

University of Windsor

## Scholarship at UWindor

---

Electronic Theses and Dissertations

Theses, Dissertations, and Major Papers

---

2007

### Ligand designs for polynuclear and heterometallic complexes

Hua Han

*University of Windsor*

Follow this and additional works at: <https://scholar.uwindsor.ca/etd>

---

#### Recommended Citation

Han, Hua, "Ligand designs for polynuclear and heterometallic complexes" (2007). *Electronic Theses and Dissertations*. 8066.

<https://scholar.uwindsor.ca/etd/8066>

This online database contains the full-text of PhD dissertations and Masters' theses of University of Windsor students from 1954 forward. These documents are made available for personal study and research purposes only, in accordance with the Canadian Copyright Act and the Creative Commons license—CC BY-NC-ND (Attribution, Non-Commercial, No Derivative Works). Under this license, works must always be attributed to the copyright holder (original author), cannot be used for any commercial purposes, and may not be altered. Any other use would require the permission of the copyright holder. Students may inquire about withdrawing their dissertation and/or thesis from this database. For additional inquiries, please contact the repository administrator via email ([scholarship@uwindsor.ca](mailto:scholarship@uwindsor.ca)) or by telephone at 519-253-3000ext. 3208.

# **Ligand Designs for Polynuclear and Heterometallic Complexes**

**By**

**Hua Han**

**A Dissertation**

**Submitted to the Faculty of Graduate Studies through the Department of  
Chemistry and Biochemistry in Partial Fulfillment of the Requirements  
for the Degree of Doctor of Philosophy at the University of Windsor**

**Windsor, Ontario, Canada  
2007**

**©2007 Hua Han**



Library and  
Archives Canada

Bibliothèque et  
Archives Canada

Published Heritage  
Branch

Direction du  
Patrimoine de l'édition

395 Wellington Street  
Ottawa ON K1A 0N4  
Canada

395, rue Wellington  
Ottawa ON K1A 0N4  
Canada

*Your file* *Votre référence*

*ISBN: 978-0-494-42376-9*

*Our file* *Notre référence*

*ISBN: 978-0-494-42376-9*

**NOTICE:**

The author has granted a non-exclusive license allowing Library and Archives Canada to reproduce, publish, archive, preserve, conserve, communicate to the public by telecommunication or on the Internet, loan, distribute and sell theses worldwide, for commercial or non-commercial purposes, in microform, paper, electronic and/or any other formats.

The author retains copyright ownership and moral rights in this thesis. Neither the thesis nor substantial extracts from it may be printed or otherwise reproduced without the author's permission.

**AVIS:**

L'auteur a accordé une licence non exclusive permettant à la Bibliothèque et Archives Canada de reproduire, publier, archiver, sauvegarder, conserver, transmettre au public par télécommunication ou par l'Internet, prêter, distribuer et vendre des thèses partout dans le monde, à des fins commerciales ou autres, sur support microforme, papier, électronique et/ou autres formats.

L'auteur conserve la propriété du droit d'auteur et des droits moraux qui protègent cette thèse. Ni la thèse ni des extraits substantiels de celle-ci ne doivent être imprimés ou autrement reproduits sans son autorisation.

---

In compliance with the Canadian Privacy Act some supporting forms may have been removed from this thesis.

Conformément à la loi canadienne sur la protection de la vie privée, quelques formulaires secondaires ont été enlevés de cette thèse.

While these forms may be included in the document page count, their removal does not represent any loss of content from the thesis.

Bien que ces formulaires aient inclus dans la pagination, il n'y aura aucun contenu manquant.



**Canada**

## Abstract

The tripodal amido ligands  $P(\text{CH}_2\text{NAr}^R)_3$  can be utilized to produce mononuclear Ti, Zr, and Ta complexes, where  $\text{Ar}^R = 3,5\text{-(CF}_3)_2\text{C}_6\text{H}_3$ , Ph, and  $3,5\text{-Me}_2\text{C}_6\text{H}_3$ . The mononuclear compound  $P(\text{CH}_2\text{N-}3,5\text{-Me}_2\text{C}_6\text{H}_3)_3\text{TiNMe}_2$  reacts with excess  $\text{Ni}(\text{CO})_4$  to afford an early-late heterobimetallic complex  $(\text{CO})_3\text{Ni}[P(\text{CH}_2\text{N-}3,5\text{-Me}_2\text{C}_6\text{H}_3)_3\text{TiNMe}_2]$  or a trinuclear complex  $(\text{CO})_2\text{Ni}[P(\text{CH}_2\text{N-}3,5\text{-Me}_2\text{C}_6\text{H}_3)_3\text{TiNMe}_2]_2$ . The reactions of 4 equiv of the mononuclear early transition metal complexes  $P(\text{CH}_2\text{NAr}^R)_3\text{TiNMe}_2$  or  $P(\text{CH}_2\text{NAr}^R)_3\text{Ta}=\text{N}^t\text{Bu}$  with  $[\text{Rh}(\text{CO})_2(\mu\text{-Cl})]_2$  produce the trinuclear *trans*-rhodiumcarbonylchlorobisphosphine complexes. The donor abilities of the phosphine complexes are affected by the direct interactions between the phosphine donors and Ti or Ta metal centers.

The reaction of phosphine ligand  $P(\text{CH}_2\text{NPh})_3$  with nickelocene  $\text{Cp}_2\text{Ni}$  produces a Ni(II) dimer  $[\text{CpNiP}(\text{CH}_2\text{NPh})_2]_2$  with a bridging diamido-phosphido ligand.  $\text{Ni}[P(\text{CH}_2\text{NPh})_3]_4$  is identified as an intermediate. The Ni(II) dimer can be used as a ligand to give the early-late transition tetranuclear heterometallic complex  $[\text{CpNiP}(\text{CH}_2\text{NPh})_2\text{Ti}(\text{NMe}_2)_2]_2$ .

The reactions of  $P[\text{CH}_2\text{NAr}^R]_3\text{ZrCl}(\text{THF})$  with cyclopentadienyllithium ( $\text{LiC}_5\text{H}_5$ ) or lithium salt of the fulvalene dianion ( $\text{Li}_2\text{C}_{10}\text{H}_8$ ) produce  $P(\text{CH}_2\text{NAr}^R)_3\text{ZrCp}$  and the bridged binuclear complexes *trans*- $[P(\text{CH}_2\text{NAr}^R)_3\text{Zr}]_2(\eta^5:\eta^5\text{-C}_{10}\text{H}_8)$ , respectively, where  $\text{Ar}^R = \text{Ph}$  and  $3,5\text{-Me}_2\text{C}_6\text{H}_3$ . The mononuclear titanium complexes  $[P(\text{CH}_2\text{NAr}^R)_3]\text{TiOC}_6\text{H}_4^t\text{Bu}$  and the binuclear species  $[P(\text{CH}_2\text{NPh})_3\text{Ti}]_2\text{-}\mu\text{-}4,4'\{\text{O}[3,3',5,5'\text{-(C}_6\text{H}_2\text{Me}_2)_2\text{O}]\}$ ,  $\{[P(\text{CH}_2\text{NPh})_3\text{Ti}]_2(\mu\text{-O})\}$ , and  $[P(\text{CH}_2\text{N-}3,5\text{-Me}_2\text{C}_6\text{H}_3)_3\text{Ti-}\mu\text{-O-Ti}(\text{NMe}_2)_3]$ , are prepared from  $[P(\text{CH}_2\text{NAr}^R)_3]\text{TiNMe}_2$  via

protonolysis. One equiv of  $\{[P(CH_2NPh)_3Ti]_2(\mu-O)\}$  precipitates a polymer of  $\{Cl(CO)Rh[P(CH_2NPh)_3Ti]_2O\}_n$ . A single CO stretch is observed in the IR spectrum of a KBr pellet at  $1972.5\text{ cm}^{-1}$ .

$Se=P(CH_2NAr^R)_3$  are prepared by oxidation of  $[P(CH_2NAr^R)_3]$ , which can react with  $AlMe_3$  to afford  $[P(CH_2NAr^R)_2Se](AlMe_2)_3$  or  $Me_3AlP(CH_2NAr^R)_2Se(AlMe_2)_3$  with the unanticipated diamidoselenophosphinito ligands, where  $Ar^R = 3,5-(CF_3)_2C_6H_3$ , Ph, and  $3,5-Me_2C_6H_3$ . Comparing the reactions with  $P(CH_2NAr^R)_3$ , only  $P(CH_2NAr^R)_3Al_2Me_3$  or  $Me_3Al-P(CH_2NAr^R)_3Al_2Me_3$  are produced without P-C bond cleavage.

$Se=P[CH_2NH-3,5-(CF_3)_2C_6H_3]_3$  reacts with *n*-butylmagnesium to produce a binuclear magnesium complex bridging with a bisphosphine ligand  $\{P_2[CH_2N-3,5-(CF_3)_2C_6H_3]_4\}(MgTHF_2)_2$  by the cleavage of the P-C bond and the Se=P bond, with concomitant loss of  $[^nBuCH_2N-3,5-(CF_3)_2C_6H_3]_2Mg$ . Byproducts include elemental selenium and  $SeMg$ .  $Se=P(CH_2NAr^R)_3$  are efficiently reduced by  $Zr(NEt_2)_4$  to produce the mononuclear zirconium complexes  $[P(CH_2NAr^R)_2SeZrNAr^RCH_2NEt_2]$ , where  $Ar^R =$  Ph and  $3,5-Me_2C_6H_3$ .

## ACKNOWLEDGEMENTS

I would like to thank my supervisor, Dr. Samuel A. Johnson for his support and guidance on the research during my graduate term at the University of Windsor.

I am grateful to Mr. Mike Fuerth (NMR), Professor James Green (GC/MS) and Dr. Guangcai Bai for their help and insightful discussions.

Many thanks go to past and present members of the Johnson group. I am especially grateful for the help of Jillian Hatnean and Meghan Doster in editing this thesis.

A special thanks is due to my parents, without whom this effort would have been worth nothing.

*This dissertation is dedicated to my family.*

## **STATEMENT OF ORIGINALITY**

I certify that this dissertation, and the research to which it refers, are the product of my own work, and that any idea or quotations from the work of other people, published or otherwise, are fully acknowledged in accordance with the standard referencing practices of the discipline.

## TABLE OF CONTENTS

ABSTRACT.....	iii
ACKNOWLEDGEMENTS.....	v
STATEMENT OF ORIGINALITY.....	vi
LIST OF TABLES.....	x
LIST OF FIGURES.....	xiii
GLOSSARY OF TERMS.....	xvi
<b>Chapter 1: Tripodal Amidometal Chemistry and Ligand Designs.....</b>	<b>1</b>
1.1 Introduction.....	1
1.2 Tripodal Amido Ligands Containing Carbon or Silicon Backbones.....	4
1.3 Tripodal Amido Amine Ligands Containing Nitrogen Backbones.....	12
1.4 Tripodal Amido Phosphine Ligands Containing Phosphorus Backbones.....	14
1.5 Scope of this Thesis.....	15
1.6 References.....	17
<b>Chapter 2: Diligating Tripodal Amido Phosphine Ligands for Heterometallic</b>	
<b>Complexes.....</b>	<b>23</b>
2.1 Introduction.....	23
2.2 Syntheses of the Ligand Precursors $P(CH_2NHAr^R)_3$ .....	26
2.3 Syntheses of the Mononuclear Titanium Complexes.....	29
2.4 Syntheses of the Mononuclear Tantalum Complexes.....	33
2.5 Mononuclear Titanium and Tantalum Complexes as Building Blocks for Heterometallic Early-Late Transition Metal Complexes.....	36
2.6 Characterization of the Phosphine Donor.....	43
2.7 Synthesis and Structure of a Ni(II) Dimer with a Bridging Diamido-phosphido Ligand.....	49
2.8 Characterization of the Intermediate and the Byproducts in the Reaction of Phosphine Ligand $[P(CH_2NHPh)_3]$ with $Cp_2Ni$ .....	53
2.9 Synthesis and Structure of the Early-Late Polynuclear Heterometallic Complex Based on the Ni (II) Dimer.....	55
2.10 Summary and Conclusions.....	58

2.11 Experimental.....	59
2.12 References.....	78
<b>Chapter 3: Bridged Dinuclear Tripodal Amido-Phosphine Complexes of Titanium and Zirconium.....</b>	<b>83</b>
3.1 Introduction.....	83
3.2 Synthesis of the Mononuclear Zirconium Chloride Complexes.....	85
3.3 Synthesis of the Mononuclear Zirconium Complexes with Unlinked Cyclopentadienyl Rings.....	87
3.4 Synthesis of the Binuclear Zirconium Complexes with the Bridging Fulvalenide Ligand and Comparison with the Analogous Mononuclear Zirconium Complexes with Unlinked Cyclopentadienyl Rings.....	94
3.5 Synthesis of the Bridged Binuclear Titanium Complexes.....	97
3.6 Polymer Synthesis.....	109
3.7 Summary and Conclusion.....	110
3.8 Experimental.....	112
3.9 References.....	124
<b>Chapter 4: Diamidoselenophosphinito Ligands by P-C bond Cleavage of Phosphine Selenides and a Comparison to Related Tripodal Triamidophosphine Complexes.....</b>	<b>127</b>
4.1 Introduction.....	127
4.2 Oxidation of $P(CH_2NHA r^R)_3$ with Selenium.....	130
4.3 Synthesis of the Trinuclear Complexes via Reactions of $Se=P(CH_2NHA r^R)_3$ with $AlMe_3$ .....	134
4.4 Synthesis of the Trimethylaluminum Adducts of $[P(CH_2NAr^R)_2Se](AlMe_2)_3$ .....	140
4.5 Synthesis of the Bimetallic Aluminum Amido Complexes with the $P(CH_2NHA r^R)_3$ ligands.....	144
4.6 Synthesis of the Adducts of the Bimetallic Aluminum Amido Complexes $Me_3Al \cdot P(CH_2NAr^R)_3 Al_2Me_3$ .....	146
4.7 Ligand Design and Bonding Modes.....	150
4.8 Summary and Conclusions.....	151

4.9 Experimental.....	152
4.10 References.....	165
<b>Chapter 5: A Binuclear Magnesium Complex Bridged by a Bisphosphine</b>	
<b>Ligand</b> .....	170
5.1 Introduction.....	170
5.2 Synthesis and Structure of a Binuclear Magnesium Complex Bridged by a Bisphosphine Ligand.....	173
5.3 Characterization of the Byproducts and the Mechanism of the Reaction of Se=P[CH <sub>2</sub> NH-3,5-(CF <sub>3</sub> ) <sub>2</sub> C <sub>6</sub> H <sub>3</sub> ] <sub>3</sub> with <i>n</i> -Butylmagnesium.....	176
5.4 Synthesis and Structures of the Zirconium Compounds with the Tripodal Diamido-selenophosphinito ligands.....	182
5.5 Summary and Conclusions.....	186
5.6 Experimental.....	186
5.7 References.....	192
<b>Chapter 6: Summary and Future Work</b> .....	194
6.1 Summary.....	200
6.2 Future Work.....	201
6.3 Experimental.....	207
6.4 References.....	208
<b>Appendix One: X-ray Crystal Structure Data</b> .....	212
<b>Vita Auctoris</b> .....	261

## List of Tables

<b>Table 2.1</b>	Selected distances (Å) and bond angles for compounds <b>2a</b> , <b>2b</b> and <b>2c</b>	32
<b>Table 2.2</b>	Metal carbonyl stretching frequencies of compounds <b>6a-c</b> , <b>7a-c</b> and <b>8a-c</b> in CH <sub>2</sub> Cl <sub>2</sub> , their <sup>1</sup> J <sub>RhP</sub> coupling constants and <sup>31</sup> P NMR shifts, and the <sup>31</sup> P NMR shifts of the phosphine donors <b>1a-c</b> , <b>2a-c</b> and <b>3a-c</b>	49
<b>Table 2.3</b>	Crystallographic data for compounds <b>1c</b> , <b>2a-c</b> , <b>3b</b> , <b>5</b> , <b>8c</b> , <b>9</b> and <b>11</b>	75
<b>Table 3.1</b>	Crystal data and structure refinement for <b>14c</b> , <b>15c</b> , <b>16c</b> , <b>17c</b> , <b>19</b> and <b>20</b>	122
<b>Table 4.1</b>	Selected bond lengths (Å) and angles (deg) of the phosphine selenides <b>22a-c</b>	134
<b>Table 4.2</b>	The <sup>1</sup> J <sub>PSe</sub> coupling constants, <sup>31</sup> P NMR shifts of <b>22a-c</b> and the carbonyl stretching frequencies of Rh(CO)Cl[P(CH <sub>2</sub> NHAr <sup>R</sup> ) <sub>3</sub> ] <sub>2</sub> .	134
<b>Table 4.3</b>	Selected bond lengths (Å) and angles (deg) of <b>23a</b> , <b>23c</b>	138
<b>Table 4.4</b>	Selected bond lengths (Å) and angles (deg) of the Lewis acid-base adducts <b>24b</b> and <b>26b</b>	150
<b>Table 4.5</b>	Crystallographic data for compounds <b>22a-c</b> , <b>23a</b> , <b>23c</b> , <b>24b</b> , <b>25b</b> , and <b>26b</b>	162
<b>Table 5.1</b>	Crystallographic data for compounds <b>27</b> , <b>35</b> and <b>37c</b>	191
<b>Table A 1.1</b>	Positional parameters and U(eq) for P[CH <sub>2</sub> NH-3,5-(CF <sub>3</sub> ) <sub>2</sub> C <sub>6</sub> H <sub>3</sub> ] <sub>3</sub> ( <b>1a</b> )	212
<b>Table A 1.2</b>	Positional parameters and U(eq) for P(CH <sub>2</sub> N-3,5-(CF <sub>3</sub> ) <sub>2</sub> C <sub>6</sub> H <sub>3</sub> ) <sub>3</sub> TiNMe <sub>2</sub> ( <b>2a</b> )	214
<b>Table A 1.3</b>	Positional parameters and U(eq) for P(CH <sub>2</sub> NPh) <sub>3</sub> TiNMe <sub>2</sub> ( <b>2b</b> )	216
<b>Table A 1.4</b>	Positional parameters and U(eq) for P(CH <sub>2</sub> NAr <sup>Me</sup> ) <sub>3</sub> TiNMe <sub>2</sub> ( <b>2c</b> )	217
<b>Table A 1.5</b>	Positional parameters and U(eq) for P(CH <sub>2</sub> NPh) <sub>3</sub> Ta=N <sup>t</sup> Bu ( <b>3b</b> )	220
<b>Table A 1.6</b>	Positional parameters and U(eq) for (CO) <sub>2</sub> Ni[P(CH <sub>2</sub> NAr <sup>Me</sup> ) <sub>3</sub> TiNMe <sub>2</sub> ] <sub>2</sub> ( <b>5</b> )	221

<b>Table A 1.7</b>	Positional parameters and U(eq) for <i>trans</i> -RhCl(CO)( <b>3c</b> ) <sub>2</sub> ( <b>8c</b> )	224
<b>Table A 1.8</b>	Positional parameters and U(eq) for [CpNiP(CH <sub>2</sub> NHPh) <sub>2</sub> ] <sub>2</sub> ( <b>9</b> )	225
<b>Table A 1.9</b>	Positional parameters and U(eq) for [CpNiP(CH <sub>2</sub> NPh) <sub>2</sub> Ti(NMe <sub>2</sub> ) <sub>2</sub> ] <sub>2</sub> ( <b>11</b> )	228
<b>Table A 1.10</b>	Positional parameters and U(eq) for P[CH <sub>2</sub> N-3,5-Me <sub>2</sub> C <sub>6</sub> H <sub>3</sub> ] <sub>3</sub> ZrCp ( <b>14c</b> )	229
<b>Table A 1.11</b>	Positional parameters and U(eq) for P[CH <sub>2</sub> NPh] <sub>3</sub> Li <sub>3</sub> (Et <sub>2</sub> O) <sub>1.5</sub> ( <b>15d</b> )	232
<b>Table A 1.12</b>	Positional parameters and U(eq) for [P(CH <sub>2</sub> N-3,5-Me <sub>2</sub> C <sub>6</sub> H <sub>3</sub> ) <sub>3</sub> Zr] <sub>2</sub> (η <sup>5</sup> :η <sup>5</sup> -C <sub>10</sub> H <sub>8</sub> ) ( <b>16c</b> )	234
<b>Table A 1.13</b>	Positional parameters and U(eq) for P[CH <sub>2</sub> N-3,5-Me <sub>2</sub> C <sub>6</sub> H <sub>3</sub> ] <sub>3</sub> TiO[4- <i>t</i> -BuC <sub>6</sub> H <sub>3</sub> ] ( <b>17c</b> )	236
<b>Table A 1.14</b>	Table A 1.12 Positional parameters and U(eq) for P[CH <sub>2</sub> NPh] <sub>3</sub> Ti-μ-O-Ti[PhNCH <sub>2</sub> ] <sub>3</sub> P ( <b>19</b> )	239
<b>Table A 1.15</b>	Positional parameters and U(eq) for P[CH <sub>2</sub> N-3,5-Me <sub>2</sub> C <sub>6</sub> H <sub>3</sub> ] <sub>3</sub> Ti-μ-O-Ti(NMe <sub>2</sub> ) <sub>3</sub> ( <b>20</b> )	240
<b>Table A 1.16</b>	Positional parameters and U(eq) for Se=P[CH <sub>2</sub> NH-3,5-(CF <sub>3</sub> ) <sub>2</sub> C <sub>6</sub> H <sub>3</sub> ] <sub>3</sub> ( <b>22a</b> )	241
<b>Table A 1.17</b>	Positional parameters and U(eq) for Se=P(CH <sub>2</sub> NHPh) <sub>3</sub> ( <b>22b</b> )	243
<b>Table A 1.18</b>	Positional parameters and U(eq) for Se=P(CH <sub>2</sub> NH-3,5-Me <sub>2</sub> C <sub>6</sub> H <sub>3</sub> ) <sub>3</sub> ( <b>22c</b> )	244
<b>Table A 1.19</b>	Positional parameters and U(eq) for P[CH <sub>2</sub> N-3,5-(CF <sub>3</sub> ) <sub>2</sub> C <sub>6</sub> H <sub>3</sub> ] <sub>2</sub> Se(AlMe <sub>2</sub> ) <sub>3</sub> ( <b>23a</b> )	245
<b>Table A 1.20</b>	Positional parameters and U(eq) for P(CH <sub>2</sub> N-3,5-Me <sub>2</sub> C <sub>6</sub> H <sub>3</sub> ) <sub>2</sub> Se(AlMe <sub>2</sub> ) <sub>3</sub> ( <b>23c</b> )	247
<b>Table A 1.21</b>	Positional parameters and U(eq) for Me <sub>3</sub> Al·P(CH <sub>2</sub> NPh) <sub>2</sub> Se(AlMe <sub>2</sub> ) <sub>3</sub> ( <b>24b</b> )	249
<b>Table A 2.22</b>	Positional parameters and U(eq) for P[CH <sub>2</sub> N-3,5-(CF <sub>3</sub> ) <sub>2</sub> C <sub>6</sub> H <sub>3</sub> ] <sub>3</sub> Al <sub>2</sub> Me <sub>3</sub> ( <b>25a</b> )	250
<b>Table A 2.23</b>	Positional parameters and U(eq) for Me <sub>3</sub> Al·P(CH <sub>2</sub> NPh) <sub>3</sub> Al <sub>2</sub> Me <sub>3</sub> ( <b>26b</b> )	252

- Table A 2.24** Positional parameters and  $U(\text{eq})$  for  $\{\text{P}[\text{CH}_2\text{N}-3,5-$  253  
 $(\text{CF}_3)_2\text{C}_6\text{H}_3]_2\text{MgTHF}_2\}_2$  (**27**)
- Table A 2.25** Positional parameters and  $U(\text{eq})$  for  $\{\text{P}[\text{CH}_2\text{N}-3,5-$  255  
 $(\text{CF}_3)_2\text{C}_6\text{H}_3]_2\text{Se}_2\}[\text{HNEt}_3]^+$  (**35**)
- Table A 2.26** Positional parameters and  $U(\text{eq})$  for  $\text{P}[\text{CH}_2\text{N}-3,5-$  259  
 $\text{Me}_2\text{C}_6\text{H}_3]_2\text{SeZrN}(-3,5-\text{Me}_2\text{C}_6\text{H}_3)\text{CH}_2\text{NEt}_2$  (**37c**)

## List of Figures

<b>Figure 1.1</b>	Tripodal amido ligands containing carbon, silicon, nitrogen or phosphorus backbones	3
<b>Figure 1.2</b>	Tripodal amido metal complexes with weakly coordinating donor functions	9
<b>Figure 2.1</b>	Potential binding mode of the $P(CH_2NHA^R)_3$ ligands to an early transition metal fragment (shown as M) and a second metal complex (shown as M') along with an illustration of the major and minor lobes of the lone pair orbital on phosphorus.	25
<b>Figure 2.2</b>	ORTEP depiction of the solid-state structure of <b>1a</b> as determined by X-ray crystallography	29
<b>Figure 2.3</b>	Solid-state molecular structure of <b>2b</b> as determined by X-ray crystallography	31
<b>Figure 2.4</b>	Solid-state molecular structure of <b>3b</b> as determined by X-ray crystallography	36
<b>Figure 2.5</b>	ORTEP depiction of the solid-state molecular structure of $(CO)_2Ni[P(CH_2N-3,5-Me_2C_6H_3)_3TiNMe_2]_2$ ( <b>5</b> )	40
<b>Figure 2.6</b>	ORTEP depiction of the solid-state molecular structure of <b>8c</b> as determined by X-ray crystallography	43
<b>Figure 2.7</b>	Phosphorus-31 NMR chemical shifts vs. carbonyl stretching frequencies for complexes <b>6a-c</b> , <b>7a-c</b> and <b>8a-c</b>	47
<b>Figure 2.8</b>	Solid-state molecular structure of <b>9</b> as determined by X-ray crystallography	53
<b>Figure 2.9</b>	Solid-state molecular structure of <b>11</b> as determined by X-ray crystallography	58
<b>Figure 3.1</b>	Solid-state molecular structure of <b>14c</b> as determined by X-ray crystallography	90
<b>Figure 3.2</b>	Solid-state molecular structure of <b>15d</b> as determined by X-ray crystallography	93

<b>Figure 3.3</b>	Solid-state molecular structure of <b>16c</b> as determined by X-ray crystallography	97
<b>Figure 3.4</b>	Solid-state molecular structure of <b>17c</b> as determined by X-ray crystallography	101
<b>Figure 3.5</b>	Solid-state molecular structure of <b>19</b> as determined by X-ray crystallography	105
<b>Figure 3.6</b>	Solid-state molecular structure of <b>19</b> viewed along the crystallographic 3-fold axis	106
<b>Figure 3.7</b>	Solid-state molecular structure of <b>20</b> as determined by X-ray crystallography	108
<b>Figure 4.1</b>	Potential bonding modes of the formally trianionic ligands $P[CH_2NHA r^R]_3$ and $Se=P[CH_2NHA r^R]_2$ with metal complexes labeled M	130
<b>Figure 4.2</b>	Solid-state molecular structure of <b>22a</b> as determined by X-ray crystallography	132
<b>Figure 4.3</b>	Solid-state molecular structure of <b>22b</b> as determined by X-ray crystallography	133
<b>Figure 4.4</b>	Solid-state molecular structure of <b>22c</b> as determined by X-ray crystallography	133
<b>Figure 4.5</b>	Solid-state molecular structure of <b>23a</b> as determined by X-ray crystallography	137
<b>Figure 4.6</b>	Solid-state molecular structure of <b>23c</b> as determined by X-ray crystallography	138
<b>Figure 4.7</b>	Solid-state molecular structure of <b>24b</b> as determined by X-ray crystallography	141
<b>Figure 4.8</b>	Solid-state molecular structure of <b>25a</b> as determined by X-ray crystallography	146
<b>Figure 4.9</b>	ORTEP depiction of the solid-state molecular structure of <b>26b</b> as determined by X-ray crystallography	148
<b>Figure 5.1</b>	Solid-state molecular structure of <b>27</b> obtained by X-ray crystallography. Selected bond lengths	175

<b>Figure 5.2</b>	Solid-state molecular structure of <b>35</b> determined by X-ray crystallography	182
<b>Figure 5.3</b>	Solid-state molecular structure of <b>37c</b> as determined by X-ray crystallography	185

## GLOSSARY OF TERM

Å	Angström
Anal.	analysis
Ar <sup>R</sup>	3,5-(CF <sub>3</sub> ) <sub>2</sub> C <sub>6</sub> H <sub>3</sub> , Ph, and 3,5-Me <sub>2</sub> C <sub>6</sub> H <sub>3</sub>
Ar <sup>Me</sup>	3,5-Me <sub>2</sub> C <sub>6</sub> H <sub>3</sub>
Ar <sup>CF<sub>3</sub></sup>	3,5-(CF <sub>3</sub> ) <sub>2</sub> C <sub>6</sub> H <sub>3</sub>
aq	aqueous
<sup>n</sup> Bu	n-butyl group
<sup>t</sup> Bu	tertiary butyl group
<sup>13</sup> C	carbon-13
Calcd.	calculated
cm	centimetres
Cp	cyclopentadienyl
d	doublet
dd	doublet of doublets
DME	1,2-dimethoxyethane
deg	degrees
°C	degrees Celsius
D	deuterium
Et	ethyl group
<sup>19</sup> F	fluorine-19
g	grams
GC/MS	gas chromatography/mass spectrometry

{ <sup>1</sup> H}	proton decoupled
<sup>1</sup> H	proton
Hz	Hertz, seconds <sup>-1</sup>
IR	infrared
K	Kelvin
<sup>7</sup> Li	lithium-7
mm	millimetres
Me	methyl group
m/e	mass/charge
Mes	mesityl group
mg	milligram
mL	milliliter
mmol	millimole
mol	mole
M	molarity
ORTEP	Oakridge Thermal Ellipsoid Plotting Program
<sup>31</sup> P	phosphorus-31
Ph	phenyl group
ppm	parts per million
reflns	reflections (X-ray crystallography)
THF	tetrahydrofuran
U (eq)	equivalent isotropic displacement parameter
$\eta^n$	n-hapto

$\lambda$

wavelength

$\delta$

chemical shift in ppm

## Chapter One

# Tripodal Amidometal Chemistry and Ligand Designs

### 1.1 Introduction

The amido-metal bond in early transition metal complexes is kinetically inert and thermodynamically stable, which is far less interesting than the corresponding carbon-metal bond.<sup>1</sup> However, amidometal chemistry has recently utilized stable amido-metal bonds for ligand designs in main group and transition metal chemistry, and to produce reactive metal centres.<sup>1-4</sup>

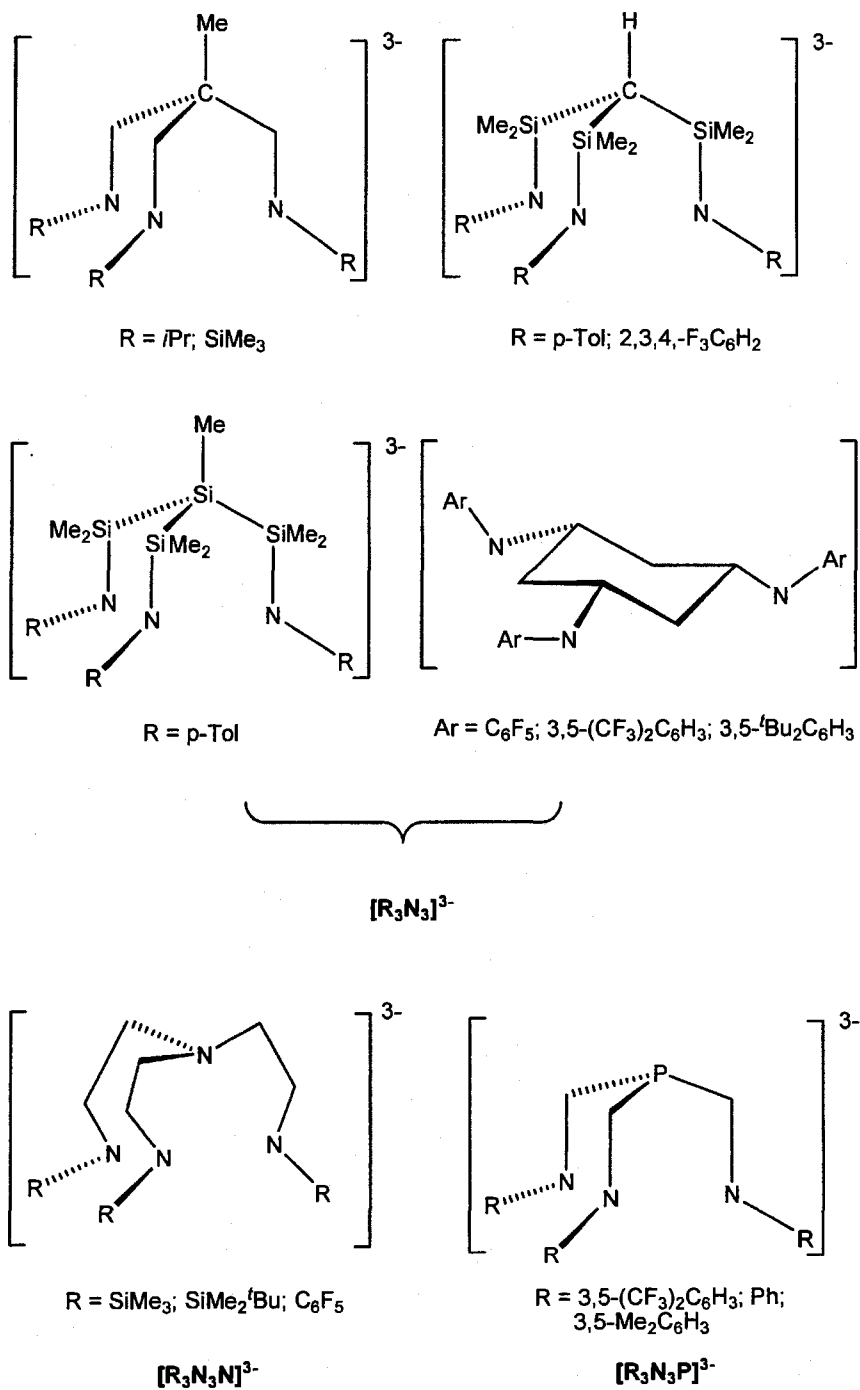
In this thesis, we first investigate and develop the ligands  $P(\text{CH}_2\text{NHA}^{\text{R}})_3$ , where  $\text{Ar}^{\text{R}} = 3,5\text{-(CF}_3)_2\text{C}_6\text{H}_3$ , Ph, and  $3,5\text{-Me}_2\text{C}_6\text{H}_3$ . Related tripodal amido ligands containing carbon, silicon or nitrogen backbones have been studied.<sup>5-7</sup> These polydentate ligands  $P(\text{CH}_2\text{NHA}^{\text{R}})_3$  combine the tripodal amido donors with a phosphine donor and have been very successfully employed in the synthesis of

polynuclear or heterometallic complexes, which will be described in Chapter 2 through 6.

In this chapter, we introduce the 3-fold-symmetrical tripodal amido ligands with variable backbones, as shown in Figure 1.1. The different reactivities of the complexes will be described. Tripodal amido ligands containing carbon or silicon backbones have been utilized to stabilize polar metal-metal bonds and are employed as building blocks in the synthesis of heterometallic complexes. Tripodal amido amine ligands containing nitrogen backbones have been employed to stabilize ‘half-naked’ trivalent transition metal complexes and ligand-metal triple bonds.

The two substituents of amido ligands  $[\text{NR}_2]^-$  play an important role in amidometal chemistry, because the electronic and steric properties of the substituents influence the metal centers.<sup>8-19</sup> By tuning the substituents, polydentate ligands can also kinetically stabilize ligand-metal bonds and sterically protect reactive metal centers. The thermodynamic stability of amidometal fragments and the kinetic stability obtained by steric shielding allow tripodal amidometal complexes to be used as stable molecular building blocks in main group and transition metal compounds. Amido functions may also be combined with other charged or neutral donor functions. This combination offers greater potential to modify reactive sites in early transition metal reagents and catalysts, as well as in ligands and complexes designed for molecular building blocks.<sup>20-31</sup>

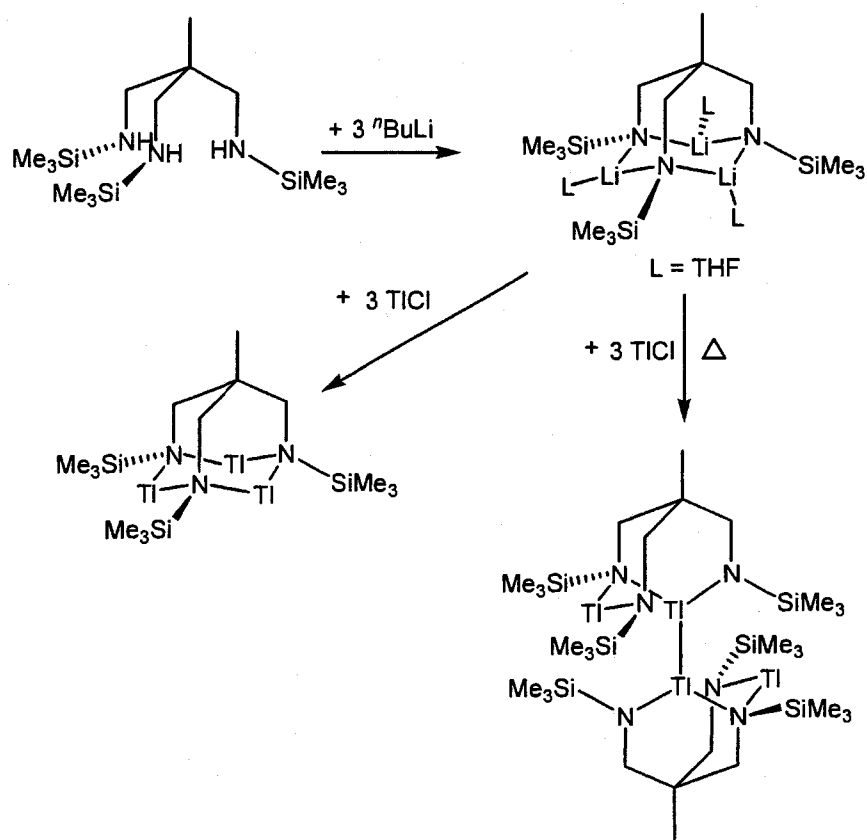
**Figure 1.1 Tripodal amido ligands containing carbon, silicon, nitrogen or phosphorus backbones**



## 1.2 Tripodal Amido Ligands Containing Carbon or Silicon Backbones

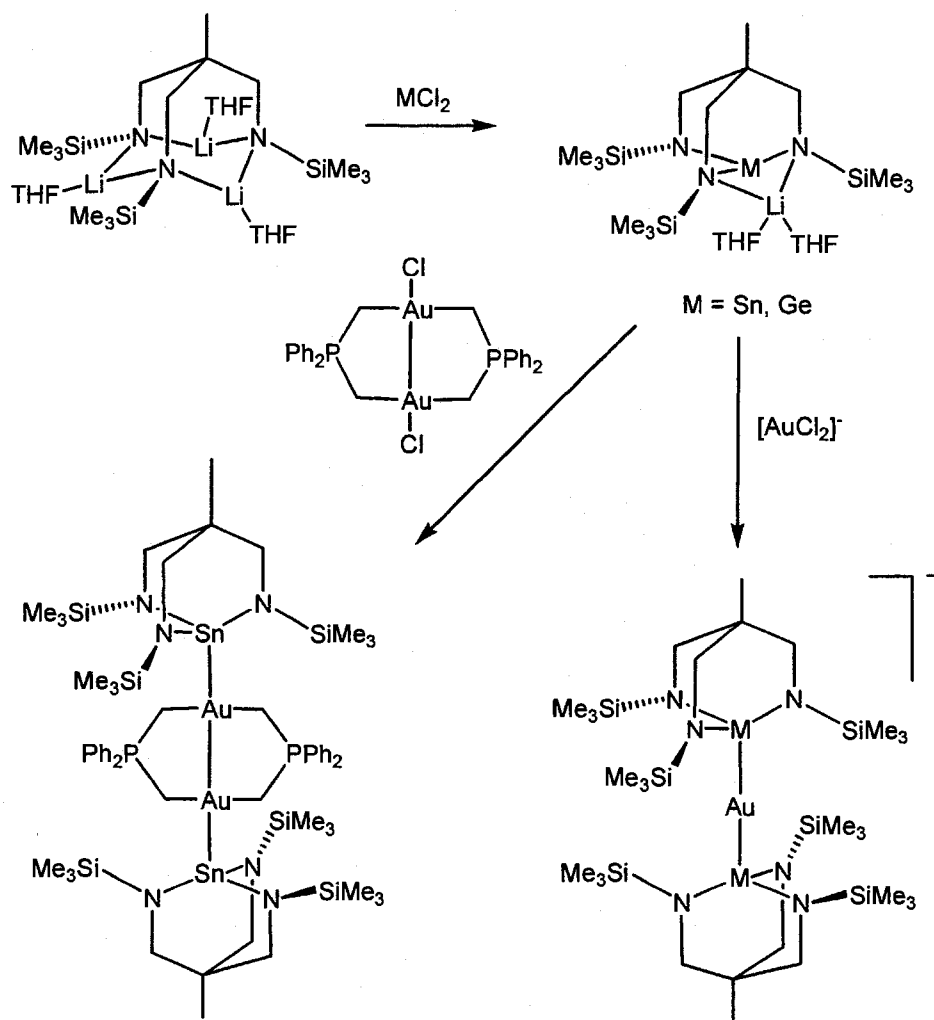
Tripodal amido ligands containing carbon or silicon backbones can be utilized to produce ligand-metal cages and have been employed as building blocks for homobinuclear complexes, heterobimetallic complexes and polynuclear complexes. For example, a tripodal amido ligand containing a carbon backbone has been used to produce a trinuclear thallium amido compound, which may be thermally converted to a tetranuclear thallium amido compound with a Tl(II)-Tl(II) bond (as shown in Scheme 1.1).<sup>10</sup>

**Scheme 1.1**



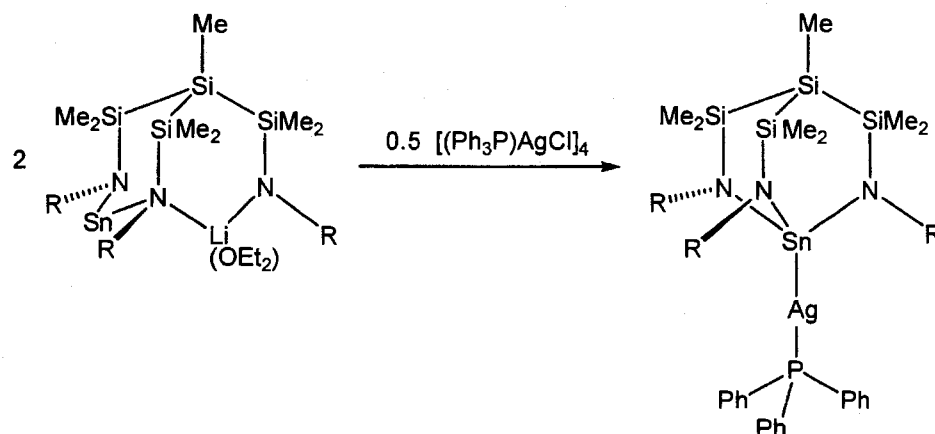
Group 14 metal complexes with tripodal amido ligands were found to act as versatile ligands in gold chemistry. The tripodal lithium amide  $\text{H}_3\text{CC}(\text{CH}_2\text{N}(\text{Li})\text{SiMe}_3)_3(\text{THF})_3$  reacted with  $\text{SnCl}_2$  and  $\text{GeCl}_2(1,4\text{-dioxane})$  in THF to give triamidometalates  $\text{H}_3\text{CC}(\text{CH}_2\text{NSiMe}_3)_3\text{MLi}(\text{THF})_2$  ( $\text{M} = \text{Sn}$  or  $\text{Ge}$ ), as shown in Scheme 1.2. A Ge-Au-Ge unit was established by the reaction with 2 equiv of  $\text{H}_3\text{CC}(\text{CH}_2\text{NSiMe}_3)_3\text{MLi}(\text{THF})_2$  and  $[\text{Q}][\text{AuX}_2]$  ( $\text{Q} = \text{Ph}_3\text{PCH}_2\text{Ph}$ ,  $\text{Ph}_4\text{P}$ ;  $\text{X} = \text{Cl}$ ,  $\text{Br}$ ). The reaction of  $[\text{MeSi}\{\text{Me}_2\text{SiN}(p\text{-tol})\}_3\text{SnLi}(\text{Et}_2\text{O})]$  with a dinuclear gold(II) derivative  $[\text{Au}_2(\text{CH}_2\text{PPh}_2\text{CH}_2)_2\text{Cl}_2]$  in a 1:2 ratio affords  $[\text{Au}_2(\text{CH}_2\text{PPh}_2\text{CH}_2)_2(\text{MeSi}\{\text{Me}_2\text{SiN}(p\text{-tol})\}_3\text{Sn})_2]$  with a Sn-Au-Au-Sn linear unit.<sup>10, 11</sup> These results show that this highly robust tripodal amido ligand is suitable for stabilizing Group 14-Au bonds and allows for the synthesis of heterometallic complexes with gold in the oxidation states +I and +III.

## Scheme 1.2



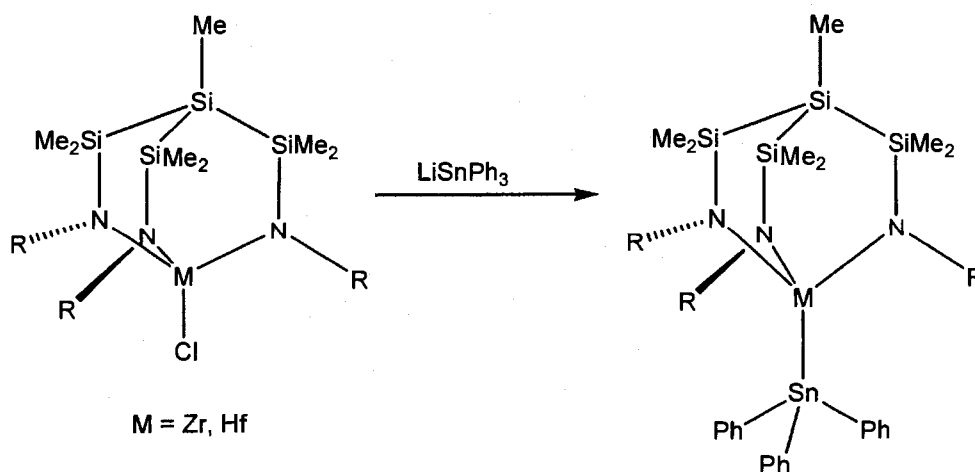
The reaction of lithium triamidostannate  $\text{MeSi}\{\text{SiMe}_2\text{N}(p\text{-Tol})\}_3\text{SnLi}(\text{OEt}_2)$  with 0.25 equiv of  $[(\text{Ph}_3\text{P})\text{AgCl}]_4$  in toluene yields a Sn-Ag complex and provides the first direct structural evidence for an Ag-Sn bond (Scheme 1.3).<sup>9</sup>

Scheme 1.3



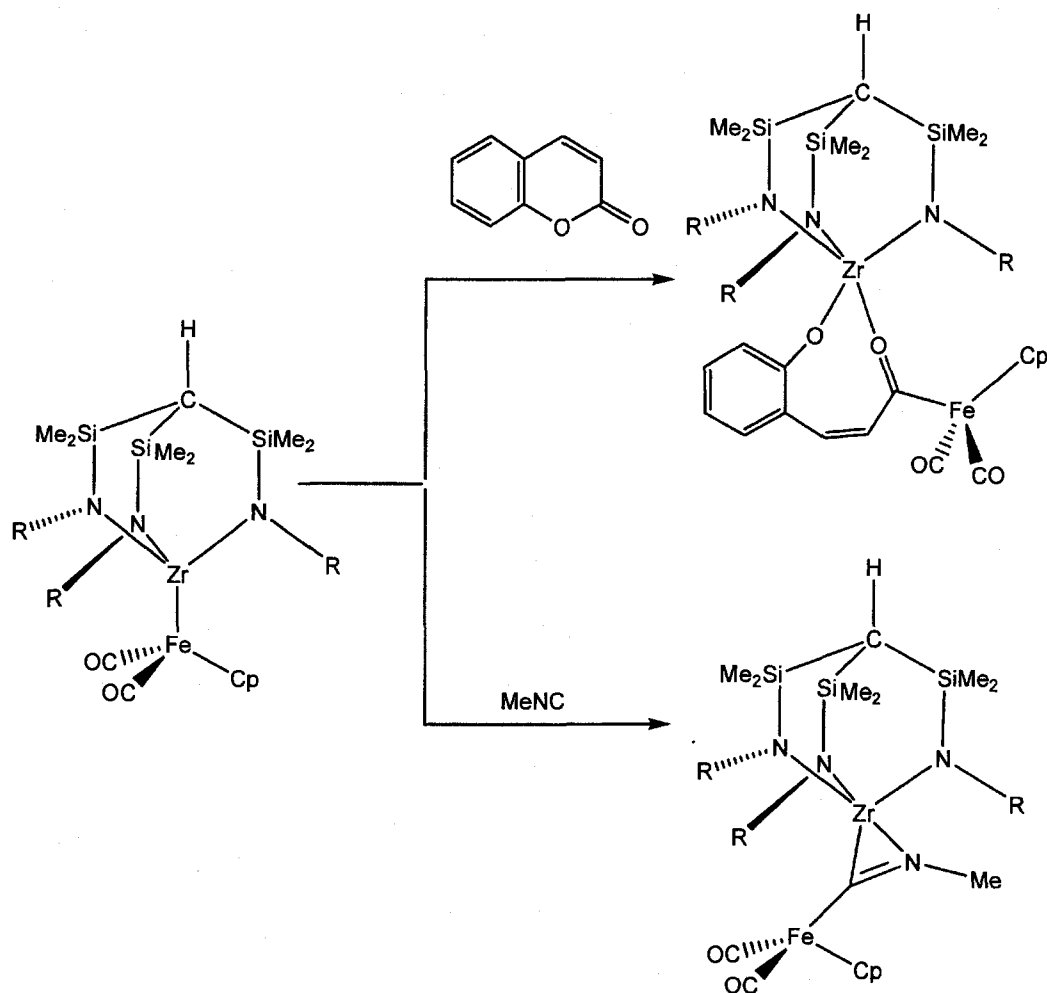
Triamidostannates can bind to the Group 4 transition metal complexes to give thermally stable heterometallic compounds.<sup>8, 13,32</sup> These ligands were successfully employed for the stabilization of tin-transition metal bonds and in the synthesis of heterometallic metal complexes (Scheme 1.4). Apart from the electronic properties of the amido ligands stabilizing the stannate units, the effective shielding of the metal-metal bonds by the ligand frameworks and periphery of the tripod play an important role.

Scheme 1.4



Tripodal amido ligands-Group 4 complexes have also been used as starting materials to synthesize early-late heterobimetallic complexes.<sup>32-39,40</sup> These complexes have been found to insert polar organic substrates, as shown in Scheme 1.5.

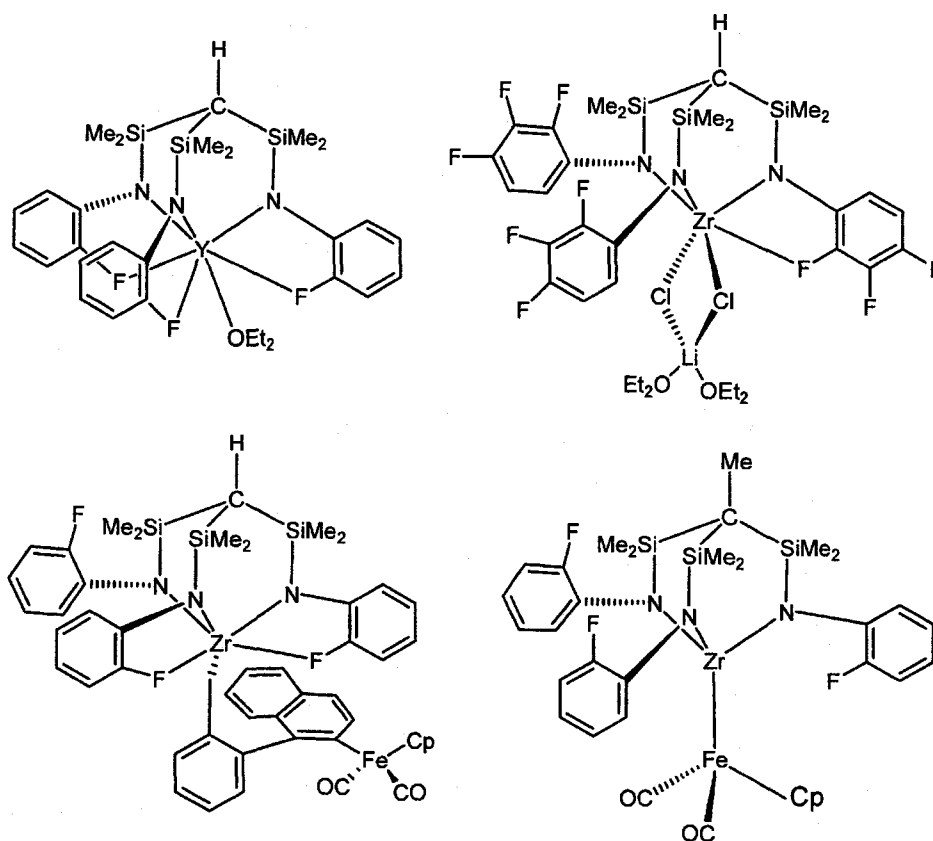
Scheme 1.5



In amido complexes, the addition of weakly coordinating donor functions may adjust the size of the reactive site at metal centers.<sup>1,2</sup> The coordination of one, two or three F atoms to metals has been studied systematically. The structures of these

complexes demonstrate the relationship between the size of the anionic monodentate ligands and the number of coordinated C-F groups, as shown in Figure 1.2.<sup>41-44,45-47</sup>

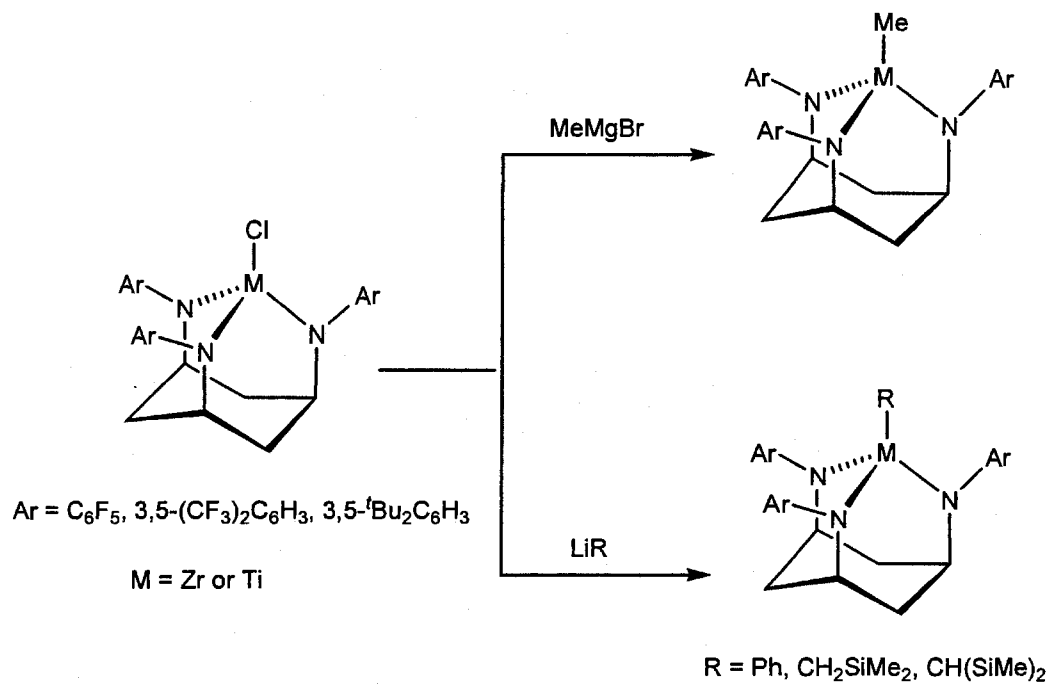
**Figure 1.2 Tripodal amido metal complexes with weakly coordinating donor functions**



Tilly and Turculet have reported the novel ligands derived from *cis, cis*-1,3,3-triaminocyclohexane (tach), which have been utilized to support reactive early transition metal complexes.<sup>48,29</sup> The steric properties of ligands affect metal centers and leave them accessible to smaller molecular reactants by inhibiting intermolecular

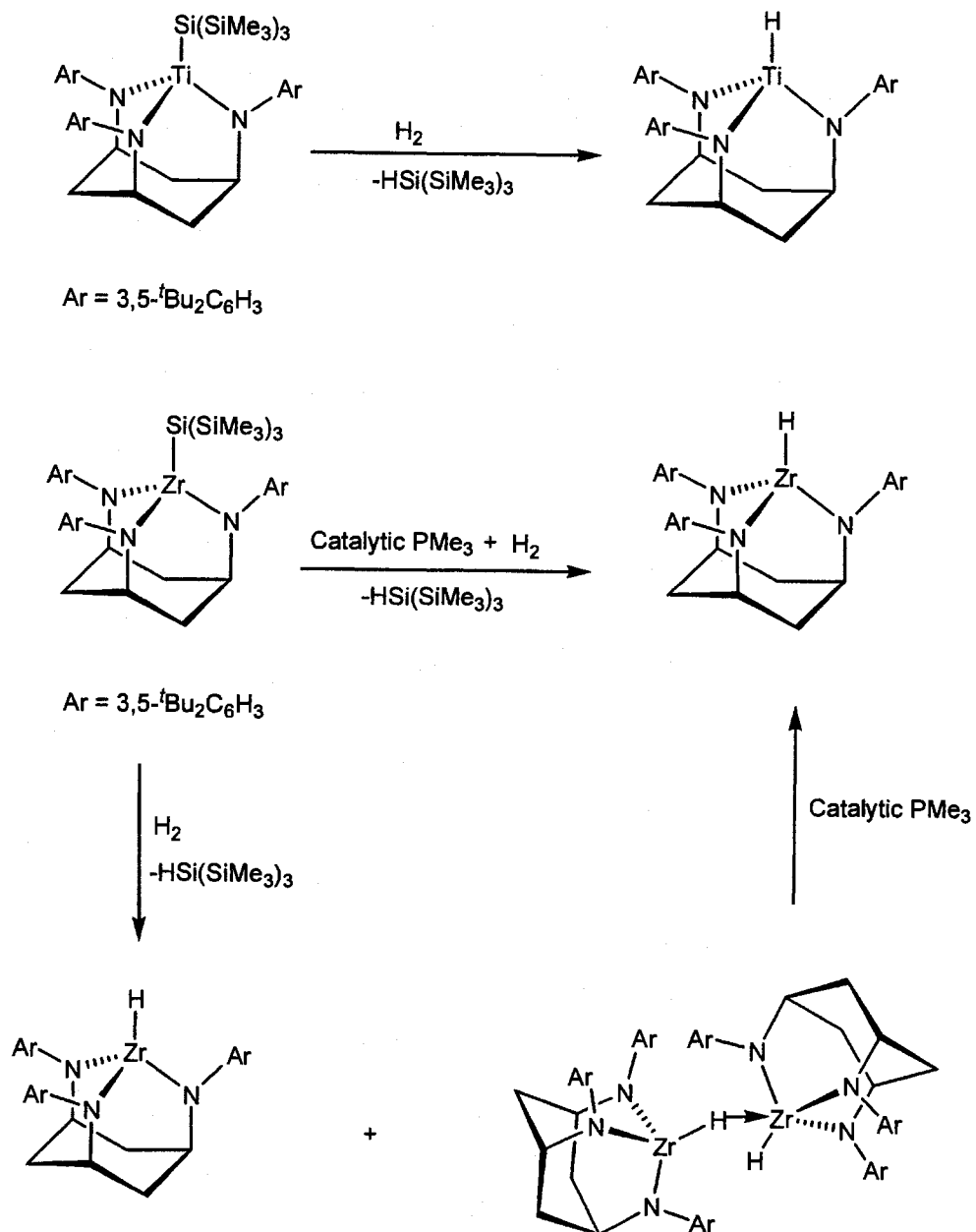
pathways. The mononuclear zirconium complexes can be alkylated by different Grignard and alkyllithium reagents, as shown in Scheme 1.6.

**Scheme 1.6**



The reaction of the Ti silyl complex with H<sub>2</sub> (1atm) affords the clean Ti mono-hydride complex and HSi(SiMe<sub>3</sub>)<sub>3</sub>. The reaction of the Zr silyl complex with H<sub>2</sub> (1atm) only results in the mixture, as shown in Scheme 1.7. However, addition of PMe<sub>3</sub> to the mixture product produces the clean hydride complex.

Scheme 1.7

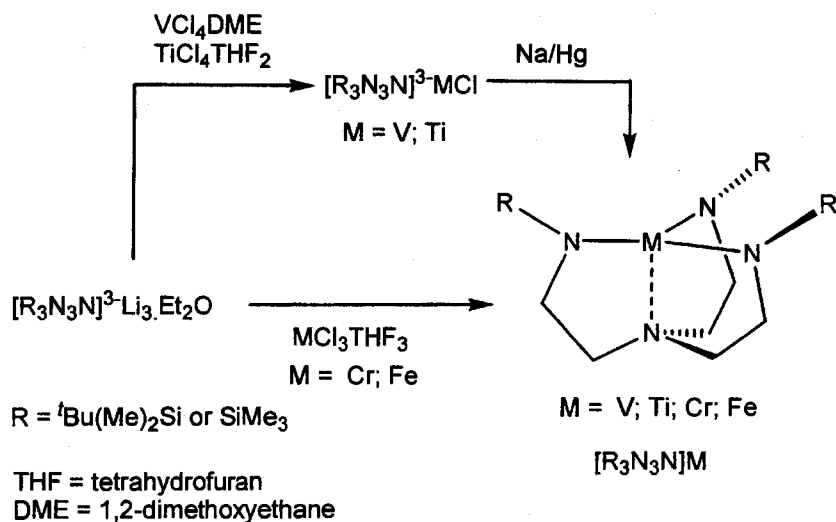


### 1.3 Tripodal Amido Amine Ligands Containing Nitrogen Backbones

The tripodal amido amine ligands may coordinate transition metals in a tetradentate manner.<sup>49</sup> These ligands have been employed to stabilize trivalent “half-naked” transition metal complexes and ligand-metal triple bonds.

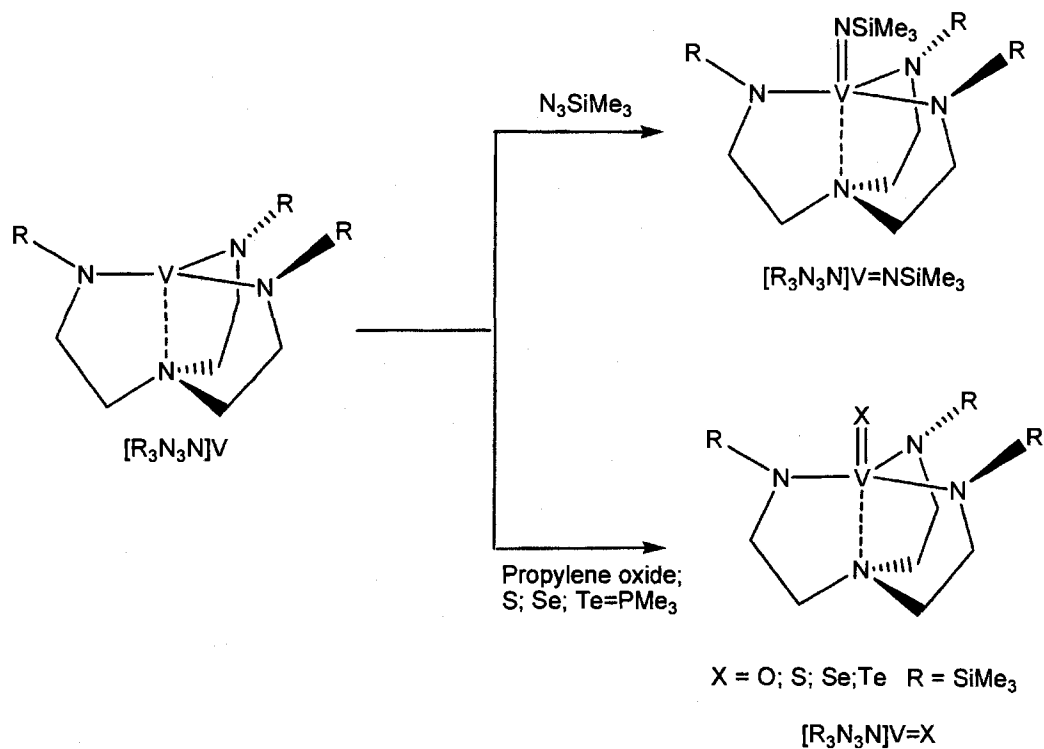
Lithium salts can be used as starting materials to synthesize the trigonal-monopyramidal M(III) complexes (M= V, Ti, Cr and Fe), as shown in Scheme 1.8.<sup>48</sup>

Scheme 1.8



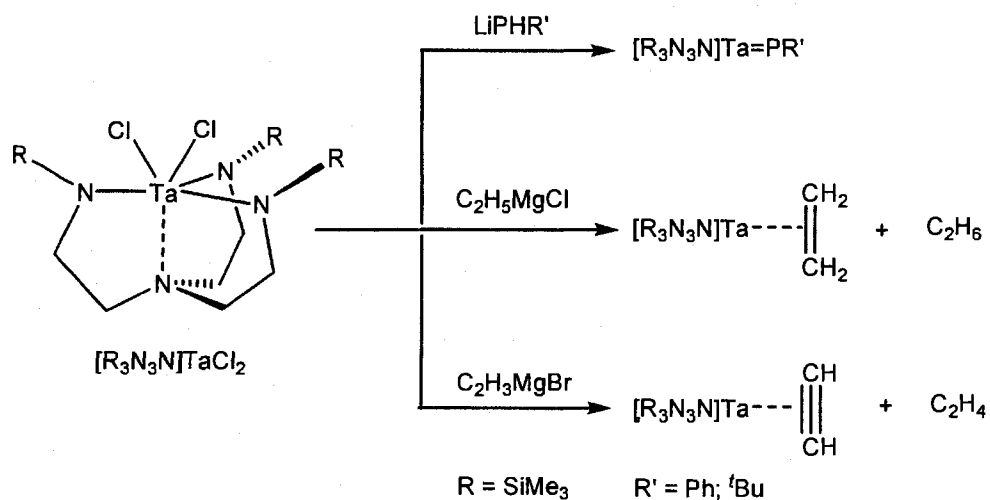
The reactions of the vanadium complexes with trimethylsilyl azide at room temperature afford the silylimido complexes, as shown in Scheme 1.9.<sup>50</sup> The reactions of vanadium complexes with propylene oxide, elemental sulfur or selenium, and  $\text{Te}=\text{PMe}_3$  produce the corresponding chalcogenide.

## Scheme 1.9



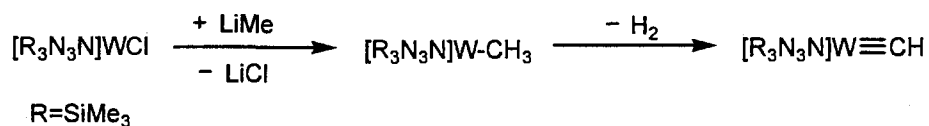
The reaction of tantalum chloride complex with  $LiPHR'$  affords phosphanidene tantalum(V) complex, as shown in Scheme 1.10.<sup>51,52,53</sup> The tantalum chloride complex reacts with ethyl or vinyl Grignard reagents to produce the corresponding ethylene or acetylene complex, which is accompanied by the elimination of ethane or ethylene.<sup>54</sup>

## Scheme 1.10



The tripodal amido amine ligands may stabilize the ligand-metal (Mo or W) triple bonds. The tungsten chloride complex can be alkylated by  $LiR'$  ( $R' = Me, Et$ ) to prepare  $n$ -alkyl complexes, which may lose  $H_2$  to form a thermodynamically favorable  $W\equiv C$  bond, as shown in Scheme 1.11.<sup>55,45,56</sup>

## Scheme 1.11



These results demonstrate that the tripodal amido amine ligands are suitable to stabilize and sterically protect transition metal centers, especially for ligand-metal triple bonds.

## 1.4 Tripodal Amido Phosphine Ligands Containing Phosphorus Backbones

Compared with tripodal amido ligands containing carbon, silicon or nitrogen backbones, the tripodal amido phosphine ligands  $P(\text{CH}_2\text{NHA}^{\text{R}})_3$  have significantly different chemical functionalities.<sup>42-47, 57-65</sup>

$P(\text{CH}_2\text{NHPh})_3$  was first synthesized in the 1970's, but never used as a ligand.<sup>66</sup> In this thesis, we first utilized and developed a series of related ligands  $P(\text{CH}_2\text{NHA}^{\text{R}})_3$ , where  $\text{Ar}^{\text{R}}$  is an aryl substituent ( $\text{Ar}^{\text{R}} = 3,5\text{-(CF}_3)_2\text{C}_6\text{H}_3$ , Ph, and 3,5- $\text{Me}_2\text{C}_6\text{H}_3$ ).<sup>67</sup> The tripodal amido phosphine ligands  $P(\text{CH}_2\text{NHA}^{\text{R}})_3$  stabilize early transition metals to produce mononuclear early transition metal complexes, which are suitable for the facile synthesis of polynuclear or heterometallic complexes.<sup>42, 68, 69</sup> These studies show that 3-fold-symmetrical tripodal amido ligands containing variable backbones display different properties and have been utilized to activate and stabilize different species and molecules.

### 1.5 Scope of this Thesis

The long-term goals of our research of amido ligand designs are to develop the synthetic methodology to prepare polynuclear clusters and polymers with ligand-metal units. In this thesis, we focus on the study of the tripodal amido phosphine ligands  $P(\text{CH}_2\text{NHA}^{\text{R}})_3$ .

This thesis is divided into five chapters aside from the introduction in Chapter one. The tripodal amido ligands  $[P(\text{CH}_2\text{NHA}^{\text{R}})_3]$  studied in Chapter 2 were originally designed for mononuclear early transition metal complexes. These mononuclear early transition metal complexes are used as building blocks to synthesize early-late polynuclear or heterobimetallic complexes. The phosphine ligand cannot bind its lone pair to the early transition metals chelated by the amido donors, but it is well situated

to bind to the late transition metal complexes. These ligands have been demonstrated to be well suited for the synthesis of early-late transition metal heterobimetallic complexes. Chapter 2 also describes the preparation of a Ni(II) dimer with a bridging diamido-phosphido ligand by cleavage P-C bond of phosphine ligand  $P(CH_2NPh)_3$ , which is accompanied with the loss of one  $-CH_2NPh$  arm. This type of the Ni(II) dimer with the bridging diamido-phosphido ligand has been used as a ligand to give early-late transition tetranuclear heterometallic complexes.

In Chapter 3, we use mononuclear tripodal amido Ti and Zr complexes to synthesize the bridged binuclear complexes and test the synthetic feasibility of preparing polymers using the diamagnetic early transition metals zirconium and titanium complexes.

In Chapter 4, the ligands  $Se=P(CH_2NAr^R)_3$  are described. These ligands provide a facile synthetic methodology to triangular trinuclear or tetranuclear complexes of the unanticipated diamidoselenophosphinito ligands by cleavage of a P-C bond, where  $Ar^R = 3,5-(CF_3)_2C_6H_3$ , Ph, and  $3,5-Me_2C_6H_3$ . Comparing the reactions with free ligand precursors  $P(CH_2NAr^R)_3$ , only the dinuclear aluminum complexes  $P(CH_2NAr^R)_3Al_2Me_3$  or trinuclear complexes  $Me_3Al \cdot P(CH_2NAr^R)_3Al_2Me_3$  are produced without P-C bond cleavage. These polydentate amido ligands combined with phosphine donor and selenium donor functionalities are demonstrated to be suitable to synthesize polynuclear main group metal complexes.

Chapter 5 discusses the coordination chemistry of the corresponding phosphine selenides with magnesium and zirconium metal compounds. When the phosphine selenide  $Se=P[CH_2NH-3,5-(CF_3)_2C_6H_3]_3$  reacts with *n*-butylmagnesium, both the P-C bond and the Se=P bond cleave easily to form a P-P bond and produce a binuclear magnesium complex bridged by a biamido bisphosphine ligand. By-products are

characterized and believed to include elemental selenium, n-butyl diselenolate salt or n-butyl selenolate salt, depending on the amount of  $n\text{-Bu}_2\text{Mg}$  added to the solution of  $\text{Se}=\text{P}[\text{CH}_2\text{NH}-3,5\text{-(CF}_3)_2\text{C}_6\text{H}_3]_3$ .  $\text{Se}[\text{P}(\text{CH}_2\text{NAr}^{\text{R}})_3]$  can also be reduced to produce mononuclear zirconium complexes  $[\text{P}(\text{CH}_2\text{NAr}^{\text{R}})_2\text{SeZrNAr}^{\text{R}}\text{CH}_2\text{NEt}_2]$  by P-C bond cleavage, where  $\text{Ar}^{\text{R}} = \text{Ph}$ , and  $3,5\text{-Me}_2\text{C}_6\text{H}_3$ .

Chapter 6 presents some possible future research of ligand designs for polymers and assemblies of metals with specific molecular properties.

## 1.6 References

1. Kempe, R. *Angew. Chem. Int. Ed.* **2000**, 39, 468-493.
2. Tandura, S. N.; Shumsky, A. N.; Ugrak, B. I.; Negrebetsky, V. V.; Bylikin, S. Y.; Kolesnikov, S. P. *Organometallics* **2005**, 24, (22), 5227-5240.
3. Cuevas, J. V.; Garcia-Herbosa, G.; Munoz, A.; Garcia-Granda, S.; Miguel, D. *Organometallics* **1997**, 16, (10), 2220-2222.
4. Parris, C. L.; Christenson, R. M. *J. Organomet. Chem.* **1960**, 25, 1888-1893.
5. Gade, L. H. *J. Organomet. Chem.* **2002**, 661, 85-94.
6. Gade, L. H. *Chem. Commun.* **2000**, (3), 173-181.
7. Gade, L. H. *Acc. Chem. Res.* **2002**, 35, (7), 575-582.
8. Lutz, M.; Findeis, B.; Haukka, M.; Pakkanen, T. A.; Gade, L. H. *Organometallics* **2001**, 20, (12), 2505-2509.
9. Findeis, B.; Gade, L. H.; Scowen, I. J.; McPartlin, M. *Inorg. Chem.* **1997**, 36, (6), 960-961.
10. Contel, M.; Hellmann, K. W.; Gade, L. H.; Scowen, I. J.; McPartlin, M.; Laguna, M. *Inorg. Chem.* **1996**, 35, (12), 3713-3715.

11. Findeis, B.; Contel, M.; Gade, L. H.; Laguna, M.; Gimeno, M. C.; Scowen, I. J.; McPartlin, M. *Inorg. Chem.* **1997**, 36, (11), 2386-2390.
12. Konrad W. Hellmann, L. H. G. A. S. D. S. F. M. *Angew. Chem. Int. Ed.* **1997**, 36, 160-163.
13. Stefan Friedrich, H. M. L. H. G. W.-S. L. M. M. *Angew. Chem. Int. Ed.* **1994**, 33, 676-678.
14. Korendovych Ivan, V.; Staples Richard, J.; Reiff William, M.; Rybak-Akimova Elena, V. *Inorg. Chem.* **2004**, 43, (13), 3930-3941.
15. Rivas Juan, C. M.; Salvagni, E.; Prabakaran, R.; de Rosales Rafael Torres, M.; Parsons, S. *Dalton Trans.* **2004**, (1), 172-177.
16. Olsher, U.; Elgavish, G. A.; Jagur-Grodzinski, J. *J. Am. Chem. Soc.* **1980**, 102, (10), 3338-3845.
17. Ravindar, V.; Lingaiah, P.; Reddy, K. V. *Inorg. Chim. Acta* **1984**, 87, (1), 35-40.
18. Korendovych, I. V.; Staples, R. J.; Reiff, W. M.; Rybak-Akimova, E. V. *Inorg. Chem.* **2004**, 43, (13), 3930-3941.
19. Desmangles, N.; Jenkins, H.; Rupp, K. B.; Gambarotta, S. *Inorg. Chim. Acta* **1996**, 250, (1-2), 1-4.
20. Memmler, H.; Gade, L. H.; Lauher, J. W. *Inorg. Chem.* **1994**, 33, (14), 3064-3071.
21. Hellmann, K. W.; Steinert, P.; Gade, L. H. *Inorg. Chem.* **1994**, 33, (18), 3859-3860.
22. Hellmann, K. W.; Gade, L. H.; Li, W.-S.; McPartlin, M. *Inorg. Chem.* **1994**, 33, (25), 5974-5977.

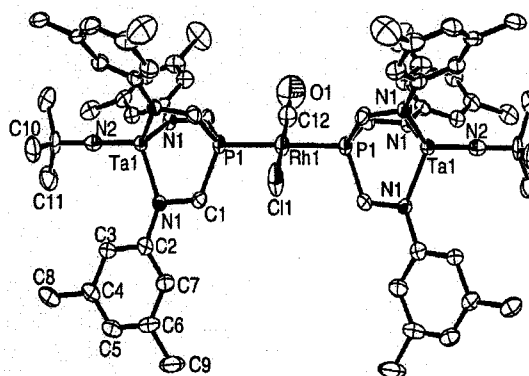
23. Beer, P. D.; Hopkins, P. K.; McKinney, J. D. *Chem. Commun.* **1999**, (13), 1253-1254.
24. Renner, P.; Galka, C.; Memmler, H.; Kauper, U.; Gade, L. H. *J. Organomet. Chem.* **1999**, 591, (1-2), 71-77.
25. Gade, L. H.; Memmler, H.; Kauper, U.; Schneider, A.; Fabre, S.; Bezougli, I.; Lutz, M.; Galka, C.; Scowen, I. J.; McPartlin, M. *Chem. Eur. J.* **2000**, 6, (4), 692-708.
26. Ballester, P.; Capo, M.; Costa, A.; Deya, P. M.; Gomila, R.; Decken, A.; Deslongchamps, G. *Org. Lett.* **2001**, 3, (2), 267-270.
27. Gade, L. H.; Renner, P.; Memmler, H.; Fecher, F.; Galka, C. H.; Laubender, M.; Radojevic, S.; McPartlin, M.; Lauher, J. W. *Chem. Eur. J.* **2001**, 7, (12), 2563-2580.
28. Ho, J.; Stephan, D. W. *Inorg. Chem.* **1994**, 33, (20), 4595-4597.
29. Turculet, L.; Tilley, T. D. *Organometallics* **2002**, 21, (19), 3961-3972.
30. Porter, R. M.; Danopoulos, A. A. *Dalton Trans.* **2004**, (16), 2556-2562.
31. Zhu, H.; Chen, E. Y. X. *Inorg. Chem.* **2007**, 46, (4), 1481-1487.
32. Memmler, H.; Kauper, U.; Gade, L. H.; Stalke, D.; Lauher, J. W. *Organometallics* **1996**, 15, (17), 3637-3639.
33. Friedrich, S.; Memmler, H.; Gade, L. H.; Li, W. S.; Scowen, I. J.; McPartlin, M.; Housecroft, C. E. *Inorg. Chem.* **1996**, 35, (9), 2433-2441.
34. Hultsch, K. C.; Spaniol, T. P.; Okuda, J. *Organometallics* **1997**, 16, (22), 4845-4856.
35. Friedrich, S.; Gade, L. H.; Scowen, I. J.; McPartlin, M. *Angew. Chem. Int. Ed.* **1996**, 35, (12), 1338-1341.
36. Friedrich, S.; Memmler, H.; Gade, L. H.; Li, W.-S.; Scowen, I. J.; McPartlin, M.; Housecroft, C. E. *Inorg. Chem.* **1996**, 35, (9), 2433-2441.

37. Findeis, B.; Schubart, M.; Platzek, C.; Gade, L. H.; Scowen, I.; McPartlin, M. *Chem. Commun.* **1996**, (2), 219-220.
38. Friedrich, S.; Gade, L. H.; Scowen, I. J.; McPartlin, M. *Organometallics* **1995**, 14, (11), 5344-5349.
39. Hitchcock, P. B.; Jang, E.; Lappert, M. F. *J. Chem. Soc. Dalton Trans.* **1995**, (19), 3179-3187.
40. Schneider, A.; Gade, L. H.; Breuning, M.; Bringmann, G.; Scowen, I. J.; McPartlin, M. *Organometallics* **1998**, 17, (9), 1643-1645.
41. Chen, J.; Woo, L. K. *J. Organomet. Chem.* **2000**, 601, (1), 57-68.
42. Klaui, W.; Hardt, T. *J. Organomet. Chem.* **1998**, 553, (1-2), 241-251.
43. Lutz H. Gade. *Chem. A. Eur. J.* **2000**, 6, (4), 692-708.
44. Stokes, S. L.; Davis, W. M.; Odom, A. L.; Cummins, C. C. *Organometallics* **1996**, 15, (21), 4521-4530.
45. Siedle, A. R.; Newmark, R. A.; Lamanna, W. M.; Huffman, J. C. *Organometallics* **1993**, 12, (5), 1491-1492.
46. Karl, J.; Erker, G.; Frohlich, R. *J. Am. Chem. Soc.* **1997**, 119, (46), 11165-11173.
47. Turculet, L.; Tilley, T. D. *Organometallics* **2004**, 23, (7), 1542-1553.
48. Schrock, R. R. *Acc. Chem. Res.* **1997**, 30, 9-16.
49. Cummins, C. C.; Schrock, R. R.; Davis, W. M. *Inorg. Chem.* **1994**, 33, (7), 1448-1457.
50. Freundlich, J. S.; Schrock, R. R.; Davis, W. M. *J. Am. Chem. Soc.* **1996**, 118, (15), 3643-3655.
51. Freundlich, J. S.; Schrock, R. R.; Davis, W. M. *Organometallics* **1996**, 15, (12), 2777-2783.

52. Johnson-Carr, J. A.; Zanetti, N. C.; Schrock, R. R.; Hopkins, M. D. *J. Am. Chem. Soc.* **1996**, 118, (45), 11305-11306.
53. Schrock, R. R.; Cummins, C. C.; Wilhelm, T.; Lin, S.; Reid, S. M.; Kol, M.; Davis, W. M. *Organometallics* **1996**, 15, (5), 1470-1476.
54. Nomura, K.; Schrock, R. R. *Inorg. Chem.* **1996**, 35, (12), 3695-3701.
55. Neuner, B.; Schrock, R. R. *Organometallics* **1996**, 15, (1), 5-6.
56. Lee, L.; Berg, D. J.; Bushnell, G. W. *Organometallics* **1995**, 14, (11), 5021-5023.
57. Lee, L.; Berg, D. J.; Bushnell, G. W. *Organometallics* **1995**, 14, (1), 8-10.
58. Braunstein, P.; Naud, F. *Angew. Chem. Int. Ed.* **2001**, 40, (4), 680-699.
59. Martinez, A. P.; Garcia, M. P.; Lahoz, F. J.; Oro, L. A. *Inorg. Chim. Acta* **2003**, 347, 86-98.
60. Romeo, R.; Scolaro, L. M.; Plutino, M. R.; Romeo, A.; Nicolo, F.; Del Zotto, A. *Eur. J. Inorg. Chem.* **2002**, (3), 629-638.
61. Kashiwabara, K.; Taguchi, N.; Takagi, H. D.; Nakajima, K.; Suzuki, T. *Polyhedron* **1998**, 17, (11-12), 1817-1829.
62. Hessler, A.; Fischer, J.; Kucken, S.; Stelzer, O. *Chem. Ber.* **1994**, 127, (3), 481-488.
63. Bressan, M.; Bonuzzi, C.; Morandini, F.; Morvillo, A. *Inorg. Chim. Acta.* **1991**, 182, (2), 153-156.
64. Grotjahn Douglas, B.; Gong, Y.; Zakharov, L.; Golen James, A.; Rheingold Arnold, L. *J. Am. Chem. Soc.* **2006**, 128, (2), 438-453.
65. Frank, A. W. D. G. L. Jr. *J. Org. Chem.* **1972**, 37, 2752-2755.
66. Kohl, S. W.; Heinemann, F. W.; Hummert, M.; Bauer, W.; Grohmann, A. *Chem. Eur. J.* **2006**, 12, (16), 4313-4320.

67. Gade, L. H. *Acc. Chem. Res.* **2002**, 35, (7), 575-582.
68. Gade, L. H. *J. Organomet. Chem.* **2002**, 661, (1-2), 85-94.

Chapter Two



**Diligating Tripodal Amido-Phosphine Ligands for Heterometallic Complexes**

**2.1 Introduction**

Due to the ability of adjacent metals to cooperatively activate substrates,<sup>1,2</sup> the chemistry of polynuclear and heterobimetallic clusters has been of interest to chemists.<sup>3-8</sup> In biological systems, clusters of metals can assist in the transfer of

electrons to activate relatively inert substrates.<sup>9,10</sup> More recently, rational cluster synthesis has been used for the tuning of physical properties, such as single-molecule magnetism,<sup>11,12</sup> and early-late heterobimetallics have been used to synthesize unusual molecular architectures via self-assembly.<sup>13-16</sup>

In order to synthesize polynuclear and heterobimetallic complexes, the ligands designs must exhibit coordinative flexibility by being able to chelate both early and late transition metals. Here, we report the ligands of the type  $P(\text{CH}_2\text{NHA}^{\text{R}})_3$ , where  $\text{Ar}^{\text{R}} = 3,5\text{-(CF}_3)_2\text{C}_6\text{H}_3$ , Ph, and  $3,5\text{-Me}_2\text{C}_6\text{H}_3$ . These polydentate ligands combine a tripodal arrangement of amido donors with a phosphine donor functionality, extending these tripodal amido ligand systems to the hybrid ligand systems that contain significantly different chemical functionalities, increasing their use in molecular chemistry.<sup>17,18</sup> It is anticipated that with a high oxidation state early transition metal, the ligand  $P(\text{CH}_2\text{NHA}^{\text{R}})_3$  will adopt the bonding mode as shown in Figure 2.1.<sup>19-21</sup> In this bonding mode the phosphine ligand cannot bind its lone pair to the early transition metals chelated by the amido donors, but is well situated to bind to a second metal complex.

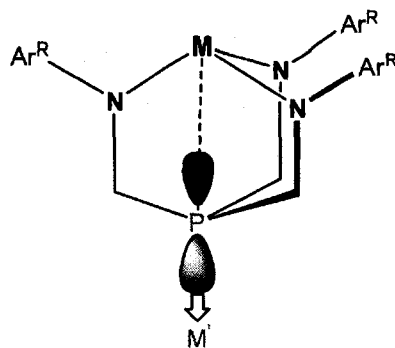


**Figure 2.1.** Potential binding mode of the  $P(\text{CH}_2\text{NHA}r^R)_3$  ligands to an early transition metal fragment (shown as M) and a second metal complex (shown as M'), along with an illustration of the major and minor lobes of the lone pair orbital on phosphorus, where  $\text{Ar}^R = 3,5\text{-(CF}_3)_2\text{C}_6\text{H}_3$ , Ph, and  $3,5\text{-Me}_2\text{C}_6\text{H}_3$ .

The nature of early transition metals M could have a significant effect on the chemistry of M' for several reasons. Firstly, the size of M could significantly alter the donor properties of the phosphine donor, because the C-P-C angles presumably increase upon the chelation of a large transition metal. Large and strained C-P-C bond angles greatly affect the donor abilities of phosphines. For example, the remarkably strong  $\sigma$ -donor properties of  $t\text{Bu}_3\text{P}$  relative to other alkyl phosphines are partly attributed to the large C-P-C angles.<sup>30</sup> Secondly, a direct through-space interaction between M and the minor lobe of the lone-pair orbital could allow for communication between metal centres due to the P-M distances being significantly shorter than the sum of van der Waals radii. Such an interaction could mitigate the transfer of electrons between metals in complexes of this type, or facilitate magnetic coupling between the metals in paramagnetic complexes.

The effect of the early transition metal M on the donor ability of the phosphine ligand can be determined by the preparation of the bis-phosphine complexes *trans*-L<sub>2</sub>Rh(CO)Cl, prepared by the reactions of the appropriate phosphines with [Rh(CO)<sub>2</sub>(μ-Cl)]<sub>2</sub>, and by a measurement of the resultant CO stretching frequencies. A more electron-donating ligand produces a more electron-rich metal center that is able to backbond to a bound carbonyl more effectively. It results in greater electron density in the carbonyl π\* orbitals. The decreasing C-O bond order may be reflected by the lowering C-O stretching frequency in the infrared spectrum. For more electron-poor ligands and less electron-rich metal centers, an increase in the C-O stretching frequency can be predicted. Thus, for a series of ligands substituted with electron-donating or electron-withdrawing groups, a trend may be observed that correlates the C-O stretching frequency with the electron-donating ligand.

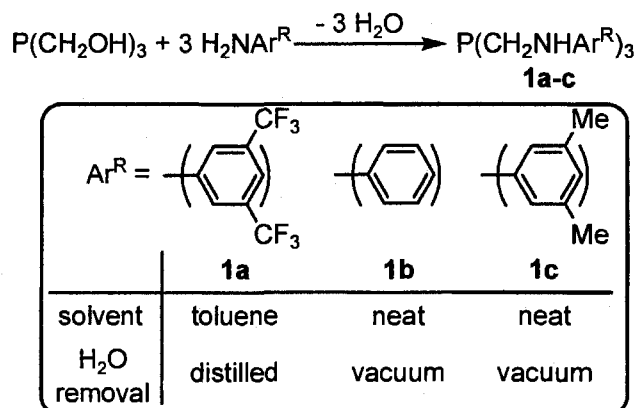
Herein we report a study that demonstrates the ability of these ligands to coordinate and stabilize early transition metals as building blocks to prepare early-late heterobimetallic and polynuclear complexes, and an investigation of the effect of the amido donors and early transition metal centres on the properties of the phosphine donors.

## 2.2 Syntheses of the Ligand Precursors P(CH<sub>2</sub>NHAr<sup>R</sup>)<sub>3</sub> (1a-1c, where Ar<sup>R</sup> = 3,5-(CF<sub>3</sub>)<sub>2</sub>C<sub>6</sub>H<sub>3</sub>, Ph, and 3,5-Me<sub>2</sub>C<sub>6</sub>H<sub>3</sub>)

The reactions of P(CH<sub>2</sub>OH)<sub>3</sub> with the appropriate aniline produce the ligand precursors P[CH<sub>2</sub>NH-3,5-(CF<sub>3</sub>)<sub>2</sub>C<sub>6</sub>H<sub>3</sub>]<sub>3</sub> (1a), P(CH<sub>2</sub>NHPh)<sub>3</sub> (1b) and

$\text{P}(\text{CH}_2\text{NH}-3,5\text{-Me}_2\text{C}_6\text{H}_3)$  (**1c**), as shown in Scheme 2.1.<sup>18</sup> As previously reported for **1b**,<sup>22</sup> this reaction can be performed in toluene and water can be removed by azeotropic distillation using a Dean-Stark apparatus, which requires the use of an excess (5 equiv) of aniline. We found that the reaction can be performed neat, with use the dynamic vacuum to remove the resultant water. The reaction occurred over 30 min and was exothermic. This procedure worked well with a stoichiometric amount of aniline, which simplified the purification procedure. The product is analytically pure when prepared in this manner, though it is easily crystallized from a saturated warm toluene solution by cooling to  $-40\text{ }^\circ\text{C}$ . A solvent free procedure also worked well using 3,5-dimethylaniline to produce **1c**, however, using 3,5-bis(trifluoromethyl)aniline resulted in no reaction. It was therefore necessary to use the original procedure with toluene as the solvent and a Dean-Stark apparatus to remove water to obtain **1a**. For simplicity, these ligand precursors will be abbreviated herein as  $[\text{P}(\text{CH}_2\text{NHAr}^{\text{R}})_3]$ , where  $\text{Ar}^{\text{R}} = 3,5\text{-(CF}_3)_2\text{C}_6\text{H}_3$ , Ph, and  $3,5\text{-Me}_2\text{C}_6\text{H}_3$ , for **a**, **b**, and **c**, respectively. Ligands **1a-c** oxidize slowly in air, and are not particularly moisture sensitive, although they were stored under a dry nitrogen atmosphere.

## Scheme 2.1.



Compounds **1b** and **1c** both crystallized as thin plates unsuitable for Crystallographic studies; however, crystals of **1a** suitable for X-ray diffraction were obtained by slow evaporation of a toluene solution. An ORTEP depiction of the solid-state structure obtained at 133 K is shown in Figure 2.2. Unfortunately, this structure suffers slightly from disorder of one of the ligand arms and rotational disorder of a majority of the CF<sub>3</sub> substituents. The C(1)-P(1)-C(2), C(1)-P(1)-C(3), and C(2)-P(1)-C(3) angles for the free ligand precursor **1c** are 99.48(11)°, 99.38(15)°, and 100.59(16)°, respectively, for a sum of 299.5(2)°; this value is fairly typical for phosphine donors, whose C-P-C angles are invariably much less than the tetrahedral angle of 109.5°. This change in sum of C-P-C angles will be used to evaluate the effects of complexation of early transition metals to the amido donors on the phosphine donor (*vide infra*).<sup>30</sup>

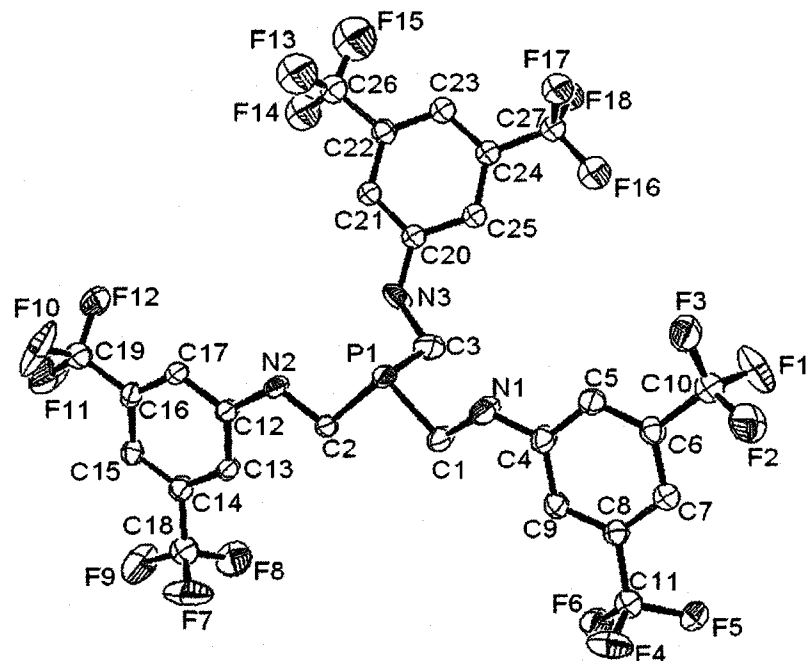
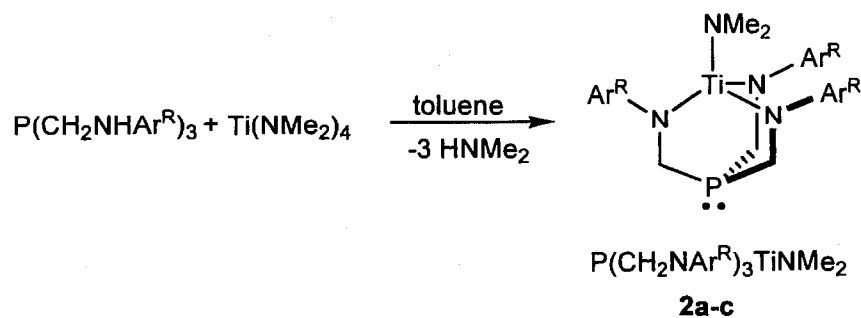


**Figure 2.2** ORTEP depiction of the solid-state structure of **1a** as determined by X-ray crystallography. Selected bond angles (deg): C(1)-P(1)-C(2), 99.48(11); C(1)-P(1)-C(3), 99.38(15); C(2)-P(1)-C(3), 100.59(16); P(1)-C(1)-N(1), 107.99(18); P(1)-C(2)-N(2), 107.79(16); C(1)-N(1)-C(4), 123.7(2); C(2)-N(2)-C(12), 120.95(19).

### 2.3 Syntheses of the Mononuclear Titanium Complexes $P(CH_2NAr^R)_3TiNMe_2$

(**2a-c**)

#### Scheme 2.2



The treatments of **1a-c** with  $\text{Ti}(\text{NMe}_2)_4$  in toluene prepare mononuclear titanium complexes  $\text{P}(\text{CH}_2\text{NAr}^{\text{R}})_3\text{TiNMe}_2$ , **2a-c**, as shown in Scheme 2.2. These reactions require 12-24 h to go to completion and no intermediates were observed by  $^1\text{H}$  or  $^{31}\text{P}\{^1\text{H}\}$  NMR spectroscopy. The resultant products are all obtained in high yields as the thermally-stable dark-red crystalline solids.

The solid-state structures of **2a-c** were determined by X-ray crystallography. The ORTEP depiction of the solid-state molecular structure of **2b** is shown in Figure 2.3; a comparison of the bond lengths and angles with those of **2a** and **2c** (Table 2.1) revealed little variation, although the quality of the structure of **2c** was hampered by the tendency of this compound to crystallize as nonmerohedral twins. As anticipated, in all three structures the tripodal ligand chelates via three amido donors, and the lone-pair of the phosphine donor is directed away from the metal centre.

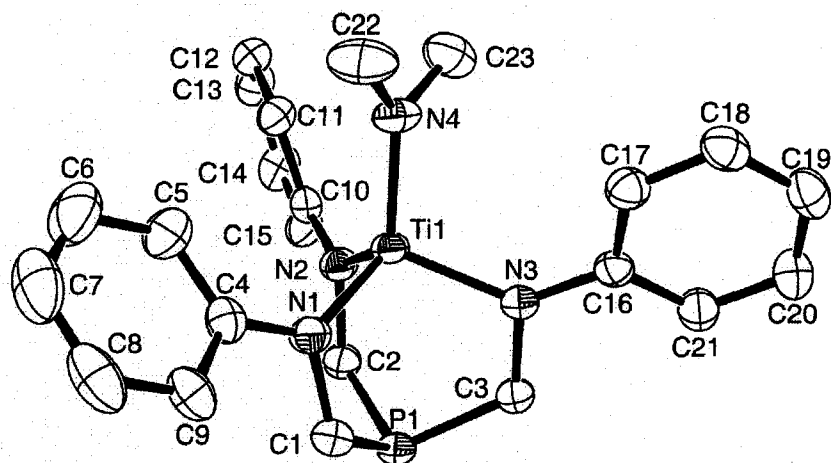


**Figure 2.3.** Solid-state molecular structure of **2b** as determined by X-ray crystallography. Hydrogen atoms are omitted for clarity. Selected distances (Å): Ti(1)···P(1), 2.9895(4); Ti(1)-N(1), 1.9239(11); Ti(1)-N(2), 1.9327(11); Ti(1)-N(3), 1.9424(11); Ti(1)-N(4), 1.8643(12). Selected bond angles (deg): C(1)-P(1)-C(2), 105.85(6); C(1)-P(1)-C(3), 102.64(6); C(2)-P(1)-C(3), 102.89(6); Ti(1)-N(4)-C(22), 130.95(11); Ti(1)-N(4)-C(23), 115.22(10); Ti(1)-N(1)-C(1), 109.48(8); Ti(1)-N(1)-C(4), 132.54(9); Ti(1)-N(2)-C(2), 108.78(8); Ti(1)-N(2)-C(10), 133.75(9); Ti(1)-N(3)-C(3), 109.80(8); Ti(1)-N(3)-C(16), 134.33(9); P(1)-C(1)-N(1), 116.64(9); P(1)-C(2)-N(2), 118.59(9); P(1)-C(3)-N(3), 117.06(9); C(1)-N(1)-C(4), 117.13(11); C(2)-N(2)-C(10), 117.47(11); C(3)-N(3)-C(16), 115.74(10).

**Table 2.1.** Selected distances (Å) and bond angles (deg) for compounds **2a**, **2b** and **2c**

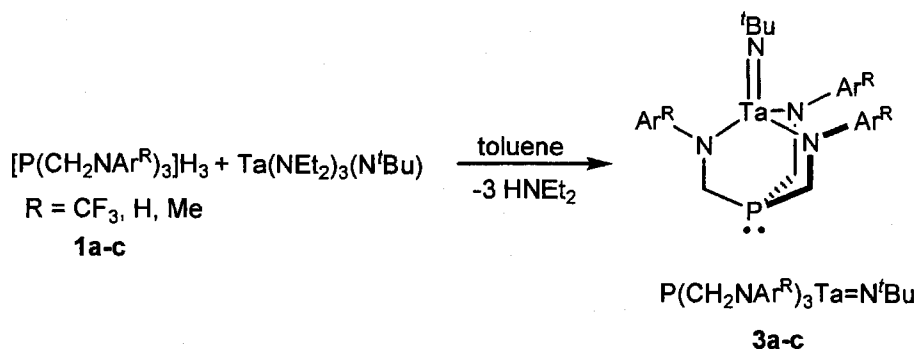
	<b>2a</b>	<b>2b</b>	<b>2c</b>
Ti(1)---P(1)	2.9963(10)	2.9895(4)	3.019(4)
Ti(1)-N(1)	1.944(3)	1.9239(11)	1.963(7)
Ti(1)-N(2)	1.915(3)	1.9327(11)	1.941(6)
Ti(1)-N(3)	1.946(3)	1.9424(11)	1.934(6)
Ti(1)-N(4)	1.862(3)	1.8643(12)	1.879(6)
C(1)-P(1)-C(2)	104.13(17)	105.85(6)	103.3(4)
C(1)-P(1)-C(3)	101.91(17)	102.64(6)	102.6(4)
C(2)-P(1)-C(3)	105.53(16)	102.89(6)	105.6(4)

Some measurements of the hybridization change at the phosphine donor are provided by a comparison of the C-P-C angles before and after the introduction of a transition metal to the triamido chelate provides, which should affect its donor properties. In **2b**, the sum of C-P-C angles is 311.4(1)° compared to 299.5(2)° in **1a**, which is a significant change. Although the phosphine donor is hybridized so that the lone-pair is formally directed away from the early transition metal, the binding of the ligand enforces P...Ti distances that are under the sum of the Van der Waals radii of these elements.<sup>23</sup> For **2b**, the P...Ti distance is 2.9895(4) Å, and is only ~6% larger than the longest reported phosphine-titanium bond length of 2.813(1) Å,<sup>24</sup> although Ti-P bond distances are more typically 2.6-2.7 Å.

Despite the fact that the phosphine lone-pair is not coordinated to the early transition metal center, the  $^{31}\text{P}\{^1\text{H}\}$  NMR shifts are strongly affected by the coordination of a transition metal to the amido donors. A small range of chemical shifts are observed for the free ligands, by  $^{31}\text{P}\{^1\text{H}\}$  NMR spectroscopy:  $\delta$  -32.6, -31.0, and -29.6 for **1a-c**, respectively. In **2a-c** both the shifts and the range covered are vastly different, with shifts of  $\delta$  -79.9, -65.6, and -61.6, respectively. The shift upfield for **2a-c** compared to their ligand precursors was unexpected; an increase in C-P-C angle usually leads to a significant shift to downfield. For example, the opposite trend of chemical shifts and C-P-C angle is observed for the alkyl phosphines  $\text{PMe}_3$ ,  $\text{PEt}_3$ , and  $\text{P}^t\text{Bu}_3$ , whose  $^{31}\text{P}$  shifts are  $\delta$  -62, -20, and +63, respectively.<sup>25,31</sup> The  $^{31}\text{P}$  NMR shifts is complex, however, these results indicate that the phosphorus donor may be directly affected by its proximity to the chelated early transition metal.

#### **2.4 Syntheses of the Mononuclear Tantalum Complexes $\text{P}(\text{CH}_2\text{NAr}^R)_3\text{Ta}=\text{N}^t\text{Bu}$ (**3a-c**)**

## Scheme 2.3



The reactions of **1a-c** with  $\text{Ta(NEt}_2\text{)}_3\text{(N}^t\text{Bu)}$  cleanly produced the tantalum imido complexes  $\text{P(CH}_2\text{NAr}^{\text{R}}\text{)}_3\text{Ta=N}^t\text{Bu}$ , **3a-c**, as shown in Scheme 2.3. The products were obtained in high yields as yellow crystalline solids. The solid-state structure of **3b** was determined by X-ray crystallography. The  $^1\text{H}$  NMR spectra of **3a-c** are consistent with apparent  $C_{3v}$  symmetry. The solid-state structure of **3b** was determined by X-ray crystallography, and an ORTEP depiction of the solid-state molecular structure of **3b** is shown in Figure 2.4. As with complexes **2a-c** the triamido donors chelate to the early transition metal, and the phosphine lone-pair is directed away from the Ta centre. The C-P-C angles for **3b** are larger than those in the titanium complexes **2a-c**, with a sum of C-P-C angles of  $315.0(2)^\circ$ . The chelation of a metal requires an increase in the bond angles at P, with the greater increase for the larger metal, Ta, although this difference is more than expected, considering the relatively small difference between the size of Ti and Ta. Despite the slightly larger size of Ta, the P $\cdots$ Ta distance in **3b** is  $2.9548(6)$  Å, which is shorter than the P $\cdots$ Ti distance in **2b**, and only 3.5 % longer than the longest reported phosphine-tantalum

bond length of 2.855 Å.<sup>26</sup>

The changes in <sup>31</sup>P NMR shifts of **1a-c** upon coordination of the amido donors to tantalum are more dramatic than those observed for titanium, though the range of observed shifts is smaller, with shifts of  $\delta$  -108.5, -100.9, and -100.1 for complexes **3a-c**, respectively. Contrary to what might be expected, the trend of phosphorus shifts for the free ligand, Ti, and Ta complexes seems to indicate that the phosphine donors are becoming poorer donors with increasing C-P-C angle; however, it is difficult to be certain that the changes in chemical shift truly represent a reduced donor ability of the phosphine donor.

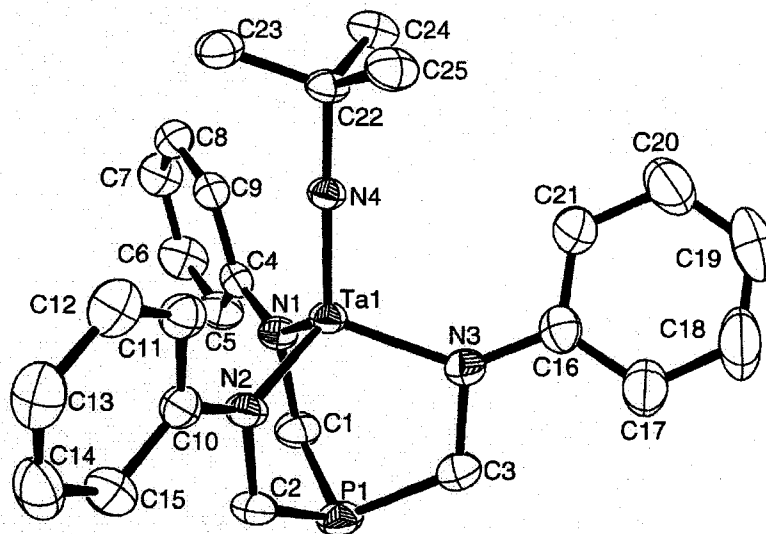


**Figure 2.4.** Solid-state molecular structure of **3b** as determined by X-ray crystallography. Hydrogen atoms are omitted for clarity. Selected distances (Å): Ta(1)···P(1), 2.9548(6); Ta(1)-N(1), 2.004(2); Ta(1)-N(2), 1.998(2); Ta(1)-N(3), 1.990(2); Ta(1)-N(4), 1.7682(18). Selected bond angles (deg): C(1)-P(1)-C(2), 103.91(13); C(1)-P(1)-C(3), 105.77(12); C(2)-P(1)-C(3), 105.27(12); Ta(1)-N(1)-C(1), 105.77(15); Ta(1)-N(1)-C(4), 137.42(15); C(1)-N(1)-C(4), 116.8(2); Ta(1)-N(2)-C(2), 105.27(15); Ta(1)-N(2)-C(10), 138.42(16); C(2)-N(2)-C(10), 116.3(2); Ta(1)-N(3)-C(16), 135.96(17).

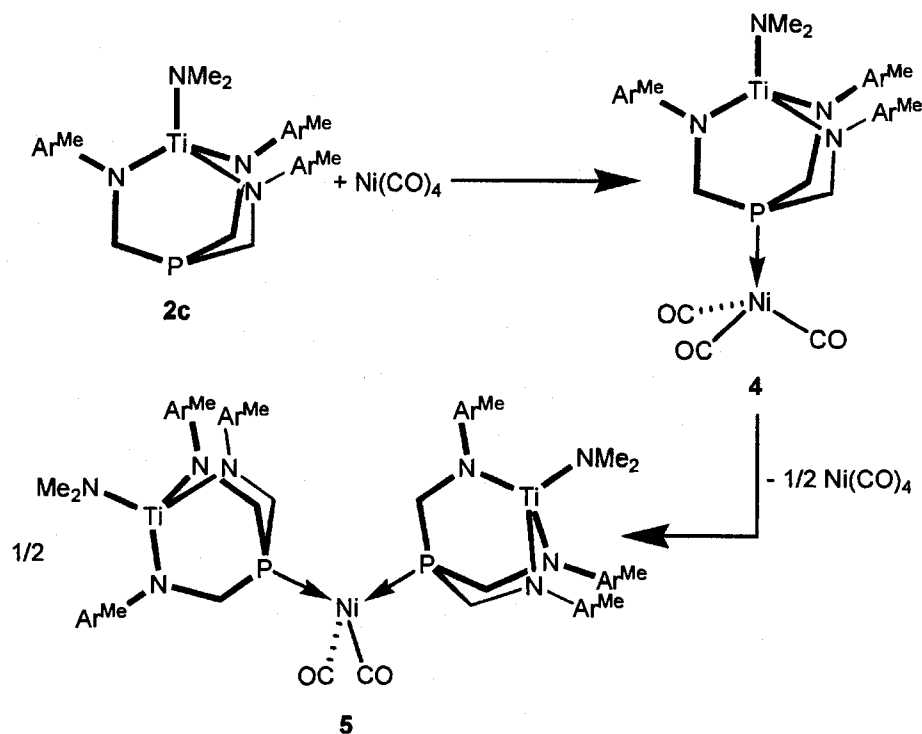
## 2.5 Mononuclear Titanium and Tantalum Complexes as Building Blocks for Heterometallic Early-Late Transition Metal Complexes

The mononuclear titanium compound  $P(\text{CH}_2\text{NAr}^R)_3\text{TiNMe}_2$  **2c** ( $\text{Ar}^R = 3,5\text{-Me}_2\text{C}_6\text{H}_3$ ) reacted instantaneously with excess  $\text{Ni}(\text{CO})_4$  to afford, a single product, which was determined to be  $(\text{CO})_3\text{Ni}[P(\text{CH}_2\text{N-}3,5\text{-Me}_2\text{C}_6\text{H}_3)_3\text{TiNMe}_2]$  (**4**),

as assessed by  $^1\text{H}$ ,  $^{13}\text{C}\{^1\text{H}\}$  and  $^{31}\text{P}\{^1\text{H}\}$  NMR spectroscopy. The coordination of phosphorus to nickel is accompanied by a large  $^{31}\text{P}\{^1\text{H}\}$  NMR shift from  $\delta$  -61.6 in **2c** to  $\delta$  4.1,<sup>27</sup> and the  $^{13}\text{C}\{^1\text{H}\}$  carbonyl carbon resonance at  $\delta$  196.3, which is doublet with a typical  $^2J_{\text{PC}}$  value of 1.1 Hz,<sup>28</sup> confirms the coordination of a single phosphine donor.

Compound **4** is not stable at room temperature, and the solution undergoes ligand redistribution over the course of 48 h to form over 50 %  $(\text{CO})_2\text{Ni}[\text{P}(\text{CH}_2\text{N}-3,5\text{-Me}_2\text{C}_6\text{H}_3)_3\text{TiNMe}_2]_2$ , **5**, presumably with loss of  $\text{Ni}(\text{CO})_4$ . This reaction sequence is depicted in Scheme 2.4. The  $^{31}\text{P}\{^1\text{H}\}$  NMR spectrum shows an additional peak at  $\delta$  7.0, and the  $^{13}\text{C}\{^1\text{H}\}$  NMR carbonyl resonance is a triplet at  $\delta$  190.0, due to the coupling of two identical phosphorus nuclei. The resonance for the methylene carbon, which is typically a doublet due to a  $^1J_{\text{PC}}$  of around 15 Hz, in this case is a virtual triplet due to the AXX' spin system. Further ligand redistribution appears to occur as the conversion to **5** increases, and results in the formation of an impurity, which is presumably the trisubstituted complex; this makes the high-yield isolation of pure **5** by this procedure difficult. The addition of an additional equivalent of **2b** to a freshly prepared sample of **4** has been proved to be the most effective synthesis of **5**.

## Scheme 2.4



The molecular structure of **5** was determined by single crystal X-ray crystallography and is shown in Figure 2.5. The bonding of the phosphine donor to nickel appears to have minor effects on the structure of the ligand. The  $\text{Ti}(1)\cdots\text{P}(1)$  and  $\text{Ti}(2)\cdots\text{P}(2)$  short contacts are 3.087(5) Å and 3.097(5) Å, respectively, whereas in **2c** a  $\text{Ti}\cdots\text{P}$  distance of 3.015(5) Å was observed. The sums of C-P-C angles for P(1) and P(2) are 307.5(3)° and 306.4(3)°, respectively, which are a slight decrease from 310.5(5)° in **2c**. This result is quite unusual, because the coordination of phosphine donors to metal centres almost invariably results in an increase of C-P-C angles by 3° or 4°.<sup>30-32</sup> Although the absence of an increase in C-P-C angles could be explained by the initial strain on the ligand to accommodate the large Ti metal centre, the decrease in C-P-C angle upon coordination to Ni is not easy to

This compression of C-P-C angles has a considerable effect on the geometry at Ti. The sum of the N(1)-Ti(1)-N(2), N(2)-Ti(1)-N(3) and N(1)-Ti(1)-N(3) angles decreases from 316.4(1)° in **2b** to 304.0(3)° in **5**, both of which deviate considerably from the 328.5° expected for a tetrahedral structure. Examination of the geometry at Ni(1) in the structure of **5** reveals a few points worthy of mention. The P(1)-Ni(1) and P(2)-Ni(1) distances are 2.1835(13) Å and 2.1900(14) Å, respectively, which is approximately 0.1 Å shorter than the average phosphine-nickel bond lengths of 2.28 Å. A direct measurement of the cone angles of these ligands yields a value of 106°, a value larger than estimated from the structure of **2b**; however, this increase is due to the shorter than average Ni-P bond length. The diminutive nature of these phosphines is apparent from the P(1)-Ni(1)-P(2) angle of 104.00(5)°, which is significantly smaller than the tetrahedral angle of 109.5°.

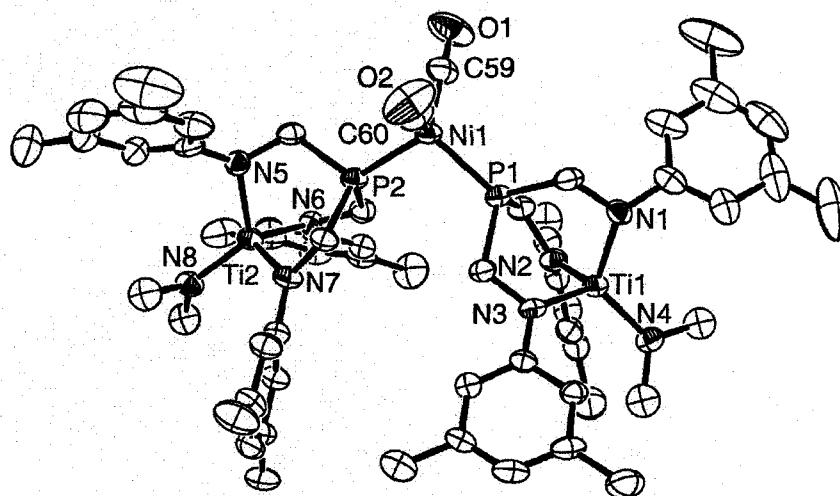
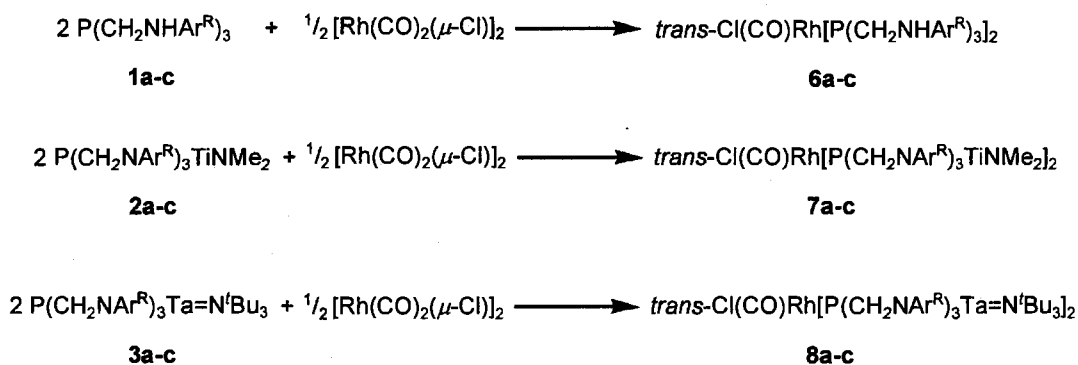


**Figure 2.5.** ORTEP depiction of the solid-state molecular structure of  $(\text{CO})_2\text{Ni}[\text{P}(\text{CH}_2\text{N}-3,5\text{-Me}_2\text{C}_6\text{H}_3)_3\text{TiNMe}_2]_2$  (**5**). Hydrogen atoms are omitted for clarity. Selected distances (Å): P(1)-Ni(1), 2.1835(13); P(2)-Ni(1), 2.1900(14); Ti(1)···P(1), 3.087(5); Ti(2)···P(2), 3.097(5); N(1)-Ti(1), 1.938(4); N(2)-Ti(1), 1.942(4); N(3)-Ti(1), 1.922(4); N(4)-Ti(1), 1.872(4); N(5)-Ti(2), 1.943(4); N(6)-Ti(2), 1.937(4); N(7)-Ti(2), 1.923(4); N(8)-Ti(2), 1.857(4). Selected bond angles (deg): P(1)-Ni(1)-P(2), 104.00(5); C(59)-Ni(1)-C(60), 111.4(2); P(1)-Ni(1)-C(59), 111.22(19); P(1)-N(1)-C(60), 109.96(17); P(2)-Ni(1)-C(59), 110.98(16); P(2)-Ni(1)-C(60), 108.97(19); C(1)-P(1)-C(2), 102.4(2); C(2)-P(1)-C(3), 103.7(2); C(3)-P(1)-C(1), 101.4(2); C(30)-P(2)-C(31), 101.3(2); C(31)-P(2)-C(32), 103.6(2); C(30)-P(2)-C(32), 101.5(2); C(1)-P(1)-Ni(1), 116.31(14); C(2)-P(1)-Ni(1), 116.34(15); C(3)-P(1)-Ni(1), 114.66(15); C(30)-P(2)-Ni(1), 114.98(14); C(31)-P(2)-Ni(1), 117.10(16); C(32)-P(2)-Ni(1), 116.09(15).

The reaction of 4 equiv of most phosphine donors with  $[\text{Rh}(\text{CO})_2(\mu\text{-Cl})]_2$  allows for the facile preparation of *trans*-rhodiumcarbonylchlorobisphosphine complexes.  $^1\text{H}$  and  $^{31}\text{P}\{^1\text{H}\}$  NMR spectroscopy was used to identify the products as the *trans*-rhodiumcarbonylchlorobisphosphine complexes **6a-c**, **7a-c**, and **8a-c** of the phosphines **1a-c**, **2a-c**, and **3a-c**, respectively, as shown in Scheme 2.5. The products were all formed within 20 min of dissolving the reagents in  $\text{CH}_2\text{Cl}_2$ .

### Scheme 2.5



The adduct of mononuclear tantalum compound **3c**, *trans*-Cl(CO)Rh[P(CH<sub>2</sub>NAr<sup>Me</sup>)<sub>3</sub>Ta=N<sup>t</sup>Bu]<sub>2</sub> (**8c**) was isolated and characterized by X-ray crystallography. The solid-state molecular structure of **8c** is shown in Figure 2.6. The crystallographically symmetry imposed in the structure of **8c** is  $C_{3h}$ . There is a three-fold disorder of the carbonyl and chloride ligands; only one location is shown in Figure 2.6. In a projection along the P-Rh-P 3-fold axis, the larger Cl ligand is staggered with respect to the P-CH<sub>2</sub> bonds, whereas the small carbonyl ligand is eclipsed. The sum of C-P-C angles is 319.0(3)°, which is approximately 4° larger

than the sum of C-P-C angles in **3b**; this increase in C-P-C angle is typical for the coordination of phosphine to metal centres, unlike the decrease of C-P-C angle noted previously for complex **5**. As a result, the tantalum centre moves further into the chelating amides compared to the structure of **3b**, and the P(1)···Ta(1) distance of 2.943(2) is 0.012(2) Å shorter than in **3b**, as might be expected considering the larger C-P-C angles. The P(1)···Ta(1) distance in **8c** is only 3.0 % longer than the longest crystallographically characterized tantalum-phosphine bonding interaction.<sup>26</sup>

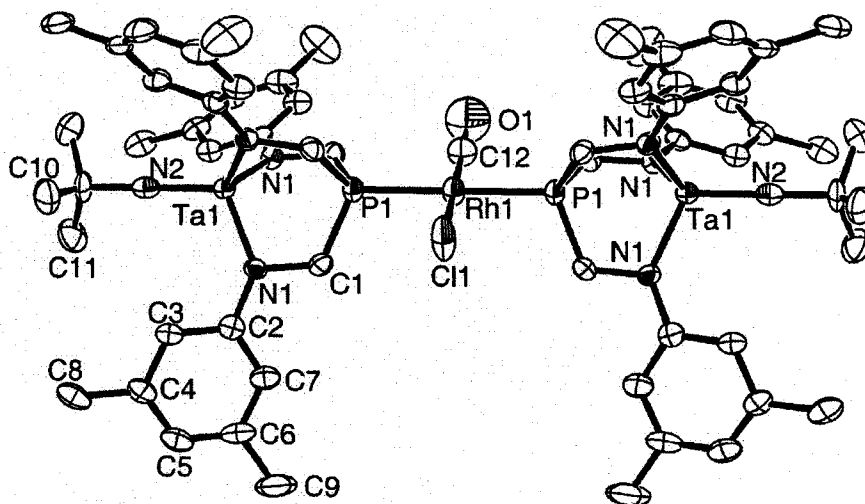


**Figure 2.6.** ORTEP depiction of the solid-state molecular structure of **8c** as determined by X-ray crystallography. Only one pair of the three disordered sites of occupancy of the Cl and CO ligands is shown, and hydrogen atoms are omitted for clarity. Selected distances (Å): P(1)···Ta(1), 2.943(2); N(1)-Ta(1), 1.995(4); N(2)-Ta(1), 1.787(9); P(1)-Rh(1), 2.292(2). Selected bond angles (deg): C(1)-P(1)-C(1), 106.33(19); Rh(1)-P(1)-C(1), 112.46(17).

## 2.6 Characterization of the Phosphine Donor

The standard measures of a phosphine donor are its electronic parameter, usually obtained from the symmetric CO stretching frequency of a carbonyl complex of the phosphine,<sup>29,30</sup> and the cone angle, as defined by Tolman with respect to Ni(CO)<sub>3</sub> complexes.<sup>31</sup> Although numerous other approaches have been described, most still attempt to classify the properties of a phosphine in terms of steric<sup>32-35</sup> and electronic effects.<sup>36-38</sup> From the structure of the titanium complex **2b**, the cone angle

of the phosphine donor can be estimated as  $100^\circ$  if the methylene hydrogens are used to define the cone angle, where the hydrogen atom is given a radius of  $0.6 \text{ \AA}$ , and a metal-P distance of  $2.28 \text{ \AA}$  is assumed, as described by Tolman. For the tantalum complex **3b**, the estimated cone angle is  $103^\circ$ , which is larger due to the increase in C-P-C angles relative to the titanium complexes. For **2a** and **2c**, the trifluoromethyl or methyl meta substituents define the cone angle, rather than the methylene hydrogens, which makes these complexes slightly larger donors, although the aryl groups are likely to rotate so the predicted cone angles from the location of these substituents overestimate the size of these donors. Regardless, these complexes display remarkably small cone angles comparable to those of the smallest phosphine donors. For comparison, the cone angles of  $\text{PMe}_3$ ,  $\text{PEt}_3$ ,  $\text{PPh}_3$  and  $\text{P(OEt)}_3$  are all larger, at  $118^\circ$ ,  $132^\circ$ ,  $145^\circ$ , and  $109^\circ$ , respectively.

The electronic properties of many phosphines have been characterized by measurement of the  $A_1$  stretching frequency of complexes prepared by replacement of a CO group in  $\text{Ni(CO)}_4$  by a single phosphine donor. Compounds that are less toxic than  $\text{Ni(CO)}_4$  are now more commonly used to characterize the electronic properties of phosphines. However, we opted to prepare a complex of  $\text{Ni(CO)}_4$  to have a chance to compare the parameters of some of these phosphine complexes directly with a large database of available data for adducts of the  $\text{Ni(CO)}_3$  moiety. The symmetric  $A_1$  carbonyl stretching frequency of a  $0.05 \text{ mol L}^{-1}$  solution of  $(\text{CO})_3\text{Ni}[\text{P}(\text{CH}_2\text{N-3,5-Me}_2\text{C}_6\text{H}_3)_3\text{TiNMe}_2]$  **4** in  $\text{CH}_2\text{Cl}_2$  was  $2073.7 \text{ cm}^{-1}$ ; this can be compared to the extensive data tabulated by Tolman.<sup>31</sup> Compared to other

phosphine ligands,  $\text{P}(\text{CH}_2\text{NAr}^{\text{R}})_3\text{TiNMe}_2$  is significantly less strongly electron-donating than common alkyl phosphines  $\text{PMe}_3$  ( $\nu_{\text{CO}}(A_1) = 2064.1 \text{ cm}^{-1}$ ), and slightly less electron donating than the ubiquitous  $\text{PPh}_3$  ( $\nu_{\text{CO}}(A_1) = 2068.9 \text{ cm}^{-1}$ ). The electronic parameter for **4** is almost identical to  $\text{PPh}_2$  ( $\nu_{\text{CO}}(A_1) = 2073.3 \text{ cm}^{-1}$ ). As a phosphine ligand, complex **4** appears to be a  $\pi$ -donor, but not as strong a  $\pi$ -acid as typical phosphites, such as  $\text{P}(\text{OEt})_3$  ( $\nu_{\text{CO}}(A_1) = 2076.3 \text{ cm}^{-1}$ ). Another method to assess the steric bulk of a phosphine is the symmetric deformation coordinate, which is defined as the difference between the sum of these C-P-C and Ni-P-C angles.<sup>35</sup> In **5**, the sum of Ni(1)-P-C angles for P(1) and P(2) are  $347.3(3)$  and  $348.2(3)^\circ$ , respectively, which results in symmetric deformation coordinates of  $39.8(4)^\circ$  and  $41.8(4)^\circ$  for P(1) and P(2), respectively. As with the cone angle, these values are indicative of a small donor.

The CO stretching frequency of *trans*-rhodiumcarbonylchlorobisphosphine complexes has been used extensively in the past to determine electronic parameters for phosphine ligands. To avoid the repeated handling of highly toxic  $\text{Ni}(\text{CO})_4$ , we chose to evaluate the electronic properties of the phosphine donor in **1a-c**, **2a-c** and **3a-c** by this method. The CO stretching frequency of  $\text{CH}_2\text{Cl}_2$  solutions of **6a-c**, **7a-c** and **8a-c** are presented in Table 2.2, and plotted versus the  $^{31}\text{P}$  chemical shifts of the precursors **1a-c**, **2a-c**, and **3a-c** in Figure 2.7. It is clear from this chart that the effect of the different aryl substituents is very significant even for the ligand precursor complexes **6a-c**, despite the distance of these substituents from the phosphine donor. Such an influence demonstrates that the lone pairs on the nitrogen atoms are

important in determining the electronic properties of these donors even in the absence of a transition metal. There is the evidence for a preferential orientation of the nitrogen lone pairs with respect to both the aromatic ring substituents and the phosphine donor in the structure of **1c**, shown in Figure 2.2. The two ligand arms associated with N(1) and N(2) are aligned, so that their aromatic substituents, C(1), C(2) and P(1) are nearly coplanar. The effect of the aryl substituents is also apparent in the CO stretching frequencies of the titanium complexes, **7a-c**. The effect of the aryl substituents for these titanium complexes is practically identical to that observed for **6a-c**, although the titanium complexes are nearly uniformly less donating than **6a-c**. In contrast, the CO stretches for the tantalum complexes **8a-c** are much less affected by the aryl substituents. The range of CO stretching frequencies for **8a-c** spans only  $3.8\text{ cm}^{-1}$  for the 3 different aryl substituents, whereas for **6a-c** and **7a-c** the ranges spanned are  $11.7$  and  $12.7\text{ cm}^{-1}$ , respectively. Complexes **8b** and **8c** have nearly identical CO stretching frequencies. There is a near linear trend of decreasing  $^{31}\text{P}$  chemical shift with the decreasing donor ability of the phosphine for each set of complexes, **6a-c**, **7a-c**, and **8a-c**. Between sets of the complexes, there is no linear trend between chemical shift and donor ability; however, the highest field  $^{31}\text{P}$  NMR chemical shifts do correlate with the weaker  $\sigma$ -donating phosphines. The most strongly donating phosphine ligands, **1b-c** and **2b-c** have similar donor properties to  $\text{PPh}_3$ , which exhibits a CO stretching frequency of  $1978\text{ cm}^{-1}$  in the complex *trans*- $\text{Rh}(\text{CO})\text{Cl}(\text{PPh}_3)_2$ .

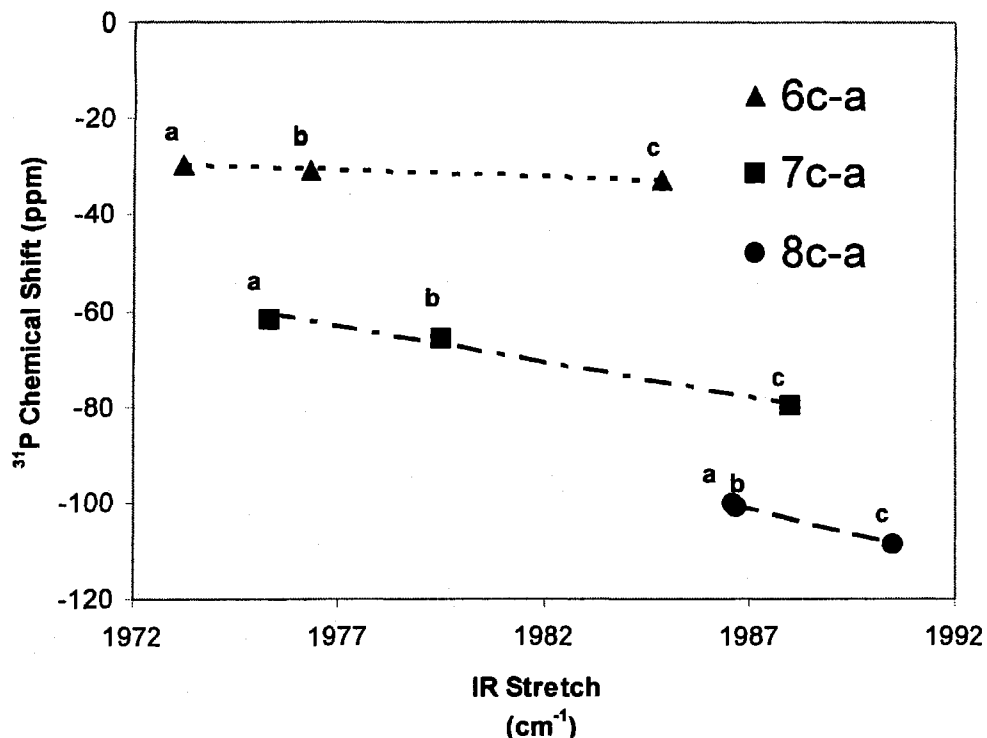


**Figure 2.7.** Phosphorus-31 NMR chemical shifts vs. carbonyl stretching frequencies for complexes **6a-c**, **7a-c** and **8a-c**.

Table 2.2 also contains the  $^{31}\text{P}$  NMR shifts and  $^1J_{\text{RhP}}$  values for complexes **6a-c**, **7a-c** and **8a-c**, along with the  $^{31}\text{P}$  NMR shifts of the phosphine donors **1a-c**, **2a-c** and **3a-c**. For complexes **6a-c** the  $^1J_{\text{RhP}}$  values range from 116.9 to 120.1 Hz, with the largest values for **6a**, which bears the most electron-withdrawing substituents. An increase in phosphine lone pair *s*-orbital character is consistent with the poorer donor ability of this phosphine, although many factors can affect Rh-P coupling constants.<sup>31</sup> The same trend is observed for complexes **7a-c**, and the poorer donor abilities of these phosphines relative to **6a-c** are consistent with their larger  $^1J_{\text{RhP}}$  values, which range from 122.5 to 130.3 Hz. For the tantalum complexes, there is a similar trend. For **8a-c**, the  $^1J_{\text{RhP}}$  values range from 136.9 to 143.6 Hz, all

of which are greater than the  $^1J_{\text{RhP}}$  values for **6a-c** and **7a-c**.

It is known that phosphines with larger cone angles have smaller changes in  $^{31}\text{P}$  NMR shift upon coordination to rhodium.<sup>39</sup> The differences in  $^{31}\text{P}$  chemical shifts between **1a-c** and their rhodium complexes **6a-c** are  $\delta$  52.2, 54.7, and 56.1, respectively, are consistent with a cone angle of approximately  $110^\circ$ . This trend of increasing shift with increasing donor ability is reversed for **2a-c** and **7a-c**; these differences in shifts are  $\delta$  83.7, 81.3, and 80.1, respectively. The significantly larger coordination shift relative to **1a-c** can be attributed to the smaller cone angle for this phosphine donor. The differences in  $^{31}\text{P}$  chemical shift for **3a-c** and **8a-c** are  $\delta$  74.3, 68.1, and 67.8, respectively, which reflect the fact that phosphines **3a-c** have slightly larger cone angles than their Ti analogues, but still smaller than **1a-c**.

**Table 2.2** Metal carbonyl stretching frequencies of compounds **6a-c**, **7a-c** and **8a-c** in CH<sub>2</sub>Cl<sub>2</sub>, their <sup>1</sup>J<sub>Rh-P</sub> coupling constants and <sup>31</sup>P NMR shifts, and the <sup>31</sup>P NMR shifts of the phosphine donors **1a-c**, **2a-c** and **3a-c**.

Rh(I) Complex	Phosphine Donors	$\nu_{\text{CO}}$ (cm <sup>-1</sup> )	<sup>1</sup> J <sub>Rh-P</sub>	<sup>31</sup> P shift	Ligand <sup>31</sup> P shift
<b>6a</b>	P(CH <sub>2</sub> NHAr <sup>CF<sub>3</sub></sup> ) <sub>3</sub>	1984.9	120.1	+22.6	-29.6 ( <b>1a</b> )
<b>6b</b>	P(CH <sub>2</sub> NHPh) <sub>3</sub>	1976.3	118.1	+23.7	-31.0 ( <b>1b</b> )
<b>6c</b>	P(CH <sub>2</sub> NHAr <sup>Me</sup> ) <sub>3</sub>	1973.2	116.9	+23.5	-32.6 ( <b>1c</b> )
<b>7a</b>	P(CH <sub>2</sub> NAr <sup>CF<sub>3</sub></sup> ) <sub>3</sub> TiNMe <sub>2</sub>	1988.0	130.3	+3.8	-79.9 ( <b>2a</b> )
<b>7b</b>	P(CH <sub>2</sub> NPh) <sub>3</sub> TiNMe <sub>2</sub>	1979.5	125.8	+15.7	-65.6 ( <b>2b</b> )
<b>7c</b>	P(CH <sub>2</sub> NAr <sup>Me</sup> ) <sub>3</sub> TiNMe <sub>2</sub>	1975.3	122.5	+18.5	-61.6 ( <b>2c</b> )
<b>8a</b>	P(CH <sub>2</sub> NAr <sup>CF<sub>3</sub></sup> ) <sub>3</sub> Ta=NC(CH <sub>3</sub> ) <sub>3</sub>	1990.5	143.6	-34.2	-108.5 ( <b>3a</b> )
<b>8b</b>	P(CH <sub>2</sub> NPh) <sub>3</sub> Ta=NC(CH <sub>3</sub> ) <sub>3</sub>	1986.7	138.1	-32.8	-100.9 ( <b>3b</b> )
<b>8c</b>	P(CH <sub>2</sub> NAr <sup>Me</sup> ) <sub>3</sub> Ta=NC(CH <sub>3</sub> ) <sub>3</sub>	1986.6	136.9	-32.3	-100.1 ( <b>3c</b> )

## 2.7 Synthesis and Structure of a Ni(II) Dimer with a Bridging Diamido-phosphido Ligand

Transition metals are known to activate the P-C bond of tertiary phosphines PR<sub>3</sub>. The reactions of transition metals with P-C bonds of tertiary phosphines PR<sub>3</sub> imply damage in the organometallic catalyst and have been studied extensively. These studies are mainly concerned with the cleavage of aryl-phosphine bonds but seldom with an alkyl-phosphine bond, which is the consequence of less favored migration of an alkyl group as compared to that of an aryl group.<sup>40</sup> The reactions of bis(diphenylphosphino)methane and the derivatives with transition metals to

synthesize the dinuclear and trinuclear complexes are special in that they undergo P-C bond cleavage at the P-CH<sub>2</sub> bond rather than at the P-phenyl bond.<sup>18,21,41-53</sup> The decomposition reactions of P-C bonds are also enhanced by the presence of electron-withdrawing substituents and inhibited by electron-donating substituents.<sup>54,55</sup> The studies have shown that the ease of P-C bond cleavage follows the order:

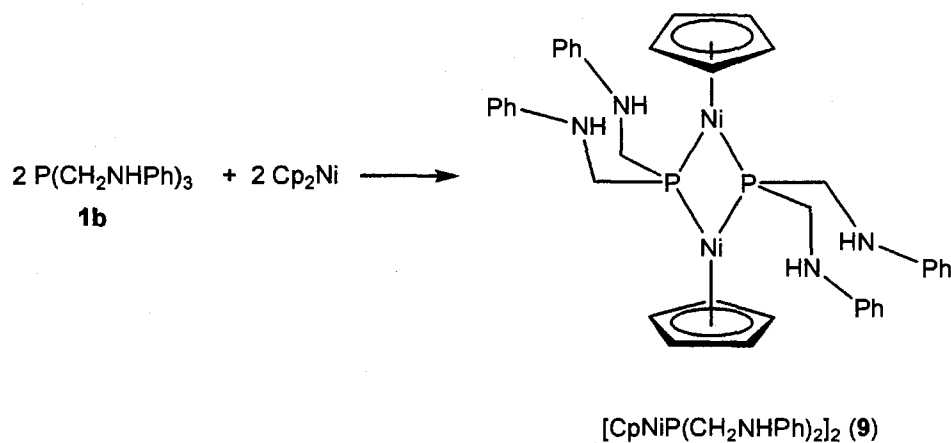


However, the cleavage of P-C bond in phosphine ligands has provided access to phosphido-bridged polymetallic complexes.<sup>56-59</sup> Diorganophosphide (PR<sub>2</sub>) ligands have been widely used to bridge early-late heterobimetallic complexes, in which the M-P-M' angles and M-M' distances range from 54° to 104° and 2.21 Å to 3.70 Å, respectively.<sup>56</sup> [Cp<sub>2</sub>M(PR<sub>2</sub>)<sub>2</sub>] complexes have been used as the starting materials in preparing Group 4 and Group 10 phosphido-bridged heterobimetallic complexes by displacing the carbonyl ligand in the Group 10 transition metal complexes.<sup>60</sup> The ligands PHR<sub>2</sub> were shown to give phosphido-bridged transition metal dimers.<sup>61,62</sup>

The reaction of phosphine ligand [P(CH<sub>2</sub>NHPh)<sub>3</sub>] with nickelocene (Cp<sub>2</sub>Ni) in toluene produces a Ni(II) dimer with a bridging diamido-phosphido ligand [CpNiP(CH<sub>2</sub>NHPh)<sub>2</sub>]<sub>2</sub> (**9**), as shown in Scheme 2.6. The reaction is slow at room temperature and requires 2 weeks to go to completion, but it only need 2 days to complete by heating at 80 °C. The resulting product was obtained in 57 % yield as a thermally stable brown solid and has been characterized by <sup>1</sup>H NMR, <sup>31</sup>P{<sup>1</sup>H} NMR,

$^{13}\text{C}\{^1\text{H}\}$  NMR, elemental analysis, and single-crystal X-ray diffraction. The  $^{31}\text{P}\{^1\text{H}\}$  NMR spectrum of  $[\text{CpNiP}(\text{CH}_2\text{NHPh})_2]_2$  (**9**) contains a single resonance for the phosphorus donor at  $\delta$  -87.5, which is shifted significantly upfield compared with the free ligand precursor  $\text{P}[\text{CH}_2\text{NHPh}]_3$ . The  $^1\text{H}$  NMR and  $^{13}\text{C}\{^1\text{H}\}$  NMR spectra of **9** exhibit one set of signals, which are consistent with a symmetric dimer. The cleavage of the P-C bond in the ligand  $\text{P}[\text{CH}_2\text{NHPh}]_3$  and loss of Cp Group in nickelocene ( $\text{Cp}_2\text{Ni}$ ) allow for the achievement of the favored 18-electron stabilization when the resulting  $-\text{P}[\text{CH}_2\text{NHPh}]_2$  ligand is considered to act as a three electron donor.

Scheme 2.6



The molecular structure of **9** in the solid state was determined by X-ray crystal structure analysis. An ORTEP depiction of the solid-state structure obtained at 173 K is shown in Figure 2.8, which features a symmetric dimer structure. The coordination geometry about the Ni atom is distorted trigonal planar, at the corners of which are the centre of Cp group and two phosphido donors. The geometry about

the P atoms could be described as distorted tetrahedron, where two Ni atoms occupy the corner positions. In contrast to the planar Ni<sub>2</sub>P<sub>2</sub> rings in the phosphido complexes (the torsion angle Ni-P...P-Ni = 180°), the Ni<sub>2</sub>P<sub>2</sub> ring in [CpNiP(CH<sub>2</sub>NHPh)<sub>2</sub>]<sub>2</sub> (**9**) is puckered and the torsion angle Ni-P...P-Ni is 160.6°. The distortion is controlled by the steric interaction of the phosphido group with the Cp ligand and with each other. A vertical C<sub>2</sub> symmetry axis runs through the center of the Ni<sub>2</sub>P<sub>2</sub> ring and relates the two halves of the dimer. The P-Ni bond lengths range from 2.1382(8) Å to 2.1513(9) Å and P-Ni-P angles are 74.30(3)° and 74.60(3)°, which are similar to those in [CpNi(μ-PPh<sub>2</sub>)<sub>2</sub>] (P-Ni=2.15(0.7) Å, 2.16(0.8) Å, P-Ni-P=77.6(2)°).<sup>63</sup> The Ni-Ni distance of 3.367(5) Å indicates the absence of a Ni-Ni bond.

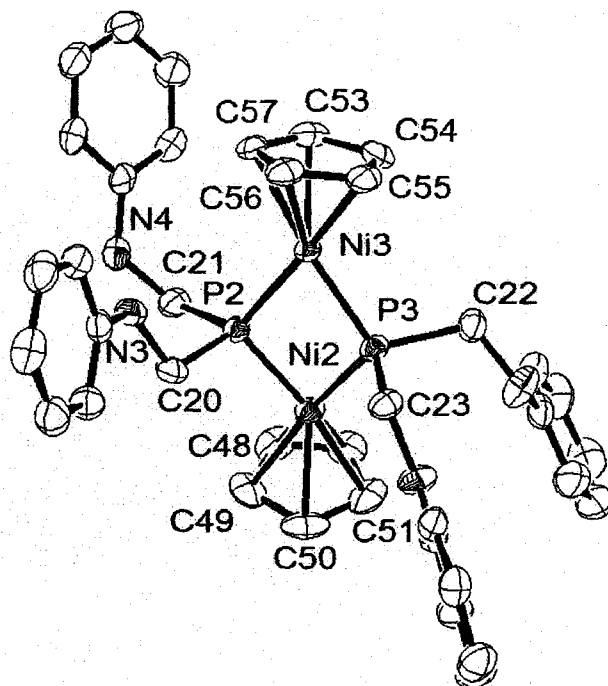


**Figure 2.8.** Solid-state molecular structure of **9** as determined by X-ray crystallography. Hydrogen atoms are omitted for clarity. Selected distances (Å): Ni(2)-P(2), 2.1458(9); Ni(2)-P(3), 2.1513(9); Ni(3)-P(2), 2.1439(9); Ni(3)-P(3), 2.1382(8); Ni(1)···Ni(1), 3.367(5); C(20)-P(2), 1.851(3); C(21)-P(2), 1.872(3); P(2)···P(3), 2.5950(11). Selected bond angles (deg): P(2)-Ni(2)-P(3); 74.30(3); P(2)-Ni(3)-P(3); 74.60(3); Ni(2)-P(2)-Ni(3), 103.42(4); Ni(2)-P(3)-Ni(3), 103.43(4); C(20)-P(2)-C(21), 102.26(15); C(22)-P(3)-C(23), 100.33(15); C(20)-P(2)-Ni(2), 110.58(10); C(21)-P(2)-Ni(2), 109.83(10).

### 2.8 Characterization of the Intermediates and the Byproducts in the Reaction of the Phosphine Ligand [P(CH<sub>2</sub>NHPh)<sub>3</sub>] with Cp<sub>2</sub>Ni

In the reaction of 4 equiv of phosphine ligand [P(CH<sub>2</sub>NHPh)<sub>3</sub>] with 5 equiv of Cp<sub>2</sub>Ni, a single intermediate is observed by <sup>31</sup>P{<sup>1</sup>H} NMR spectroscopy after the

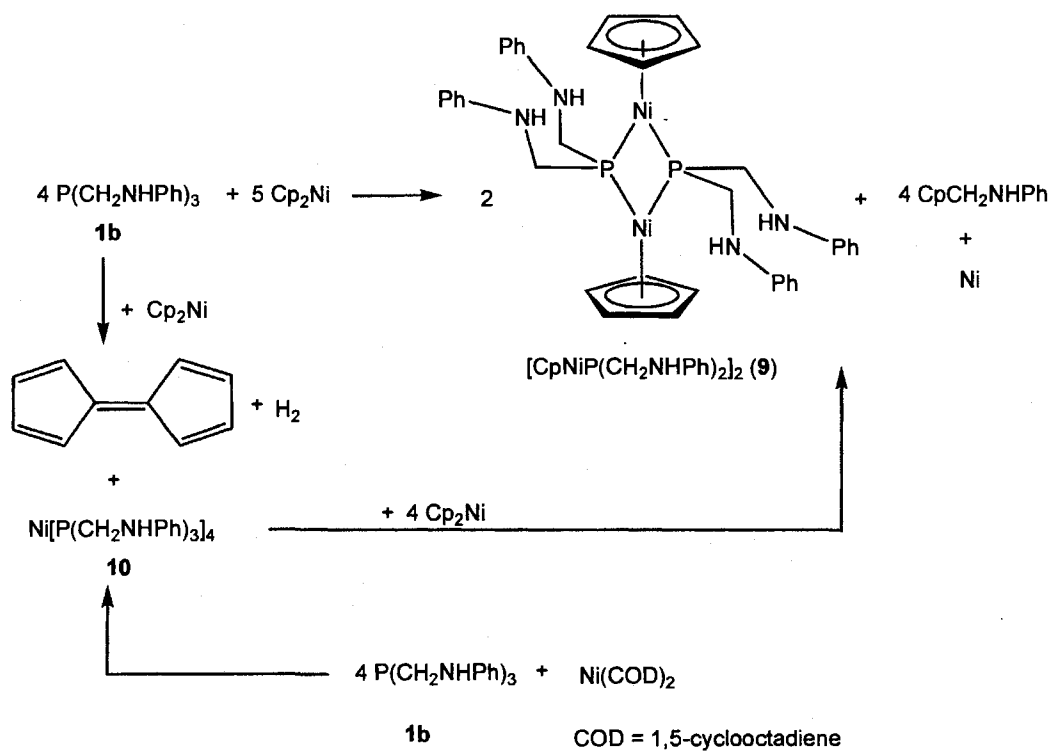
mixture is heated to 80 °C for a few minutes. The  $^{31}\text{P}\{^1\text{H}\}$  NMR spectrum of the intermediate shows a singlet at  $\delta$  15.9, which is shifted downfield compared to the corresponding phosphine ligand  $[\text{P}(\text{CH}_2\text{NHPH})_3]$  at  $\delta$  -32.1. The intermediate was identified to be  $\text{Ni}[\text{P}(\text{CH}_2\text{NHPH})_3]_4$  (**10**) (vide infra).<sup>64,65</sup> One equiv of nickelocene reacts with four equiv of phosphine ligand  $[\text{P}(\text{CH}_2\text{NHPH})_3]$  to initially form a mixture of the Ni(0) complex  $\text{Ni}[\text{P}(\text{CH}_2\text{NHPH})_3]_4$  (**10**) and pentafulvalene.<sup>66,30</sup> Leadbeater's group has previously reported that phosphines react with  $\text{Cp}_2\text{Ni}$  to produce Ni(0) tetrakisphosphine adducts; the cyclopentadiene groups displaced dimerise to form pentafulvalene, which did not partake in any further carbon-carbon bond forming reactions.<sup>64</sup>

$\text{Ni}[\text{P}(\text{CH}_2\text{NHPH})_3]_4$  (**10**) reacts with 4 equiv of nickelocene to generate 2 equiv of Ni(II) dimer with a bridging diamido-phosphido ligand  $[\text{CpNiP}(\text{CH}_2\text{NHPH})_2]_2$  (**9**), as shown in Scheme 2.7. The byproducts are much more soluble in pentane than the scarcely soluble  $[\text{CpNiP}(\text{CH}_2\text{NHPH})_2]_2$  (**9**), and are easily rinsed from the product and the filtrate is collected. The solvent of the filtrate is removed by vacuum to produce the dark brown solid. The hydrolysis product of the dark brown solid was identified as  $\text{CpCH}_2\text{N}(\text{H})\text{Ph}$  by GC/MS and  $^1\text{H}$  NMR spectroscopy. However, the exact mechanism by which  $\text{Ni}[\text{P}(\text{CH}_2\text{NHPH})_3]_4$  (**10**) is oxidized to the Ni(II) dimer is not clear. The speculative byproduct in the reaction of  $\text{Ni}[\text{P}(\text{CH}_2\text{NHPH})_3]_4$  (**10**) with 4 equiv of nickelocene could be Ni metal.

The Ni(0) complex  $\text{Ni}[\text{P}(\text{CH}_2\text{NHPH})_3]_4$  (**10**) also can be prepared by the treatment of  $\text{Ni}(\text{COD})_2$  [COD = 1,5-cyclooctadiene] with 4 equiv of phosphine

ligand  $[P(CH_2NHPH)_3]$  (Scheme 2.7), which was characterized by  $^1H$ ,  $^{13}C\{^1H\}$ , and  $^{31}P\{^1H\}$  NMR spectroscopy.

Scheme 2.7

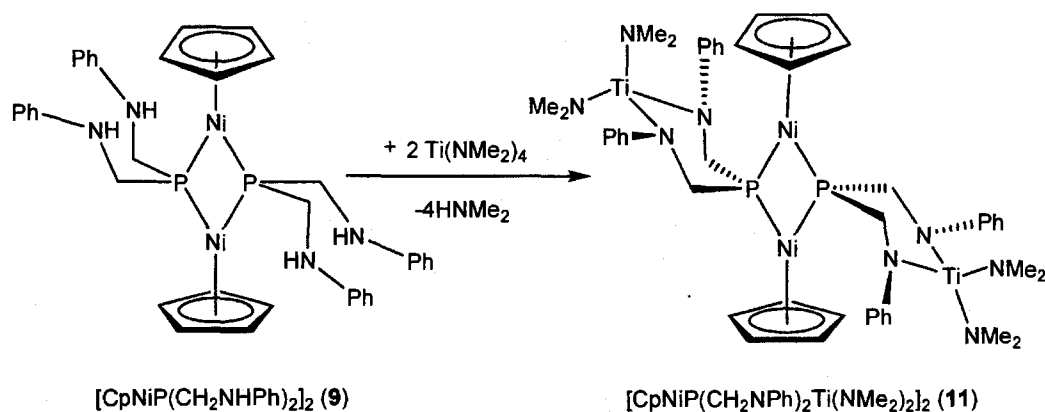


## 2.9 Synthesis and Structure of an Early-Late Polynuclear Heterometallic Complex Based on the Ni (II) Dimer

Treatment of  $[CpNiP(CH_2NHPH)_2]_2$  (**9**) with 2 equiv of  $Ti(NMe_2)_4$  in toluene affords the early-late polynuclear heterometallic complex  $[CpNiP(CH_2NHPH)_2Ti(NMe_2)_2]_2$  (**11**) in 89.8 % yield, as shown in Scheme 2.8. The  $^{31}P\{^1H\}$  NMR spectrum of  $[CpNiP(CH_2NHPH)_2Ti(NMe_2)_2]_2$  (**11**) shows a singlet at  $\delta$

-80.5, which is shifted slightly downfield compared to the Ni(II) dimer  $[\text{CpNiP}(\text{CH}_2\text{NHPh})_2]_2$  (**9**). This indicates that phosphorus is not coordinated to the early transition metal centre.<sup>67</sup> The  $^1\text{H}$  NMR and  $^{13}\text{C}\{^1\text{H}\}$  NMR spectra of **11** are consistent with an apparent  $C_2$  symmetry. The change in  $^1\text{H}$  NMR chemical shift of the Cp group (**11**: 5.02; **9**: 4.91) is small, which also indicates only a slight effect of the Ni(II) metal center from the Ti-Ni heterometallic complex **11** upon the Ni(II) dimer (**9**).

Scheme 2.8



The solid-state structure of  $[\text{CpNiP}(\text{CH}_2\text{NPh})_2\text{Ti}(\text{NMe}_2)_2]_2$  (**11**) was determined by X-ray crystallography and depicted in Figure 2.9. The diamido-phosphido ligand binds the titanium metal center by two amido donors. Both of the Ti centers have approximately tetrahedral geometries, and each contains two  $\text{-NMe}_2$  groups. The phosphido ligand and a Ti atom form a six-membered  $\text{TiN}_2\text{C}_2\text{P}$  ring, which adopts a chair conformation. Although the distance of  $\text{Ti}\cdots\text{Ni}$  is

4.638(5) Å, binding of the Ti metal center to the amido donors in [CpNiP(CH<sub>2</sub>NPh)<sub>2</sub>Ti(NMe<sub>2</sub>)<sub>2</sub>]<sub>2</sub> (**11**) has only a slight effect on the Ni metal center in the Ni(II) dimer [CpNiP(CH<sub>2</sub>NHPh)<sub>2</sub>]<sub>2</sub> (**9**). The P-Ni bond lengths in **11** range from 2.1447(11) to 2.1427(11) Å, which are similar to those in the Ni(II) dimer **9**. The P-Ni-P angle of 75.02(5)° is slightly larger than those in **9** (74.30(3)° and 74.60(3)°). Compared with the puckered Ni<sub>2</sub>P<sub>2</sub> ring with the torsion angle Ni-P-P-Ni of 160.6° in [CpNiP(CH<sub>2</sub>NHPh)<sub>2</sub>]<sub>2</sub> (**9**), the Ni<sub>2</sub>P<sub>2</sub> ring in [CpNiP(CH<sub>2</sub>NPh)<sub>2</sub>Ti(NMe<sub>2</sub>)<sub>2</sub>]<sub>2</sub> (**11**) is planar and the torsion angle Ni-P···P-Ni is 180.0°. The change in <sup>1</sup>H NMR chemical shift of the Cp group (**11**: 5.02; **9**: 4.91) is small, which also indicates a slight effect of the Ni (II) metal center from the Ti-Ni heterometallic complex **11**.

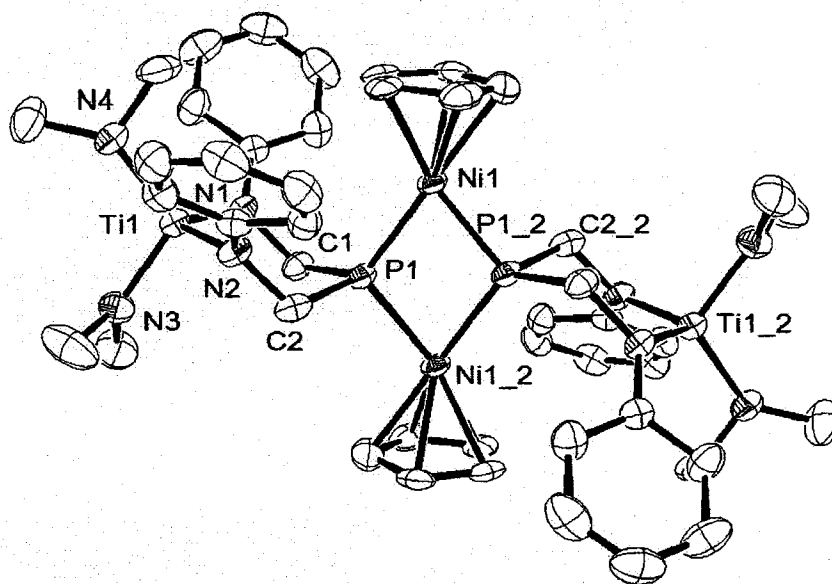


**Figure 2.9.** Solid-state molecular structure of **11** as determined by X-ray crystallography. Hydrogen atoms are omitted for clarity. Selected distances (Å): Ni(1)-P(1), 2.1427(11); Ni(1)-P(1), 2.1447(11); Ni(1)···Ni(1), 3.4009(10); P(1)···P(1), 2.611(5); Ni(1)···Ti(1), 4.638(5); Ti(1)-N(1), 1.949(3); Ti(1)-N(2), 1.951(3); Ti(1)-N(3), 1.876(3); Ti(1)-N(4), 1.866(3); C(1)-P(1), 1.863(4); C(2)-P(1), 1.862(4). Selected bond angles (deg): P(1)-Ni(1)-P(1); 75.02(5); Ni(1)-P(1)-Ni(1), 104.98(5); C(1)-P(1)-C(2), 99.44(18); C(2)-P(1)-Ni(1), 115.56(13); C(1)-P(1)-Ni(1), 119.11(13); N(1)-Ti(1)-N(2), 108.66(13); N(1)-Ti(1)-N(3), 106.28(14); N(1)-Ti(1)-N(4), 114.45(14); N(2)-Ti(1)-N(3), 105.39(14); N(2)-Ti(1)-N(4), 110.19(14); N(3)-Ti(1)-N(4), 111.40(15).

## 2.10 Summary and Conclusions

The ligand precursors P[CH<sub>2</sub>N-3,5-(CF<sub>3</sub>)<sub>2</sub>C<sub>6</sub>H<sub>3</sub>]<sub>3</sub>H<sub>3</sub> (**1a**), P[CH<sub>2</sub>NPh]<sub>3</sub>H<sub>3</sub> (**1b**), and P[CH<sub>2</sub>N-3,5-Me<sub>2</sub>C<sub>6</sub>H<sub>3</sub>]<sub>3</sub>H<sub>3</sub> (**1c**), react with the reagents Ti(NMe<sub>2</sub>)<sub>4</sub> and

'BuN=Ta(NEt<sub>2</sub>)<sub>3</sub> to generate metal complexes of the type P[CH<sub>2</sub>NAr<sup>R</sup>]<sub>3</sub>TiNMe<sub>2</sub> (**2a-c**) and P[CH<sub>2</sub>NAr<sup>R</sup>]<sub>3</sub>Ta=N'Bu (**3a-c**). Due to ring strain, the phosphine lone-pair cannot chelate and is available to bind a second metal, despite quite short P...Ti and P...Ta distance. The reaction of **2c** with Ni(CO)<sub>4</sub> produces at first the early-late heterobimetallic complex (CO)<sub>3</sub>Ni[P(CH<sub>2</sub>N-3,5-Me<sub>2</sub>C<sub>6</sub>H<sub>3</sub>)<sub>3</sub>TiNMe<sub>2</sub>] (**4**), which gradually converts to the early-late trimetallic complex (CO)<sub>2</sub>Ni[P(CH<sub>2</sub>N-3,5-Me<sub>2</sub>C<sub>6</sub>H<sub>3</sub>)<sub>3</sub>TiNMe<sub>2</sub>]<sub>2</sub> (**5**).

The effect of the complexation of Ti and Ta fragments on the donor ability of the phosphine ligands was determined by the preparation of the bis-phosphine complexes *trans*-L<sub>2</sub>Rh(CO)Cl, (where L = **1a-c**, **2a-c**, and **3a-c**) prepared by the reactions of the appropriate phosphines with [Rh(CO)<sub>2</sub>(μ-Cl)]<sub>2</sub>, and a measurement of the resultant CO stretching frequencies. The early transition metal centres were affecting the property of the phosphine donors in the building blocks for heterometallic complexes, despite the fact that the phosphine lone-pair is not coordinated to the metal centers. Although the lone pair of the phosphine donor is aimed away from the early transition metal centres, the donor abilities of the phosphines are affected by direct interactions between the early transition metals and the phosphine donors.

Nickelocene Cp<sub>2</sub>Ni reacts with the phosphine ligand [P(CH<sub>2</sub>NPh)<sub>3</sub>H<sub>3</sub>] to give a Ni(II) dimer with a bridging diamido-phosphido ligand [CpNiP(CH<sub>2</sub>NHPh)<sub>2</sub>]<sub>2</sub> (**9**). The intermediates of the reaction are Ni[P(CH<sub>2</sub>NHPh)<sub>3</sub>]<sub>4</sub> (**10**) and pentafulvalene, which react with 4 equiv of nickelocene to generate 2 equiv of Ni(II) dimer

$[\text{CpNiP}(\text{CH}_2\text{NHPH})_2]_2$  (**9**) and 4 equiv of  $\text{CpCH}_2\text{N}(\text{H})\text{Ph}$ . The Ni(II) dimer **9** readily binds the titanium metal center using amido donors, which allows for the facile synthesis of the early-late tetranuclear heterometallic complex  $[\text{CpNiP}(\text{CH}_2\text{NPh})_2\text{Ti}(\text{NMe}_2)_2]_2$  (**11**). The binding of the Ti metal center to the amido donors in  $[\text{CpNiP}(\text{CH}_2\text{NPh})_2\text{Ti}(\text{NMe}_2)_2]_2$  (**11**) has a slight effect on the Ni metal center in the Ni(II) dimer  $[\text{CpNiP}(\text{CH}_2\text{NHPH})_2]_2$  (**9**).

## 2.11 Experimental

### 2.11.1 General Procedures

Unless otherwise stated, all manipulations were performed under an inert atmosphere of nitrogen using either standard Schlenk techniques or an MBraun glove box. Dry, oxygen-free solvents were employed throughout. Anhydrous pentane, toluene, diethyl ether and THF were purchased from Aldrich, sparged with dinitrogen, and passed through activated alumina under a positive pressure of nitrogen gas; toluene and hexanes were further deoxygenated using Ridox catalyst columns.<sup>68</sup> Deuterated benzene was dried by heating at reflux with sodium/potassium alloy in a sealed vessel under partial pressure, then trap-to-trap distilled, and freeze-pump-thaw degassed three times. Deuterated methylene chloride was heated in a sealed vessel over  $\text{CaH}_2$ , then trap-to-trap distilled, and freeze-pump-thaw degassed three times. NMR spectra were recorded on Bruker AMX (300 MHz) or Bruker AMX (500 MHz) spectrometer. All chemical shifts are

reported in ppm, and all coupling constants are in Hz. For  $^{19}\text{F}\{^1\text{H}\}$  NMR spectra, trifluoroacetic acid was used as the external reference at 0.00 ppm.  $^1\text{H}$  NMR spectra were referenced to residual protons ( $\text{C}_6\text{D}_5\text{H}$ ,  $\delta$  7.15;  $\text{C}_7\text{D}_7\text{H}$ ,  $\delta$  2.09;  $\text{CHDCl}_2$ ,  $\delta$  5.35) with respect to tetramethylsilane at  $\delta$  0.00.  $^{31}\text{P}\{^1\text{H}\}$  NMR spectra were referenced to external 85 %  $\text{H}_3\text{PO}_4$  at  $\delta$  0.0.  $^{13}\text{C}\{^1\text{H}\}$  spectra were referenced relative to solvent resonances ( $\text{C}_6\text{D}_6$ ,  $\delta$  128.0;  $\text{C}_7\text{D}_8$ ,  $\delta$  20.4;  $\text{CD}_2\text{Cl}_2$ ,  $\delta$  54.00). Elemental analyses were performed by the Centre for Catalysis and Materials Research (CCMR), Windsor, Ontario, Canada. The compounds tris(hydroxymethyl)phosphine, aniline, 3,5-dimethylaniline, 3,5-bis(trifluoromethyl)aniline,  $\text{Ni}(\text{CO})_4$ ,  $\text{TiCl}_4$ ,  $\text{LiNMe}_2$ ,  $\text{Ta}(\text{NEt}_2)_3(\text{N}^t\text{Bu})$ ,  $[(\text{CO})_2\text{Rh}(\mu\text{-Cl})]_2$  were purchased from Aldrich, and used as received. The complex  $\text{Ti}(\text{NMe}_2)_4$  was prepared from the reaction of  $\text{TiCl}_4$  and  $\text{LiNMe}_2$  and distilled prior to use.<sup>69</sup> Nickel tetracarbonyl,  $\text{Ni}(\text{CO})_4$ , is highly toxic and should be handled with care.

### 2.11.2 Synthesis of Complexes

**$\text{P}[\text{CH}_2\text{NH-3,5-(CF}_3)_2\text{C}_6\text{H}_3]_3$  (1a).** A mixture of  $\text{P}(\text{CH}_2\text{OH})_3$  (5.0 g, 90 %, 0.0362 mol), 3,5-bis(trifluoromethyl)aniline (28 mL, 41.5 g, 5 equiv) and toluene (60 mL) were mixed in a 250 mL 3 neck flask equipped with a Dean Stark trap and a condenser. The solution was heated to reflux for 30 min, and the water was collected and removed from the trap. The solution was allowed to cool, and then the remaining solvent was removed under vacuum. The addition of pentane (80 mL) dissolved the

excess 3,5-bis(trifluoromethyl)aniline, and precipitated the product as a fine white solid which was collected by filtration and dried under vacuum. X-ray quality crystals were obtained from slow evaporation of the toluene solution. Yield 20.2 g, 73 %.  $^1\text{H}$  NMR ( $\text{C}_6\text{D}_6$ , 300 MHz, 298 K):  $\delta$  2.55 (dd,  $^3J_{\text{HH}} = 5.2$  Hz,  $^2J_{\text{PH}} = 5.2$  Hz, 6H,  $\text{PCH}_2$ ), 3.13 (b, 3H,  $\text{NH}$ ), 6.59 (s, 6H, Ph  $o\text{-H}$ ), 7.27 (s, 3H, Ph  $p\text{-H}$ ).  $^{13}\text{C}\{^1\text{H}\}$  NMR ( $\text{C}_6\text{D}_6$ , 125.8 MHz, 298 K):  $\delta$  39.4 (d,  $J_{\text{PC}} = 12.2$  Hz,  $\text{PCH}_2$ ), 111.2 and 122.1 (s, Ph  $o\text{-C}$  and  $m\text{-C}$ ), 112.5 (s, Ph  $p\text{-C}$ ), 132.9 (q,  $J = 32.9$  Hz, Ph  $\text{C-F}_3$ ), 148.9 (d,  $J = 5.5$  Hz,  $ipso\text{-C}$ ).  $^{31}\text{P}\{^1\text{H}\}$  NMR ( $\text{C}_6\text{D}_6$ , 121.5 MHz, 298 K):  $\delta$  -32.6 (s).  $^{19}\text{F}\{^1\text{H}\}$  NMR ( $\text{C}_6\text{D}_6$ , 282.1 MHz, 298 K):  $\delta$  14.71 (s). Anal. Calc'd for  $\text{C}_{27}\text{H}_{18}\text{F}_3\text{N}_3\text{P}$ : F.W.: 757.10. C, 42.82; H, 2.40; N, 5.55. Found: C, 43.00; H, 2.49 N, 5.41.

**$\text{P}(\text{CH}_2\text{NHPh})_3$  (1b).**<sup>22</sup> A mixture of  $\text{P}(\text{CH}_2\text{OH})_3$  (7.5 g, 0.0605 mol) and aniline (16.5 mL, 3 equiv) was stirred under dynamic vacuum. The solution became warm after 1 min and then cooled after 10 min. Shortly thereafter, the mixture solidified and was left under vacuum for two hours. The addition of ether to the mixture and filtering the resulting solid removed any trace remaining aniline. The sample was crystallized by cooling a warm saturated toluene solution sample at  $-40$  °C. The white solid was filtered, rinsed with pentane and dried (15.8 g, 75 %).  $^1\text{H}$  NMR ( $\text{C}_6\text{D}_6$ , 300 MHz, 298 K):  $\delta$  3.23 (d,  $^2J_{\text{PH}} = 4.8$  Hz, 6H,  $\text{PCH}_2$ ), 3.47 (b, 3H,  $\text{NH}$ ), 6.48 (dd, 6H, Ph  $o\text{-H}$ ), 6.76 (t, 3H, Ph  $p\text{-H}$ ), 7.16 (m, Ph  $m\text{-H}$ ).  $^{13}\text{C}\{^1\text{H}\}$  NMR ( $\text{C}_6\text{D}_6$ , 125.8 MHz, 298 K):  $\delta$  40.6 (d,  $J_{\text{PC}} = 12.5$  Hz,  $\text{PCH}_2$ ), 113.2 and 118.2 (s, Ph  $o\text{-C}$  and  $m\text{-C}$ ), 117.0 (s, Ph  $p\text{-C}$ ), 148.5 (d,  $J = 4.5$  Hz,  $ipso\text{-C}$ ).  $^{31}\text{P}\{^1\text{H}\}$  NMR ( $\text{C}_6\text{D}_6$ , 121.5

MHz, 298 K):  $\delta$  -32.1 (s). Anal. Calc'd for  $C_{21}H_{24}N_3P$ : F.W.: 349.41; C, 72.19; H, 6.92; N, 12.03. Found: C, 72.55; H, 7.00 N, 11.64.

**$P(CH_2NH-3,5-Me_2C_6H_3)_3$  (1c).** The mixture of  $P(CH_2OH)_3$  (17.36 g, 0.126 mol) and 3,5-dimethylaniline (45.8 g, 3 equiv) were stirred under dynamic vacuum. The solution became warm after 1 min and then cooled after 10 min. Shortly thereafter, the mixture solidified. Residual 3,5-dimethylaniline was removed by adding pentane to the mixture and filtering the resulting solid. The sample was crystallized by cooling a warm saturated toluene solution to  $-40$  °C. The white solid was filtered, rinsed with pentane and dried (42.7 g, 78 %).  $^1H$  NMR ( $C_6D_6$ , 300 MHz, 298 K):  $\delta$  2.18 (s, 18H, Ph CH3), 3.23 (d,  $^2J_{PH} = 5.2$  Hz, 6H, PCH2), 3.49 (b, 3H, NH), 6.23 (s, 6H, Ph *o*-H), 6.42 (s, 3H, Ph *p*-H).  $^{13}C\{^1H\}$  NMR ( $C_6D_6$ , 125.8 MHz, 298 K):  $\delta$  22.1 (s, Ph CH3), 41.1 (d,  $J_{PC} = 13.1$  Hz, PCH2), 112.2 and 120.9 (s, Ph *o*-C and *m*-C), 139.1 (s, Ph *p*-C), 149.3 (d,  $J = 4.8$  Hz, *ipso*-C).  $^{31}P\{^1H\}$  NMR ( $C_6D_6$ , 121.5 MHz, 298 K):  $\delta$  -29.6 (s). Anal. Calc'd for  $C_{27}H_{36}N_3P$ : F.W.: 433.57; C, 74.80; H, 8.37; N, 9.69. Found: C, 74.50; H, 8.49 N, 9.40.

**$P[(CH_2N-3,5-(CF_3)_2C_6H_3)_3TiNMe_2$  (2a).** A solution of  $Ti(NMe_2)_4$  (754.78 mg, 3.37 mmol) in toluene (60 mL) was added to a solution of **1a** (2.55 g, 3.37 mmol) in 50mL toluene. The pale yellow solution was stirred 10 h and turned dark red. The solvent was removed under vacuum and the remaining dark red solid was rinsed with a small portion of pentane, and then dried under vacuum (2.45 g, 85 %). X-ray

quality crystals were obtained by slow evaporation of a benzene solution.  $^1\text{H}$  NMR ( $\text{C}_6\text{D}_6$ , 300 MHz, 298 K):  $\delta$  2.85 (s, 6H,  $\text{NCH}_3$ ), 3.18 (d, 6H,  $^2J_{\text{PH}} = 7.0$  Hz,  $\text{PCH}_2$ ), 6.81 (s, 6H, Ph *o-H*), 7.40 (s, 3H, Ph *p-H*).  $^{13}\text{C}\{^1\text{H}\}$  NMR ( $\text{C}_6\text{D}_6$ , 125.8 MHz, 298 K):  $\delta$  41.2 (s,  $\text{TiNCH}_3$ ), 44.1 (d,  $J_{\text{PC}} = 24.2$  Hz,  $\text{PCH}_2$ ), 113.4 and 122.1 (s, Ph *o-C* and *m-C*), 116.0 (s, Ph *p-C*), 132.6 (q,  $J = 32.9$  Hz, Ph *C-F*), 152.9 (d, *ipso-C*).  $^{31}\text{P}\{^1\text{H}\}$  NMR ( $\text{C}_6\text{D}_6$ , 121.5 MHz, 298 K):  $\delta$  -79.9 (s).  $^{19}\text{F}\{^1\text{H}\}$  NMR ( $\text{C}_6\text{D}_6$ , 282.1 MHz, 298 K):  $\delta$  14.88 (s). Anal. Calc'd for  $\text{C}_{29}\text{H}_{21}\text{F}_{18}\text{N}_4\text{PTi}$ , F.W.: 846.32. C, 41.16; H, 2.50; N, 6.62. Found: C, 40.72; H, 2.70; N, 6.71.

**$\text{P}(\text{CH}_2\text{NPh})_3\text{TiNMe}_2$  (2b).** Prepared in an analogous manner to **2a** from  $\text{Ti}(\text{NMe}_2)_4$  (2.63 g, 11.73 mmol) and **1b** (4.09 g, 11.73 mmol) using a reaction time of 12 h. Yield 4.10 g (83 %).  $^1\text{H}$  NMR ( $\text{C}_6\text{D}_6$ , 500.1 MHz, 298 K):  $\delta$  2.98 (s, 6H,  $\text{TiNMe}_2$ ), 3.84 (d, 6H,  $^2J_{\text{PH}} = 6.7$  Hz,  $\text{PCH}_2$ ), 6.72 (d, 6H,  $^3J_{\text{HH}} = 8.3$  Hz, Ph *o-H*), 6.86 (t, 3H, Ph *p-H*), 7.20 (m, 6H, Ph *m-H*).  $^{13}\text{C}\{^1\text{H}\}$  NMR ( $\text{C}_6\text{D}_6$ , 125.8 MHz, 298 K):  $\delta$  42.4 (s,  $\text{TiNMe}_2$ ), 45.9 (d,  $J_{\text{PC}} = 20.2$  Hz,  $\text{PCH}_2$ ), 117.7 and 129.7 (s, Ph *o-C* and *m-C*), 120.9 (s, Ph *p-C*), 154.2 (m, *ipso-C*).  $^{31}\text{P}\{^1\text{H}\}$  NMR ( $\text{C}_6\text{D}_6$ , 202.5 MHz, 298 K):  $\delta$  -65.6 (s). Anal. Calc'd for  $\text{C}_{23}\text{H}_{27}\text{N}_4\text{PTi}$ : F.W.: 438.33. C, 63.02; H, 6.21; N, 12.78. Found: C, 63.24; H, 6.25 N, 12.44.

**$\text{P}(\text{CH}_2\text{N-3,5-Me}_2\text{C}_6\text{H}_3)_3\text{TiNMe}_2$  (2c).** A solution of  $\text{Ti}(\text{NMe}_2)_4$  (2.63 g, 11.73 mmol) in toluene (50 mL) was added to a solution of **1c** (5.08 g, 11.73 mmol) in 50 mL toluene. The solution gradually turned dark red over 24 H. The solution was

evaporated to dryness, and 5 mL pentane and 10 mL hexamethyldisiloxane were added. The solution was filtered and the dark red solid dried under vacuum (5.62 g, 92 %). X-ray quality crystals were obtained from slow evaporation of a pentane solution.  $^1\text{H}$  NMR ( $\text{C}_6\text{D}_6$ , 500 MHz, 298 K):  $\delta$  2.22 (s, 18H, ArCH $\underline{3}$ ), 3.15 (s, 6H, NMe $\underline{2}$ ), 3.95 (d,  $^2J_{\text{PH}} = 7.3$  Hz, 6H, PCH $\underline{2}$ ), 6.49 (s, 6H, *o*-H), 6.53 (s, 3H, *p*-H).  $^{13}\text{C}\{^1\text{H}\}$  NMR ( $\text{C}_6\text{D}_6$ , 125.8 MHz, 298 K):  $\delta$  222.2 (s, ArCH $\underline{3}$ ), 42.8 (s, NMe $\underline{2}$ ), 46.3 (d,  $J_{\text{PC}} = 19.9$  Hz, PCH $\underline{2}$ ), 115.9, 122.7, and 138.7 (s, PH *o*-C, *m*-C and *p*-C), 154.4 (d,  $^3J = 1.6$  Hz, *ipso*-C).  $^{31}\text{P}\{^1\text{H}\}$  NMR ( $\text{C}_6\text{D}_6$ , 202.5 MHz, 298 K):  $\delta$  -61.6 (s). Anal. Calc'd for  $\text{C}_{29}\text{H}_{39}\text{N}_4\text{PTi}$ , F.W.: 522.49. C, 66.66; H, 7.52; N, 10.72. Found: C, 67.02; H, 7.71; N, 11.01.

**P[(CH $\underline{2}$ N-3,5-(CF $\underline{3}$ ) $\underline{2}$ C $\underline{6}$ H $\underline{3}$ ) $\underline{3}$ Ta=N $\underline{t}$ Bu (3a).** A solution of (Et $\underline{2}$ N) $\underline{3}$ Ta=N $\underline{t}$ Bu (234.3 mg, 0.5 mmol) in 10 mL toluene was added to a solution of **1b** (379 mg, 0.5 mmol) in 30 mL toluene. The solution was stirred overnight. The solvent was removed under vacuum and the remaining pale yellow solid was rinsed with a small portion of pentane, and then dried under vacuum (315 mg, 60 %).  $^1\text{H}$  NMR ( $\text{C}_6\text{D}_6$ , 300 MHz, 298 K):  $\delta$  1.65 (s, 9H, Ta=NCMe $\underline{3}$ ), 3.10 (d, 6H,  $^2J_{\text{PH}} = 6.7$  Hz, PCH $\underline{2}$ ), 7.15 (s, 3H, Ph *p*-H), 7.54 (s, 6H, Ph *o*-H).  $^{13}\text{C}\{^1\text{H}\}$  NMR ( $\text{C}_6\text{D}_6$ , 125.8 MHz, 298 K):  $\delta$  32.6 (s, 9H, Ta=NCMe $\underline{3}$ ), 41.8 (d,  $J_{\text{PC}} = 30.1$  Hz, PCH $\underline{2}$ ), 70.4 (s, Ta=NCMe $\underline{3}$ ), 118.4 and 129.6 (s, Ph *o*-C and *m*-C), 125.9 (s, Ph *p*-C), 132.8 (q,  $J = 32.9$  Hz, Ph C-F $\underline{3}$ ), 152.5 (s, *ipso*-C).  $^{31}\text{P}\{^1\text{H}\}$  NMR ( $\text{C}_6\text{D}_6$ , 121.5 MHz, 298 K):  $\delta$  -108.5 (s).  $^{19}\text{F}\{^1\text{H}\}$  NMR ( $\text{C}_6\text{D}_6$ , 282.1 MHz, 298 K):  $\delta$  14.2 (s). Anal. Calc'd for  $\text{C}_{31}\text{H}_{24}\text{F}_{18}\text{N}_4\text{PTa}\cdot(0.5$

$C_7H_8$ ): C, 39.34; H, 2.7; N, 5.32. Found: C, 39.71; H, 3.30; N, 5.29.

**$P(CH_2NPh)_3Ta=N^tBu$  (3b).** Prepared in an analogous manner to **3a** using  $(Et_2N)_3Ta=N^tBu$  (234.3 mg, 0.5 mmol) and **1b** (173 mg, 0.5 mmol). Yield 389 mg (65 %).  $^1H$  NMR ( $C_6D_6$ , 500.1 MHz, 298 K):  $\delta$  1.62 (s, 9H,  $Ta=NCMe_3$ ), 3.67 (d, 6H,  $^2J_{PH} = 7.3$  Hz,  $PCH_2$ ), 6.90 (t, 6H,  $^3J_{HH} = 7.3$  Hz, Ph *o-H*), 7.27 (t, 3H,  $^3J_{HH} = 7.8$  Hz, Ph *p-H*), 7.40 (m, 6H, Ph *m-H*).  $^{13}C\{^1H\}$  NMR ( $C_6D_6$ , 125.8 MHz, 298 K):  $\delta$  33.8 (s,  $Ta=NCMe_3$ ), 42.6 (d,  $J_{PC} = 26.8$  Hz,  $PCH_2$ ), 69.1 (s,  $Ta=NCMe_3$ ), 119.1 and 129.1 (s, Ph *o-C* and *m-C*), 121.5 (s, Ph *p-C*), 152.3 (s, *ipso-C*).  $^{31}P\{^1H\}$  NMR ( $C_6D_6$ , 202.5 MHz, 298 K):  $\delta$  -100.9 (s). Anal. Calc'd for  $C_{25}H_{30}N_4PTa$ : F.W.: 598.45. C, 50.17; H, 5.05; N, 9.36. Found: C, 50.65; H, 5.25; N, 9.01.

**$P(CH_2N-3,5-Me_2C_6H_3)_3Ta=N^tBu$  (3c).** Prepared in an analogous manner to **3a** using  $(Et_2N)_3Ta=N^tBu$  (234.3 mg, 0.5 mmol) and **1c** (215 mg, 0.5 mmol) and a reaction time of 72 h. Yield 204.6 mg (60 %). X-ray quality crystals were obtained from slow evaporation of the benzene solution.  $^1H$  NMR ( $C_6D_6$ , 300 MHz, 298 K):  $\delta$  1.71 (s, 9H,  $Ta=NCMe_3$ ), 2.32 (s, 18H,  $ArCH_3$ ), 3.73 (d,  $^2J_{PH} = 6.7$  Hz, 6H,  $PCH_2$ ), 6.61 (s, 6H, *o-H*), 7.11 (s, 3H, *p-H*).  $^{13}C\{^1H\}$  NMR ( $C_6D_6$ , 125.8 MHz, 298 K):  $\delta$  821.9 (s,  $ArCH_3$ ), 33.6 (s, 9H,  $Ta=NCMe_3$ ), 42.7 (d,  $J_{PC} = 26.3$  Hz,  $NMe_2$ ), 68.9 (s,  $Ta=NCMe_3$ ), 116.2 (s, Ph *o-C*), 117.9 (s, Ph *m-C*), 138.7 (s, Ph *p-C*), 152.5 (s, *ipso-C*).  $^{31}P\{^1H\}$  NMR ( $C_6D_6$ , 202.5 MHz, 298 K):  $\delta$  -100.1 (s). Anal. Calc'd for  $C_{31}H_{42}N_4PTa$ , F.W.: 682.61. C, 54.55; H, 6.20; N, 8.21. Found: C, 54.07; H, 6.11; N,

8.77.

$(\text{CO})_3\text{Ni}(\text{CH}_2\text{N-3,5-Me}_2\text{C}_6\text{H}_3)_3\text{TiNMe}_2$  (**4**). Excess  $\text{Ni}(\text{CO})_4$  was vacuum transferred onto a solution of **2c** (1.25 g, 2.87 mmol) in 50 mL toluene. The dark red solution was stirred 5 min and then evaporated to dryness to provide a dark red product (1.77 g, 93 %). The product was stable for short durations in  $\text{CH}_2\text{Cl}_2$ , as judged by  $^{31}\text{P}\{^1\text{H}\}$  NMR spectroscopy, and the IR spectrum of a 0.05 M solution was obtained in this solvent. Solutions kept at room temperature are not stable and gradually undergo ligand redistribution with loss of  $\text{Ni}(\text{CO})_4$ , and thus should be handled with care.  $^1\text{H}$  NMR ( $\text{C}_6\text{D}_6$ , 500 MHz, 298 K):  $\delta$  2.17 (s, 18H, Ar $\underline{\text{CH3}}$ ), 3.06 (s, 6H, N $\underline{\text{Me}_2}$ ), 4.07 (s, 6H, P $\underline{\text{CH}_2}$ ), 6.46 (s, 6H, *o*-H), 6.52 (s, 3H, *p*-H).  $^{13}\text{C}\{^1\text{H}\}$  NMR ( $\text{C}_6\text{D}_6$ , 125.8 MHz, 298 K):  $\delta$  22.0 (s, Ar $\underline{\text{CH3}}$ ), 42.9 (s, N $\underline{\text{Me}_2}$ ), 52.5 (d,  $J_{\text{PC}} = 15.5$  Hz, P $\underline{\text{CH}_2}$ ), 116.1, 123.6, and 139.1 (s, Ph *o*- $\underline{\text{C}}$ , *m*- $\underline{\text{C}}$  and *p*- $\underline{\text{C}}$ ), 153.8 (d,  $^3J_{\text{PC}} = 6.9$  Hz, *ipso*- $\underline{\text{C}}$ ), 196.3 (d,  $^2J_{\text{PC}} = 1.1$  Hz,  $\text{Ni}(\text{CO})_3$ ).  $^{31}\text{P}\{^1\text{H}\}$  NMR ( $\text{C}_6\text{D}_6$ , 202.5 MHz, 298 K):  $\delta$  4.1 (s). Anal. Calc'd for  $\text{C}_{32}\text{H}_{39}\text{N}_4\text{O}_3\text{PTi}$ : F.W.: 665.21; C, 57.78; H, 5.91; N, 8.42. Found: C, 58.01; H, 5.94; N, 8.39. IR: ( $\text{CH}_2\text{Cl}_2$ , 0.05M) 2073.7  $\text{cm}^{-1}$  (s,  $A_1$ ), 2041.0  $\text{cm}^{-1}$  (w), 2000.0  $\text{cm}^{-1}$  (br,  $E$ ).

$(\text{CO})_2\text{Ni}[(\text{CH}_2\text{N-3,5-Me}_2\text{C}_6\text{H}_3)_3\text{TiNMe}_2]_2$  (**5**). Solid **1c** (482.8 mg, 0.924mmol) was added to a solution of **4** (614.9mg, 0.924mmol) in 50 mL toluene. The solution was stirred for 48 h and evaporated to dryness, and 15 mL pentane was added. The solution was filtered and the remaining dark red solid was rinsed with a small

portion of pentane, and then dried under vacuum. The complex is slightly soluble in pentane, and X-ray crystals were obtained by cooling a pentane solution to  $-40\text{ }^{\circ}\text{C}$ .  $^1\text{H}$  NMR ( $\text{C}_6\text{D}_6$ , 500 MHz, 298 K):  $\delta$  2.17 (s, 18H, ArCH<sub>3</sub>), 3.06 (s, 6H, NMe<sub>2</sub>),  $^1\text{H}$  NMR ( $\text{C}_6\text{D}_6$ , 500 MHz, 298 K):  $\delta$  2.15 (s, 18H, ArCH<sub>3</sub>), 3.12 (s, 6H, NMe<sub>2</sub>), 4.37 (s, 6H, PCH<sub>2</sub>), 6.51 (s, 3H, *p*-H), 6.56 (s, 6H, *o*-H).  $^{13}\text{C}\{^1\text{H}\}$  NMR ( $\text{C}_6\text{D}_6$ , 125.8 MHz, 298 K):  $\delta$  22.0 (s, ArCH<sub>3</sub>), 42.9 (s, NMe<sub>2</sub>), 54.0 (vt,  $J_{\text{PC}} = 15.5\text{ Hz}$ , PCH<sub>2</sub>), 116.0, 123.4, and 139.0 (s, Ph *o*-C, *m*-C and *p*-C), 153.8 (d,  $^3J_{\text{PC}} = 6.9\text{ Hz}$ , *ipso*-C), 190.0 (t,  $^2J_{\text{PC}} = 1.1\text{ Hz}$ , Ni(CO)<sub>3</sub>).  $^{31}\text{P}\{^1\text{H}\}$  NMR ( $\text{C}_6\text{D}_6$ , 202.5 MHz, 298 K):  $\delta$  7.03 (s). Anal. Calc'd for  $\text{C}_{60}\text{H}_{78}\text{N}_8\text{NiO}_2\text{P}_2\text{Ti}_2$ : F.W.: 1159.69; C, 62.14; H, 6.78; N, 9.66. Found: C, 62.33; H, 6.96; N, 9.47.

***trans*-RhCl(CO)(1a)<sub>2</sub> (6a).** A solution of **1a** (60.8mg, 0.08 mmol) in 0.4 mL of CD<sub>2</sub>Cl<sub>2</sub> was added to [RhCl(CO)<sub>2</sub>]<sub>2</sub> (7.8mg, 0.02 mmol) in 0.4 mL CD<sub>2</sub>Cl<sub>2</sub>. Gas evolution was observed and the solution turned dark orange over the course of 20 min.  $^1\text{H}$  NMR (CD<sub>2</sub>Cl<sub>2</sub>, 300 MHz, 298 K):  $\delta$  3.1 (s, 6H, PCH<sub>2</sub>), 4.82 (s, 3H, NH), 7.05 (s, 6H, Ph *o*-H), 7.24 (s, 3H, Ph *p*-H).  $^{13}\text{C}\{^1\text{H}\}$  NMR (CD<sub>2</sub>Cl<sub>2</sub>, 125.8 MHz, 298 K):  $\delta$  39.1 (s, PCH<sub>2</sub>), 112.8 (s, CO), 113.2 and 122.1 (s, Ph *o*-C and *m*-C), 118.5 (s, Ph *p*-C), 132.9 (q,  $J = 33.1\text{ Hz}$ , Ph C-F<sub>3</sub>), 148.9 (s, *ipso*-C).  $^{31}\text{P}\{^1\text{H}\}$  NMR (CD<sub>2</sub>Cl<sub>2</sub>, 121.5 MHz, 298 K):  $\delta$  22.6 (d,  $J_{\text{PRh}} = 120.1\text{ Hz}$ ).  $^{19}\text{F}\{^1\text{H}\}$  NMR (CD<sub>2</sub>Cl<sub>2</sub>, 282.1 MHz, 298 K):  $\delta$  14.00 (s). IR: 1984.9 cm<sup>-1</sup>.

***trans*-RhCl(CO)(1b)<sub>2</sub> (6b).** A solution of 28.0 mg (0.08 mmol) of **1b** in 0.4 mL of

CD<sub>2</sub>Cl<sub>2</sub> was added to [RhCl(CO)<sub>2</sub>]<sub>2</sub> (7.8 mg, 0.02 mmol) in 0.4 mL CD<sub>2</sub>Cl<sub>2</sub>. <sup>1</sup>H NMR (CD<sub>2</sub>Cl<sub>2</sub>, 300.1 MHz, 298 K): δ 3.95 (s, 6H, PCH<sub>2</sub>), 4.28 (b, 3H, NH), 6.78 (m, 6H, Ph *o*-H), 7.20 (t, 3H, Ph *p*-H), 7.35 (s, 6H, Ph *m*-H). <sup>13</sup>C{<sup>1</sup>H} NMR (CD<sub>2</sub>Cl<sub>2</sub>, 125.8 MHz, 298 K): δ 39.7 (t, J<sub>PC</sub> = 14.5 Hz, PCH<sub>2</sub>), 114.2 (s, CO), 119.3 and 129.9 (s, Ph *o*-C and *m*-C), 128.8 (s, Ph *p*-C), 148.2 (m, *ipso*-C). <sup>31</sup>P{<sup>1</sup>H} NMR (CD<sub>2</sub>Cl<sub>2</sub>, 202.5 MHz, 298 K): δ 23.7 (d, J<sub>PRh</sub> = 118.1 Hz). IR: 1976.3 cm<sup>-1</sup>.

***trans*-RhCl(CO)(1c)<sub>2</sub> (6c).** A solution of 1c (34.4 mg, 0.08 mmol) in 0.4 mL of CD<sub>2</sub>Cl<sub>2</sub> was added to [RhCl(CO)<sub>2</sub>]<sub>2</sub> (7.8 mg, 0.02 mmol) in 0.4 mL CD<sub>2</sub>Cl<sub>2</sub>. <sup>1</sup>H NMR (CD<sub>2</sub>Cl<sub>2</sub>, 300 MHz, 298 K): δ 2.20 (s, 18H, PH CH<sub>3</sub>), 3.93 (s, 6H, PCH<sub>2</sub>), 4.24 (b, 3H, NH), 6.32 (s, 6H, Ph *o*-H), 6.43 (s, 3H, Ph *p*-H). <sup>13</sup>C{<sup>1</sup>H} NMR (CD<sub>2</sub>Cl<sub>2</sub>, 125.8 MHz, 298 K): δ 21.7 (s, Ph CH<sub>3</sub>), 39.6 (t, J<sub>PC</sub> = 13.4 Hz, PCH<sub>2</sub>), 116.0 (s, CO), 112.0 and 121.2 (s, Ph *o*-C and *m*-C), 139.6 (s, Ph *p*-C), 148.3 (t, *ipso*-C). <sup>31</sup>P{<sup>1</sup>H} NMR (CD<sub>2</sub>Cl<sub>2</sub>, 121.5 MHz, 298 K): δ 23.5 (d, J<sub>PRh</sub> = 116.9 Hz). IR: 1973.2 cm<sup>-1</sup>.

***trans*-RhCl(CO)(2a)<sub>2</sub> (7a).** A solution of 2a (64.1 mg, 0.08 mmol) in 0.4 mL of CD<sub>2</sub>Cl<sub>2</sub> was added to [RhCl(CO)<sub>2</sub>]<sub>2</sub> (7.8 mg, 0.02 mmol) in 0.4 mL CD<sub>2</sub>Cl<sub>2</sub>. <sup>1</sup>H NMR (CD<sub>2</sub>Cl<sub>2</sub>, 300 MHz, 298 K): δ 3.5 (s, 6H, NCH<sub>3</sub>), 4.8 (s, PCH<sub>2</sub>), 7.29 (s, 6H, Ph *o*-H), 7.54 (s, 3H, Ph *p*-H). <sup>13</sup>C{<sup>1</sup>H} NMR (CD<sub>2</sub>Cl<sub>2</sub>, 125.8 MHz, 298 K): δ 42.7 (s, TiNCH<sub>3</sub>), 49.3 (s, PCH<sub>2</sub>), 115.2 (s, CO), 113.4 and 122.1 (s, Ph *o*-C and *m*-C), 117.3 (s, Ph *p*-C), 133.1 (q, J = 32.8 Hz, Ph C-F<sub>3</sub>), 153.2 (s, *ipso*-C). <sup>31</sup>P{<sup>1</sup>H} NMR (CD<sub>2</sub>Cl<sub>2</sub>, 121.5 MHz, 298 K): δ 3.8 (d, J<sub>PRh</sub> = 130.3 Hz). <sup>19</sup>F{<sup>1</sup>H} NMR (CD<sub>2</sub>Cl<sub>2</sub>,

282.1 MHz, 298 K):  $\delta$  14.3 (s). IR: 1988.1  $\text{cm}^{-1}$ .

***trans*-RhCl(CO)(2b)<sub>2</sub> (7b).** A solution of **2b** (35.2 mg, 0.08 mmol) in 0.4 mL of CD<sub>2</sub>Cl<sub>2</sub> was added to 7.8 mg (0.02 mmol) of [RhCl(CO)<sub>2</sub>]<sub>2</sub> in 0.4 mL CD<sub>2</sub>Cl<sub>2</sub>. <sup>1</sup>H NMR (CD<sub>2</sub>Cl<sub>2</sub>, 300 MHz, 298 K):  $\delta$  3.3 (s, 6H, TiNMe<sub>2</sub>), 4.6 (s, PCH<sub>2</sub>), 6.82 (d, 6H, <sup>3</sup>J<sub>HH</sub> = 7.8 Hz, Ph *o*-H), 6.89 (t, 3H, Ph *p*-H), 7.30 (t, 6H, Ph *m*-H). <sup>13</sup>C{<sup>1</sup>H} NMR (CD<sub>2</sub>Cl<sub>2</sub>, 125.8 MHz, 298 K):  $\delta$  43.0 (s, TiNMe<sub>2</sub>), 49.7 (s, PCH<sub>2</sub>), 117.5 (s, CO), 117.7 and 129.7 (s, Ph *o*-C and *m*-C), 121.6 (s, Ph *p*-C), 153.5 (m, *ipso*-C). <sup>31</sup>P{<sup>1</sup>H} NMR (CD<sub>2</sub>Cl<sub>2</sub>, 202.5 MHz, 298 K):  $\delta$  15.7 (d, J<sub>PRh</sub> = 125.8 Hz). IR: 1979.6  $\text{cm}^{-1}$ .

***trans*-RhCl(CO)(2c)<sub>2</sub> (7c).** A solution of **2c** (42.0 mg, 0.08 mmol) in 0.4 mL of CD<sub>2</sub>Cl<sub>2</sub> was added to [RhCl(CO)<sub>2</sub>]<sub>2</sub> (7.8 mg, 0.02 mmol) in 0.4 mL CD<sub>2</sub>Cl<sub>2</sub>. <sup>1</sup>H NMR (CD<sub>2</sub>Cl<sub>2</sub>, 300 MHz, 298 K):  $\delta$  2.28 (s, 18H, ArCH<sub>3</sub>), 3.26 (s, 6H, NMe<sub>2</sub>), 4.56 (s, 6H, PCH<sub>2</sub>), 6.46 (s, 6H, Ph *o*-H), 6.47 (s, 3H, Ph *p*-H). <sup>13</sup>C{<sup>1</sup>H} NMR (CD<sub>2</sub>Cl<sub>2</sub>, 125.8 MHz, 298 K):  $\delta$  21.9 (s, ArCH<sub>3</sub>), 43.3 (s, NMe<sub>2</sub>), 49.6 (s, PCH<sub>2</sub>), 112.1 (s, CO), 115.6, 123.2, and 139.2 (s, Ph *o*-C, *m*-C and *p*-C), 153.5 (s, Ph *ipso*-C). <sup>31</sup>P{<sup>1</sup>H} NMR (CD<sub>2</sub>Cl<sub>2</sub>, 202.5 MHz, 298 K):  $\delta$  18.51 (d, J<sub>PRh</sub> = 122.5 Hz). IR: 1974.8  $\text{cm}^{-1}$ .

***trans*-RhCl(CO)(3a)<sub>2</sub> (8a).** A solution of **3a** (80.5 mg, 0.08 mmol) in 0.4 mL of CD<sub>2</sub>Cl<sub>2</sub> was added to 7.8 mg (0.02 mmol) of [RhCl(CO)<sub>2</sub>]<sub>2</sub> in 0.4 mL CD<sub>2</sub>Cl<sub>2</sub>. <sup>1</sup>H NMR (CD<sub>2</sub>Cl<sub>2</sub>, 300 MHz, 298 K):  $\delta$  1.59 (s, 9H, Ta=NCMe<sub>3</sub>), 4.90 (s, PCH<sub>2</sub>), 7.55 (s,

3H, Ph *p*-H), 7.82 (s, 6H, Ph *o*-H).  $^{13}\text{C}\{^1\text{H}\}$  NMR ( $\text{CD}_2\text{Cl}_2$ , 125.8 MHz, 298 K):  $\delta$  32.9 (s, 9H, Ta=NCMe<sub>3</sub>), 53.3 (d,  $J_{\text{PC}} = 30.1$  Hz, PCH<sub>2</sub>), 72.2 (s, Ta=NCMe<sub>3</sub>), 116.2 and 129.6 (s, Ph *o*-C and *m*-C), 125.9 (s, Ph *p*-C), 132.8 (q,  $J = 33.2$  Hz, Ph C-F<sub>3</sub>), 152.8 (t, *ipso*-C).  $^{31}\text{P}\{^1\text{H}\}$  NMR ( $\text{CD}_2\text{Cl}_2$ , 121.5 MHz, 298 K):  $\delta$  -34.2 (d,  $J_{\text{PRh}} = 143.6$  Hz).  $^{19}\text{F}\{^1\text{H}\}$  NMR ( $\text{CD}_2\text{Cl}_2$ , 282.1 MHz, 298 K):  $\delta$  14.9 (s). IR: 1990.5  $\text{cm}^{-1}$ .

***trans*-RhCl(CO)(3b)<sub>2</sub> (8b).** A solution of **3b** (48.0 mg, 0.08 mmol) in 0.4 mL of  $\text{CD}_2\text{Cl}_2$  was added to  $[\text{RhCl}(\text{CO})_2]_2$  (7.8 mg, 0.02 mmol) in 0.4 mL  $\text{CD}_2\text{Cl}_2$ .  $^1\text{H}$  NMR ( $\text{CD}_2\text{Cl}_2$ , 300.1 MHz, 298 K):  $\delta$  1.59 (s, 9H, Ta=NCMe<sub>3</sub>), 4.82 (s, PCH<sub>2</sub>), 6.95 (t, 6H,  $^3J_{\text{HH}} = 7.3$  Hz, Ph *o*-H), 7.3 (t, 3H,  $^3J_{\text{HH}} = 7.8$  Hz, Ph *p*-H), 7.44 (d, 6H, Ph *m*-H).  $^{13}\text{C}\{^1\text{H}\}$  NMR ( $\text{CD}_2\text{Cl}_2$ , 125.8 MHz, 298 K):  $\delta$  32.9 (s, Ta=NCMe<sub>3</sub>), 46.7 (s, PCH<sub>2</sub>), 69.8 (s, Ta=NCMe<sub>3</sub>), 117.7 (s, CO), 118.4 and 128.5 (s, Ph *o*-C and *m*-C), 121.3 (s, Ph *p*-C), 151.0 (s, *ipso*-C).  $^{31}\text{P}\{^1\text{H}\}$  NMR ( $\text{CD}_2\text{Cl}_2$ , 202.5 MHz, 298 K):  $\delta$  -32.8 (d,  $J_{\text{PRh}} = 138.11$  Hz). IR: 1986.7  $\text{cm}^{-1}$ .

***trans*-RhCl(CO)(3c)<sub>2</sub> (8c).** A solution of **3c** (54.6 mg, 0.08 mmol) in 0.4 mL of  $\text{CD}_2\text{Cl}_2$  was added to 7.8 mg (0.02 mmol) of  $[\text{RhCl}(\text{CO})_2]_2$  in 0.4 mL  $\text{CD}_2\text{Cl}_2$ . X-ray quality crystals were obtained from slow evaporation of the  $\text{CD}_2\text{Cl}_2$  solution at  $-40$  °C.  $^1\text{H}$  NMR ( $\text{CD}_2\text{Cl}_2$ , 300 MHz, 298 K):  $\delta$  1.63 (s, 9H, Ta=NCMe<sub>3</sub>), 2.32 (s, 18H, ArCH<sub>3</sub>), 4.77 (s, 6H, PCH<sub>2</sub>), 6.61 (s, 6H, *o*-H), 7.08 (s, 3H, *p*-H).  $^{13}\text{C}\{^1\text{H}\}$  NMR ( $\text{CD}_2\text{Cl}_2$ , 125.8 MHz, 298 K):  $\delta$  21.7 (s, ArCH<sub>3</sub>), 33.5 (s, Ta=NCMe<sub>3</sub>), 47.4 (s,

$NMe_2$ ), 70.4 (s, Ta=N $\underline{C}Me_3$ ), 116.3 (s,  $\underline{C}O$ ), 116.9 (s, Ph  $o$ - $\underline{C}$ ), 123.9 (s, Ph  $m$ - $\underline{C}$ ), 138.9 (s, Ph  $p$ - $\underline{C}$ ), 151.9 (s,  $ipso$ - $\underline{C}$ ).  $^{31}P\{^1H\}$  NMR ( $CD_2Cl_2$ , 202.5 MHz, 298 K):  $\delta$  -32.3 (d,  $J_{PRh} = 136.9$  Hz). IR: 1986.6  $cm^{-1}$ . Anal. Calc'd for  $C_{63}H_{84}N_8OCIP_2Ta_2$ : C, 49.40; H, 5.53; N, 7.32. Found: C, 49.09; H, 5.64; N, 7.27.

**[CpNiP(CH<sub>2</sub>NHPh)<sub>2</sub>]<sub>2</sub> (9).** NiCp<sub>2</sub> (2.37 g, 12.5 mmol) was added to a solution of P(CH<sub>2</sub>NHPh)<sub>3</sub> (3.46 g, 10 mmol) in 50 mL of toluene. The solution was stirred 2 weeks. The solvent was removed under vacuum and the remaining dark red solid was rinsed with a small portion of pentane, and then dried under vacuum (2.09 g, 57 %). X-ray quality crystals were obtained from slow evaporation of a toluene solution.  $^1H$  NMR ( $C_6D_6$ , 300 MHz, 298 K):  $\delta$  3.15 (d,  $^2J_{PH} = 6.2$  Hz, 8H, P $\underline{C}H_2$ ), 4.02 (b, 4H, N $\underline{H}$ ), 4.91 (s, 10H,  $C_5$  $\underline{H}_5$ ), 6.65 (d,  $^3J_{HH} = 7.8$  Hz, 8H, Ph  $o$ - $\underline{H}$ ), 6.79 (t,  $^3J_{HH} = 7.3$  Hz, 4H, Ph  $p$ - $\underline{H}$ ), 7.20 (t,  $^3J_{HH} = 8.3$  Hz, 8H, Ph  $m$ - $\underline{H}$ ).  $^{13}C\{^1H\}$  NMR ( $C_6D_6$ , 125.8 MHz, 298 K):  $\delta$  45.77 (s, P $\underline{C}H_2$ ), 88.7 (s,  $\underline{C}_5H_5$ ), 114.0 and 118.8 (s, Ph  $o$ - $\underline{C}$  and  $m$ - $\underline{C}$ ), 130.2 (s, Ph  $p$ - $\underline{C}$ ), 148.9 (s, Ph  $ipso$ - $\underline{C}$ ).  $^{31}P\{^1H\}$  NMR ( $C_6D_6$ , 121.5 MHz, 298 K):  $\delta$  -87.5 (s). Anal. Calc'd for  $C_{34}H_{42}N_4P_2Ni_2$ , F.W.: 734.10; C, 62.17; H, 5.77; N, 7.63. Found: C, 61.80; H, 5.98, N, 7.44.

**Ni[P(CH<sub>2</sub>NHPh)<sub>3</sub>]<sub>4</sub> (10).** [P(CH<sub>2</sub>NHPh)<sub>3</sub>] (28 mg, 0.08 mmol) was added to a solution of Ni(COD)<sub>4</sub> (5.6 mg, 0.02mmol) in 0.8 mL of  $C_6D_6$ .  $^1H$  NMR ( $C_6D_6$ , 300 MHz, 298 K):  $\delta$  3.55 (d,  $^2J_{PH} = 4.8$  Hz, 6H, P $\underline{C}H_2$ ), 4.75 (b, 3H, N $\underline{H}$ ), 6.58 (d,  $^3J_{HH} = 7.9$  Hz, 6H, Ph  $o$ - $\underline{H}$ ), 6.74 (t,  $^3J_{HH} = 7.3$  Hz, 3H, Ph  $p$ - $\underline{H}$ ), 7.05 (t,  $^3J_{HH} = 7.6$  Hz, 6H,

Ph *m-H*).  $^{13}\text{C}\{^1\text{H}\}$  NMR ( $\text{C}_6\text{D}_6$ , 125.8 MHz, 298 K):  $\delta$  47.3 (p,  $J_{\text{PC}} = 9.9$  Hz,  $\text{PCH}_2$ ), 114.9 and 130.0 (s, Ph *o-C* and *m-C*), 119.9 (s, Ph *p-C*), 148.2 (s, Ph *ipso-C*).  $^{31}\text{P}\{^1\text{H}\}$  NMR ( $\text{C}_6\text{D}_6$ , 121.5 MHz, 298 K):  $\delta$  15.9 (s).

$[\text{CpNiP}(\text{CH}_2\text{NPh})_2\text{Ti}(\text{NMe}_2)_2]_2$  (11).  $\text{Ti}(\text{NMe}_2)_4$  (448.34 mg, 2 mmol) was added to a solution of  $[\text{CpNiP}(\text{CH}_2\text{NHP})_2]_2$  (734.10 mg, 1 mmol) in 50 mL of toluene. The solution was stirred 2 days. The solvent was removed under vacuum and the remaining dark red solid was rinsed with a small portion of pentane, and then dried under vacuum (901 mg, 89.8 %). X-ray quality crystals were obtained from slow evaporation of a toluene solution.  $^1\text{H}$  NMR ( $\text{C}_6\text{D}_6$ , 300 MHz, 298 K):  $\delta$  3.04 (s, 24H,  $\text{NMe}_2$ ), 4.4 (s, 8H,  $\text{PCH}_2$ ), 5.02 (s, 10H,  $\text{C}_5\text{H}_5$ ), 6.87 (t,  $^3J_{\text{HH}} = 7.3$  Hz, 4H, Ph *p-H*), 7.19 (m, 8H, Ph *o-H*), 7.29 (t,  $^3J_{\text{HH}} = 7.8$  Hz, 8H, Ph *m-H*).  $^{13}\text{C}\{^1\text{H}\}$  NMR ( $\text{C}_6\text{D}_6$ , 125.8 MHz, 298 K):  $\delta$  45.77 (s,  $\text{PCH}_2$ ), 88.7 (s,  $\text{C}_5\text{H}_5$ ), 114.0 and 118.8 (s, Ph *o-C* and *m-C*), 130.2 (s, Ph *p-C*), 148.9 (s, Ph *ipso-C*).  $^{31}\text{P}\{^1\text{H}\}$  NMR ( $\text{C}_6\text{D}_6$ , 121.5 MHz, 298 K):  $\delta$  -80.5 (s). Anal. Calc'd for  $\text{C}_{46}\text{H}_{62}\text{N}_8\text{P}_4\text{Ni}_2\text{Ti}_2$ , F.W.: 1002.11; C, 55.13; H, 6.24; N, 11.18. Found: C, 55.42; H, 6.62, N, 11.02.

**X-ray Crystallography.** The X-ray structures were obtained at low temperature, with each crystal covered in Paratone and placed rapidly into the cold  $\text{N}_2$  stream of the Kryo-Flex low-temperature device. The data were collected using the SMART software on a Bruker APEX CCD diffractometer using a graphite monochromator with  $\text{Mo K}\alpha$  radiation ( $\lambda = 0.71073$  Å). A hemisphere of data was collected using a

counting time of 10 to 30 s per frame. Details of crystal data, data collection, and structure refinement are listed in Table 2.3. Data reductions were performed using the SAINT software, and the data were corrected for absorption using SADABS. The structures were solved by direct methods using SIR97 and refined by full-matrix least-squares on  $F^2$  with anisotropic displacement parameters for the non-H atoms using SHELXL-97 and the WinGX software package, and thermal ellipsoid plots were produced using ORTEP32.<sup>70</sup> The thermal parameters for the carbonyl fragment in **8c** were modeled isotropically, due to problems arising from its three-fold disorder.

### 2.11.3 Crystal Data and Structure Refinement

**Table 2.3.** Crystallographic data for compounds **1a**, **2a-c**, **3b**, **5**, **8c**, **9** and **11**

	<b>1a</b>	<b>2a</b>	<b>2b</b>
Empirical Formula	C <sub>27</sub> H <sub>18</sub> F <sub>18</sub> N <sub>3</sub> P	C <sub>34</sub> H <sub>24</sub> F <sub>18</sub> N <sub>4</sub> PTi	C <sub>23</sub> H <sub>27</sub> N <sub>4</sub> PTi
Formula Weight	757.41	909.44	439.33
Crystal System	Orthorhombic	Orthorhombic	Monoclinic
<i>a</i>	15.620(2) Å	31.221(4) Å	11.9600(8) Å
<i>b</i>	16.410(2) Å	13.8559(17) Å	14.4825(9) Å
<i>c</i>	22.386(3) Å	17.048(2) Å	12.8136(8) Å
$\alpha$	90°	90°	90°
$\beta$	90°	90°	90.081(1)°
$\gamma$	90°	90°	90°
V, Å <sup>3</sup>	5738.0(13)	7375.0(16)	2219.45(2)
Space Group	<i>Pbca</i>	<i>Pccn</i>	<i>P2<sub>1</sub>/n</i>
Z value	8	8	4
$\mu$ (MoK $\alpha$ )	0.239 mm <sup>-1</sup>	0.399 mm <sup>-1</sup>	0.474 mm <sup>-1</sup>
Temperature	133 K	143 K	173 K
No. Variables	505	650	264
No. of Unique Reflns	6569 ( $R_{int} = 0.0282$ )	6500 ( $R_{int} = 0.0454$ )	3903 ( $R_{int} = 0.019$ )
Residuals: R; wR <sub>2</sub> (all data)	0.077; 0.187	0.0742, 0.1692	0.034; 0.090

**Table 2.3 cont'd.**

	<b>2c</b>	<b>3b</b>	<b>5</b>
Empirical Formula	C <sub>121</sub> H <sub>168</sub> N <sub>16</sub> P <sub>4</sub> Ti <sub>4</sub>	C <sub>25</sub> H <sub>30</sub> N <sub>4</sub> P <sub>4</sub> Ta	C <sub>65</sub> H <sub>90</sub> N <sub>8</sub> NiO <sub>2</sub> Ti <sub>2</sub>
Formula Weight	2160.45	598.45	1231.90
Crystal System	Triclinic	Monoclinic	Triclinic
<i>a</i>	11.68(2) Å	27.980(3) Å	15.417(3) Å
<i>b</i>	14.93(2) Å	11.7166(12) Å	15.812(3) Å
<i>c</i>	18.19(3) Å	19.371(2) Å	16.336(3) Å
$\alpha$	92.11(3)°	90°	111.303(2)°
$\beta$	99.84(2)°	131.3410(10)°	109.839(2)°
$\gamma$	103.46(3)°	90°	95.691(2)°
V, Å <sup>3</sup>	3030(8)	4767.9(8)	3375.6(11)
Space Group	P-1	C2/c	P-1
Z value	1	8	2
$\mu$ (MoK $\alpha$ )	0.359 mm <sup>-1</sup>	4.697 mm <sup>-1</sup>	0.601 mm <sup>-1</sup>
Temperature	173 K	173 K	173 K
No. Variables	629	283	695
No. of Unique Reflns	17866 ( $R_{int} = 0.0000$ )	5417 ( $R_{int} = 0.021$ )	11867 ( $R_{int} = 0.069$ )
Residuals: R; wR <sub>2</sub> (all data)	0.1626, 0.3202	0.022; 0.046	0.109; 0.174

Table 2.3 cont'd.

	8c	9	11
Empirical formula	C <sub>63</sub> H <sub>84</sub> ClN <sub>8</sub> OP <sub>2</sub> RhTa <sub>2</sub>	C <sub>40.33</sub> H <sub>43.33</sub> N <sub>4</sub> Ni <sub>2</sub> P <sub>2</sub>	C <sub>46</sub> H <sub>62</sub> N <sub>8</sub> Ni <sub>2</sub> P <sub>2</sub> Ti <sub>2</sub>
Formula weight	1531.58	763.48	1001.46
Crystal System	Hexagonal	Triclinic	Triclinic
Space group	<i>P</i> 63/m	<i>P</i> -1	<i>P</i> -1
a	14.2228(8) Å	10.0671(13) Å	10.528(2) Å
b	14.2228(8) Å	13.8241(17) Å	10.991(2) Å
c	25.594(3) Å	21.291(3) Å	11.593(2) Å
α	90 °	108.2090(10)°	66.712(2)°
β	90 °	90.0110(10)°	78.470(2)°
γ	120 °	105.3660(10)°	87.357(2)°
Volume Å <sup>3</sup>	4483.7(6)	2702.8(6)	1206.5(4)
Z	2	3	1
μ(MoKα)	2.714 mm <sup>-1</sup>	1.169 mm <sup>-1</sup>	1.194 mm <sup>-1</sup>
Temperature	173 K	173 K	173 K
No. Variables	129	682	275
Total No. of Reflns	49687	30865	11489
No. of Unique Reflns	3513 ( <i>R</i> <sub>int</sub> = 0.0429)	12166 ( <i>R</i> <sub>int</sub> = 0.0390)	4232 ( <i>R</i> <sub>int</sub> = 0.0430)
Residuals: R; wR <sub>2</sub> (all data)	0.056; 0.1254	0.0687, 0.1215	0.0700, 0.1124

## 2.12 References

- (1) Stephan, D. W. *Coord. Chem. Rev.* **1989**, *95*, 41-107.
- (2) Wheatley, N.; Kalck, P. *Chem. Rev.* **1999**, *99*, 3379-3419.
- (3) Braunstein, P.; Naud, F. *Angew. Chem. Int. Ed.* **2001**, *40*, 680-699.
- (4) Hernandez-Gruel, M. A. F.; Perez-Torrente, J. J.; Ciriano, M. A.; Rivas, A. B.; Lahoz, F. J.; Dobrinovitch, I. T.; Oro, L. A. *Organometallics* **2003**, *22*, 1237-1249.
- (5) Kabashima, S.-i.; Kuwata, S.; Hidai, M. *J. Am. Chem. Soc.* **1999**, *121*, 7837-7845.
- (6) Graham, T. W.; Llamazares, A.; McDonald, R.; Cowie, M. *Organometallics* **1999**, *18*, 3502-3510.
- (7) Spannenberg, A.; Oberthur, M.; Noss, H.; Tillack, A.; Arndt, P.; Kempe, R. *Angew. Chem. Int. Ed.* **1998**, *37*, 2079-2082.
- (8) Renner, P.; Galka, C.; Memmler, H.; Kauper, U.; Gade, L. H. *J. Organomet. Chem.* **1999**, *591*, 71-77.
- (9) Gray, H. B.; Malmstroem, B. G. *Biochemistry* **1989**, *28*, 7499-7505.
- (10) Messerschmidt, A.; Huber, R.; Wieghardt, K.; Poulos, T. *Handbook of Metalloproteins, Volume 1*, 2001.
- (11) Christou, G.; Gatteschi, D.; Hendrickson, D. N.; Sessoli, R. *MRS Bulletin* **2000**, *25*, 66-71.
- (12) Gatteschi, D.; Sessoli, R. *Angew. Chem. Int. Ed.* **2003**, *42*, 268-297.
- (13) Alvarez-Vergara, M. C.; Casado, M. A.; Martin, M. L.; Lahoz, F. J.; Oro, L. A.; Perez-Torrente, J. J. *Organometallics* **2005**, *24*, 5929-5936.

- (14) Stang, P. J.; Persky, N. E. *Chem. Commun.* **1997**, 77-78.
- (15) Mokuolu, Q. F.; Avent, A. G.; Hitchcock, P. B.; Love, J. B. *J. Chem. Soc. Dalton Trans.* **2001**, 2551-2553.
- (16) Mokuolu, Q. F.; Duckmanton, P. A.; Hitchcock, P. B.; Wilson, C.; Blake, A. J.; Shukla, L.; Love, J. B. *Dalton Trans.* **2004**, 1960-1970.
- (17) Han, H.; Elsmaili, M.; Johnson, S. A. *Inorg. Chem.* **2006**, *45*, 7435-7445. Keen, A. L.; Doster, M.; Han, H.; Johnson, S. A. *Chem. Comm.* **2006**, 1221-1223.
- (18) Fryzuk, M. D.; Kozak, C. M.; Bowdridge, M. R.; Jin, W.; Tung, D.; Patrick, B. O.; Rettig, S. J. *Organometallics* **2001**, *20*, 3752-3761.
- (19) Gade, L. H. *Acc. Chem. Res.* **2002**, *35*, 575-582.
- (20) Gade, L. H. *J. Organomet. Chem.* **2002**, *661*, 85-94.
- (21) Jia, L.; Ding, E.; Rheingold, A. L.; Rhatigan, B. *Organometallics* **2000**, *19*, 963-965.
- (22) Frank, A. W. D., G. L. Jr. *J. Org. Chem.* **1972**, *37*, 2752-2755.
- (23) Bondi, A. *J. Phy. Chem.* **1964**, *68*, 441-451.
- (24) Shao, M.-Y.; Gau, H.-M. *Organometallics* **1998**, *17*, 4822-4827.
- (25) Feindel, K. W.; Wasylshen, R. E. *Can. J. Chem.* **2004**, *82*, 27-44.
- (26) van Doorn, J. A.; van der Heijden, H.; Orpen, A. G. *Organometallics* **1994**, *13*, 4271-4277.
- (27) Mathieu, R.; Lenzi, M.; Poilblanc, R. *Inorg. Chem.* **1970**, *9*, 2030-2034.
- (28) Bodner, G. M.; May, M. P.; McKinney, L. E. *Inorg. Chem.* **1980**, *19*, 1951-1958.
- (29) Strohmeier, W.; Mueller, F. J. *Chem. Ber.* **1967**, *100*, 2812-2821.

- (30) Tolman, C. A. *J. Am. Chem. Soc.* **1970**, *92*, 2953-2956.
- (31) Tolman, C. A. *Chem. Rev.* **1977**, *77*, 313-348.
- (32) Bunten, K. A.; Chen, L.; Fernandez, A. L.; Poe, A. J. *Coord. Chem. Rev.* **2002**, *233-234*, 41-51.
- (33) Ferguson, G.; Roberts, P. J.; Alyea, E. C.; Khan, M. *Inorg. Chem.* **1978**, *17*, 2965-2967.
- (34) Cooney Katharine, D.; Cundari Thomas, R.; Hoffman Norris, W.; Pittard Karl, A.; Temple, M. D.; Zhao, Y. *J. Am. Chem. Soc.* **2003**, *125*, 4318-4324.
- (35) Dunne, B. J.; Morris, R. B.; Orpen, A. G. *J. Chem. Soc. Dalton Trans.* **1991**, 653-661.
- (36) Rahman, M. M.; Liu, H. Y.; Eriks, K.; Prock, A.; Giering, W. P. *Organometallics* **1989**, *8*, 1-7.
- (37) Bush, R. C.; Angelici, R. J. *Inorg. Chem.* **1988**, *27*, 681-686.
- (38) Suresh, C. H.; Koga, N. *Inorg. Chem.* **2002**, *41*, 1573-1578.
- (39) Shaw, B. L.; Mann, B. E.; Masters, C. J. *J. Chem. Soc.* **1971**, 1104-1106.
- (40) Kashiwabara, K.; Taguchi, N.; Takagi, H. D.; Nakajima, K.; Suzuki, T. *Polyhedron* **1998**, *17*, 1817-1829.
- (41) Watson, W. H.; Kandala, S.; Richmond, M. G. *J. Organomet. Chem.* **2007**, *692*, 968-975.
- (42) Ruiz, J.; Garcia-Granda, S.; Diaz, M. R.; Quesada, R. *Dalton Trans.* **2006**, 4371-4376.
- (43) Kohl, S. W.; Heinemann, F. W.; Hummert, M.; Bauer, W.; Grohmann, A. *Chem.*

*Eur. J.* **2006**, *12*, 4313-4320.

(44) Watson, W. H.; Wu, G.; Richmond, M. G. *Organometallics* **2006**, *25*, 930-945.

(45) Kabir, S. E.; Miah, M. A.; Sarker, N. C.; Hussain, G. M. G.; Hardcastle, K. I.; Nordlander, E.; Rosenberg, E. *Organometallics* **2005**, *24*, 3315-3320.

(46) Knabel, K.; Klapoetke, T. M.; Noeth, H.; Paine, R. T.; Schwab, I. *Eur. J. Inorg. Chem.* **2005**, 1099-1108.

(47) Shima, T.; Suzuki, H. *Organometallics* **2005**, *24*, 1703-1708.

(48) Caballero, A.; Jalon, F. A.; Manzano, B. R.; Espino, G.; Perez-Manrique, M.; Mucientes, A.; Poblete, F. J.; Maestro, M. *Organometallics* **2004**, *23*, 5694-5706.

(49) Geldbach, T. J.; Pregosin, P. S. *Eur. J. Inorg. Chem.* **2002**, 1907-1918.

(50) Heyn, R. H.; Goerbitz, C. H. *Organometallics* **2002**, *21*, 2781-2784.

(51) Koch, T.; Blaurock, S.; Somoza, F. B., Jr.; Voigt, A.; Kirmse, R.; Hey-Hawkins, E. *Organometallics* **2000**, *19*, 4186.

(52) Dogan, J.; Schulte, J. B.; Swigers, G. F.; Wild, S. B. *J. Org. Chem.* **2000**, *65*, 4782.

(53) Kim, D. Y. *Synth. Commun.* **2000**, *30*, 1205-1212.

(54) Dogan, J.; Schulte, J. B.; Swiegers, G. F.; Wild, S. B. *J. Org. Chem.* **2000**, *65*, 951-957.

(55) Ho, J.; Stephan, D. W. *Inorg. Chem.* **1994**, *33*, 4595-4597.

(56) Macgregor, S. A. *Chem. Soc. Rev.* **2007**, *36*, 67-76.

(57) Garrou, P. E. *Chem. Rev.* **1985**, *85*, 171-185.

(58) Baker, R. T.; Fultz, W. C.; Marder, T. B.; Williams, I. D. *Organometallics* **1990**,

9, 2357-2367.

(59)Lindenberg, F.; Shribman, T.; Sieler, J.; Hey-Hawkins, E.; Eisen, M. S. *J. Organomet. Chem.* **1996**, *515*, 19-25.

(60)Amor, I.; Garcia-Vivo, D.; Garcia, M. E.; Ruiz, M. A.; Saez, D.; Hamidov, H.; Jeffery, J. C. *Organometallics* **2007**, *26*, 466-468.

(61)Zheng, P. Y.; Nadasdi, T. T.; Stephan, D. W. *Organometallics* **1989**, *8*, 1393-1398.

(62)Stephan, D. W. *Coord. Chem. Rev.* **1989**, *95*, 41.

(63)Maslennikov, S. V.; Glueck, D. S.; Yap, G. P. A.; Rheingold, A. L. *Organometallics* **1996**, *15*, 2483-2488.

(64)Leadbeater, N. E. *J. Org. Chem.* **2001**, *66*, 7539-7541.

(65)Melenkivitz, R.; Mindiola Daniel, J.; Hillhouse Gregory, L. *J. Am. Chem. Soc.* **2002**, *124*, 3846-3647.

(66)Diamond, G. M.; Jordan, R. F.; Petersen, J. L. *Organometallics* **1996**, *15*, 4030-4037.

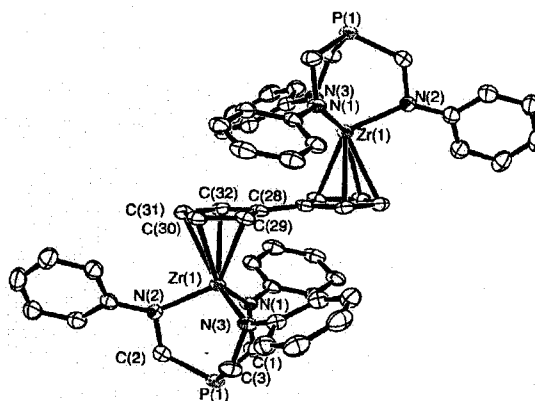
(67)Niecke, E.; Kramer, B.; Nieger, M. *Organometallics* **1991**, *10*, 10-11.

(68)Kuhn, N.; Heuser, N.; Winter, M. *J. Organomet. Chemistry* **1984**, *267*, 221-227.

(69)Chien, P.-S.; Liang, L.-C. *Inorg. Chem.* **2005**, *44*, 5147-5151.

(70)Pangborn, A. B.; Giardello, M. A.; Grubbs, R. H.; Rosen, R. K.; Timmers, F. J. *Organometallics* **1996**, *15*, 1518-1520.

Chapter Three



**Bridged Dinuclear Tripodal Amido-Phosphine Complexes of  
Titanium and Zirconium**

**3.1 Introduction**

Ligand designs to incorporate metal complexes into polymers or 2-D and 3-D structures are of current interest due to the additional physical properties, such as magnetism chemistry.<sup>1-3</sup> A variety of methods have been used to incorporate metal

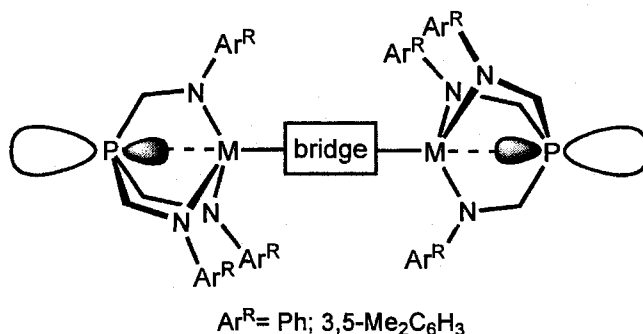
centers in polymers or extended supermolecular networks,<sup>4</sup> which include the use of divergent diligating donors incapable of coordinating to a single metal center.<sup>5-8</sup>

In Chapter two, the synthesis and initial study of the tripodal amido phosphine ligands  $P(\text{CH}_2\text{NAr}^R)_3$  were described.<sup>9</sup> The ligands  $P(\text{CH}_2\text{NAr}^R)_3$  have been demonstrated to be well suited for the facile synthesis of early-late transition metal polynuclear or heterobimetallic complexes, where  $\text{Ar}^R = 3,5\text{-(CF}_3)_2\text{C}_6\text{H}_3$ , Ph, and  $3,5\text{-Me}_2\text{C}_6\text{H}_3$ . The ligand precursors  $P(\text{CH}_2\text{NH-}3,5\text{-(CF}_3)_2\text{C}_6\text{H}_3)_3$ ,  $P(\text{CH}_2\text{NHPh})_3$ , and  $P(\text{CH}_2\text{NH-}3,5\text{-Me}_2\text{C}_6\text{H}_3)_3$ , react with the reagents  $\text{Ti}(\text{NMe}_2)_4$  and  ${}^t\text{BuN}=\text{Ta}(\text{NEt}_2)_3$  to generate the metal complexes of the type  $P(\text{CH}_2\text{NAr}^R)_3\text{TiNMe}_2$  (**2a-c**) and  $P(\text{CH}_2\text{NAr}^R)_3\text{Ta}=\text{N}^t\text{Bu}$  (**3a-c**). The electron density of the metal centre affects the phosphine donor, despite the fact that the phosphine lone-pair is not coordinated to the metal center.<sup>9, 10</sup>

Due to ring strain, the phosphine lone-pair cannot chelate the early transition metal centres and is available to bind a second metal. With suitable building-blocks, this interaction could be used to create 1-D wires, and 2-D or 3-D networks that could have properties that result from through-space exchange-coupling, or through-space electron-transfer.<sup>11-17</sup> The target bis(phosphine) building blocks for such an approach are shown in Scheme 3.1. The addition of suitable late-transition metal fragments capable of bonding to two phosphine moieties, provides a facile route to the polymers containing transition metals. Although there are a plethora of examples of bis(phosphines) used as bridging ligands<sup>18</sup>, these complexes could provide rare examples of the linear bis(phosphine) building-blocks,<sup>19-24</sup> where through-space

interactions provide the potential for extended interactions. In this chapter, we test the synthetic feasibility of preparing such building blocks using the diamagnetic early transition metals zirconium and titanium, with the goal of introducing redox active and paramagnetic metal-bridge fragments in future endeavours.

### Scheme 3.1



### 3.2 Synthesis of the Mononuclear Zirconium Chloride Complexes

The reactions of the phosphine ligands  $\text{P}[\text{CH}_2\text{NAr}^{\text{R}}]_3\text{H}_3$ <sup>9</sup> with 1 equiv of  $\text{Zr}(\text{NEt}_2)_4$  cleanly produced the mononuclear zirconium complexes  $[\text{P}(\text{CH}_2\text{NAr}^{\text{R}})_3]\text{ZrNEt}_2$  (**12b**,  $\text{Ar}^{\text{R}} = \text{Ph}$ ; **12c**,  $\text{Ar}^{\text{R}} = 3,5\text{-Me}_2\text{C}_6\text{H}_3$ ), which were accompanied by elimination of 3 equiv of  $\text{HNEt}_2$ , as shown in Scheme 3.2. The 3,5- $(\text{CF}_3)_2\text{C}_6\text{H}_3$  substituents bearing ligand precursors did not produce a clean reaction product. These reactions require 24-48 h to go to completion and no intermediates were observed by  $^1\text{H}$  or  $^{31}\text{P}\{^1\text{H}\}$  NMR spectroscopy. The resultant products are all obtained in 69-86 % yields as thermally-stable yellow solids. The  $^1\text{H}$  NMR spectra of  $[\text{P}(\text{CH}_2\text{NAr}^{\text{R}})_3]\text{ZrNEt}_2$  (**12b-c**) exhibit the presence of one  $\text{Zr-NEt}_2$

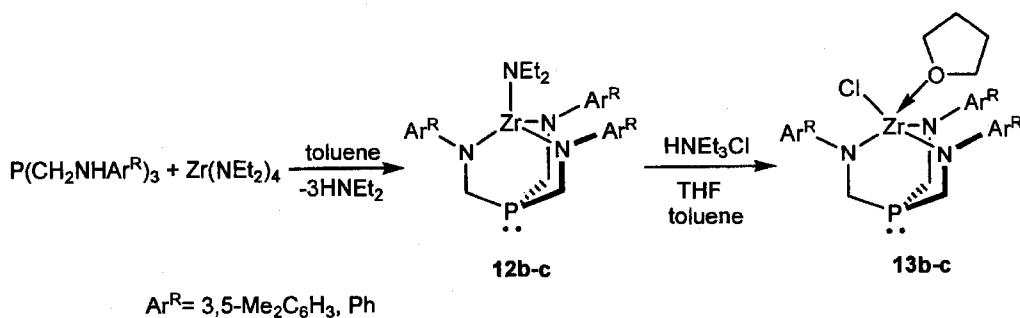
moiety and one set of aromatic resonances, corresponding to 3-fold symmetric complexes in solution, similar to that of  $[\text{P}(\text{CH}_2\text{NAr}^{\text{R}})_3]\text{TiNMe}_2$ . The protons of Zr-NEt<sub>2</sub> group are observed as triplet (**12b**:  $\delta$  1.0, 3H,  $J_{\text{HH}} = 7.0$  Hz; **12c**:  $\delta$  1.1, 3H,  $J_{\text{HH}} = 7.1$  Hz) and quadruplet (**12b**:  $\delta$  3.2, 2H,  $J_{\text{HH}} = 7.0$  Hz; **12c**:  $\delta$  3.3, 2H,  $J_{\text{HH}} = 7.1$  Hz). The Zr-NEt<sub>2</sub> group of complexes **12b-c** was also identified by the <sup>13</sup>C NMR signals at  $\delta$  14.5 and  $\delta$  42.8. The <sup>31</sup>P{<sup>1</sup>H} NMR spectra of  $[\text{P}(\text{CH}_2\text{NAr}^{\text{R}})_3]\text{ZrNEt}_2$  reveal the singlet resonances for the phosphorus donors at  $\delta$  -70.8 and -75.2, respectively, where Ar<sup>R</sup> = Ph and 3,5-Me<sub>2</sub>C<sub>6</sub>H<sub>3</sub>. Compared with shifts of  $\delta$  -31.0, and -29.6 for free ligand precursors  $\text{P}[\text{CH}_2\text{NAr}^{\text{R}}]_3\text{H}_3$ , the changes of the chemical shift to upfield for **12b-c** are significant.<sup>25</sup>

The zirconium chloride complexes  $[\text{P}(\text{CH}_2\text{NAr}^{\text{R}})_3]\text{ZrCl}(\text{THF})$  (**13b-c**) were readily prepared by reactions of  $[\text{P}(\text{CH}_2\text{NAr}^{\text{R}})_3]\text{ZrNEt}_2$  (**12b-c**) with HNEt<sub>3</sub>Cl, and were isolated in 84-89 % yields as yellow solids. The reactions were carried out in toluene at room temperature. After 1 h, THF was added before the solvent was removed. If the solvent was removed without first adding THF, however, the product decomposed. The chloride complex formed in the absence of THF is likely stabilized by HNEt<sub>2</sub>, which is removed under vacuum. When the reaction of  $[\text{P}(\text{CH}_2\text{NAr}^{\text{R}})_3]\text{ZrNEt}_2$  with HNEt<sub>3</sub>Cl was performed using THF as the solvent, it took more than 48 h to go to completion and a plethora of long-lived intermediates were observed by <sup>31</sup>P{<sup>1</sup>H} NMR spectroscopy. This probably indicates that the amido donors of the free ligands are protonated as easily as diethylamido ligand and the THF solvent molecules can then behave as donors that coordinate to the zirconium metal

center and block proton transfer pathways, thus rendering the formation of the thermodynamic products quite slow.

The  $^{31}\text{P}\{^1\text{H}\}$  NMR spectra of  $[\text{P}(\text{CH}_2\text{NAr}^{\text{R}})_3]\text{ZrCl}(\text{THF})$  (**13b-c**) reveal single resonances for the phosphorus donor at  $\delta$  -66.0 and -71.5, respectively, which are shifted downfield compared with that of  $[\text{P}(\text{CH}_2\text{NAr}^{\text{R}})_3]\text{ZrNEt}_2$  (**12b-c**). The room temperature  $^1\text{H}$  NMR and  $^{13}\text{C}$  NMR spectra identify the presence of 1 equiv of coordinated THF and disappearance of the  $-\text{NEt}_2$  resonances.  $[\text{P}(\text{CH}_2\text{NAr}^{\text{R}})_3]\text{ZrCl}(\text{THF})$  (**13b-c**) exhibit 3-fold symmetry in solution, which are indicated by the presence of one set of aromatic resonances and one  $\text{PhCH}_3$  resonance.

### Scheme 3.2



### 3.3 Synthesis of the Mononuclear Zirconium Complexes with Unlinked Cyclopentadienyl Rings

The treatments of zirconium chloride complexes  $[\text{P}(\text{CH}_2\text{NAr}^{\text{R}})_3]\text{ZrCl}(\text{THF})$

(**13b-c**) with LiCp in toluene at room temperature generated  $[\text{P}(\text{CH}_2\text{NAr}^{\text{R}})_3]\text{ZrCp}$  (**14b-c**) (Scheme 3.3), which were isolated as the yellow microcrystalline solids, following crystallization from toluene. The molecular structure of **14c** in the solid state was determined by X-ray crystal structure analysis, however, compound **14b** crystallized as thin needles unsuitable for crystallographic studies. An ORTEP depiction of the solid-state structure obtained at 173 K is shown in Figure 3.1, which features a mononuclear zirconium complex. The tripodal ligand chelates the zirconium metal centre via three amido donors, and the lone-pair electrons of the phosphine donor is directed away from the metal centre. The coordination geometry of the zirconium atom is distorted tetrahedron, at the corners of which are the centre of Cp group and three amido donors of the ligand. Two independent molecules of **14c** are found in the unit cell, which have same bond lengths and angles. The binding of the ligand enforces the P...Zr distances of 3.0523(6) Å, which is under the sum of Van der Waals radii of these elements, suggesting a weak through-space interaction.<sup>9</sup> This value can be compared to typical P-Zr bond distance of 2.7-2.9 Å,<sup>26,27</sup> and is nearly identical to the longest reported Zr-P bond length of 3.033 Å, which was observed in an organometallic  $\text{PMe}_3$  adduct.<sup>28</sup>

The  $^{31}\text{P}\{^1\text{H}\}$  NMR spectra of  $[\text{P}(\text{CH}_2\text{NAr}^{\text{R}})_3]\text{ZrCp}$  (**14b-c**) contain single resonances for the phosphorus donor at  $\delta$  -67.5 and -66.9, respectively, both of which are shifted significantly upfield compared with corresponding ligand precursors  $\text{P}[\text{CH}_2\text{NAr}^{\text{R}}]_3\text{H}_3$ .<sup>25</sup> The  $^1\text{H}$  NMR spectra of **14c** and **14b** are consistent with an apparent  $C_{3v}$  symmetry. The N-Zr bond distances range from 2.0536(18) to 2.0986(17)

Å, which are in the normal range.<sup>8</sup> All the nitrogen atoms coordinated to the zirconium metal centre have the trigonal-planar geometries. The N(1)-Zr(1)-N(3) bond angle (99.37(7)°) is smaller than the angles N(1)-Zr(1)-N(2) (104.91(7)°) and N(2)-Zr(1)-N(3) (106.38(7)°) because of the influence of the bulky Cp group coordinated to Zr metal centre and different orientation of -Ar<sup>R</sup> groups. The C-P-C angles for **14c** are 104.93(12)°, 106.40(12)° and 104.66(11)°, respectively, with a sum of C-P-C angles of 315.99(35)°, which are larger than that of free ligands and titanium compounds reported previously.<sup>9</sup> Compared with titanium compounds, the chelation of a larger metal centre Zr requires an increase in the bond angles at the centre of phosphorus.<sup>9</sup>

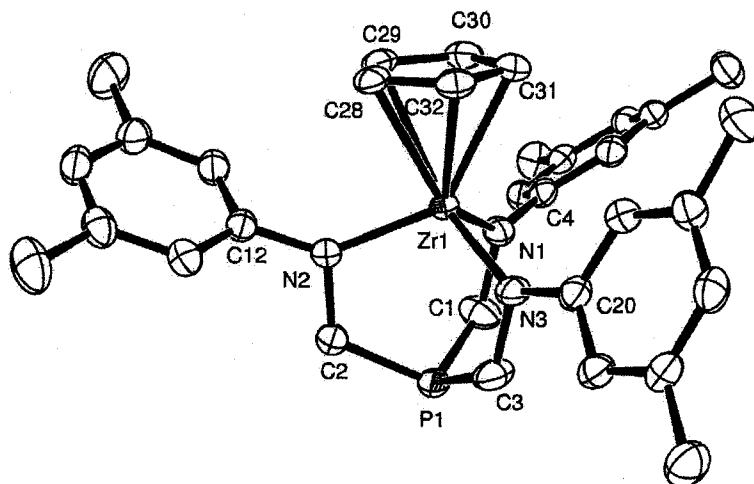
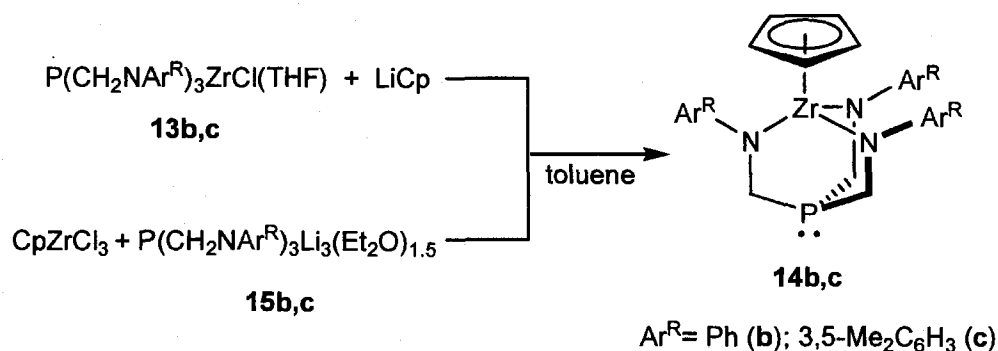


**Figure 3.1.** Solid-state molecular structure of **14c** as determined by X-ray crystallography. Hydrogen atoms are omitted for clarity. Selected distances (Å): Zr(1)···P(1), 3.0523(6); Zr(1)-N(1), 2.0536(18); Zr(1)-N(2), 2.0624(17); Zr(1)-N(3), 2.0986(17); P(1)-C(1), 1.850(2); P(1)-C(2), 1.846(2); P(1)-C(3), 1.857(2). Selected bond angles (deg): C(1)-P(1)-C(2), 104.93(12); C(1)-P(1)-C(3), 106.40(12); C(2)-P(1)-C(3), 104.66(11); P(1)-C(1)-N(1), 120.31(16); P(1)-C(2)-N(2), 118.48(15); P(1)-C(3)-N(3), 121.69(16); C(1)-N(1)-C(4), 113.62(17); C(2)-N(2)-C(12), 112.46(16); C(3)-N(3)-C(20), 113.60(17); N(1)-Zr(1)-N(2), 104.91(7); N(1)-Zr(1)-N(3), 99.37(7); N(2)-Zr(1)-N(3), 106.38(7).

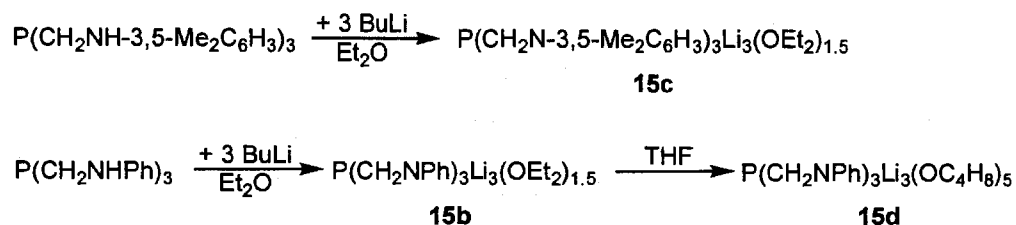
## Scheme 3.3



Alternatively,  $[\text{P}(\text{CH}_2\text{NAr}^{\text{R}})_3]\text{ZrCp}$  (**14b-c**) could be prepared via the reactions of the lithium salts  $[\text{P}(\text{CH}_2\text{NAr}^{\text{R}})_3]\text{Li}_3(\text{OEt}_2)_{1.5}$  (**15b-c**) with  $\text{CpZrCl}_3$  (Scheme 3.3). The lithium salts of the phenyl substituents bearing ligands were easily obtained by the reaction of a slurry of  $\text{P}(\text{CH}_2\text{NPh})_3$  in diethyl ether with 3 equiv of  $n\text{BuLi}$ , as shown in Scheme 3.4. After the addition of 2 equiv of  $n\text{BuLi}$ , the solids dissolved, and the addition of the third equiv resulted in the precipitation of the analytically pure products,  $\text{P}(\text{CH}_2\text{NPh})_3\text{Li}_3(\text{OEt}_2)_{1.5}$  (**15b**). The lithium salt  $\text{P}(\text{CH}_2\text{N-3,5-Me}_2\text{C}_6\text{H}_3)_3\text{Li}_3(\text{OEt}_2)_{1.5}$  (**15c**) was prepared in an analogous manner from **15b**.

The complexes **15b-c** are insoluble in toluene, diethyl ether and methylene chloride, but soluble in THF. The dissolution of THF results in the displacement of the diethyl ether donors as demonstrated by the crystallization of  $\text{P}(\text{CH}_2\text{NPh})_3\text{Li}_3(\text{THF})_5$  (**15d**) by cooling a THF solution of **15b**. This THF adduct is soluble in cold  $\text{CH}_2\text{Cl}_2$ , but solutions decomposes over the course of 1 h at room temperature in this solvent.

## Scheme 3.4



The solid-state molecular structure of **15d** was determined by X-ray crystallography and is shown in Figure 3.2. The complex has an approximate mirror plane of symmetry, with the central Li ion chelated by all three amido donors and bearing a single THF donor. The two remaining Li ions bridge between amido donors, and adopt four-coordinate geometries by binding to two THF moieties. Lithium salts of tripodal amido donors are known to adopt a plethora of bonding motifs in the solid state,<sup>29</sup> and structurally related tripodal amido lithium salts are known.<sup>30</sup> Although the lone-pair of the phosphine is directed away from the central Li(3), the Li(3)⋯P(1) distance of 3.074(6) Å is only ~0.4 Å longer than typical Li-P bond distances; this short contact with phosphorus is common for metals chelated by the amido donors of these tris(amido)phosphine ligands. In the structure of **15d**, the sum of C-P-C angles is 313.7(3)°, which is intermediate between the values we previously reported for the complexes P(CH<sub>2</sub>NPh)<sub>3</sub>TiNMe<sub>2</sub> and P(CH<sub>2</sub>NPh)<sub>3</sub>Ta=N<sup>t</sup>Bu, which were 311.4(1)° and 315.0(2)°, respectively.

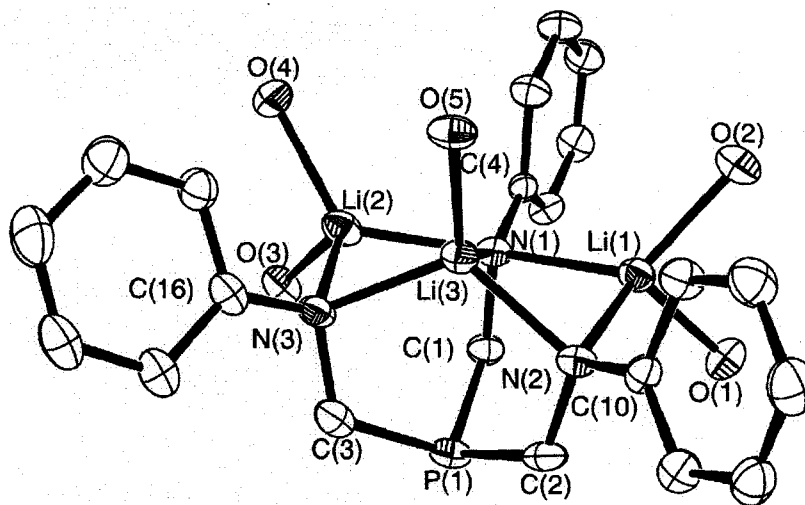


**Figure 3.2.** Solid-state molecular structure of **15d** as determined by X-ray crystallography. Hydrogen atoms are omitted and only the oxygen atoms associated with the THF donors are shown for clarity. Selected distances (Å): Li(1)-N(2), 2.069(7); Li(1)-N(1), 2.189(8); Li(2)-N(1), 2.150(9); Li(2)-N(3), 2.053(7); Li(3)-N(3), 2.063(7); Li(3)-N(2), 2.088(7); Li(3)-N(1), 2.149(7); Li(3)⋯P(1), 3.074(6). Selected bond angles (deg): C(2)-P(1)-C(1), 104.38(18); C(2)-P(1)-C(3) 101.5(2); C(1)-P(1)-C(3), 107.84(19).

The room-temperature  $^1\text{H}$ ,  $^7\text{Li}$ , and  $^{13}\text{C}\{^1\text{H}\}$  NMR spectra of both **15c** and **15b** are consistent with high symmetry species. The  $^1\text{H}$  NMR spectrum of **15b** in  $d_8$ -THF consists of a single  $\text{PCH}_2$  resonance and a set of three aromatic resonances, and the  $^7\text{Li}$  NMR spectrum displays a single lithium environment. The fluxional nature of Li salts of related species is well documented.<sup>30</sup> The  $^{31}\text{P}\{^1\text{H}\}$  NMR spectra of **15b-c** and in  $d_8$ -THF display singlets at  $\delta$  -21.7 and -22.2, respectively, which are only slightly altered from the chemical shift observed in the free ligand precursors. The change of

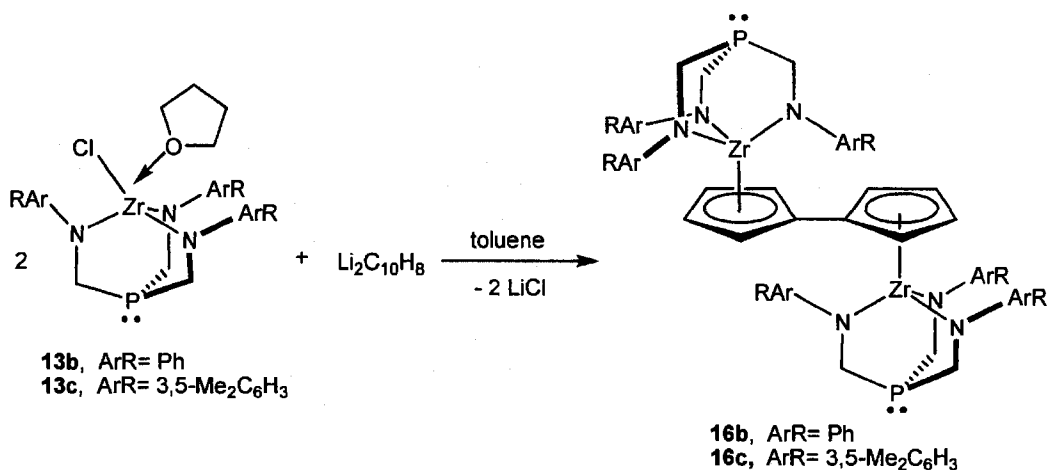
shift is in the opposite direction we have previously observed for early transition metal complexes of these ligands, which exhibit  $^{31}\text{P}$  chemical shifts as low as  $\delta$  -108.5.<sup>9</sup>

### 3.4 Synthesis of the Binuclear Zirconium Complexes with the Bridging Fulvalenide Ligand and Comparison with the Analogous Mononuclear Zirconium Complexes with Unlinked Cyclopentadienyl Rings.

The stabilities of the cyclopentadienyl zirconium complexes **14b-c** suggested that the most versatile dinuclear zirconium building-blocks should bear polyhaptoligands. The fulvalene dianion  $[(\text{C}_5\text{H}_4)_2]^{2-}$  exhibits electron delocalization between the rings,<sup>31,32</sup> and its obvious relation to the Cp ligand suggests that these complexes should be stable and isolable. Fulvalene-metal complexes also offer the opportunity to investigate the cooperative interaction between the two metals across a delocalized bridging ligand by comparing the properties of analogous mono and binuclear complexes. Here, we prepare the binuclear zirconium complexes by nucleophilic substitution reactions of metal substrates with the fulvalene dianion. As the procedure of Vollhardt and Weidman,<sup>33</sup> the lithium salt of the fulvalene dianion  $\text{Li}_2\text{C}_{10}\text{H}_8$  was isolated via deprotonation of hydrofulvalene with  $n\text{BuLi}$ .<sup>33</sup> Reactions of 2 equiv of  $\text{P}(\text{CH}_2\text{NAr}^{\text{R}})_3\text{ZrCl}(\text{THF})$  (**13b-c**) with 1 equiv of  $\text{Li}_2\text{C}_{10}\text{H}_8$  result in the binuclear zirconium complexes *trans*- $[\text{P}(\text{CH}_2\text{NAr}^{\text{R}})_3\text{Zr}]_2(\mu\text{-}\eta^5\text{:}\eta^5\text{-C}_{10}\text{H}_8)$  (**16b-c**) at room temperature, as shown in Scheme 3.5, which are soluble in hydrocarbon solvents and can be recrystallized from a mixture of benzene and hexamethyldisiloxane solution to

give thermally-stable yellow crystals.

**Scheme 3.5**



The structure of the compound **16c** was confirmed by X-ray diffraction and an ORTEP depiction of the solid-state molecular structure is shown in Figure 3.3, together with selected bond distances and bond angles. The molecule crystallizes with a center of symmetry. Thus, the two metal centers are crystallographically equivalent and are coordinated to the bridging fulvalene ligand in a *trans* manner, which is probably primarily due to steric reasons.<sup>34</sup> Both  $^1\text{H}$  and  $^{31}\text{P}\{^1\text{H}\}$  NMR spectroscopy support the presence of only the *trans* isomer; the  $^{31}\text{P}\{^1\text{H}\}$  NMR spectra of complexes **16c** and **16b** exhibit one signal each at  $\delta$  -56.3 and  $\delta$  -57.1, respectively. The central fulvalene C-C bond length of 1.471(6) Å is within the normal range found in fulvalene metal complexes with a degree of multiple bonding between the rings.<sup>35</sup> The bond distances and angles of the binuclear compound **16c** are similar to those of the analogous mononuclear compound **14c**. The P...Zr distance of 3.0698(9) Å for **16c** is

slightly larger than that of 3.0523(6) Å for **14c**.

The  $^1\text{H}$  NMR spectrum provides the convenient tool to characterize the binuclear fulvalene complexes and their corresponding monomers. In the  $^1\text{H}$  NMR spectra of *trans*-[P(CH<sub>2</sub>NAr<sup>R</sup>)<sub>3</sub>Zr]<sub>2</sub>( $\eta^5$ : $\eta^5$ -C<sub>10</sub>H<sub>8</sub>) (**16b-c**), the fulvalene protons appear as a pair of triplets, indicating that molecule possesses a mirror plane bisecting the central C-C bond linking the fulvalene rings.<sup>33</sup> However, the  $^1\text{H}$  NMR spectra of P(CH<sub>2</sub>NAr<sup>R</sup>)<sub>3</sub>ZrCp only show singlets at  $\delta$  6.18 and 5.95, respectively, due to the unlinked Cp ligand. The change of the  $^{31}\text{P}$  NMR shift downfield is observed for complexes **16b** and **16c** (**16b**: -57.1; **16c**:  $\delta$  -56.2), comparing to their corresponding mononuclear zirconium complexes **14b** and **14c** (**14b**: -67.5; **14c**:  $\delta$  -66.9).

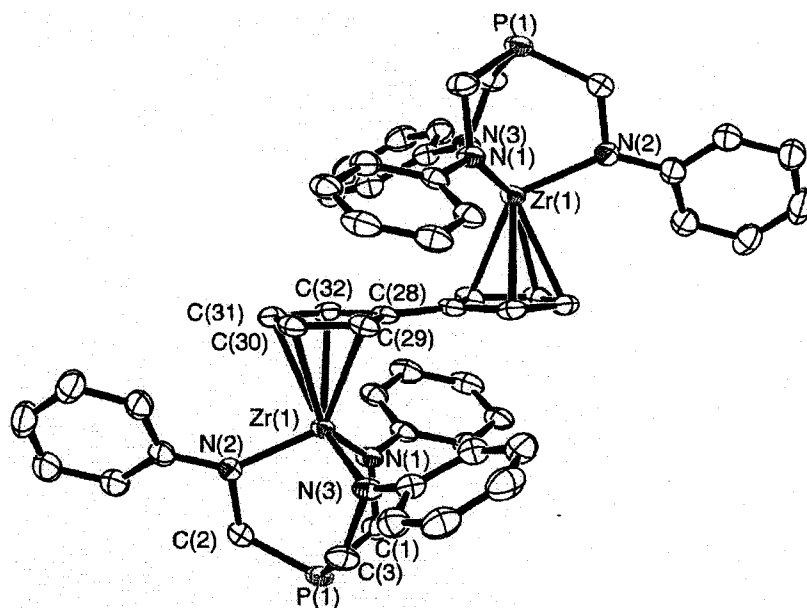


**Figure 3.3.** Solid-state molecular structure of **16c** as determined by X-ray crystallography. Hydrogen atoms and 3,5-methyl substituents are omitted for clarity. Selected distances (Å): Zr(1)···P(1), 3.0698(9); Zr(1)-N(1), 2.052(2); Zr(1)-N(2), 2.093(3); Zr(1)-N(3), 2.073(3); P(1)-C(1), 1.853(3); P(1)-C(2), 1.848(3); P(1)-C(3), 1.852(3). Selected bond angles (deg): C(1)-P(1)-C(2), 104.50(15); C(1)-P(1)-C(3), 105.38(15); C(2)-P(1)-C(3), 103.13(16); P(1)-C(1)-N(1), 118.8(2); P(1)-C(2)-N(2), 118.5(2); P(1)-C(3)-N(3), 118.3(2); C(1)-N(1)-C(4), 111.9(2); C(2)-N(2)-C(12), 112.8(2); C(3)-N(3)-C(20), 113.1(2); N(1)-Zr(1)-N(2), 103.15(10); N(1)-Zr(1)-N(3), 102.71(10); N(2)-Zr(1)-N(3), 102.19(10).

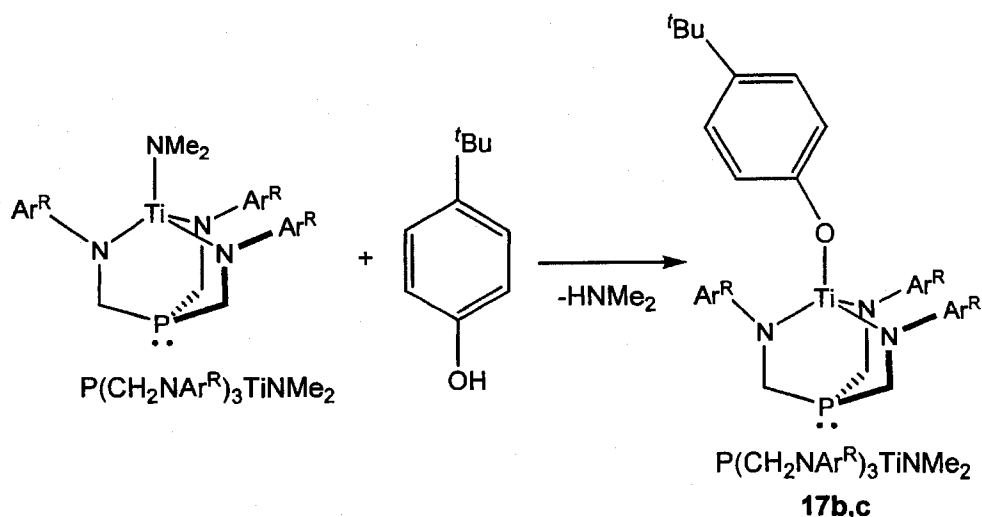
### 3.5 Synthesis of the Bridged Binuclear Titanium Complexes

A variety of synthetic approaches to  $P(\text{CH}_2\text{NAr}^R)_3\text{TiCl}$  were attempted, due to the fact that it could serve as a potential precursor to a variety of bridged dinuclear complexes via salt metathesis. Unfortunately, the direct reactions of the lithium salts

**15b-c** with  $\text{TiCl}_4$  produced a mixture of products. The reaction of the ligand precursors  $\text{P}(\text{CH}_2\text{NAr}^{\text{R}})_3$  with stoichiometric quantities of  $(\text{Me}_2\text{N})_3\text{TiCl}$  also failed to produce the desired products, and the previously characterized  $\text{P}(\text{CH}_2\text{NAr}^{\text{R}})_3\text{TiNMe}_2$  and unreacted  $\text{P}(\text{CH}_2\text{NAr}^{\text{R}})_3$  were identified as two of the major components of the reaction mixture in each case, where  $\text{Ar}^{\text{R}} = \text{Ph}$  and 3,5- $\text{Me}_2\text{C}_6\text{H}_3$ . Similarly, the reactions of  $\text{P}(\text{CH}_2\text{NAr}^{\text{R}})_3\text{TiNMe}_2$  with the ammonium salt  $\text{HNEt}_3\text{Cl}$  and  $\text{Me}_3\text{SiCl}$  failed to yield the desired chloride complexes.

Due to the difficulty in accessing the chloride complex, we attempted to demonstrate that the amido complexes,  $\text{P}(\text{CH}_2\text{NAr}^{\text{R}})_3\text{TiNMe}_2$ , could act as precursors to the bridged binuclear complexes via protonolysis reactions. To test this hypothesis, we prepared the mononuclear complexes  $[\text{P}(\text{CH}_2\text{NAr}^{\text{R}})_3]\text{TiOC}_6\text{H}_4^t\text{Bu}$  (**17b,c**) via the reaction of 1,4- $\text{HOC}_6\text{H}_4^t\text{Bu}$  with  $\text{P}(\text{CH}_2\text{NAr}^{\text{R}})_3\text{TiNMe}_2$  ( $\text{Ar}^{\text{R}} = 3,5\text{-Me}_2\text{C}_6\text{H}_3$  and Ph) in toluene, as shown in Scheme 3.6. The reactions are slow at room temperature, and required 48 h to go to completion. The resultant products are thermally-stable dark-red solids. The reaction where  $\text{Ar}^{\text{R}} = 3,5\text{-(CF}_3)_2\text{C}_6\text{H}_3$  produces only a mixture of products.

## Scheme 3.6



Crystalline **17c** was obtained by slow evaporation of a pentane solution and the solid-state molecular structure was determined by X-ray crystallography. The unit cells contain two crystallographically distinct molecules of **17c** in the asymmetric unit, and an ORTEP depiction of one of these is shown in Figure 3.4. The structure could be described as distorted trigonal bipyramid with the phosphine lone pair formally directing away from the titanium center, in which P atom and O atom occupy the apical positions. The angle between the two axial positions O(1)-Ti(1)-P(1) is 178.20(12)° and close to the idealized value of 180° in the trigonal bipyramid. The Ti(1)-O(1)-C(28) bond angle (160.20(3)°) and Ti-O distance (1.784(3) Å) are in the normal ranges.<sup>36</sup> The Ti-N<sub>amido</sub> bonds of **17c** (1.918(4) Å, 1.918(4) Å, 1.926(4) Å) are shorter than those of [P(CH<sub>2</sub>NAr<sup>R</sup>)]TiNMe<sub>2</sub> (1.963(7) Å, 1.941(6) Å, 1.934(6) Å),

reflecting stronger  $\sigma$ -bonding together with additional p-d  $\pi$  donation in the compound **17c**.<sup>37</sup> In the  $^{13}\text{C}\{^1\text{H}\}$  NMR spectra of **17b-c**, the chemical shifts of the *ipso* carbons bonded directly to the oxygen atoms are at  $\delta$  153.3 and 164.2, respectively, which indicate the difference of electronic density around the titanium metal centre.<sup>36</sup> For compound **17c**, the signal is shifted upfield relative to **17b**, as the result of electron-donating property of the methyl groups in the ligand of the compound **11**. Comparing the structure of **17c** with the parent titanium compound  $[\text{P}(\text{CH}_2\text{NAr}^{\text{R}})_3]\text{TiNMe}_2$ , the sum of C-P-C bond angles and the P...Ti distances are similar, indicating that the coordinated ( $-\text{OC}_6\text{H}_4^t\text{Bu}$ ) ligand does not alter the geometry of the remaining parts. However, the chemical shifts observed by  $^{31}\text{P}\{^1\text{H}\}$  NMR spectroscopy of  $[\text{P}(\text{CH}_2\text{NAr}^{\text{R}})_3]\text{Ti-OC}_6\text{H}_4^t\text{Bu}$  (**17b-c**) (**17c**,  $\delta$  -77.9; **17b**, -81.07) compared with that of  $[\text{P}(\text{CH}_2\text{NAr}^{\text{R}})_3]\text{TiNMe}_2$  ( $\delta$  -61.6, -65.6) and free ligand precursors  $\text{P}(\text{CH}_2\text{NAr}^{\text{R}})_3\text{H}_3$  ( $\delta$  -29.6, -31.0), which corroborate our previous observations that the electron density at the chelated metal center affects the properties of the phosphine donor, despite the fact that the phosphine lone-pair is not coordinated to the metal center.<sup>9</sup>

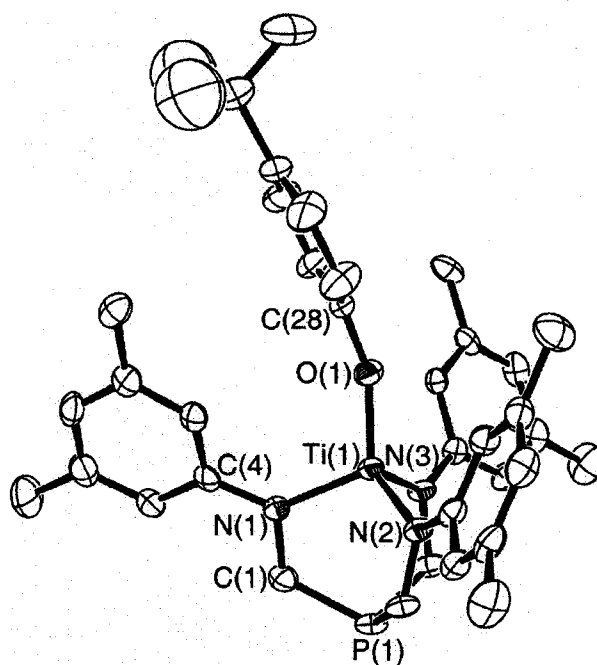
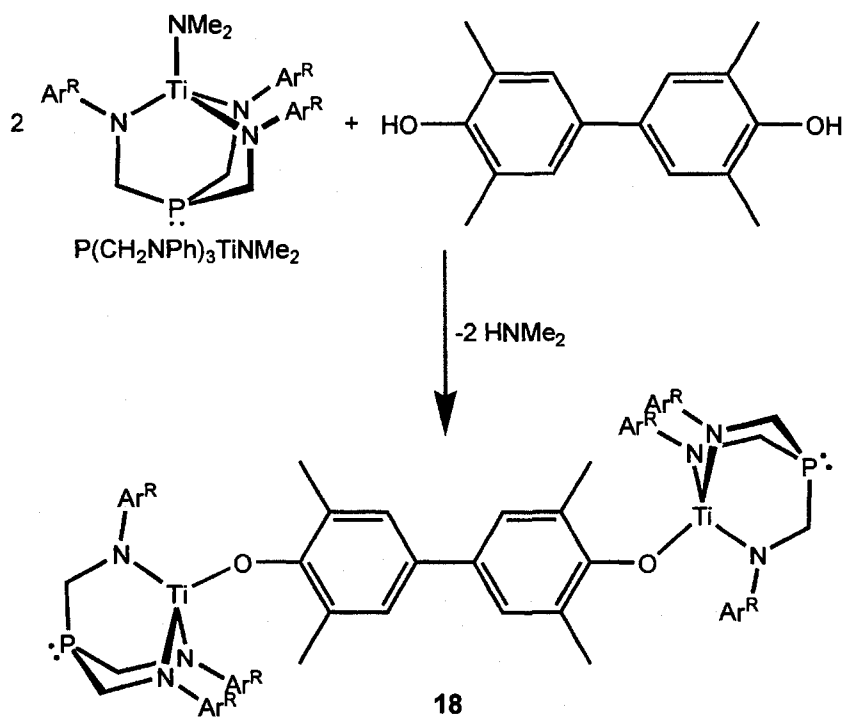


**Figure 3.4.** Solid-state molecular structure of 17c as determined by X-ray crystallography. Hydrogen atoms are omitted for clarity. Selected distances (Å): Ti(1)···P(1), 3.0150(16); Ti(1)-N(1), 1.918(4); Ti(1)-N(2), 1.926(4); Ti(1)-N(3), 1.918(4); Ti(1)-O(1), 1.784(3); O(1)-C(28), 1.369(5); P(1)-C(1), 1.854(5); P(1)-C(2), 1.861(5); P(1)-C(3), 1.863(5). Selected bond angles (deg): O(1)-Ti(1)-P(1), 178.20(12); Ti(1)-O(1)-C(28), 160.20(3); C(1)-P(1)-C(2), 102.8(2); C(1)-P(1)-C(3), 102.8(2); C(2)-P(1)-C(3), 102.8(2); N(1)-Ti(1)-O(1), 112.66(16); N(2)-Ti(1)-O(1), 115.74(16); N(3)-Ti(1)-O(1), 113.82(16); N(1)-Ti(1)-N(3), 105.73(17); N(2)-Ti(1)-N(3), 104.02(16); N(2)-Ti(1)-N(1), 103.77(16).

Aryloxy ligands have been utilized in the past as bridging ligands to generate the binuclear or larger complexes with cyclopentadienyl substituted titanium and zirconium complexes.<sup>38-40</sup> The reaction of {4,4'-HO[3,3',5,5'-(C<sub>6</sub>H<sub>2</sub>Me<sub>2</sub>)<sub>2</sub>]OH} with 2 equiv of [P(CH<sub>2</sub>NPh)<sub>3</sub>]TiNMe<sub>2</sub> gave the red solid of binuclear compound

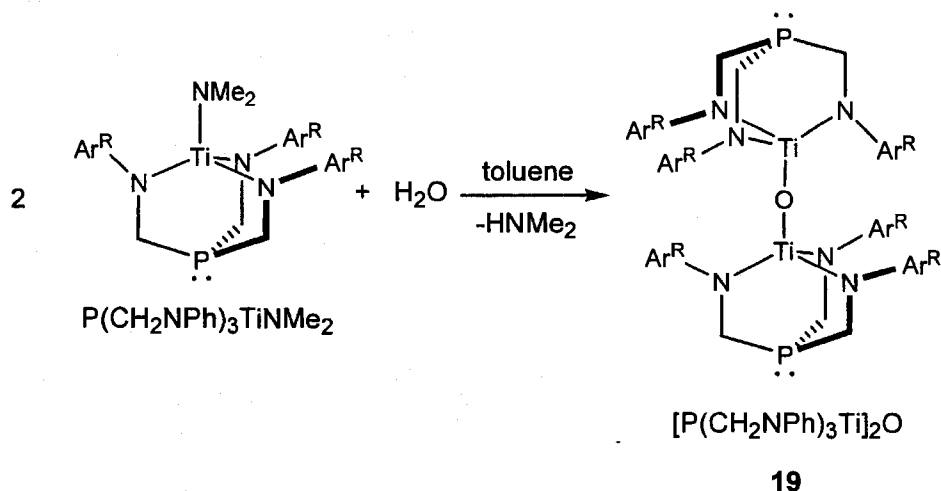
$[\text{P}(\text{CH}_2\text{NPh})_3\text{Ti}]_2\{\mu\text{-O-}3,3',5,5'\text{-(Me}_2\text{C}_6\text{H}_2)_2\text{O-}\}$  (**18**) in 85 % yield, as shown in Scheme 3.7. Compound **18** is soluble in aromatic hydrocarbons such as toluene and benzene. The NMR data and elemental analysis for the compound **18** are consistent with the structure depicted in Scheme 3.7. The  $^1\text{H}$  NMR and  $^{13}\text{C}\{^1\text{H}\}$  NMR spectra of the compound **18** show the disappearance of  $\text{-NMe}_2$  ligand and equivalence of the two Ti metal fragments, as well as one set of aromatic resonances. In the  $^1\text{H}$  NMR spectrum, the aromatic protons of the  $\{\mu\text{-O}[3,3',5,5'\text{-(C}_6\text{H}_2\text{Me}_2)_2\text{O-}]\}^{2-}$  ligand are equivalent and appear as a singlet at  $\delta$  7.2. The  $^{31}\text{P}\{^1\text{H}\}$  NMR spectrum displays a singlet at  $\delta$  -78.6, which is comparable to that of  $\text{P}(\text{CH}_2\text{NPh})_3\text{TiOC}_6\text{H}_4^t\text{Bu}$  (**17b**) at  $\delta$  -81.1. Unfortunately, the analogous complexes could not be prepared from  $[\text{P}(\text{CH}_2\text{N-}3,5\text{-(CF}_3)_2\text{C}_6\text{H}_3)_3]\text{TiNMe}_2$  and  $[\text{P}(\text{CH}_2\text{NH-}3,5\text{-Me}_2\text{C}_6\text{H}_3)_3]\text{TiNMe}_2$  by this method, and attempts to prepare crystals of **18** suitable for study by X-ray diffraction only generated the solid of **18**.

### Scheme 3.7



Carrying out the reaction of  $[\text{P}(\text{CH}_2\text{NPh})_3\text{TiNMe}_2]$  with 1 equiv of  $\text{H}_2\text{O}$  results in a colorless to pale red precipitate that likely consists of  $\text{TiO}_2$ . However, the slow addition of a stoichiometric amount of water by using the hydrated salt  $\text{Na}_2\text{SO}_4 \cdot 10\text{H}_2\text{O}$  resulted in the formation of the *oxo*-bridged binuclear compound  $[\text{P}(\text{CH}_2\text{NPh})_3\text{Ti}]_2(\mu\text{-O})$  (**19**), as shown in Scheme 3.8.

## Scheme 3.8



The bridging oxo formulation was confirmed by X-ray crystallography, and an ORTEP depiction of the solid-state molecular structure is shown in Figure 3.5 & 3.6. Complex **19** crystallized from toluene in a trigonal space group and possesses crystallographically imposed  $S_6$  symmetry. A second monoclinic pseudopolymorph containing cocrystallized toluene was also characterized, however, no significant structural differences were observed. The molecule has a strictly linear P-Ti-O-Ti-P unit, which defines the  $S_6$  axis. As expected, the <sup>1</sup>H NMR spectrum of **19** contains one PCH<sub>2</sub> and three aromatic resonances associated with the ancillary ligand. The <sup>31</sup>P{<sup>1</sup>H} NMR shift of -39.4 is unusual, compared the chemical shift of **17b** and **18b**, which are more negative by almost 40 ppm. A reasonable rationale for this shift might be that the steric interaction between the two ancillary ligand moieties in **19** results in a strained ligand conformation with larger N-Ti-O angles and P-Ti distances. The bond angles and lengths corroborate this hypothesis. For example, the Ti(1)···P(1) separation of 3.051(2) Å is the longest we have observed in the Ti complexes of these ancillary ligands.

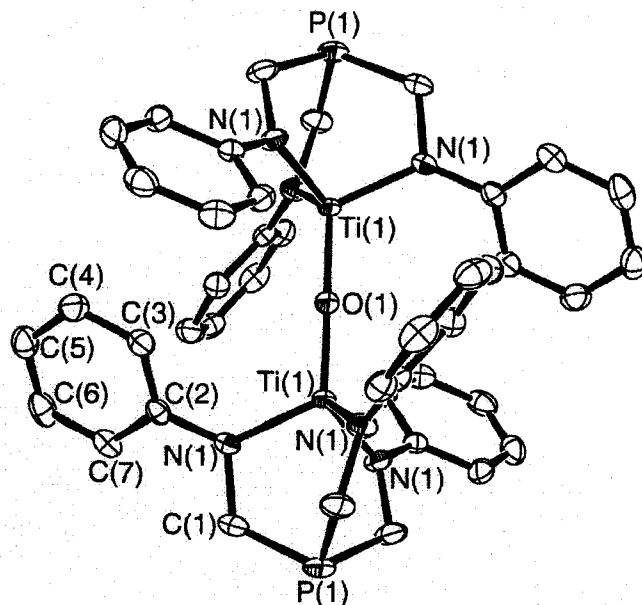


**Figure 3.5.** Solid-state molecular structure of **19** as determined by X-ray crystallography. Hydrogen atoms are omitted for clarity. Selected distances (Å): Ti(1)···P(1), 3.051(2); Ti(1)-N(1), 1.907(2); Ti(1)-O(1), 1.802(8); C(1)-P(1), 1.855(3); C(1)-N(1), 1.467(4); C(2)-N(1), 1.397(3); Selected bond angles (deg): P(1)-Ti(1)-O(1)-Ti(2), 180.00(0); N(1)-Ti(1)-O(1), 115.46(7); N(1)-C(1)-P(2), 115.53(2); C(1)-N(1)-C(2), 118.29(2); C(2)-N(1)-Ti(1), 129.96(18); C(1)-N(1)-Ti(1), 110.61(18); C(1)-P(1)-C(1), 102.05(11).

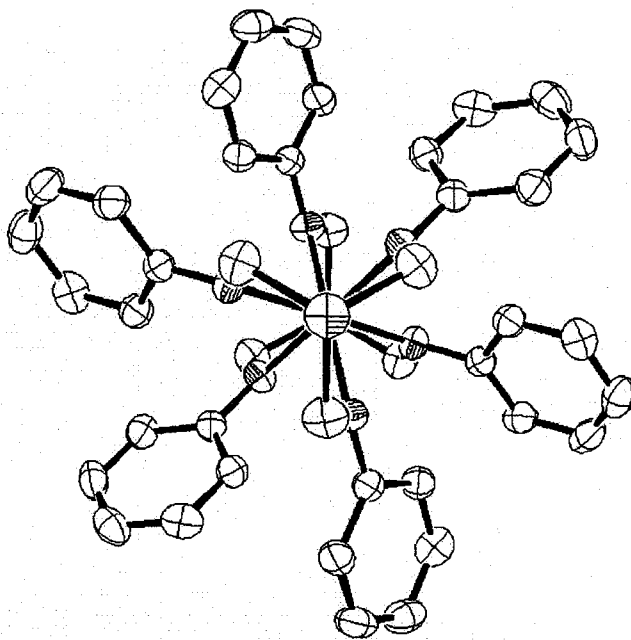


**Figure 3.6.** Solid-state molecular structure of **19** viewed along the crystallographic 3-fold axis. Hydrogen atoms are omitted for clarity.

Attempts to make an analogous bridging *oxo*-complex with  $\text{P}(\text{CH}_2\text{N}-3,5\text{-Me}_2\text{C}_6\text{H}_3)_3\text{TiNMe}_2$  and  $\text{P}[\text{CH}_2\text{N}-3,5\text{-(CF}_3)_2\text{C}_6\text{H}_3]_3\text{TiNMe}_2$  have so far failed, possibly due to the steric bulk afforded by these ligands, however, it may be that kinetic factors prevent their facile preparation. In an attempt to find an alternate route to these complexes,  $\text{P}(\text{CH}_2\text{N}-3,5\text{-Me}_2\text{C}_6\text{H}_3)_3\text{TiNMe}_2$  was reacted with 1 equiv of  $\text{H}_2\text{O}$  and excess  $\text{Ti}(\text{NMe}_2)_4$  at room temperature to yield the binuclear titanium complex  $[\text{P}(\text{CH}_2\text{N}-3,5\text{-Me}_2\text{C}_6\text{H}_3)_3]\text{Ti}-\mu\text{-O}-\text{Ti}(\text{NMe}_2)_3$  (**20**), as shown in Scheme 3.9. Crystals suitable for an X-ray structure analysis were grown by slow evaporation of toluene solution at  $-30\text{ }^\circ\text{C}$ . Unfortunately, attempts to react **20** with  $\text{P}(\text{CH}_2\text{NH}-3,5\text{-Me}_2\text{C}_6\text{H}_3)_3$  failed to produce the desired product,  $[\text{P}(\text{CH}_2\text{N}-3,5\text{-Me}_2\text{C}_6\text{H}_3)_3\text{Ti}]_2(\mu\text{-O})$ .

## Scheme 3.9

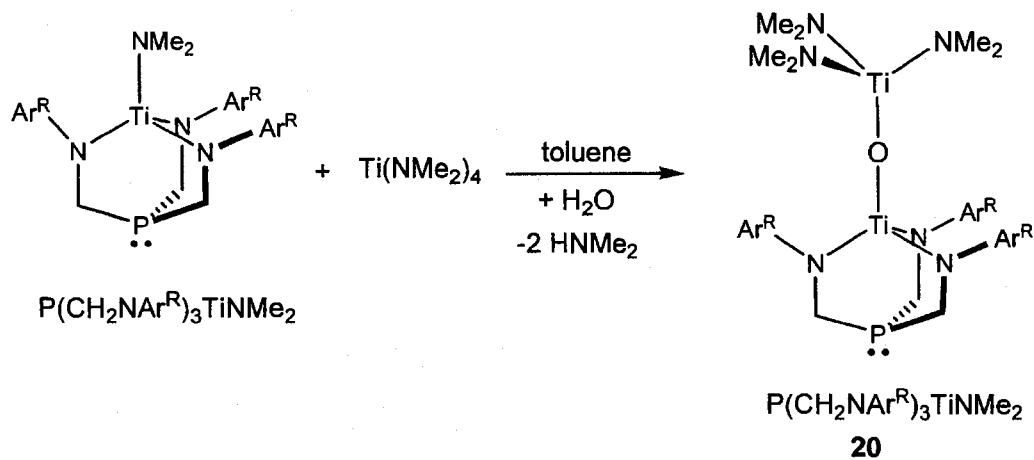
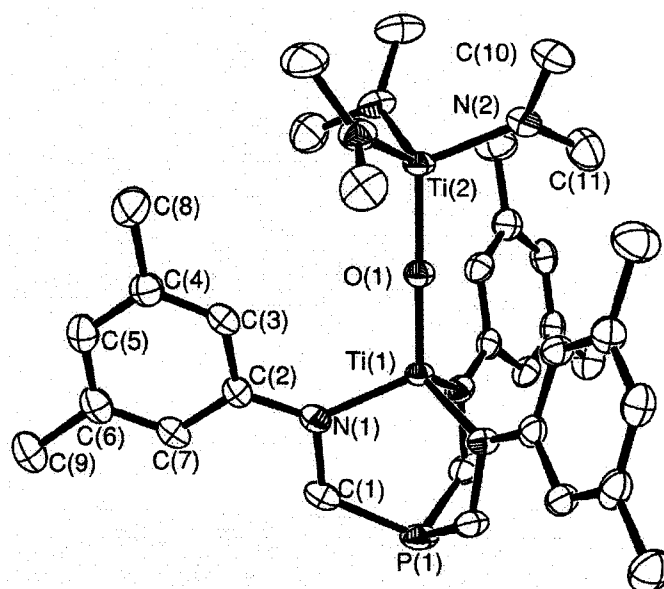


Figure 3.7 shows the solid-state molecular structure of **20**, as well as the selected bond lengths and bond angles. The binuclear compound of **20** crystallizes in the rhombohedral space group  $R\bar{3}$  and the molecular structure has crystallographically imposed  $C_3$  symmetry. Both titanium atoms are connected by a linear  $\mu$ -oxo bridge, and the Ti(1)-O(1) bond length of 1.757(3) Å is shorter than the Ti(2)-O(1) bond length of 1.886(3) Å. This is likely due to significantly greater  $\pi$ -donation via the oxygen donor to Ti(1).<sup>41</sup> The aromatic substituents render the ancillary ligand amido donors less potent than the  $-NMe_2$  groups, but also the hindered rotation of the chelating amido donors prevents optimal overlap of these orbitals with the available d-orbitals on Ti(1). The Ti(1)··P(1) distance of 2.968(14) Å is just slightly shorter than observed for  $[P(CH_2N-3,5-Me_2C_6H_3)_3]TiNMe_2$  and  $[P(CH_2NAr^R)_3]Ti-OC_6H_4^tBu$  (**17c**), 3.015(5) and 3.015(16) Å, respectively. Also noteworthy is the  $^{31}P\{^1H\}$  NMR shift of  $\delta$  -62.9, which is significantly different than

the shift of -39.4 observed for **19**.

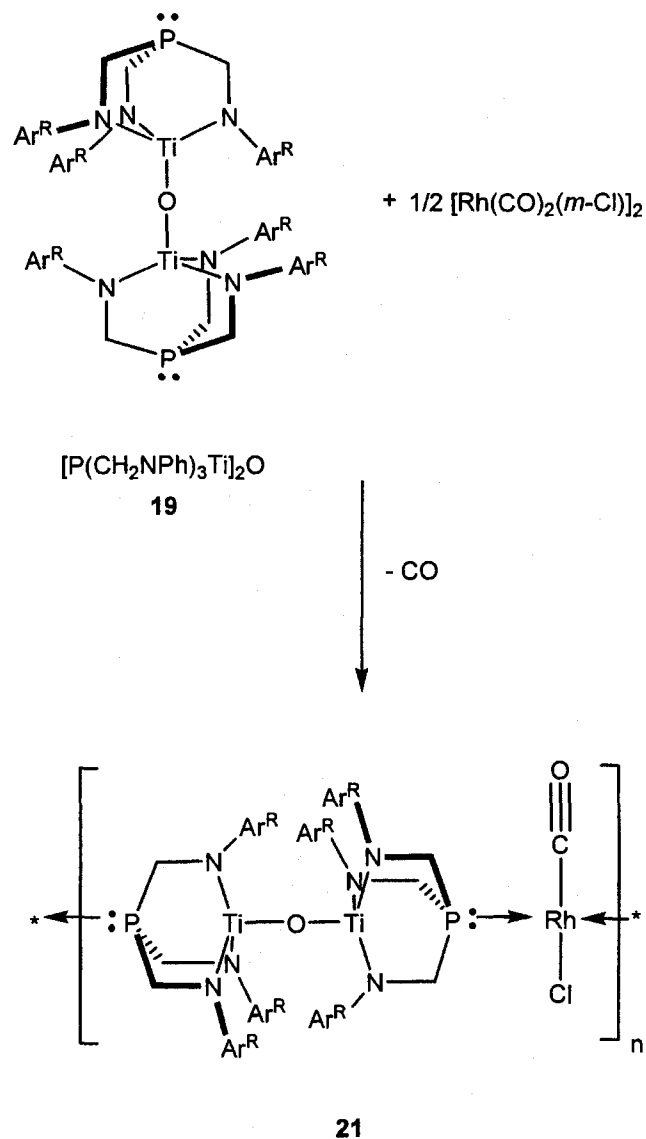


**Figure 3.7.** Solid-state molecular structure of **20** as determined by X-ray crystallography. Hydrogen atoms are omitted for clarity. Selected distances (Å): Ti(1)···P(1), 2.968(14); Ti(1)-N(1), 1.935(2); Ti(1)-O(1), 1.757(3); Ti(2)···P(1), 6.612; Ti(2)-N(2), 1.881(2); Ti(2)-O(1), 1.886(3); C(1)-P(1), 1.850(3); C(1)-N(1), 1.461(3); Selected bond angles (deg): Ti(1)-O(1)-Ti(2), 180.0; N(1)-Ti(1)-N(1), 106.15(7); N(1)-Ti(1)-O(1), 112.62(6); N(2)-Ti(2)-N(2), 105.13(8); N(2)-Ti(2)-O(1), 113.52(7); C(1)-P(1)-C(1), 103.65(10); C(1)-N(1)-C(2), 115.74(2); C(1)-N(1)-Ti(1), 108.01(16); C(2)-N(1)-Ti(1), 135.87(16); C(10)-N(2)-C(11), 112.45(2); C(10)-N(2)-Ti(2), 129.37(2); C(11)-N(2)-Ti(2), 117.99(18).

### 3.6 Polymer Synthesis

The bridging binuclear complexes we have prepared should provide a facile route to polymeric materials that contain transition metals along the main polymer chain, and we chose to demonstrate the synthetic viability of this approach using the complex **19**. We have previously shown that two equivalents of the mononuclear complexes  $\text{P}(\text{CH}_2\text{NAr}^{\text{R}})\text{TiNMe}_2$  react cleanly with  $[\text{Rh}(\text{CO})_2(\mu\text{-Cl})]_2$  to generate the heterobimetallic complexes *trans*- $\text{Cl}(\text{CO})\text{Rh}[\text{P}(\text{CH}_2\text{NAr}^{\text{R}})_3\text{TiNMe}_2]_2$ , as shown in Scheme 3.10. An analogous reaction with one equivalent of the dinuclear oxo-bridged titanium complex **19** precipitated a red insoluble polymer  $\text{Cl}(\text{CO})\text{Rh}[\text{P}(\text{CH}_2\text{NPh})_3\text{Ti}]_2\text{O}$  (**21**). A single CO stretch is observed in the IR spectrum of a KBr pellet of **21** at  $1972.5\text{ cm}^{-1}$ .

Scheme 3.10



### 3.7 Summary and Conclusion

The reactions of the phosphine ligands  $\text{P}[\text{CH}_2\text{NAr}^R]_3\text{H}_3$ <sup>9</sup> with 1 equiv of  $\text{Zr}(\text{NEt}_2)_4$  afforded the mononuclear zirconium complexes  $[\text{P}(\text{CH}_2\text{NAr}^R)_3]\text{ZrNEt}_2$  (**12b**,  $\text{Ar}^R = \text{Ph}$ ; **12c**,  $\text{Ar}^R = 3,5\text{-Me}_2\text{C}_6\text{H}_3$ ). The chloride complexes  $[\text{P}(\text{CH}_2\text{NAr}^R)_3]\text{ZrCl}(\text{THF})$  (**13b-c**) were prepared by the treatments of  $\text{HNEt}_3\text{Cl}$  with

**12b-c.** The complexes **13b-c** reacted with cyclopentadienyllithium ( $C_5H_5Li$ ) to produce  $P[CH_2NAr^R]_3ZrCp$  (**14b-c**). Alternatively, **14b-c** could be prepared from the reactions of the lithium salts **15b-c** with  $CpZrCl_3$ . The reactions of the lithium salts of the fulvalene dianion ( $Li_2C_{10}H_8$ ) with **13b-c** produce the dinuclear complexes *trans*- $[P(CH_2NAr^R)_3Zr]_2(\eta^5:\eta^5-C_{10}H_8)$  (**16b-c**). Attempts to make the chloride complexes  $[P(CH_2NAr^R)_3]TiCl$  have failed; however, the mononuclear titanium complexes  $[P(CH_2NAr^R)_3]TiOC_6H_4^tBu$  (**17b-c**) and the dinuclear species  $[P(CH_2NPh)_3TiNMe_2]_{2-\mu-1,1'}\{O[3,3',5,5'-(C_6H_2Me_2)_2]O\}$  (**18**),  $\{[P(CH_2NPh)_3]Ti\}_2(\mu-O)$  (**19**) and  $[P(CH_2N-3,5-Me_2C_6H_3)_3]Ti-\mu-O-Ti(NMe_2)_3$  (**20**), can be prepared from  $[P(CH_2NAr^R)_3]TiNMe_2$  via protonolysis.

The ligands  $P(CH_2NHAr^R)_3$  have been demonstrated to stabilize mononuclear early transition metal complexes, which were well suited for bridged early transition homobimetallic complexes. The design of divergent metal-containing building blocks provides a facile route to linear rigid metal-containing polymers. With the smaller metal Ti, it is proved possible to generate bridges with  $\eta^1$  bound ligands, whereas with the larger metal Zr, attempts to generate bridged complexes only succeeded by utilizing polyhapto ligands. Our future goals include the inclusion of redox active or paramagnetic metal-ligand fragments in lieu of Ti and Zr in the bisphosphine moieties, as well as an in-depth investigation into the properties and characteristics of these polymers and the use of these building blocks in the assembly of higher-dimensional networks with functional physical properties.

### 3.8 Experimental

#### 3.8.1 General Procedures

Unless otherwise stated, general procedures were performed according to Section 2.11.1.

#### 3.8.2 Synthesis of Complexes

**[CH<sub>2</sub>NPh]<sub>3</sub>ZrNEt<sub>2</sub> (12b)**. Liquid Zr(NEt<sub>2</sub>)<sub>4</sub> (3.246 g, 8.55 mmol) was added to a solution of P[CH<sub>2</sub>NPh]<sub>3</sub>H<sub>3</sub> (2.987 g, 8.55 mmol) in 30 mL of toluene. The pale yellow solution was stirred 24 h. The solvent was removed under vacuum and the remaining yellow solid was rinsed with a small portion of pentane, and then dried under vacuum (3.76 g, 86 %). <sup>1</sup>H NMR (C<sub>6</sub>D<sub>6</sub>, 300 MHz, 298 K): δ 1.01 (t, <sup>3</sup>J = 7.0 Hz, 6H, NCH<sub>2</sub>CH<sub>3</sub>), 3.20 (q, 4H, <sup>3</sup>J = 7.0 Hz, NCH<sub>2</sub>CH<sub>3</sub>), 3.83 (d, 6H, <sup>2</sup>J<sub>PH</sub> = 6.4 Hz, PCH<sub>2</sub>), 6.80 (d, 6H, Ph *o*-H), 6.85 (t, 3H, Ph *p*-H), 7.23 (m, 6H, Ph *m*-H). <sup>13</sup>C {<sup>1</sup>H} NMR (C<sub>6</sub>D<sub>6</sub>, 125.8 MHz, 298 K): δ 14.5 (s, NCH<sub>2</sub>CH<sub>3</sub>), 42.8 (s, ZrNCH<sub>2</sub>CH<sub>3</sub>), 44.5 (d, J<sub>PC</sub> = 23 Hz, PCH<sub>2</sub>), 117.8 and 129.7 (s, Ph *o*-C and *m*-C), 120.2 (s, Ph *p*-C), 153.6 (d, *ipso*-C). <sup>31</sup>P {<sup>1</sup>H} NMR (C<sub>6</sub>D<sub>6</sub>, 121.5 MHz, 298 K): δ -75.2 (s). Anal. Calc'd for C<sub>25</sub>H<sub>31</sub>N<sub>4</sub>PZr: C, 58.91; H, 6.13; N, 10.99. Found: C, 58.55; H, 6.17; N, 10.77.

**P[CH<sub>2</sub>N-3,5-Me<sub>2</sub>C<sub>6</sub>H<sub>3</sub>]<sub>3</sub>ZrNEt<sub>2</sub> (12c)**. Liquid Zr(NEt<sub>2</sub>)<sub>4</sub> (3.79 g, 10.0 mmol) was added to a solution of P[CH<sub>2</sub>N-3,5-Me<sub>2</sub>C<sub>6</sub>H<sub>3</sub>]<sub>3</sub>H<sub>3</sub> (4.30 g, 10.0 mmol) in 50 mL of toluene. The pale yellow solution was stirred 48 h. The solvent was removed under

vacuum and the remaining yellow solid was rinsed with a small portion of pentane, and then dried under vacuum (4.12 g, 69.4 %). The product has only moderate solubility in benzene at room temperature, but is quite soluble in hot benzene.  $^1\text{H}$  NMR ( $\text{C}_6\text{D}_6$ , 300 MHz, 298 K):  $\delta$  1.12 (t,  $^3J = 7.1$  Hz, 6H,  $\text{NCH}_2\text{CH}_3$ ), 2.23 (s, 18H,  $\text{PhCH}_3$ ), 3.37 (q, 4H,  $^3J = 7.1$  Hz,  $\text{NCH}_2\text{CH}_3$ ), 3.95 (d, 6H,  $^2J_{\text{PH}} = 6.8$  Hz,  $\text{PCH}_2$ ), 6.52 (s, 6H, Ph *o-H*), 6.55 (s, 3H, Ph *p-H*).  $^{13}\text{C}\{^1\text{H}\}$  NMR ( $\text{C}_6\text{D}_6$ , 125.8 MHz, 298 K):  $\delta$  14.6 (s,  $\text{NCH}_2\text{CH}_3$ ), 22.1 (s,  $\text{PhCH}_3$ ), 42.8 (s,  $\text{ZrNCH}_2\text{CH}_3$ ), 44.9 (d,  $J_{\text{PC}} = 22.0$  Hz,  $\text{PCH}_2$ ), 115.9 and 122.2 (s, Ph *o-C* and *m-C*), 138.9 (s, Ph *p-C*), 153.8 (d,  $J_{\text{CC}} = 2.7$  Hz, *ipso-C*).  $^{31}\text{P}\{^1\text{H}\}$  NMR ( $\text{C}_6\text{D}_6$ , 121.5 MHz, 298 K):  $\delta$  -70.8 (s). Anal. Calc'd for  $\text{C}_{31}\text{H}_{43}\text{N}_4\text{PZr}$ : F.W.: 593.9; C, 62.69; H, 7.30; N, 9.43. Found: C, 62.50; H, 6.99; N, 9.12.

**$\text{P}[\text{CH}_2\text{NPh}]_3\text{ZrCl}(\text{THF})$  (13b).**  $\text{P}[\text{CH}_2\text{NPh}]_3\text{ZrNEt}_2$  (1.17 g, 2.0 mmol) was added to a solution of  $\text{HNEt}_3\text{Cl}$  (0.275 g, 2.0 mmol) in 50 mL of toluene. The pale yellow solution was stirred 1 h, then was added 5 mL THF. The solvent was removed under vacuum and the remaining yellow solid was rinsed with a small portion of pentane, and then dried under vacuum (910 mg, 84.1 %).  $^1\text{H}$  NMR ( $\text{C}_6\text{D}_6$ , 300 MHz, 298 K):  $\delta$  0.74 (m, 4H, THF), 3.47 (m, 4H, THF), 3.81 (d, 6H,  $^2J_{\text{PH}} = 7.0$  Hz,  $\text{PCH}_2$ ), 6.77 (t, 3H, Ph *p-H*), 6.98 (d, 6H, Ph *o-H*), 7.16 (m, 6H, Ph *m-H*).  $^{13}\text{C}\{^1\text{H}\}$  NMR ( $\text{C}_6\text{D}_6$ , 125.8 MHz, 298 K):  $\delta$  25.4 (s, THF), 44.1 (d,  $J_{\text{PC}} = 21$  Hz,  $\text{PCH}_2$ ), 72.8 (s, THF), 117.8 and 129.5 (s, Ph *o-C* and *m-C*), 120.4 (s, Ph *p-C*), 153.4 (d, *ipso-C*).  $^{31}\text{P}\{^1\text{H}\}$  NMR ( $\text{C}_6\text{D}_6$ , 121.5 MHz, 298 K):  $\delta$  -71.5 (s). Anal. Calc'd for  $\text{C}_{25}\text{H}_{29}\text{ClN}_3\text{OPZr}$ : F.W.

545.17; C, 55.08; H, 5.36; N, 7.71. Found: C, 54.83; H, 5.48; N, 8.02.

**P[CH<sub>2</sub>N-3,5-Me<sub>2</sub>C<sub>6</sub>H<sub>3</sub>]<sub>3</sub>ZrCl(THF) (13c).** P[CH<sub>2</sub>N-3,5-Me<sub>2</sub>C<sub>6</sub>H<sub>3</sub>]<sub>3</sub>ZrNEt<sub>2</sub> (2.93 g, 5.0 mmol) was added to a solution of HNEt<sub>3</sub>Cl (0.688 g, 5.0 mmol) in 120 mL of toluene. The pale yellow solution was stirred 1 h, then was added 12 mL THF. The solvent was removed under vacuum and the remaining yellow solid was rinsed with a small portion of pentane, and then dried under vacuum (2.80 g, 90 %). <sup>1</sup>H NMR (C<sub>6</sub>D<sub>6</sub>, 300 MHz, 298 K): δ 0.79 (2H, THF), 2.20 (s, 18H, PhCH<sub>3</sub>), 3.55 (2H, THF), 3.92 (d, <sup>2</sup>J<sub>PH</sub> = 6.4 Hz, 6H, PCH<sub>2</sub>), 6.45 (s, 6H, Ph *o*-H), 6.72 (s, 3H, Ph *p*-H). <sup>13</sup>C{<sup>1</sup>H} NMR (C<sub>6</sub>D<sub>6</sub>, 125.8 MHz, 298 K): δ 21.7 (s, PhCH<sub>3</sub>), 25.1 (s, THF), 44.1 (d, J<sub>PC</sub> = 19.8 Hz, PCH<sub>2</sub>), 72.5 (s, THF), 115.5 and 122.1 (s, Ph *o*-C and *m*-C), 138.2 (s, Ph *p*-C), 153.1 (d, J<sub>CC</sub> = 2.7 Hz, *ipso*-C). <sup>31</sup>P{<sup>1</sup>H} NMR (C<sub>6</sub>D<sub>6</sub>, 121.5 MHz, 298 K): δ -66.0 (s). Anal. Calc'd for C<sub>31</sub>H<sub>41</sub>ClN<sub>3</sub>OPZr: F.W.: 629.33; C, 59.16; H, 6.57; N, 6.68. Found: C, 59.12; H, 6.29; N, 6.79.

**P[CH<sub>2</sub>NPh]<sub>3</sub>ZrCp (14b).** P[CH<sub>2</sub>NPh]<sub>3</sub>ZrCl(THF) (4) (545.17 mg, 1.0 mmol) was added to a solution of CpLi (72.03 mg, 1.0 mmol) in 50 mL of toluene. The yellow solution was stirred 20 h. The solvent was removed under vacuum and the remaining yellow solid was rinsed with a small portion of pentane, and then dried under vacuum (420 mg, 80 %). <sup>1</sup>H NMR (C<sub>6</sub>D<sub>6</sub>, 300 MHz, 298 K): δ 3.90 (d, 6H, <sup>2</sup>J<sub>PH</sub> = 7.3 Hz, PCH<sub>2</sub>), 5.95 (s, 5H, Cp), 6.85 (d, 6H, Ph *o*-H), 6.92 (t, 3H, Ph *p*-H), 7.20 (m, 6H, Ph *m*-H). <sup>13</sup>C{<sup>1</sup>H} NMR (C<sub>6</sub>D<sub>6</sub>, 125.8 MHz, 298 K): δ 46.8 (d, J<sub>PC</sub> = 23.1 Hz, PCH<sub>2</sub>),

72.8 (s, THF), 114.6, 121.9, 122.8, 129.3(s, Ph *o*-C, *m*-C, *p*-C, Cp), 153.4 (s, *ipso*-C).

$^{31}\text{P}\{^1\text{H}\}$  NMR ( $\text{C}_6\text{D}_6$ , 121.5 MHz, 298 K):  $\delta$  -67.5 (s). Anal. Calc'd for  $\text{C}_{26}\text{H}_{26}\text{N}_3\text{PZr}$ : F.W. 502.7; C, 62.12; H, 5.21; N, 8.36. Found: C, 62.37; H, 5.48; N, 8.02.

**P[CH<sub>2</sub>N-3,5-Me<sub>2</sub>C<sub>6</sub>H<sub>3</sub>]<sub>3</sub>ZrCp (14c).** P[CH<sub>2</sub>N-3,5-Me<sub>2</sub>C<sub>6</sub>H<sub>3</sub>]<sub>3</sub>ZrCl(THF) (3) (629.33 mg, 1.0 mmol) was added to a solution of CpLi (72.03 mg, 1.0 mmol) in 50 mL of toluene. The yellow solution was stirred 20 h. The solvent was removed under vacuum and the remaining yellow solid was rinsed with a small portion of pentane, and then dried under vacuum (530 mg, 90 %). X-ray quality crystals were obtained from slow evaporation of a toluene solution.  $^1\text{H}$  NMR ( $\text{C}_6\text{D}_6$ , 300 MHz, 298 K):  $\delta$  2.23 (s, 18H, PhCH<sub>3</sub>), 4.00 (d,  $^2J_{\text{PH}} = 6.7$  Hz, 6H, PCH<sub>2</sub>), 6.18 (s, 5H, Cp), 6.60 (s, 3H, Ph *p*-H), 6.68 (s, 6H, Ph *o*-H).  $^{13}\text{C}\{^1\text{H}\}$  NMR ( $\text{C}_6\text{D}_6$ , 125.8 MHz, 298 K):  $\delta$  21.8 (s, PhCH<sub>3</sub>), 47.0 (d,  $J_{\text{PC}} = 23.1$  Hz, PCH<sub>2</sub>), 114.6, 120.8, 123.8, 138.4 (s, Ph *o*-C, *m*-C, *p*-C, Cp), 159.9 (s, *ipso*-C).  $^{31}\text{P}\{^1\text{H}\}$  NMR ( $\text{C}_6\text{D}_6$ , 121.5 MHz, 298 K):  $\delta$  -66.9 (s). Anal. Calc'd for  $\text{C}_{32}\text{H}_{38}\text{N}_3\text{PZr}$ : F.W. 586.86; C, 65.49; H, 6.53; N, 7.16. Found: C, 65.68; H, 6.64; N, 6.69.

**P[CH<sub>2</sub>NPh]<sub>3</sub>Li<sub>3</sub>(Et<sub>2</sub>O)<sub>1.5</sub> (15b).** A 1.6 M solution of <sup>n</sup>BuLi (28.0 mL, 17.5 mmol, 3 equiv) in hexanes was added dropwise to a stirred slurry of P(CH<sub>2</sub>NPh)<sub>3</sub>H<sub>3</sub> (2.04 g, 5.84 mmol) in ether (80 mL) at 0 °C. After the addition of 2 equiv of <sup>n</sup>BuLi the solution was clear. The addition of the third equivalent precipitated a white solid. The solid was filtered and dried under vacuum (yield 80 %). The product is insoluble

in toluene, ether, or  $\text{CH}_2\text{Cl}_2$ . The addition of THF generates the more soluble THF adduct. This adduct is soluble in THF and  $\text{CH}_2\text{Cl}_2$  but decomposes within an hour at room temperature in the latter. Crystals of the THF adduct suitable for characterization by X-ray diffraction were obtained from THF by slow evaporation.  $^1\text{H}$  NMR ( $d_8$ -THF, 500.1 MHz, 298 K):  $\delta$  1.12 (t, 9H,  $^3J = 7.0$  Hz,  $\text{OCH}_2\text{CH}_3$ ) 3.39 (q, 6H,  $^3J = 7.0$  Hz,  $\text{OCH}_2\text{CH}_3$ ), 3.47 (d, 6H,  $^2J_{\text{PC}} = 7.0$  Hz,  $\text{PCH}_2$ ), 6.09 (t, 3H, Ph *p*-H), 6.42 (d, 6H,  $^3J_{\text{HH}} = 8.3$  Hz, Ph *o*-H), 6.85 (m, 6H, Ph *m*-H).  $^{31}\text{P}\{^1\text{H}\}$  NMR ( $d_8$ -THF, 202.5 MHz, 298 K):  $\delta$  -22.15 (s).  $^{13}\text{C}\{^1\text{H}\}$  NMR ( $d_8$ -THF, 125.8 MHz, 298 K):  $\delta$  15.9 (s,  $\text{OCH}_2\text{CH}_3$ ), 50.3 (d,  $J_{\text{PC}} = 12$  Hz,  $\text{PCH}_2$ ), 110.9, 114.2, 129.3 (s, *o*, *m*, *p*-C), 164.2 (m, *ipso*-C).  $^7\text{Li}$  NMR ( $d_8$ -THF, 116.7 MHz, 298 K):  $\delta$  1.34 (s). Anal. Calc'd for  $\text{C}_{27}\text{H}_{36}\text{Li}_3\text{N}_3\text{O}_{1.5}\text{P}$ : C, 67.79; H, 7.58; N, 8.78. Found: C, 68.08; H 7.49, N, 8.74.

**$\text{P}[\text{CH}_2\text{N}-3,5\text{-Me}_2\text{C}_6\text{H}_3]_3\text{Li}_3(\text{Et}_2\text{O})_{1.5}$  (15c).** A 1.6 M solution of  $n\text{BuLi}$  (9.4 mL, 15 mmol) in hexanes was added dropwise to a stirred slurry of  $\text{P}[\text{CH}_2\text{N}-3,5\text{-Me}_2\text{C}_6\text{H}_3]_3\text{H}_3$  (2.15 g, 5 mmol) in ether (50 mL) at  $0^\circ\text{C}$  and stirred at r.t. for 1 hour. The solid was filtered and dried under vacuum (2.12 g, 75 %).  $^1\text{H}$  NMR ( $d_8$ -THF, 500.1 MHz, 298 K):  $\delta$  1.11 (t, 9H,  $^3J = 6.9$  Hz,  $\text{OCH}_2\text{CH}_3$ ), 2.08 (s, 18H,  $\text{ArCH}_3$ ), 3.38 (m, 6H,  $^3J = 7.0$  Hz,  $\text{OCH}_2\text{CH}_3$  &  $\text{PCH}_2$ ), 5.80 (s, 3H, *p*-H), 6.10 (s, 6H, *o*-H).  $^{31}\text{P}\{^1\text{H}\}$  NMR ( $d_8$ -THF, 202.5 MHz, 298 K):  $\delta$  -21.7 (s).  $^{13}\text{C}\{^1\text{H}\}$  NMR ( $d_8$ -THF, 125.8 MHz, 298 K):  $\delta$  15.6 (s,  $\text{OCH}_2\text{CH}_3$ ), 22.1 (s,  $\text{PhCH}_3$ ), 50.1 (d,  $J_{\text{PC}} = 11$  Hz,  $\text{PCH}_2$ ), 66.3 (s,  $\text{OCH}_2\text{CH}_3$ ), 112.0, 112.8, 137.3 (s, *o*, *m*, *p*-C), 164.2 (m, *ipso*-C).  $^7\text{Li}$  NMR ( $d_8$ -THF, 116.7 MHz, 298 K):  $\delta$  1.06 (s). Anal. Calc'd for

$C_{33}H_{48}Li_3N_3O_{1.5}P$ : C, 73.58; H, 7.92; N, 6.60. Found: C, 73.05; H, 7.55; N, 6.99.

**[P(CH<sub>2</sub>NPh)<sub>3</sub>Zr]<sub>2</sub>(η<sup>5</sup>:η<sup>5</sup>-C<sub>10</sub>H<sub>8</sub>) (16b).** P[CH<sub>2</sub>NPh]<sub>3</sub>ZrCl(THF) (4) (545.17 mg, 1.0 mmol) was added to a solution of Cp<sub>2</sub>Li<sub>2</sub> (72 mg, 0.5 mmol) in 50 mL of toluene. The solution was stirred 12 h and filtered to remove the solid. The solvent was removed under vacuum and the remaining yellow solid was rinsed with a small portion of pentane, and then dried under vacuum (205 mg, 40 %). <sup>1</sup>H NMR (C<sub>6</sub>D<sub>6</sub>, 300 MHz, 298 K): δ 3.89 (d, <sup>2</sup>J<sub>PH</sub> = 7.3 Hz, 12H, PCH<sub>2</sub>), 5.49 (s, 4H, Cp), 5.93 (s, 4H, Cp), 6.70 (d, 6H, Ph o-H), 6.90 (t, 3H, Ph p-H), 7.20 (m, 6H, Ph m-H). <sup>13</sup>C{<sup>1</sup>H} NMR (C<sub>6</sub>D<sub>6</sub>, 125.8 MHz, 298 K): δ 46.9 (d, J<sub>PC</sub> = 23.0 Hz, PCH<sub>2</sub>), 113.9 and 118.8, 123.1, 129.2, 129.8, 138.9 (s, Ph o-C, m-C, p-C, Cp), 158.8 (s, ipso-C). <sup>31</sup>P{<sup>1</sup>H} NMR (C<sub>6</sub>D<sub>6</sub>, 121.5 MHz, 298 K): δ -57.1 (s). Anal. Calc'd for (C<sub>26</sub>H<sub>26</sub>N<sub>3</sub>PZr)<sub>2</sub>: F.W. 1005.4; C, 62.12; H, 5.21; N, 8.36. Found: C, 61.79; H, 5.64; N, 8.47.

**[P(CH<sub>2</sub>N-3,5-Me<sub>2</sub>C<sub>6</sub>H<sub>3</sub>)<sub>3</sub>Zr]<sub>2</sub>(η<sup>5</sup>:η<sup>5</sup>-C<sub>10</sub>H<sub>8</sub>) (16c).**

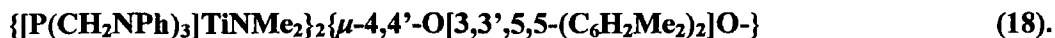
P[CH<sub>2</sub>N-3,5-Me<sub>2</sub>C<sub>6</sub>H<sub>3</sub>]<sub>3</sub>ZrCl(THF) (3) (629.33 mg, 1.0 mmol) was added to a solution of Cp<sub>2</sub>Li<sub>2</sub> (72 mg, 0.5 mmol) in 50 mL of toluene. The solution was stirred 12 h and filtered to remove the solid. The solvent was removed under vacuum and the remaining yellow solid was rinsed with a small portion of pentane, and then dried under vacuum (280 mg, 48 %). X-ray quality crystals were obtained from slow evaporation of a mixture of benzene and hexamethyldisiloxane solution. <sup>1</sup>H NMR (C<sub>6</sub>D<sub>6</sub>, 300 MHz, 298 K): δ 2.18 (s, 36H, PhCH<sub>3</sub>), 3.86 (d, <sup>2</sup>J<sub>PH</sub> = 7.2 Hz, 12H, PCH<sub>2</sub>),

5.70 (s, 4H, Cp), 6.17 (s, 4H, Cp), 6.50 (s, 6H, Ph o-H), 6.55 (s, 3H, Ph p-H). <sup>13</sup>C{<sup>1</sup>H} NMR (C<sub>6</sub>D<sub>6</sub>, 125.8 MHz, 298 K): δ 21.8 (s, PhCH<sub>3</sub>), 48.1 (d, *J*<sub>PC</sub> = 22.2 Hz, PCH<sub>2</sub>), 110.1 and 112.6, 121.8, 124.0, 128.8, 138.2 (s, Ph o-C, m-C, p-C, Cp), 158.9 (s, *ipso-C*). <sup>31</sup>P{<sup>1</sup>H} NMR (C<sub>6</sub>D<sub>6</sub>, 121.5 MHz, 298 K): δ -56.3 (s). Anal. Calc'd for (C<sub>32</sub>H<sub>38</sub>N<sub>3</sub>PZr)<sub>2</sub>: F.W. 1173.72; C, 65.49; H, 6.53; N, 7.16. Found: C, 65.76; H, 6.83; N, 7.53.

**P[CH<sub>2</sub>NPh]<sub>3</sub>TiO[4-*t*-BuC<sub>6</sub>H<sub>3</sub>] (17b).** HO-(4-*t*-BuC<sub>6</sub>H<sub>3</sub>) (150 mg, 1.0mmol) were added to a solution of P[CH<sub>2</sub>NPh]<sub>3</sub>TiNMe<sub>2</sub> (438.3 mg, 1 mmol) in 50 mL toluene. The solution was stirred for 48 h. The solvent was removed under vacuum and the remaining red solid was rinsed with a small portion of cold pentane, and then dried under vacuum (277 mg, 51 %). <sup>1</sup>H NMR (C<sub>6</sub>D<sub>6</sub>, 300 MHz, 298 K): δ 1.19 (s, 9H, C(CH<sub>3</sub>)<sub>3</sub>), 3.85 (d, <sup>2</sup>*J*<sub>PH</sub> = 7.0 Hz, 6H, PCH<sub>2</sub>), 6.81 (m, 3H, Ph p-H), 7.04 (m, 2H, C<sub>6</sub>H<sub>4</sub>), 7.06 (m, 6H, Ph m-H), 7.13 (m, 2H, C<sub>6</sub>H<sub>4</sub>), 7.18(m, 6H, Ph o-H). <sup>13</sup>C{<sup>1</sup>H} NMR (C<sub>6</sub>D<sub>6</sub>, 125.8 MHz, 298 K): δ 1.35 (s, C(CH<sub>3</sub>)<sub>3</sub>), 31.7 (s, C(CH<sub>3</sub>)<sub>3</sub>), 44.1 (d, *J*<sub>PC</sub> = 20.0 Hz, PCH<sub>2</sub>), 116.4, 119.8, 121.1, 127.0, 129.8, 146.5, and 153.3 (s, C<sub>6</sub>H<sub>5</sub>, C<sub>6</sub>H<sub>4</sub>), 164.2 (s, *ipso-C*). <sup>31</sup>P{<sup>1</sup>H} NMR (C<sub>6</sub>D<sub>6</sub>, 202.5 MHz, 298 K): δ -81.07 (s). Anal. Calc'd for C<sub>31</sub>H<sub>34</sub>N<sub>3</sub>OPTi: F.W.: 543.5; C, 68.51; H, 6.31; N, 7.73. Found: C, 68.92; H, 6.85; N, 7.27.

**P[CH<sub>2</sub>N-3,5-Me<sub>2</sub>C<sub>6</sub>H<sub>3</sub>]<sub>3</sub>TiO[4-*t*-BuC<sub>6</sub>H<sub>3</sub>] (17c).** HO-(4-*t*-BuC<sub>6</sub>H<sub>3</sub>) (150 mg, 1.0 mmol) were added to a solution of P[CH<sub>2</sub>N-3,5-Me<sub>2</sub>C<sub>6</sub>H<sub>3</sub>]<sub>3</sub>TiNMe<sub>2</sub> (522.3 mg, 1

mmol) in 50 mL toluene. The solution was stirred for 48 h. The solvent was removed under vacuum and the remaining red solid was rinsed with a small portion of cold pentane, and then dried under vacuum (378 mg, 60 %). X-ray quality crystals were obtained from toluene by slow evaporation.  $^1\text{H}$  NMR ( $\text{C}_6\text{D}_6$ , 300 MHz, 298 K):  $\delta$  0.29 (s, 9H,  $\text{C}(\underline{\text{C}}\text{H}_3)_3$ ), 1.90 (s, 18H,  $\text{Ar}\underline{\text{C}}\text{H}_3$ ), 3.97 (d,  $^2J_{\text{PH}} = 6.8$  Hz, 6H,  $\text{P}\underline{\text{C}}\text{H}_2$ ), 6.23 (m, 2H,  $\text{C}_6\underline{\text{H}}_4$ ), 6.25 (s, 3H,  $\text{Ph } p\text{-}\underline{\text{H}}$ ), 6.45 (m, 2H,  $\text{C}_6\underline{\text{H}}_4$ ), 6.59 (s, 6H,  $\text{Ph } o\text{-}\underline{\text{H}}$ ).  $^{13}\text{C}\{^1\text{H}\}$  NMR ( $\text{C}_6\text{D}_6$ , 125.8 MHz, 298 K):  $\delta$  1.7 (s,  $\text{C}(\underline{\text{C}}\text{H}_3)_3$ ), 21.3 (s,  $\text{Ar}\underline{\text{C}}\text{H}_3$ ), 21.9 (s,  $\underline{\text{C}}(\text{CH}_3)_3$ ), 45.3 (d,  $J_{\text{PC}} = 18.4$  Hz,  $\text{P}\underline{\text{C}}\text{H}_2$ ), 112.0, 114.2, 116.0, 116.5, 120.8, 123.5, and 138.6 (s,  $\underline{\text{C}}_6\text{H}_5$ ,  $\underline{\text{C}}_6\text{H}_4$ ), 153.3 (s, *ipso*- $\underline{\text{C}}$ ).  $^{31}\text{P}\{^1\text{H}\}$  NMR ( $\text{C}_6\text{D}_6$ , 202.5 MHz, 298 K):  $\delta$  -77.9 (s). Anal. Calc'd for  $\text{C}_{37}\text{H}_{46}\text{N}_3\text{OPTi}$ : F.W.: 627.6; C, 70.81; H, 7.39; N, 6.70. Found: C, 69.59; H, 7.61; N, 6.99.



{1,1-HO[2,2,6,6-( $\text{C}_6\text{H}_2\text{Me}_2$ ) $_2$ ]OH} (121 mg, 0.5 mmol) were added to a solution of  $\text{P}[\text{CH}_2\text{NPh}]_3\text{TiNMe}_2$  (438.3 mg, 1 mmol) in 50 mL toluene. The solution was stirred for 48 h. The solvent was removed under vacuum and the remaining red solid was rinsed with a small portion of cold pentane, and then dried under vacuum (277 mg, 51 %).  $^1\text{H}$  NMR ( $\text{C}_6\text{D}_6$ , 300 MHz, 298 K):  $\delta$  2.24 (s, 12H,  $\text{C}_6\text{H}_2(\underline{\text{C}}\text{H}_3)_2$ ), 3.93 (d,  $^2J_{\text{PH}} = 7.0$  Hz, 12H,  $\text{P}\underline{\text{C}}\text{H}_2$ ), 6.73 (t, 6H,  $J = 8.3$  Hz,  $\text{Ph } p\text{-}\underline{\text{H}}$ ), 6.95 (d,  $J = 8.3$  Hz, 12H,  $\text{Ph } o\text{-}\underline{\text{H}}$ ), 7.10 (m, 12H,  $\text{Ph } m\text{-}\underline{\text{H}}$ ), 7.17 (s, 4H,  $\text{C}_6\underline{\text{H}}_2$ ).  $^{13}\text{C}\{^1\text{H}\}$  NMR ( $\text{C}_6\text{D}_6$ , 125.8 MHz, 298 K):  $\delta$  18.4 (s,  $\text{C}_6\text{H}_2(\underline{\text{C}}\text{H}_3)_2$ ), 45.6 (d,  $J_{\text{PC}} = 20.7$  Hz,  $\text{P}\underline{\text{C}}\text{H}_2$ ), 113.8, 117.0, 121.5, 127.7, 129.5, and 135.7 (s,  $\underline{\text{C}}_6\text{H}_5$ ,  $\underline{\text{C}}_6\text{H}_2$ ), 153.9 (s, *ipso*- $\underline{\text{C}}_6\text{H}_5$ ), 164.2 (s, *ipso*- $\text{O}-\underline{\text{C}}_6\text{H}_2$ ).

$^{31}\text{P}\{^1\text{H}\}$  NMR ( $\text{C}_6\text{D}_6$ , 202.5 MHz, 298 K):  $\delta$  -78.6 (s). Anal. Calc'd for  $\text{C}_{58}\text{H}_{58}\text{N}_6\text{O}_2\text{P}_2\text{Ti}_2$ : F.W.: 543.5; C, 67.71; H, 5.68; N, 8.17. Found: C, 67.37; H, 5.58; N, 7.89.

**$\text{P}[\text{CH}_2\text{NPh}]_3\text{Ti}-\mu\text{-O}-\text{Ti}[\text{PhNCH}_2]_3\text{P}$  (19).**  $\text{Na}_2\text{SO}_4 \cdot 10\text{H}_2\text{O}$  (161.1 mg, 0.5 mmol) were added to a solution of  $\text{P}[\text{CH}_2\text{NPh}]_3\text{TiNMe}_2$  (438.3 mg, 1 mmol) in mixture of 50 mL toluene and 10 mL THF. The solution was stirred for two weeks. The solvent was removed under vacuum and the remaining red solid was rinsed with a small portion of cold pentane, and then dried under vacuum (200 mg, 49 %).  $^1\text{H}$  NMR ( $\text{C}_6\text{D}_6$ , 300 MHz, 298 K):  $\delta$  3.68 (d,  $^2J_{\text{PH}} = 7.8$  Hz, 12H,  $\text{PCH}_2$ ), 6.68 (t, 6H,  $J = 7.3$  Hz, Ph *p-H*), 6.80 (d,  $J = 8.2$  Hz, 6H, Ph *o-H*), 6.92 (t, 6H,  $J = 7.8$  Hz, Ph *m-H*).  $^{13}\text{C}\{^1\text{H}\}$  NMR ( $\text{C}_6\text{D}_6$ , 125.8 MHz, 298 K):  $\delta$  45.4 (d,  $J_{\text{PC}} = 19.8$  Hz,  $\text{PCH}_2$ ), 117.2, 121.6 and 129.4 (s,  $\text{C}_6\text{H}_5$ ), 153.8 (s, *ipso-C*).  $^{31}\text{P}\{^1\text{H}\}$  NMR ( $\text{C}_6\text{D}_6$ , 202.5 MHz, 298 K):  $\delta$  -39.3 (s). Anal. Calc'd for  $\text{C}_{42}\text{H}_{42}\text{N}_6\text{OP}_2\text{Ti}_2$ : F.W.: 804.5; C, 62.7; H, 5.26; N, 10.45. Found: C, 62.40; H, 5.14; N, 10.52.

**$\text{P}[\text{CH}_2\text{N}-3,5\text{-Me}_2\text{C}_6\text{H}_3]_3\text{Ti}-\mu\text{-O}-\text{Ti}(\text{NMe}_2)_3$  (20).**  $\text{Ti}(\text{NMe}_2)_4$  (224.2 mg, 1.0 mmol) and 1 mL  $\text{H}_2\text{O}/\text{Ether}$  (1M) were added to a solution of  $\text{P}[\text{CH}_2\text{N}-3,5\text{-Me}_2\text{C}_6\text{H}_3]_3\text{TiNMe}_2$  (522.3 mg, 1 mmol) in 50 mL toluene. The solution was stirred for 24 h and evaporated to dryness, and 5 mL pentane and 10 mL hexamethyldisiloxane were added. The solution was filtered and the remaining orange red solid was rinsed with a small portion of pentane, and then dried under vacuum (370 mg, 55 %).  $^1\text{H}$  NMR

(C<sub>6</sub>D<sub>6</sub>, 500 MHz, 298 K):  $\delta$  2.27 (s, 18H, ArCH<sub>3</sub>), 3.03 (s, 18H, NMe<sub>2</sub>), 3.84 (d, <sup>2</sup>J<sub>PH</sub> = 7.0 Hz, 6H, PCH<sub>2</sub>), 6.60 (s, 6H, Ph *o*-H), 6.87 (s, 3H, Ph *p*-H). <sup>13</sup>C{<sup>1</sup>H} NMR (C<sub>6</sub>D<sub>6</sub>, 125.8 MHz, 298 K):  $\delta$  22.1 (s, ArCH<sub>3</sub>), 44.3 (s, NMe<sub>2</sub>), 44.8 (d, J<sub>PC</sub> = 19.7 Hz, PCH<sub>2</sub>), 114.5, 122.2, and 138.3 (s, Ph *o*-C, *m*-C and *p*-C), 153.8 (s, *ipso*-C). <sup>31</sup>P{<sup>1</sup>H} NMR (C<sub>6</sub>D<sub>6</sub>, 202.5 MHz, 298 K):  $\delta$  -62.9 (s). Anal. Calc'd for C<sub>33</sub>H<sub>51</sub>N<sub>6</sub>OPTi<sub>2</sub>: F.W.: 674.57; C, 58.76; H, 7.62; N, 12.46. Found: C, 58.59; H, 7.41; N, 11.99.

[*trans*-RhCl(CO)(19)]<sub>n</sub> (21). A solution of 16 (80.0 mg, 0.1 mmol) in 20 mL of CD<sub>2</sub>Cl<sub>2</sub> was added to 18.9 mg (0.1 mmol) of [RhCl(CO)<sub>2</sub>]<sub>2</sub> in 10 mL CD<sub>2</sub>Cl<sub>2</sub>. Red solids were obtained by evaporation of the CD<sub>2</sub>Cl<sub>2</sub> solution. IR: 1972.5 cm<sup>-1</sup>. Anal. Calc'd for C<sub>43</sub>H<sub>42</sub>ClN<sub>6</sub>O<sub>2</sub>ClRhP<sub>2</sub>Ti<sub>2</sub>: C, 53.20; H, 4.36; N, 8.66. Found: C, 52.78; H, 4.41; N, 8.41.

### 3.8.3 Crystal Data and Structure Refinement

**Table 3.1.** Crystal data and structure refinement for **14c**, **15d**, **16c**, **17c**, **19** and **20**.

	<b>14c</b>	<b>15d</b>	<b>16c</b>
Empirical formula	C <sub>32</sub> H <sub>38</sub> N <sub>3</sub> PZr	C <sub>20.5</sub> H <sub>30.5</sub> Li <sub>1.5</sub> N <sub>1.5</sub> O <sub>2.5</sub> P <sub>0.5</sub>	C <sub>76</sub> H <sub>86</sub> N <sub>6</sub> P <sub>2</sub> Zr <sub>2</sub>
Formula weight	586.84	363.86	1327.89
Temperature	173(2) K	173(2) K	173(2) K
Crystal system	Triclinic	Orthorhombic	Monoclinic
a	11.4611(9) Å	25.863(14) Å	15.120(2) Å
b	15.4190(12) Å	14.907(8) Å	13.8406(19) Å
c	18.5870(14) Å	10.978(6) Å	18.128(3) Å
α	101.28(10)°	90.00°	90.00°
β	107.86(10)°	90.00°	113.68(10)
γ	102.39(10)°	90.00°	90.00°
Volume Å <sup>3</sup>	2930.1(4)	4232(4)	3474.2(8)
Z	4	8	2
Density (calculated)	1.330 mg/m <sup>3</sup>	1.142 mg/m <sup>3</sup>	1.269 mg/m <sup>3</sup>
μ(MoKα)	0.455 mm <sup>-1</sup>	0.108 mm <sup>-1</sup>	0.392 mm <sup>-1</sup>
No. Variables	679	471	394
Total No. of Reflns	33013	17451	37628
Residuals: R; wR <sub>2</sub> (all data)	0.0397, 0.0902	0.0786, 0.1438	0.0661, 0.1192
Residual Density, e <sup>-</sup> /Å <sup>3</sup>	0.556, -0.305	0.423, -0.198	0.786, -0.66

Table 3.2 cont'd.

	17c	19	20
Empirical formula	C <sub>39.5</sub> H <sub>52</sub> N <sub>30</sub> PTi	C <sub>33</sub> H <sub>51</sub> N <sub>60</sub> PTi <sub>2</sub>	C <sub>42</sub> H <sub>42</sub> N <sub>60</sub> P <sub>2</sub> Ti <sub>2</sub>
Formula weight	663.71	674.57	804.56
Temperature	173(2) K	173(2) K	173(2) K
Crystal system	Monoclinic	Rhombohedral	Trigonal
a	14.225(3) Å	12.2710(19) Å	13.0770(14) Å
b	14.471(3) Å	12.2710(19) Å	13.0770(14) Å
c	20.351(5) Å	12.2710(19) Å	20.452(4) Å
$\alpha$	77.687(3)°	80.53°	90.00°
$\beta$	77.687(3)°	80.53°	90.00°
$\gamma$	68.183(3)°	80.53°	120.00°
Volume Å <sup>3</sup>	3661.6(14)	1779.6(5)	3028.8(8)
Z	4	2	3
Density (calculated)	1.204 mg/m <sup>3</sup>	1.259 mg/m <sup>3</sup>	1.323 mg/m <sup>3</sup>
$\mu$ (MoK $\alpha$ )	0.311 mm <sup>-1</sup>	0.527 mm <sup>-1</sup>	0.515 mm <sup>-1</sup>
Total No. of Reflns	41175	17140	11068
No. Variables	786	134	81
No. of Unique Reflns	16230 ( $R_{int}$ = 0.0587)	2755 ( $R_{int}$ = 0.0413)	1548 ( $R_{int}$ = 0.0496)
Residuals: R; wR <sub>2</sub> (all data)	0.1357, 0.2529	0.0803, 0.1233	0.0708, 0.1328
Residual Density, e <sup>-</sup> /Å <sup>3</sup>	1.4, -0.651	0.482, -0.439	0.564, -0.438

### 3.9 References

- (1) Kempe, R. *Angew. Chem. Int. Ed.* **2000**, *39*, 468-493.
- (2) Cotton, F. A.; Lin, C.; Murillo, C. A. *Acc. Chem. Res.* **2001**, *34*, 759-771.
- (3) Swiegers, G. F.; Malefetse, T. J. *Coord. Chem. Rev.* **2002**, *225*, 91-121.
- (4) Barnett, S. A.; Champness, N. R. *Coord. Chem. Rev.* **2003**, *246*, 145-168.
- (5) Axenov, K. V.; Kilpelainen, I.; Klinga, M.; Leskelae, M.; Repo, T. *Organometallics* **2006**, *25*, 463-471.
- (6) Porter, R. M.; Danopoulos, A. A. *Dalton Trans.* **2004**, 2556-2562.
- (7) Ramos, C.; Royo, P.; Lanfranchi, M.; Pellinghelli, M. A.; Tiripicchio, A. *Eur. J. Inorg. Chem.* **2005**, 3962-3970.
- (8) Jeon, Y.-M.; Heo, J.; Lee, W. M.; Chang, T.; Kim, K. *Organometallics* **1999**, *18*, 4107-4113.
- (9) Fryzuk, M. D.; Kozak, C. M.; Bowdridge, M. R.; Jin, W.; Tung, D.; Patrick, B. O.; Rettig, S. J. *Organometallics* **2001**, *20*, 3752-3761.
- (10) Han, H.; Elsmaili, M.; Johnson, S. A. *Inorg. Chem.* **2006**, *45*, 7435-7445. Keen, A. L.; Doster, M.; Han, H.; Johnson, S. A. *Chem. Commun.* **2006**, 1221-1223.
- (11) Lutz, M.; Haukka, M.; Pakkanen, T. A.; Gade, L. H. *Inorg. Chem.* **2003**, *42*, 2798-2804.
- (12) Findeis, R. A.; Gade, L. H. *Dalton Trans.* **2003**, 249-254.
- (13) Findeis, R. A.; Gade, L. H. *Eur. J. Inorg. Chem.* **2003**, 99-110.
- (14) Gade, L. H. *J. Organomet. Chem.* **2002**, *661*, 85-94.
- (15) Lutz, M.; Haukka, M.; Pakkanen, T. A.; Gade, L. H. *Organometallics* **2002**, *21*,

3477-3480.

(16)Gade, L. H. *Eur. J. Inorg. Chem.* **2002**, 1257-1268.

(17)Gade, L. H. *Acc. Chem. Res.* **2002**, 35, 575-582.

(18)Harvey, P. D. *Frontiers in Transition Metal-Containing Polymers* **2007**, 321-368.

(19)Alder, R. W.; Butts, C. P.; Orpen, A. G.; Read, D.; Oliva, J. M. *J. Chem. Soc. Perkin Trans.* **2001**, 282-287.

(20)Alder, R. W.; Ellis, D. D.; Gleiter, R.; Harris, C. J.; Lange, H.; Orpen, A. G.; Read, D.; Taylor, P. N. *J. Chem. Soc. Perkin Trans.* **1998**, 1657-1668.

(21)Alder, R. W.; Ellis, D. D.; Orpen, A. G.; Taylor, P. N. *Chem. Commun.* **1996**, 539-540.

(22)Diel, B. N.; Norman, A. D. *Phosphorus and Sulfur and the Related Elements* **1982**, 12, 227-235.

(23)Kisanga, P.; Verkade, J. *Heteroatom Chem.* **2001**, 12, 114-117.

(24)Keller, H.; Regitz, M. *Tetrahedron Lett.* **1988**, 29, 925-928.

(25)Chien, P.-S.; Liang, L.-C. *Inorg. Chem.* **2005**, 44, 5147-5151.

(26)Urnezius, E.; Klippenstein, S. J.; Protasiewicz, J. D. *Inorg. Chim. Acta* **2000**, 297, 181-190.

(27)Fan, M.; Zhang, H.; Lattman, M. *Inorg. Chem.* **2006**, 45, 6490-6496.

(28)Baumann, R.; Stumpf, R.; Davis, W. M.; Liang, L.-C.; Schrock, R. R. *J. Am. Chem. Soc.* **1999**, 121, 7822-7836.

(29)Gade, L. H.; Mahr, N. *J. Chem. Soc. Dalton Trans.* **1986**, 489-494.

(30)Hellmann, K. W.; Gade, L. H.; Li, W.-S.; McPartlin, M. *Inorg. Chem.* **1994**, 33,

5974-5977.

(31) Davis, J. H.; Sinn, E.; Grimes, R. N. *J. Am. Chem. Soc.* **1989**, *111*, 4784-4790.

(32) Kang, Y. K.; Shin, K. S.; Lee, S.-G.; Lee, I. S.; Chung, Y. K. *Organometallics* **1999**, *18*, 180-186.

(33) Curtis, C. J.; Haltiwanger, R. C. *Organometallics* **1991**, *10*, 3220-3226.

(34) Moreno, C.; Macazaga, M.-J.; Medina, R.-M.; Farrar, D. H.; Delgado, S. *Organometallics* **1998**, *17*, 3733-3738.

(35) Drage, J. S.; Vollhardt, K. P. C. *Organometallics* **1986**, *5*, 280-297.

(36) Arvalo, S.; Bonillo, M. R.; de Jess, E.; de la Mata, F. J.; Flores, J. C.; Gmez, R.; Gmez-Sal, P.; Ortega, P. *J. Organomet. Chemistry* **2003**, *681*, 228 - 236.

(37) Bieller, S.; Bolte, M.; Lerner, H.-W.; Wagner, M. *Inorg. Chem.* **2005**, *44*, 9489-9496.

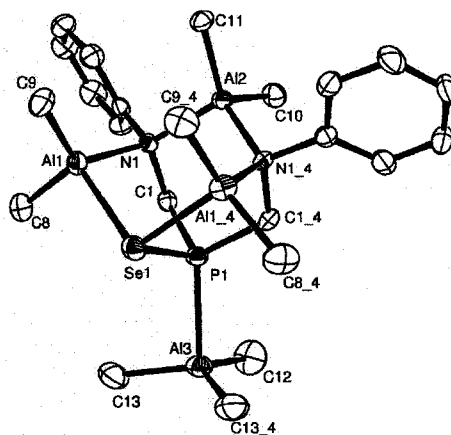
(38) Arevalo, S.; Bonillo, M. R.; De Jesus, E.; De la Mata, F. J.; Flores, J. C.; Gomez, R.; Gomez-Sal, P.; Ortega, P. *J. Organomet. Chem.* **2003**, *681*, 228-236.

(39) Arevalo, S.; Benito, J. M.; De Jesus, E.; De la Mata, F. J.; Flores, J. C.; Gomez, R. *J. Organomet. Chem.* **1999**, *592*, 265-270.

(40) Kuenzel, A.; Sokolow, M.; Liu, F.-Q.; Roesky, H. W.; Noltemeyer, M.; Schmidt, H.-G.; Uson, I. *J. Chem. Soc. Dalton Trans.* **1996**, 913-919.

(41) Hagadorn, J. R.; Arnold, J. *J. Am. Chem. Soc.* **1996**, *118*, 893-894.

Chapter Four



**Diamidoselenophosphinito Ligands by P-C bond Cleavage of  
Phosphine Selenides and a Comparison to Related Tripodal  
Triamidophosphine Complexes**

**4.1 Introduction**

The design of multidentate ligands has been of great interest, especially ligands with a combination of hard (N) and soft E (P, S, Se, or Te) donor sites,<sup>1-5</sup> which exhibit remarkable coordinative flexibility by being able to chelate main

group metals and transition metals with N, N or N, E bonding modes.<sup>6-9</sup> The availability of these combined multidentate ligands has contributed much to the synthesis of metal chalcogenates mono- and polynuclear complexes<sup>10,11</sup> with desirable structures and functions, as well as the synthesis of extended inorganic solids with novel magnetic, electronic and optical properties<sup>12-19</sup>.

Our studies have utilized the trianionic triamidophosphine donors  $P(CH_2NHAr^R)_3$  as an ancillary ligand for polynuclear complex assembly, where  $Ar^R = 3,5-(CF_3)_2C_6H_3$ , Ph, and 3,5-Me<sub>2</sub>C<sub>6</sub>H<sub>3</sub>. The mononuclear early transition metal complexes with tripodal amido-phosphine ligands were used as building block to synthesize early-late polynuclear or heterobimetallic complexes, as well as bridged binuclear early transition metal complexes.<sup>20,21</sup>

The factors which led us to investigate the donor functions in polydentate ligand designs that favor polynuclear complex formation were both the increased polarizability of the heavier chalcogenides, which should encourage electronic communication between metal centres, as well as their propensity to bridge metal centers. In this chapter we report the synthesis of diamidoselenophosphinito ancillary ligands, and the biamido-selenophosphine(III) (N, N, Se) complexes with three aluminum metal centres by the treatment of the ligands  $SeP[CH_2NAr^R]_3H_3$  with 4 equiv AlMe<sub>3</sub>, which are accompanied by the P-C bond cleavage (as shown in Figure 4.1, bonding mode A). Anionic Se donors are much less common than their oxygen and sulfur analogs,<sup>22</sup> and selenophosphinito donors ( $R_2PSe^-$ ) have not

previously been incorporated into multidentate donor ligands, to the best of our knowledge, although related ligands are known.<sup>8,16,18,23-25</sup> These ligands are anticipated to be an improvement to the  $P(\text{CH}_2\text{NHA}^{\text{R}})_3$  ligands for the formation of polynuclear clusters of paramagnetic metals, where strong magnetic coupling between metal centers is desired, due to the increased polarizability of the selenophosphinito donor relative to amido donors.

In addition, we also present the dinuclear aluminum compounds from the ligand precursors  $[P(\text{CH}_2\text{NHA}^{\text{R}})_3]$  (bonding mode **B**). For both types of aluminum complexes, there is no chelation between P and Al centre, and the lone pair electrons on the P centre can coordinate to  $\text{AlMe}_3$  to yield corresponding Lewis acid-base adducts.

The similar ionic radius of Al(III) to the radii of the trivalent first row transition metals and its diamagnetic nature make it a convenient starting point for the study of this new ancillary ligand. Numerous amidophosphines,<sup>26-28</sup> as well as monodentate,<sup>29-34</sup> bidentate,<sup>35-39</sup> tridentate<sup>40</sup> and tripodal<sup>41</sup> amido complexes of aluminum are known. These complexes have been studied largely as potential precursors for materials and catalysts.<sup>42,43</sup>

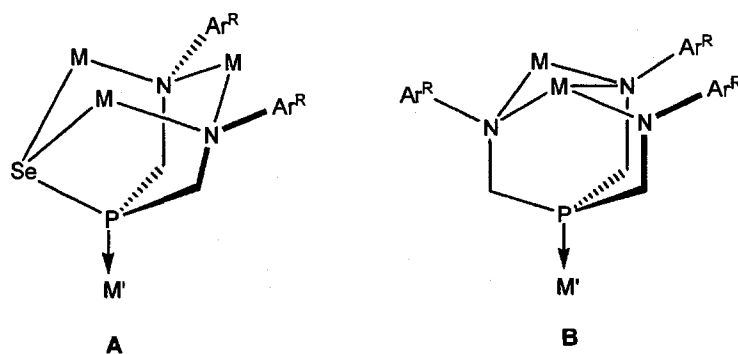
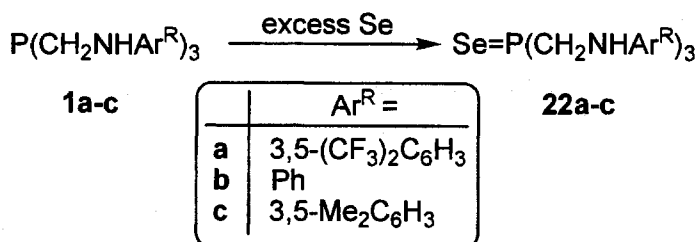


**Figure 4.1.** Potential bonding modes of  $P[CH_2NHAr^R]_3$  and  $Se=P[CH_2NHAr^R]_3$  with metal complexes labeled M and second metal complexes labeled M'.

#### 4.2 Oxidation of $P(CH_2NHAr^R)_3$ with Selenium

The treatments of the triamidophosphines  $P(CH_2NHAr^R)_3$  **1a-c**,<sup>21</sup> (where  $Ar^R = 3,5-(CF_3)_2C_6H_3$ , Ph, and 3,5-Me<sub>2</sub>C<sub>6</sub>H<sub>3</sub> for **a**, **b**, and **c**, respectively) with excess elemental selenium in toluene afforded the phosphine selenides  $SeP(CH_2NHAr^R)_3$ , as shown in Scheme 4.1. These white solids were isolated in yields ranging from 80-87 % and are neither air nor moisture sensitive.

**Scheme 4.1**



Colorless crystals of **22a-c** suitable for X-ray diffraction were grown by slow evaporation of solutions of equal amounts of ethanol and acetone. The solid-state molecular structures of **22a-c** are shown in Figure 4.2-4. The C(1)-P(1)-C(2), C(1)-P(1)-C(3), and C(2)-P(1)-C(3) angles for the free ligand precursor **22c** are 105.84(13)°, 105.56(11)° and 108.39(11)°, respectively, which are comparable to the tetrahedral angle of 109.5°. Comparison of the structure of phosphine selenide **22a** with that of the parent phosphine ligand **1a**,<sup>21</sup> reveals that the average P-C bond length of **22a** is shorter by 0.017 Å, and the sum of C-P-C bond angles is wider by about 13.3° (312.85(23)° for **22a**, 299.51(20)° for **1a**<sup>21</sup>). These differences correlate with the larger covalent radii of P(III) compared to P(V), as well as the larger repulsion of the lone pair of P(III) vs the P=Se bond. In **22a-22c**, the P-Se bond lengths are 2.0973(12), 2.1026(12) and 2.0960(7) Å, respectively, which are similar to those observed in the selenides of substituted arylphosphines.<sup>44,45</sup> The <sup>31</sup>P{<sup>1</sup>H} NMR spectra display singlets at δ 42.6, 46.3 and 44.5 and selenium satellites (<sup>77</sup>Se, I = 1/2, 7.6 %) with <sup>1</sup>J<sub>SeP</sub> values of 743.7, 719.7 and 716.1 Hz for **22a-c**, respectively. These values

are within the range expected for  $R_3P=Se$  functional groups.<sup>46,47</sup> The magnitude of  $^1J_{SeP}$  has been used to characterize the lone-pair  $s$ -orbital character of phosphine donors, and thus their  $\sigma$ -donor ability.<sup>48</sup> A larger value of  $^1J_{SeP}$  corresponds to greater  $s$ -orbital character of the phosphorus lone pair and a weaker electron-donor ability of the phosphine ligand.<sup>49</sup> The donor abilities of the phosphines in precursors **1a-c** are affected by the nature of the aryl substituents, with the most electron-withdrawing aryl group providing the phosphine selenide with the largest  $^1J_{SeP}$  value, 743.7 Hz. In comparison,  $Se=PPh_3$  has a  $^1J_{SeP}$  value of 733 Hz,<sup>48,50</sup> which predicts that **1a-c** should have similar donor properties to triphenylphosphine. A similar conclusion regarding the donor abilities of **1a-c** was reached via a study of the CO stretching frequencies<sup>51</sup> of the complexes  $trans\text{-Rh}(\text{CO})\text{Cl}[\text{P}(\text{CH}_2\text{NHA}^R)_3]_2$ , as previously reported.<sup>21</sup>

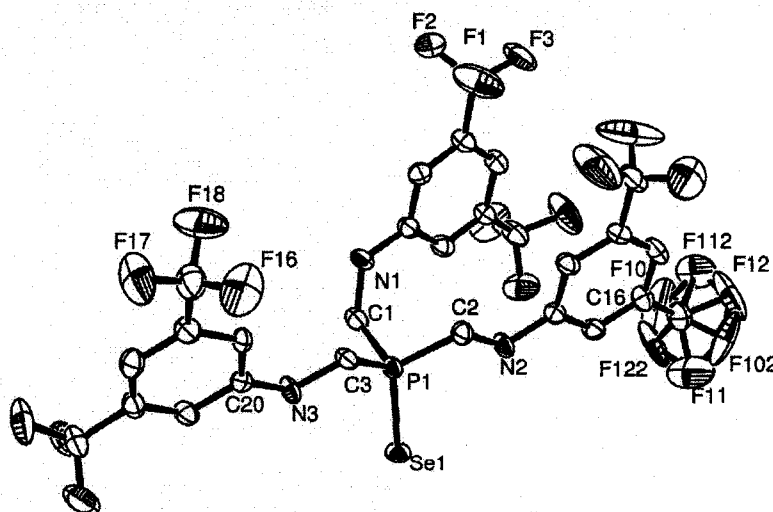


**Figure 4.2.** Solid-state molecular structure of **22a** as determined by X-ray crystallography. Hydrogen atoms are omitted for clarity. The  $CF_3$  substituents are disorder.

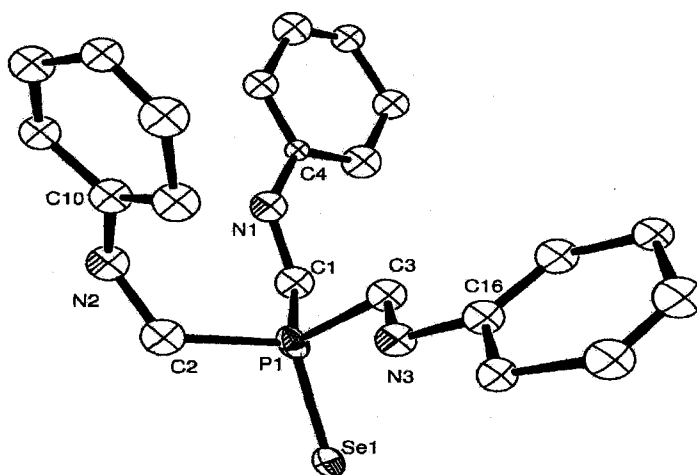


**Figure 4.3.** Solid-state molecular structure of **22b** as determined by X-ray crystallography. Hydrogen atoms are omitted for clarity.

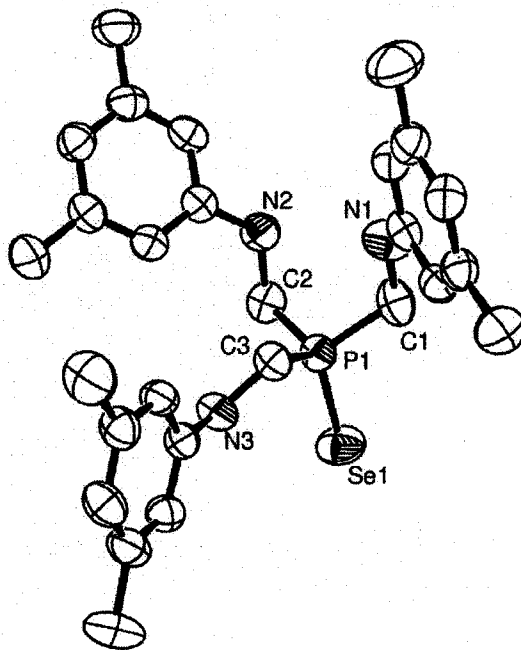


**Figure 4.4.** Solid-state molecular structure of **22c** as determined by X-ray crystallography. Hydrogen atoms are omitted for clarity.

**Table 4.1.** Selected bond lengths (Å) and angles (deg) of the phosphine selenides

**22a-c**

	<b>22a</b>	<b>22b</b>	<b>22c</b>	<b>1a</b> <sup>Ref 19</sup>
Se(1)=P(1)	2.0973(12)	2.1026(12)	2.0960(7)	-
C(1)-P(1)	1.844(4)	1.844(4)	1.829(3)	1.844(4)
C(2)-P(1)	1.826(4)	1.820(4)	1.822(3)	1.844(4)
C(3)-P(1)	1.817(4)	1.815(4)	1.821(2)	1.850(6)
C(1)-P(1)-Se(1)	113.44(14)	109.83(13)	112.12(10)	-
C(2)-P(1)-Se(1)	115.47(14)	112.28(13)	111.37(8)	-
C(3)-P(1)-Se(1)	113.85(14)	112.86(13)	113.14(8)	-
C(1)-P(1)-C(2)	107.2(2)	110.06(19)	105.84(13)	99.51(16)
C(1)-P(1)-C(3)	103.6(2)	108.37(19)	105.56(11)	99.5(2)
C(2)-P(1)-C(3)	102.05(19)	103.22(18)	108.39(11)	100.5(2)

**Table 4.2.** The  $^1J_{\text{PSe}}$  coupling constants,  $^{31}\text{P}$  NMR shifts of **22a-c** and the carbonyl stretching frequencies of  $\text{Rh}(\text{CO})\text{Cl}[\text{P}(\text{CH}_2\text{NHA}^{\text{R}})_3]_2$ .

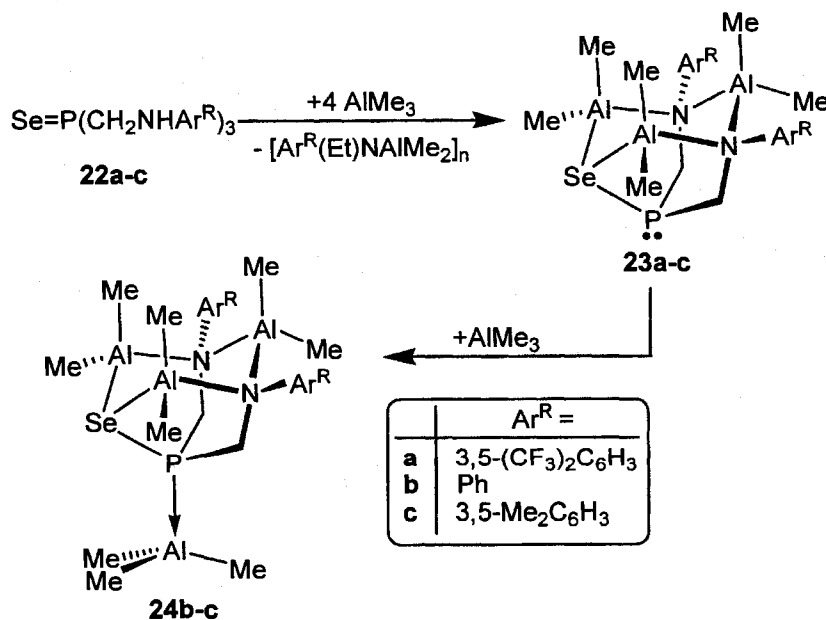
Phosphine Selenides	$^1J_{\text{PSe}}$ (Hz)	$^{31}\text{P}$ shift (ppm)	$\nu_{\text{CO}}$ (cm <sup>-1</sup> ) of $\text{Rh}(\text{CO})\text{Cl}[\text{P}(\text{CH}_2\text{NHA}^{\text{R}})_3]_2$
<b>22a</b>	743.7	42.6	<b>1a</b> : 1984.9
<b>22b</b>	719.7	46.3	<b>1b</b> : 1976.3
<b>22c</b>	716.1	44.3	<b>1c</b> : 1973.2

### 4.3 Synthesis of the Trinuclear Complexes via Reactions of $\text{Se}=\text{P}(\text{CH}_2\text{NHA}^{\text{R}})_3$ with $\text{AlMe}_3$

Se insertion reactions into polar M-R bonds and the use of the oxidized selenols as starting materials are normal methods to synthesize organic selenolates.<sup>12-19</sup> We are investigating phosphine selenides  $\text{SeP}(\text{CH}_2\text{NHA}^{\text{R}})_3$  as chelating ligands to afford metal selenides with the N, N', Se bonding mode by P-C bond cleavage and loss of one arm  $-\text{CH}_2\text{NHA}^{\text{R}}$  under mild conditions. The phosphine selenides  $\text{Se}=\text{P}(\text{CH}_2\text{NHA}^{\text{R}})_3$  (**22a-22c**) react with 4 equiv of  $\text{AlMe}_3$  in toluene at room temperature to give  $[\text{P}(\text{CH}_2\text{NAr}^{\text{R}})_2\text{Se}](\text{AlMe}_2)_3$  (**23a-23c**), as shown in Scheme 4.1. The reactions proceed over the course of 24 h, with the putative and unisolable amine-trimethylaluminum adducts as the only intermediates observable by  $^1\text{H}$  NMR spectroscopy; the observation of such adducts is not uncommon.<sup>36,52</sup> The use of 4 equiv of  $\text{AlMe}_3$  was necessary because the overall reaction involves the loss of 1 ligand  $-\text{CH}_2\text{NHA}^{\text{R}}$  arm. This is a new synthetic route to selenophosphinito ligands, which are poorly studied, and more commonly prepared by the insertion of 1 equiv of Se into a metal-phosphido bond.<sup>15,53</sup> The byproducts are much more soluble in pentane than the scarcely soluble **23a-23c**, and were easily rinsed from the crude product mixtures without significant loss of yield. The  $^1\text{H}$  NMR spectra of these byproducts are complicated and exhibit a variety of triplet and quartet resonances, as would be expected for ethyl substituents bound to nitrogen. The byproducts are believed to be dimers of the type  $[\text{CH}_3\text{CH}_2\text{N}(\text{Ar}^{\text{R}})\text{AlMe}_2]_2$ , and their complex  $^1\text{H}$  NMR spectra are likely due to the presence of *cis* and *trans* isomers, and perhaps also larger oligomers.<sup>31,52,54-56</sup> Definitive proof regarding the nature of the byproduct was

obtained by the hydrolysis of the pentane fraction used to rinse the crude product mixture in the synthesis of **23a**. The hydrolysis product was identified as  $\text{CH}_3\text{CH}_2\text{N}(\text{H})\text{-3,5-(CF}_3)_2\text{C}_6\text{H}_3$  by  $^1\text{H}$  and  $^{13}\text{C}$  NMR spectroscopy. The exact mechanism by which the ligand arm loss occurs is not clear, and a mechanism with an imine intermediate ( $\text{CH}_2=\text{NAr}^{\text{R}}$ ) cannot be distinguished from the direct reaction of the ligand precursors with  $\text{AlMe}_3$  to liberate  $\text{CH}_3\text{CH}_2\text{N}(\text{Ar}^{\text{R}})\text{AlMe}_2$ . The resultant products are obtained in 50-60 % yields as white crystalline solids. The phosphorus (V) centres are reduced to phosphorus (III) and the P=Se double bond is changed into P-Se single bond as Se coordinated to the Al metal centres together with the amido-donors.

Scheme 4.2



The solid-state molecular structures of **23a** and **23c** were determined by X-ray crystallography. The complex **23b** crystallized as thin needles that were unsuitable for crystallographic studies. An ORTEP depiction of the structure of **23c** is shown in Figure 4.5-6. Although there is no crystallographically imposed symmetry, these complexes have approximate  $C_s$  symmetry. The  $^1\text{H}$  and  $^{13}\text{C}\{^1\text{H}\}$  spectra of these complexes dissolved in  $\text{C}_6\text{D}_6$  are consistent with an identical solution structure.

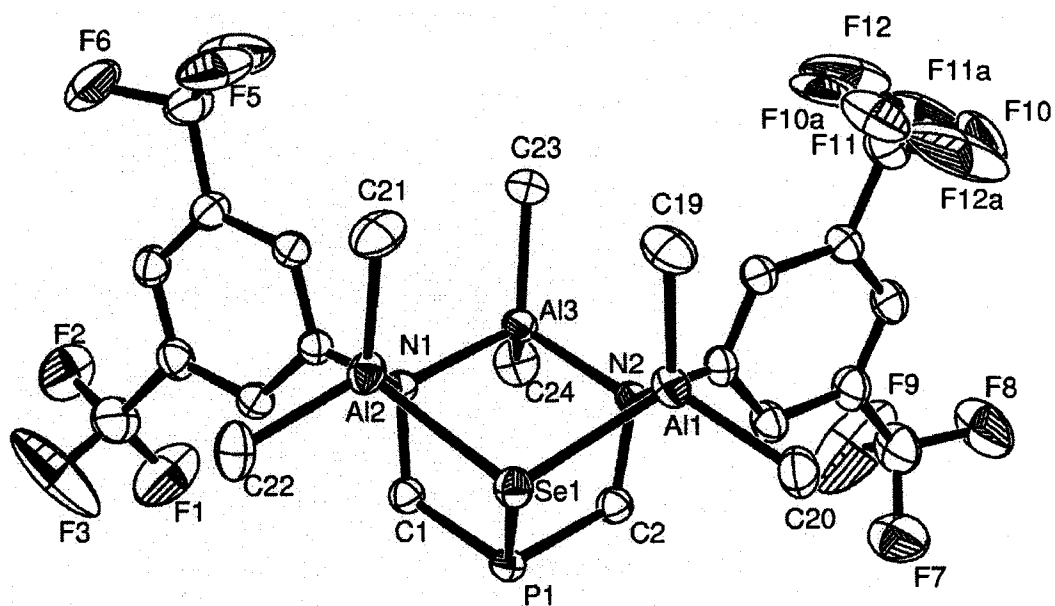


**Figure 4.5.** Solid-state molecular structure of **23a** as determined by X-ray crystallography. Hydrogen atoms are omitted for clarity. The  $\text{CF}_3$  substituents are disorder.

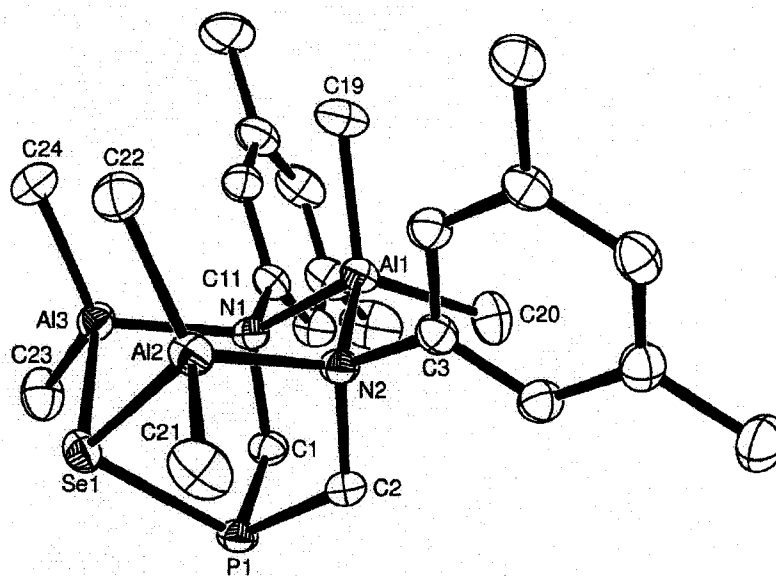


**Figure 4.6.** ORTEP depiction of the solid-state molecular structure of **23c** as determined by X-ray crystallography. Hydrogen atoms are omitted for clarity.

**Table 4.3.** Selected bond lengths (Å) and angles (deg) of **23a**, **23c**

	<b>23a</b>	<b>23b</b>
Se(1)=P(1)	2.2799(6)	2.2793(7)
C(1)-P(1)	1.844(2)	1.852(3)
C(2)-P(1)	1.849(2)	1.846(3)
Se(1)-Al(2)	2.4866(8)	2.4909(9)
Se(1)-Al(3)(1)	2.4760(8)	2.4979(9)
C(1)-P(1)-Se(1)	100.70(7)	101.23(8)
C(2)-P(1)-Se(1)	100.55(7)	100.65(8)
C(1)-P(1)-C(2)	99.81(10)	99.06(11)
Al(2)-Se(1)-P(1)	91.71(3)	91.85(3)
Al(3)(1)-Se(1)-P(1),	92.22(2)	90.37(3)

The tripodal ligand in **23c** binds three aluminum centers via one selenide and two amide donors, all of which act as bridging ligands. The three aluminum centers all have approximately tetrahedral geometries and each retains two methyl groups. The lone pair of the phosphine donor is directed away from the aluminum centers. The donors and aluminum atoms form a six-membered  $\text{Al}_3\text{N}_2\text{Se}$  ring, which adopts a boat conformation. The Al-N bond lengths in **23a** and **23c** vary from 1.977(2) to 2.0137(18) Å and the Al-Se bond lengths range from 2.4760(8) to 2.4979(9) Å. These lengths, as well as the N-Al-N angles (**23a**, 102.85(8)°; **23c**, 102.65(7)°) are in the expected range.<sup>27,29,30,35,40,57,58</sup> Both the P-Se bond lengths (**23a**: 2.2799(6) Å; **23c**, 2.2793(7) Å) and the  $^1J_{\text{SeP}}$  values (**23a**, 176.6 Hz; **23b**, 179.9; **23c**, 181.3 Hz) are within the range expected for P-Se single bonds,<sup>59</sup> and thus the selenophosphinito donor in this case is best described by a resonance structure where the selenium atom bears a formal negative charge, rather than one where the phosphorus donor is formally anionic.<sup>16</sup>

Chalcogenophosphinites ( $\text{R}_2\text{PE}^-$ , where E = O, S, Se, or Te) can be protonated at either the P or E sites to provide the tautomers  $\text{R}_2\text{P}(\text{H})=\text{E}$  and  $\text{R}_2\text{P}-\text{EH}$ .<sup>16,60</sup> The ratio of these products depends on the nature of R. Likewise, transition metals can bind to  $\text{R}_2\text{PE}^-$  ligands by a variety of bonding modes involving either the E or P centers, or both.<sup>16</sup> Only a handful of examples of complexes containing  $\text{R}_2\text{PSe}^-$  donors have been reported,<sup>15,16,53,61-63</sup> and few have been structurally characterized. The  $\eta^2$ -binding mode has been observed in complexes of  $\text{Mo}^{61}$  and  $\text{Ru}^{62}$  but for the

more electropositive metals the only crystallographically characterized structure is that of the lithium salt, [(TMEDA)Li- $\mu$ - $\eta^1$ :-SePPh<sub>2</sub>]<sub>2</sub>;<sup>15</sup> however, it is reasonable to assume that the selenophosphinito complexes of the electropositive metals will be comparable to those of the thiophosphinito ligands, which prefer to coordinate metals via the chalcogenide,<sup>64</sup> as is observed in complexes **23a-c**.

#### 4.4 Synthesis of the Trimethylaluminum Adducts of [P(CH<sub>2</sub>NAr<sup>R</sup>)<sub>2</sub>Se](AlMe<sub>2</sub>)<sub>3</sub>

The reactions of SeP(CH<sub>2</sub>NHAr<sup>R</sup>)<sub>3</sub> **22b** and **22c** with excess AlMe<sub>3</sub> lead to the formation of the Lewis acid-base adducts Me<sub>3</sub>AlP(CH<sub>2</sub>NAr<sup>R</sup>)<sub>2</sub>Se(AlMe<sub>2</sub>)<sub>3</sub> (**24b-24c**) at room temperature. The fourth AlMe<sub>3</sub> is coordinated to P by Lewis acid-base interactions in **24b-24c**. Me<sub>3</sub>AlP(CH<sub>2</sub>NAr<sup>R</sup>)<sub>2</sub>Se(AlMe<sub>2</sub>)<sub>3</sub> (**24b-24c**) can also be obtained by the addition AlMe<sub>3</sub> to **23b-c**, as shown in Scheme 4.2. The trimethylaluminum adduct of **23a** is too thermally unstable to be isolated in the solid state. Both **24b** and **24c** were obtained as white crystalline solids at room temperature, and in this state are stable with respect to decomposition for several days. Single crystals of **24b** suitable for X-ray diffraction were obtained from toluene at -30 °C. The solid-state molecular structure is shown in Figure 4.7, along with selected bond lengths and bond angles.

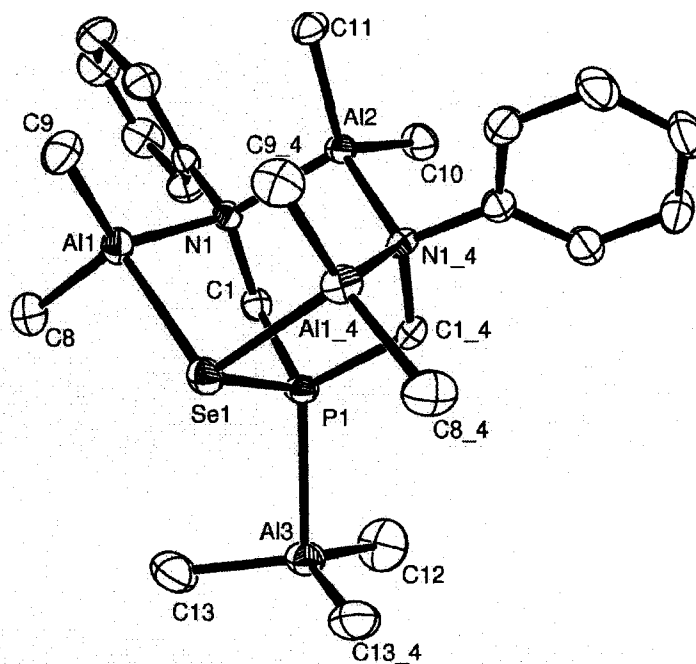


**Figure 4.7.** Solid-state molecular structure of **24b** as determined by X-ray crystallography. Hydrogen atoms are omitted for clarity. Selected distances (Å): Al(3)-P(1), 2.553(2); Al(3)-C(13), 1.958(5); Al(3)-C(12), 1.951(7); Se(1)-P(1), 2.2388(16); Se(1)-Al(1), 2.5104(13); P(1)-C(1), 1.822(4); N(1)-Al(1), 1.990(3); N(1)-Al(2), 2.011(3). Selected bond angles (deg): C(1)-P(1)-C(1), 101.4(3); C(1)-P(1)-Se(1), 103.61(13); C(1)-P(1)-Al(3), 118.84(13); Al(1)-Se(1)-Al(1), 104.07(6); P(1)-Se(1)-Al(1), 89.86(4); N(1)-Al(1)-Se(1), 93.83(11); Al(1)-N(1)-Al(2), 122.26(17); C(1)-N(1)-Al(1), 104.1(2); C(1)-N(1)-Al(2), 108.2(2); C(12)-Al(3)-C(13), 119.12(18); C(13)-Al(3)-C(13), 115.0(3); C(13)-Al(3)-P(1), 97.45(16); C(12)-Al(3)-P(1), 101.1(3).

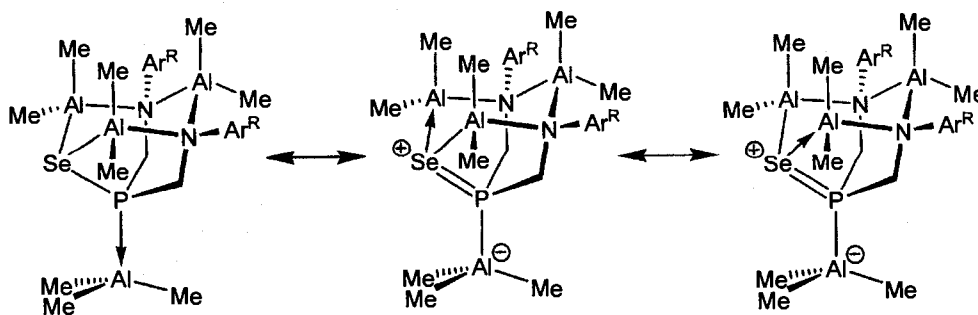
The solid-state molecular structure of **24b** has crystallographically imposed  $C_s$  symmetry. The connectivity is the same as that observed for **23b**, but with an additional  $\text{AlMe}_3$  moiety bound to the phosphine lone pair. The Al-P distance of 2.553(2) Å is significantly elongated in comparison to the sum of the covalent radii (2.350 Å) of Al and P, but within the range observed for aluminum-phosphine adducts.<sup>65,66</sup> In the solid-state structure of **24b** the sum of C-Al(3)-C angles is 353.24(39)°, which is close to that for a trigonal planar system. The C(12-13)-Al(3) bond lengths range from 1.951(7) to 1.958(5) Å, which are almost identical to that of free  $\text{AlMe}_3$ .<sup>67</sup> The changes in  $^{13}\text{C}\{\text{H}\}$  NMR chemical shifts of the Al-Me<sub>3</sub> groups (**24b**,  $\delta$  -8.0; **24c**,  $\delta$  -7.8; free  $\text{AlMe}_3$ ,  $\delta$  -8.1) are small, which also indicate only a slight distortion from planarity upon adduct formation.<sup>46</sup> All these factors are consistent with the poor  $\sigma$ -donor ability of the phosphine towards  $\text{AlMe}_3$  in **24b** and **24c**.

The binding of trimethylaluminum to the phosphine donor in **24b** has an effect on the ancillary ligand bond lengths. In particular, the P-Se bond length of 2.2388(16) Å in **24b** is approximately 0.04 Å shorter than in either **23a** or **23c**. Additionally, the Se(1)-Al(1) bond length of 2.5104(13) Å in **24b** is slightly longer than the Se-Al bond lengths in **23a**, which are 2.4760(8) and 2.4866(8) Å, or in **23c**, where the bond lengths are 2.4909(9) and 2.4979(9) Å. These bond lengths can be interpreted in terms of a slight contribution from resonance structures where the phosphine moiety formally bears the negative charge of the selenophosphinito moiety,<sup>16</sup> as shown in

Scheme 4.3, though the structure is still best described as containing a P-Se single bond.

The  $^1\text{H}$  NMR spectra of **24b-c** are consistent with the  $C_s$  symmetry observed in the solid-state structure of **24b**. The  $^{31}\text{P}\{^1\text{H}\}$  NMR spectra of **24b** and **24c** consist of singlets at  $\delta$  -8.4 and -9.4, and display selenium satellites with  $^1J_{\text{SeP}}$  values of 349.7 and 312.9 Hz, respectively. The change in the  $^{31}\text{P}$  chemical shifts upon forming the adducts **24b-c** from **23b-c** to slightly higher field is fairly typical for phosphine donors with moderately large cone angles ( $\Delta\delta = -4.3$  for **b**;  $-6.0$  for **c**).<sup>66</sup> The  $^1J_{\text{SeP}}$  values are within the range expected for the P-Se single bonds,<sup>59</sup> but much greater than the values observed for **23b-c**. Moreover, the difference in these  $^1J_{\text{SeP}}$  values of 36.8 Hz is much larger than in complexes **23b-c**, where the difference in  $^1J_{\text{SeP}}$  is only 1.4 Hz. The vastly different  $^1J_{\text{SeP}}$  values in **24b-c** indicate a large influence of the aryl substituents on the bonding in these complexes, and their importance in determining the relative contributions of the resonance structures shown in Scheme 4.3.

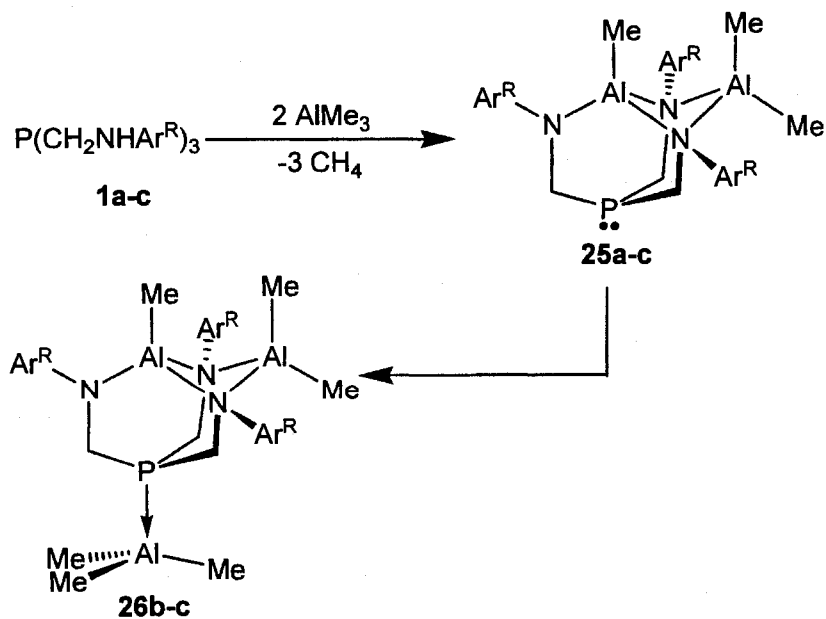
Scheme 4.3



#### 4.5 Synthesis of the Bimetallic Aluminum Amido Complexes with the $P(CH_2NHA r^R)_3$ ligands

The room temperature reactions of **1a-c** with 2 equiv  $AlMe_3$  over 24 h cleanly provide the bimetallic aluminum amido complexes  $[P(CH_2NAr^R)_3]Al_2Me_3$  (**25a-c**) as white crystalline solids, as shown in Scheme 4.4. These products were obtained as white crystalline solids at room temperature over 24h. The  $^1H$  and  $^{13}C\{^1H\}$  NMR spectra of these complexes in  $C_6D_6$  are consistent with complexes of  $C_s$  symmetry with the connectivity shown. For example, there are 3 Al-Me environments of equal intensities observed in the  $^1H$  NMR of each of these complexes, and three  $PCH_2$  environments are observed, in a 2:2:2 ratio, a pair of which are due to diastereotopic environments.

Scheme 4.4



The solid-state structure of **25a** was determined by X-ray crystallography, and is depicted in Figure 4.8. The triamidophosphine ligand binds to a central AlMe fragment with three nitrogen atoms, and two of these amido donors bridge to an AlMe<sub>2</sub> moiety. The phosphine donor is directed away from the central aluminum atom. Both geometries around the two aluminum centers are distorted tetrahedral. For example, the N(2)-Al(2)-N(3) angle of 81.40(9)°, is more acute than the C(29)-Al(2)-C(30) angle of 117.77(17). The bond length of 1.964(2) Å for Al(1)-N(2) is about 0.032 Å shorter than that of 1.996(3) Å for Al(2)-N(2), but both distances are considerably longer than the terminal amido Al(1)-N(1) bond length of 1.829(3) Å, which is possibly caused by the different orientation of the nitrogen substituents and the lower coordination number for N(1).<sup>25</sup> The aromatic substituent on the terminal amido donor is aligned such that its π-system has considerable overlap with the lone pair on the nitrogen, whereas the aromatic substituents associated with the bridging amido donors are aligned so that aromatic π-system is nearly orthogonal to the lone-pair *p*-orbital.

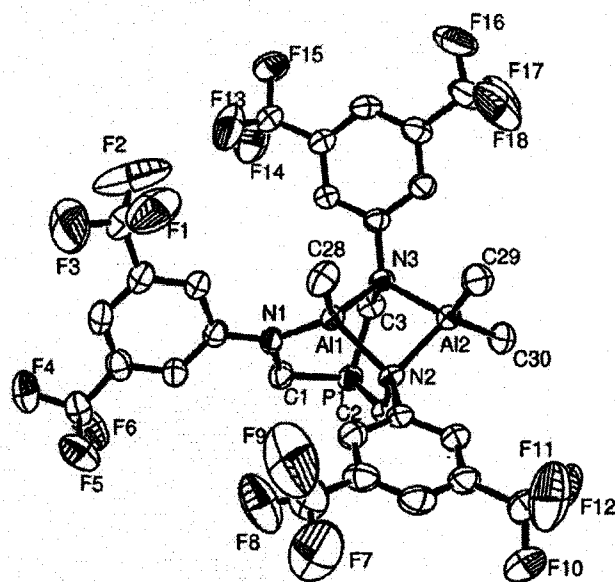


**Figure 4.8.** Solid-state molecular structure of **25a** as determined by X-ray crystallography. Hydrogen atoms are omitted for clarity. Selected distances (Å): P(1)-C(1), 1.844(3); P(1)-C(2), 1.844(3); P(1)-C(3), 1.856(3); N(1)-Al(1), 1.829(3); N(2)-Al(1), 1.964(2); N(3)-Al(1), 1.958(2); N(2)-Al(2), 1.996(3); N(3)-Al(2), 1.997(2); C(28)-Al(1), 1.930(3); C(29)-Al(2), 1.948(4); C(30)-Al(2), 1.947(4). Selected bond angles (deg): C(1)-P(1)-C(2), 99.06(15); C(1)-P(1)-C(3), 101.71(14); C(2)-P(1)-C(3), 103.39(14); N(1)-Al(1)-C(28), 119.30(14); N(1)-Al(1)-N(2), 111.15(11); N(1)-Al(1)-N(3), 107.67(11); N(2)-Al(1)-N(3), 83.18(10); C(29)-Al(2)-C(30), 117.77(17); N(2)-Al(2)-C(29), 110.60(14); N(3)-Al(2)-C(29), 114.06(13); N(2)-Al(2)-N(3), 81.40(10).

#### 4.6 Synthesis of the Adducts of Bimetallic Aluminum Amido Complexes



The reactions of the triaminophosphines (**1b-1c**) with excess  $\text{AlMe}_3$  at room temperature provide the Lewis acid-base adducts of **5b-c**,  $\text{Me}_3\text{Al}\cdot\text{P}(\text{CH}_2\text{NAr}^{\text{R}})_3\text{Al}_2\text{Me}_3$  (**26b-c**). These complexes could also be generated by the addition of  $\text{AlMe}_3$  to **25b-c**, as shown in Scheme 4.4. Similar to **23a**, adducts of **25a** could not be isolated. Single crystals of **26b** suitable for X-ray diffraction were obtained from toluene at  $-30\text{ }^\circ\text{C}$ . An ORTEP depiction is shown in Figure 4.9, along with selected bond lengths and bond angles.

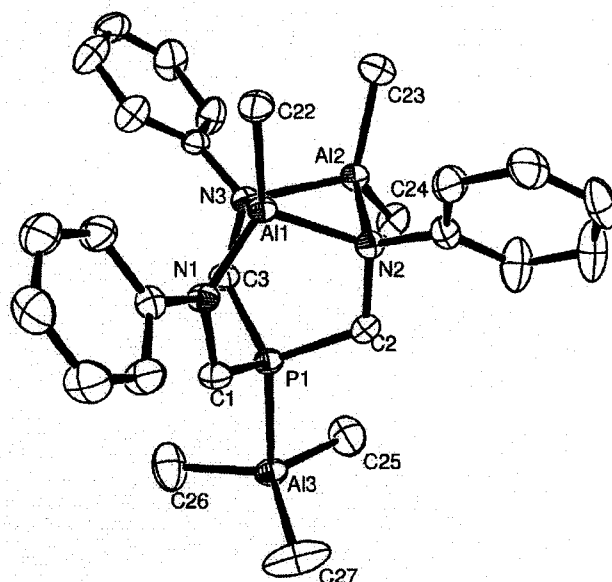


**Figure 4.9.** ORTEP depiction of the solid-state molecular structure of **26b** as determined by X-ray crystallography. Hydrogen atoms are omitted for clarity. Selected distances (Å): P(1)-Al(3), 2.5151(7); P(1)-C(1), 1.8222(18); P(1)-C(2), 1.8328(19); P(1)-C(3), 1.8426(18); N(1)-Al(1), 1.8253(16); N(2)-Al(1), 1.9903(16); N(3)-Al(1), 1.9645(15); N(2)-Al(2), 1.9970(15); N(3)-Al(2), 1.9833(16); C(22)-Al(1), 1.9474(19); Al(3)-C(25), 1.960(2); Al(3)-C(26), 1.966(3); Al(3)-C(27), 1.946(3). Selected bond angles (deg): C(1)-P(1)-C(2), 101.96(9); C(1)-P(1)-C(3), 104.48(8); C(2)-P(1)-C(3), 105.72(8); C(2)-P(1)-Al(3), 114.35(6); C(3)-P(1)-Al(3), 112.73(6); N(1)-Al(1)-C(22), 118.28(8); N(1)-Al(1)-N(2), 110.19(7); N(1)-Al(1)-N(3), 107.88(7); N(2)-Al(1)-N(3), 82.66(6); C(23)-Al(2)-C(24), 117.82(9); N(2)-Al(2)-C(24), 113.97(8); N(3)-Al(2)-C(24), 115.08(8); N(2)-Al(2)-N(3), 82.02(6); C(26)-Al(3)-C(27), 116.59(16); C(25)-Al(3)-C(27), 117.27(15); C(27)-Al(3)-P(1), 101.32(9); C(26)-Al(3)-P(1), 99.28(8); C(25)-Al(3)-P(1), 99.23(7).

The connectivity in **26b** is essentially the same as that observed for complexes **25a-c**, but with an additional  $\text{AlMe}_3$  moiety bound to the phosphine lone pair. The sum of C-Al(3)-C angles is  $351.25(43)^\circ$  and C-Al(3) bond lengths range from  $1.946(3)$  Å to  $1.966(3)$  Å. The small change in  $^{13}\text{C}$  chemical shifts of Al-Me<sub>3</sub> groups also indicates the slight distortion from planarity of aluminum.<sup>66</sup> The  $^{31}\text{P}\{^1\text{H}\}$  NMR spectra of **26b** and **26c** contain resonances at  $\delta$  -45.5 and -44.5, respectively, which are shifted downfield by approximately +6 ppm compared to that of the compounds **25b-c**. Adduct **26b** has slightly longer Al-C bond distances and the smaller C-Al-C angles for the  $\text{AlMe}_3$  moiety than in **24b**, which indicates that slightly stronger Lewis acid-base interactions occur in **26b**.<sup>36</sup> This is consistent with the shorter Al-P distance of  $2.5151(7)$  Å in **26b** than that of  $2.553(2)$  Å in **24b**.<sup>66</sup> For the compounds **23b-c** and **25b-c**, adduct formation doesn't lead to a drastic increase of the Al-C bond lengths, but a decrease of the C-Al-C angles compared to those of the uncomplexed  $\text{AlMe}_3$ .

**Table 4.4.** Selected bond lengths (Å) and angles (deg) of the Lewis acid-base adducts **24b** and **26b**

	<b>24b</b>	<b>26b</b>
Al-P	2.553(2)	2.5151(7)
Al-C	1.958(5)	1.960(2)
Al-C	1.958(5)	1.966(3)
Al-C	1.951(7)	1.946(3)
C-Al-C	119.12(18)	116.59(16)
C-Al-C	115.0(3)	117.39(12)
C-Al-C	115.0(3)	117.27(15)
C-Al-P	97.45(16)	101.32(9)
C-Al-P	97.45(16)	99.28(8)
C-Al-P	101.1(3)	99.23(7)
P-C (Se)	2.2388(16)	1.8222(18);
P-C	1.822(4)	1.8328(19)
P-C	1.822(4)	1.8426(18)
C-P-C (Se)	103.61(13)	101.96(9)
C-P-C	101.4(3)	104.48(8)
C-P-C	101.4(3)	105.72(8)

#### 4.7 Ligand Design and Bonding Modes

Both the amido and selenophosphinito donors show a propensity to bridge, and so this cannot be the only factor that leads to the formation of triangular complexes for **23a-c**, but not for **24a-c**. To improve these ligand designs to assemble triangular complexes with a variety of metal precursors requires a better understanding of what factors promote polynuclear complex formation. The

geometry of the ligand plays a role in the assembly of the trinuclear complexes in the case of **23a-c**. For the supporting diamidoselenophosphinito donor to chelate all its anionic donors to a central aluminum atom would require the formation of a [2.2.1] bicyclic. The resultant two five-membered rings and one six-membered ring seem ideal in terms of chelate ring sizes, but the fused nature of these rings leads to considerable strain and results in less than tetrahedral bond angles. For example, the analogous hydrocarbon norbornane possesses 71.8 kJ/mol of ring strain.<sup>68</sup>

#### 4.8 Summary and Conclusions

The reactions of the triaminophosphines  $P(\text{CH}_2\text{NHA}^{\text{R}})_3$  (**1a-c**, where  $\text{Ar}^{\text{R}} = 3,5\text{-(CF}_3)_2\text{C}_6\text{H}_3$  for **a**;  $\text{Ar}^{\text{R}} = \text{Ph}$  for **b**,  $\text{Ar}^{\text{R}} = 3,5\text{-Me}_2\text{C}_6\text{H}_3$  for **c**) with selenium afford the triaminophosphine selenides  $\text{Se}=\text{P}(\text{CH}_2\text{NHA}^{\text{R}})_3$ . The treatment of the ligand precursors  $\text{Se}=\text{P}(\text{CH}_2\text{NHA}^{\text{R}})_3$  (**22a-c**) with 4 equiv of  $\text{AlMe}_3$  provide the facile synthetic routes to the triangular trinuclear complexes (**23a-c**) of the unanticipated diamidoselenophosphinito ligands, with concomitant loss of one equiv of  $[\text{Et}(\text{Ar}^{\text{R}})\text{NAlMe}_2]_n$ . The byproduct was hydrolyzed and provided  $\text{CH}_3\text{CH}_2\text{N}(\text{H})\text{-}3,5\text{-(CF}_3)_2\text{C}_6\text{H}_3$ . Tetranuclear complexes can be obtained by the formation of adducts with  $\text{AlMe}_3$  at the phosphine donor. The large influence of adduct formation on the  $^1J_{\text{SeP}}$  values as well the sensitivity of these values to the nature of  $\text{Ar}^{\text{R}}$  indicates that considerable delocalization of bonding occurs.

The reactions of  $\text{P}(\text{CH}_2\text{NHAr}^{\text{R}})_3$  (**1a-c**) with 2 equiv of  $\text{AlMe}_3$  produce the dinuclear aluminum complexes  $\text{P}(\text{CH}_2\text{NAr}^{\text{R}})_3\text{Al}_2\text{Me}_3$  (**25a-c**). When **1b-c** react with excess  $\text{AlMe}_3$ , the Lewis acid-base adducts  $\text{Me}_3\text{Al}\cdot\text{P}(\text{CH}_2\text{NAr}^{\text{R}})_3\text{Al}_2\text{Me}_3$  (**26b-c**) are isolated.

The polydentate ligands combine the tripodal amido donors with the phosphine donor and selenium donor functionalities, which are demonstrated to be well suited for the facile synthesis of the polynuclear main group metal complexes. The preference of the diamidoselenophosphinito ligands in **22a-c** to form trinuclear structures, as opposed to adopting a  $\kappa \text{Se}, \text{N}, \text{N}$  bonding mode similar to the  $\kappa \text{N}, \text{N}, \text{N}$  bonding observed in complexes **23a-c**, can be ascribed to the ring strain associated with [2.2.1] bicyclic systems.<sup>69</sup>

## 4.9 Experimental

### 4.9.1 General Procedures

Unless otherwise stated, general procedures were performed according to Section 2.11.1.

### 4.9.2 Synthesis of Complexes

$\text{Se}=\text{P}[\text{CH}_2\text{NH}-3,5-(\text{CF}_3)_2\text{C}_6\text{H}_3]_3$  (**22a**). Selenium (789 mg, 10 mmol) was added

to a solution of  $\text{P}(\text{CH}_2\text{NH}-3,5\text{-(CF}_3)_2\text{C}_6\text{H}_3)_3$  (**1a**) (3.78 g, 5 mmol) in 50 mL of toluene. The solution was stirred 24 h and then filtered to remove the excess selenium. The solvent was removed under vacuum and the remaining white solid was rinsed with a small portion of pentane, and then dried under vacuum (3.55 g, 85 %). Single crystals were grown from a mixture of ethanol (50 %) and acetone (50 %) at  $-30\text{ }^\circ\text{C}$ .  $^1\text{H}$  NMR ( $\text{C}_6\text{D}_6$ , 300 MHz, 298 K):  $\delta$  2.77 (dd,  $^3J_{\text{HH}} = 5.8\text{ Hz}$ ,  $^2J_{\text{PH}} = 5.2\text{ Hz}$ , 6H,  $\text{PCH}_2$ ), 3.94 (q, 3H,  $\text{NH}$ ), 6.56 (s, 6H, Ph *o-H*), 7.28 (s, 3H, Ph *p-H*).  $^{13}\text{C}\{^1\text{H}\}$  NMR ( $\text{C}_6\text{D}_6$ , 125.8 MHz, 298 K):  $\delta$  40.3 (d,  $J_{\text{PC}} = 49.4\text{ Hz}$ ,  $\text{PCH}_2$ ), 113.3 and 122.4 (s, Ph *o-C* and *m-C*), 113.6 (s, Ph *p-C*), 133.4 (q,  $J = 33.5\text{ Hz}$ , Ph  $\text{C-F}_3$ ), 147.8 (d,  $J = 8.8\text{ Hz}$ , *ipso-C*).  $^{31}\text{P}\{^1\text{H}\}$  NMR ( $\text{C}_6\text{D}_6$ , 121.5 MHz, 298 K):  $\delta$  42.6 (s with satellites,  $J_{\text{SeP}} = 743.7\text{ Hz}$ ).  $^{77}\text{Se}\{^1\text{H}\}$  NMR ( $\text{C}_6\text{D}_6$ , 121.5 MHz, 298 K):  $\delta$  -463.8 (d,  $J_{\text{SeP}} = 743.7\text{ Hz}$ ).  $^{19}\text{F}$  NMR ( $\text{C}_6\text{D}_6$ , 282.1 MHz, 298 K):  $\delta$  14.68 (s). Anal. Calc'd for  $\text{C}_{27}\text{H}_{18}\text{F}_{18}\text{N}_3\text{SeP}$ : C, 38.75; H, 2.17; N, 5.02. Found: C, 39.1; H, 2.46; N, 5.06.

$\text{Se}=\text{P}(\text{CH}_2\text{NHPh})_3$  (**22b**). Prepared in an analogous manner to **22a** using  $\text{P}(\text{CH}_2\text{NHPh})_3$  (**1b**) (1.75 g, 5 mmol) in lieu of **1a** with a yield of 1.92 g, 80 %. Single crystals were grown from a mixture of ethanol (50 %) and acetone (50 %) at  $-30\text{ }^\circ\text{C}$ .  $^1\text{H}$  NMR ( $\text{C}_6\text{D}_6$ , 300 MHz, 298 K):  $\delta$  3.30 (dd,  $^3J_{\text{HH}} = 5.6\text{ Hz}$ ,  $^2J_{\text{PH}} = 5.6\text{ Hz}$ , 6H,  $\text{PCH}_2$ ), 5.1 (b, 3H,  $\text{NH}$ ), 6.36 (d,  $^3J_{\text{HH}} = 8.5\text{ Hz}$ , 6H, Ph *o-H*), 6.71 (t,  $^3J_{\text{HH}} = 7.5\text{ Hz}$ , 3H, Ph *p-H*), 7.03 (m, 6H, Ph *m-H*).  $^{13}\text{C}\{^1\text{H}\}$  NMR ( $\text{C}_6\text{D}_6$ , 125.8 MHz, 298 K):

$\delta$  42.1 (d,  $J_{PC} = 47.8$  Hz,  $P\text{C}\underline{H}_2$ ), 114.5 and 119.9 (s, Ph  $o\text{-}\underline{C}$  and  $m\text{-}\underline{C}$ ), 130.1 (s, Ph  $p\text{-}\underline{C}$ ), 147.6 (d,  $J = 7.1$  Hz,  $ipso\text{-}\underline{C}$ ).  $^{31}\text{P}\{^1\text{H}\}$  NMR ( $\text{C}_6\text{D}_6$ , 121.5 MHz, 298 K):  $\delta$  46.3 (s with satellites,  $J_{SeP} = 719.7$  Hz.).  $^{77}\text{Se}\{^1\text{H}\}$  NMR ( $\text{C}_6\text{D}_6$ , 57.2 MHz, 298 K):  $\delta$  -455.2 (d,  $J_{SeP} = 719.7$  Hz.). Anal. Calc'd for  $\text{C}_{21}\text{H}_{24}\text{N}_3\text{PSe}$ : C, 58.88; H, 5.65; N, 9.81. Found: C, 58.95; H, 5.47, N, 9.44.

**Se=P(CH<sub>2</sub>NH-3,5-Me<sub>2</sub>C<sub>6</sub>H<sub>3</sub>)<sub>3</sub> (22c).** Prepared in an analogous manner to **22a** using P(CH<sub>2</sub>NH-3,5-Me<sub>2</sub>C<sub>6</sub>H<sub>3</sub>)<sub>3</sub> (**1c**) (1.75 g, 5 mmol) in lieu of **1a** with a yield of 2.22 g, 87 %. Single crystals were grown from a mixture of ethanol (50%) and acetone (50%) at -30 °C.  $^1\text{H}$  NMR ( $\text{C}_6\text{D}_6$ , 300 MHz, 298 K):  $\delta$  2.18 (s, 18H, Ph $\underline{C}\underline{H}_3$ ), 3.51 (dd,  $^3J_{\text{HH}} = 5.7$  Hz,  $^2J_{\text{PH}} = 5.7$  Hz, 6H,  $P\text{C}\underline{H}_2$ ), 4.05 (b, 3H,  $\text{N}\underline{H}$ ), 6.16 (s, 6H, Ph  $o\text{-}\underline{H}$ ), 6.40 (s, 3H, Ph  $p\text{-}\underline{H}$ ).  $^{13}\text{C}\{^1\text{H}\}$  NMR ( $\text{C}_6\text{D}_6$ , 125.8 MHz, 298 K):  $\delta$  21.8 (s, Ph $\underline{C}\underline{H}_3$ ), 42.1 (d,  $J_{PC} = 47.2$  Hz,  $P\text{C}\underline{H}_2$ ), 112.5 and 121.9 (s, Ph  $o\text{-}\underline{C}$  and  $m\text{-}\underline{C}$ ), 139.4 (s, Ph  $p\text{-}\underline{C}$ ), 147.6 (d,  $J = 7.1$  Hz,  $ipso\text{-}\underline{C}$ ).  $^{31}\text{P}\{^1\text{H}\}$  NMR ( $\text{C}_6\text{D}_6$ , 121.5 MHz, 298 K):  $\delta$  44.46 (s with satellites,  $J_{SeP} = 716.1$  Hz.).  $^{77}\text{Se}\{^1\text{H}\}$  NMR ( $\text{C}_6\text{D}_6$ , 57.2 MHz, 298 K):  $\delta$  -453.2 (d,  $J_{SeP} = 716.1$  Hz.). Anal. Calc'd for  $\text{C}_{27}\text{H}_{36}\text{N}_3\text{PSe}$ : C, 63.27; H, 7.08; N, 8.20. Found: C, 63.51; H, 6.9; N, 7.93.

**P[CH<sub>2</sub>N-3,5-(CF<sub>3</sub>)<sub>2</sub>C<sub>6</sub>H<sub>3</sub>]<sub>2</sub>Se(AlMe<sub>2</sub>)<sub>3</sub> (23a).** A 2.0 M solution of AlMe<sub>3</sub> in toluene (2.0 mL, 4.0 mmol) was added to a solution of **22a** (836.1 mg, 1 mmol) in 25 mL toluene. The solution was stirred at room temperature for 24 h. The solution was

evaporated to dryness, and the remaining solid was rinsed by pentane. The white solid was collected by filtration and dried (382 mg, 50 %). X-ray quality crystals were obtained from slow evaporation of a benzene solution.  $^1\text{H}$  NMR ( $\text{C}_6\text{D}_6$ , 300 MHz, 298 K):  $\delta$  -1.71 and -0.28 (s, 3H each,  $\text{N,N}'\text{-AlMe}_2$ ), -0.98 and 0.05 (s, 6H each, Se,  $\text{N-AlMe}_2$ ), 2.93 (s, 2H,  $\text{PCH}_2$ ), 2.95 (d, 2H,  $\text{PCH}_2$ ), 7.44 (s, 2H, Ph *o*-H), 7.69 (s, 4H, Ph *p*-H).  $^{13}\text{C}\{^1\text{H}\}$  NMR ( $\text{C}_6\text{D}_6$ , 125.8 MHz, 298 K):  $\delta$  -9.4, -7.9, -3.9 and -2.8 (s,  $\text{AlMe}_2$ ),  $\delta$  46.4 (d,  $J_{\text{PC}} = 41.2$  Hz,  $\text{PCH}_2$ ), 118.3 and 123.5 (s, Ph *o*-C and *m*-C), 121.5 (s, Ph *p*-C), 133.6 (q,  $J = 33.4$  Hz,  $\text{PhC-F}_3$ ), 148.0 (s, *ipso*-C).  $^{31}\text{P}\{^1\text{H}\}$  NMR ( $\text{C}_6\text{D}_6$ , 202.5 MHz, 298 K):  $\delta$  -4.7 (s with satellites,  $J_{\text{SeP}} = 176.6$  Hz).  $^{19}\text{F}$  NMR ( $\text{C}_6\text{D}_6$ , 282.1 MHz, 298 K):  $\delta$  14.81 (s).  $^{77}\text{Se}\{^1\text{H}\}$  NMR ( $\text{C}_6\text{D}_6$ , 121.5 MHz, 298 K):  $\delta$  -430.0 (d,  $J_{\text{SeP}} = 176.6$  Hz).  $\text{C}_{24}\text{H}_{28}\text{Al}_3\text{F}_{12}\text{N}_2\text{PSe}$ : C, 37.76; H, 3.70; N, 3.67. Found: C, 38.20; H, 3.58 N, 3.76.

The pentane rinse was hydrolyzed with water, with the evolution of gas. The sample was extracted into  $\text{C}_6\text{D}_6$  and passed through a short plug of alumina.  $^1\text{H}$  NMR ( $\text{C}_6\text{D}_6$ , 300 MHz, 298 K):  $\delta$  0.62 (t, 3H,  $^3J_{\text{HH}} = 7.3$  Hz,  $\text{CH}_2\text{CH}_3$ ), 2.26 (qd, 2H,  $^3J_{\text{HH}} = 7.3$  Hz,  $^3J_{\text{HH}} = 5.2$  Hz,  $\text{NHCH}_2\text{CH}_3$ ), 5.2 (br, 1H,  $\text{NH}$ ), 6.42 (s, 2H, Ph *o*-H), 7.21 (s, 1H, Ph *p*-H), consistent with  $\text{EtN(H)-3,5-(CF}_3)_2\text{C}_6\text{H}_3$ .

**$\text{P}(\text{CH}_2\text{NPh})_2\text{Se}(\text{AlMe}_2)_3$  (23b).** Prepared in an analogous manner to **23a** using **(2b)** (428.4 mg, 1.0 mmol) in lieu of **19a** with an isolated yield of 245.6 mg, 50 %.  $^1\text{H}$  NMR ( $\text{C}_6\text{D}_6$ , 300 MHz, 298 K):  $\delta$  -1.36 and -0.04 (s, 3H each,  $\text{N,N}'\text{-AlMe}_2$ ), -0.81,

0.23, (s, 6H each, Se, N- $\text{AlMe}_2$ ), 3.24 and 3.24 (m, 4H total,  $\text{PCH}_2$ ), 6.81 (t, 2H,  $J = 7.3$  Hz, Ph *p*-H), 7.0 (dd, 4H, Ph *m*-H), 7.17 (d, 4H, Ph *o*-H).  $^{13}\text{C}\{^1\text{H}\}$  NMR ( $\text{C}_6\text{D}_6$ , 125.8 MHz, 298 K):  $\delta$  -15.1, -8.6, -5.8 and -2.7 (s,  $\text{AlMe}_2$ ),  $\delta$  46.7 (d,  $J_{\text{PC}} = 36.5$  Hz,  $\text{PCH}_2$ ), 122.05 and 125.5 (s, Ph *o*- $\text{C}$  and *m*- $\text{C}$ ), 130.0 (s, Ph *p*- $\text{C}$ ), 145.9 (s, *ipso*- $\text{C}$ ).  $^{31}\text{P}\{^1\text{H}\}$  NMR ( $\text{C}_6\text{D}_6$ , 202.5 MHz, 298 K):  $\delta$  -4.1 (s with satellites,  $J_{\text{SeP}} = 179.9$  Hz).  $^{77}\text{Se}\{^1\text{H}\}$  NMR ( $\text{C}_6\text{D}_6$ , 121.5 MHz, 298 K):  $\delta$  -433.0 (d,  $J_{\text{SeP}} = 179.9$  Hz.).  $\text{C}_{20}\text{H}_{32}\text{Al}_3\text{N}_2\text{PSe}$ : C, 48.89; H, 6.56; N, 5.70. Found: C, 48.48; H, 6.23; N, 5.89.

**$\text{P}(\text{CH}_2\text{N}-3,5\text{-Me}_2\text{C}_6\text{H}_3)_2\text{Se}(\text{AlMe}_2)_3$  (23c).** Prepared in an analogous manner to **23a** using **2c** (512.5 mg, 1.0 mmol) in lieu of **19a** with an isolated yield of 328.5 mg, 60 %. X-ray quality crystals were obtained from slow evaporation of a benzene solution.  $^1\text{H}$  NMR ( $\text{C}_6\text{D}_6$ , 300 MHz, 298 K):  $\delta$  -1.24 and 0.03 (s, 3H each, N,N'- $\text{AlMe}_2$ ), -0.74 and 0.30 (s, 6H each, Se, N- $\text{AlMe}_2$ ), 2.05 (s, 12H,  $\text{PhCH}_3$ ), 3.30 (s, 2H,  $\text{PCH}_2$ ), 3.32 (d, 2H,  $\text{PCH}_2$ ), 6.51 (s, 2H, Ph *o*-H), 6.96 (s, 4H, Ph *p*-H).  $^{13}\text{C}\{^1\text{H}\}$  NMR ( $\text{C}_6\text{D}_6$ , 125.8 MHz, 298 K):  $\delta$  -14.8, -8.4, -5.6 and -2.3 (s,  $\text{AlMe}_2$ ), 21.8 (s,  $\text{PhCH}_3$ ), 46.7 (d,  $J_{\text{PC}} = 37.3$  Hz,  $\text{PCH}_2$ ), 120.1 and 127.4 (s, Ph *o*- $\text{C}$  and *m*- $\text{C}$ ), 137.8 (s, Ph *p*- $\text{C}$ ), 146.1 (s, *ipso*- $\text{C}$ ).  $^{31}\text{P}\{^1\text{H}\}$  NMR ( $\text{C}_6\text{D}_6$ , 202.5 MHz, 298 K):  $\delta$  -3.4 (s with satellites,  $J_{\text{SeP}} = 181.3$  Hz).  $^{77}\text{Se}\{^1\text{H}\}$  NMR ( $\text{C}_6\text{D}_6$ , 121.5 MHz, 298 K):  $\delta$  -434.9 (d,  $J_{\text{SeP}} = 181.3$  Hz.).  $\text{C}_{24}\text{H}_{40}\text{Al}_3\text{N}_2\text{PSe}$ : C, 52.65; H, 7.36; N, 5.12. Found: C, 52.29; H, 6.99; N, 4.75.

**Me<sub>3</sub>Al·P(CH<sub>2</sub>NPh)<sub>2</sub>Se(AlMe<sub>2</sub>)<sub>3</sub> (24b).** A solution of AlMe<sub>3</sub> in toluene (3.0 mL, 2.0 M, 6.0 mmol) was added to a solution of **23b** (428.4 mg, 1.0 mmol) in 25 mL toluene. The solution was stirred at room temperature for 24 h. The solution was evaporated to dryness, and the remaining solid was rinsed by pentane. The white solid was collected by filtration and dried (310 mg, 55 %). X-ray quality crystals were obtained from toluene solution at -30 °C. <sup>1</sup>H NMR (C<sub>6</sub>D<sub>6</sub>, 300 MHz, 298 K): δ -1.04 and -0.69 (s, 3H each, N,N'-AlMe<sub>2</sub>), -0.80, 0.13, (s, 6H, Se, N-AlMe<sub>2</sub>), -0.46 (s, 9H, P-AlMe<sub>3</sub>), 3.54 (m, 4H, PCH<sub>2</sub>), 2.83 (m, 2H, PCH<sub>2</sub>), 6.81 (m, 4H, Ph *o*-H), 7.07 (m, 6H, Ph *p*-H & Ph *m*-H). <sup>13</sup>C{<sup>1</sup>H} NMR (C<sub>6</sub>D<sub>6</sub>, 125.8 MHz, 298 K): δ -14.7, -8.5, -5.4 and -2.1 (s, AlMe<sub>2</sub>), -8.0 (s, P-AlMe<sub>3</sub>), 46.3 (d, J<sub>PC</sub> = 36.7 Hz, PCH<sub>2</sub>), 121.05 and 126.0 (s, Ph *o*-C and *m*-C), 130.0 (s, Ph *p*-C), 145.6 (s, *ipso*-C). <sup>31</sup>P{<sup>1</sup>H} NMR (C<sub>6</sub>D<sub>6</sub>, 202.5 MHz, 298 K): δ -8.4 (s with satellites, J<sub>SeP</sub> = 349.7 Hz). <sup>77</sup>Se{<sup>1</sup>H} NMR (C<sub>6</sub>D<sub>6</sub>, 121.5 MHz, 298 K): δ -435.0 (d, J<sub>SeP</sub> = 349.7 Hz). Anal. Calc'd for C<sub>23</sub>H<sub>41</sub>Al<sub>4</sub>N<sub>2</sub>PSe: C, 49.03; H, 7.33; N, 4.91. Found: C, 49.43; H, 6.99; N, 4.87.

**Me<sub>3</sub>Al·P(CH<sub>2</sub>N-3,5-Me<sub>2</sub>C<sub>6</sub>H<sub>3</sub>)<sub>2</sub>Se(AlMe<sub>2</sub>)<sub>3</sub> (24c).** A solution of AlMe<sub>3</sub> in toluene (3 mL, 2.0 M, 6 mmol) was added to a solution of **19c** (512.5 mg, 1 mmol) in 25 mL toluene. The solution was stirred at room temperature for 24 h. The solution was evaporated to dryness, and the remaining solid was rinsed by pentane. The white solid was collected by filtration and dried (403 mg, 65 %). <sup>1</sup>H NMR (C<sub>6</sub>D<sub>6</sub>, 300 MHz, 298 K): δ -0.837 and -0.63 (s, 3H each, N,N'-AlMe<sub>2</sub>), -0.171 and 0.291 (s, 6H

each, Se, N- $\text{AlMe}_2$ ), -0.447 (s, 9H, P- $\text{AlMe}_3$ ), 1.866, 1.994 (s, 6H each, Ph $\text{CH}_3$ ), 2.56 (dd, 1H, P $\text{CH}_2$ ), 3.50 (m, 1H, P $\text{CH}_2$ ), 3.67 (m, 1H, P $\text{CH}_2$ ), 3.86 (dd, 1H, P $\text{CH}_2$ ), 6.5 (s, 2H, Ph *o*-H), 6.6 (s, 4H, Ph *p*-H).  $^{13}\text{C}\{^1\text{H}\}$  NMR ( $\text{C}_6\text{D}_6$ , 125.8 MHz, 298 K):  $\delta$  -14.1, -8.1 -2.25 and -1.63 (s,  $\text{AlMe}_2$ ), -7.8 (s, P- $\text{AlMe}_3$ ), 21.8 (s, Ph $\text{CH}_3$ ),  $\delta$  47.3 (m, P $\text{CH}_2$ ), 120.0 and 127.5 (s, Ph *o*-C and *m*-C), 142.7 (s, Ph *p*-C), 146.1 (d,  $J = 19.5$  Hz, *ipso*-C).  $^{31}\text{P}\{^1\text{H}\}$  NMR ( $\text{C}_6\text{D}_6$ , 202.5 MHz, 298 K):  $\delta$  -9.4 (s with satellites,  $J_{\text{SeP}} = 312.9$  Hz).  $^{77}\text{Se}\{^1\text{H}\}$  NMR ( $\text{C}_6\text{D}_6$ , 121.5 MHz, 298 K):  $\delta$  -436.1 (d,  $J_{\text{SeP}} = 312.9$  Hz.).  $\text{C}_{27}\text{H}_{49}\text{Al}_4\text{N}_2\text{PSe}$ : C, 52.3; H, 7.97; N, 4.52. Found: C, 52.79; H, 7.68; N, 4.26.

**$\text{P}[\text{CH}_2\text{N}-3,5-(\text{CF}_3)_2\text{C}_6\text{H}_3]_3\text{Al}_2\text{Me}_3$  (25a).** A solution of  $\text{AlMe}_3$  in toluene (3.09 mL, 2.0 M, 6.18 mmol) was added to a solution of **1a** (2.34 g, 3.09 mmol) in 15 mL toluene. The solution was left for 12 h. The solution was evaporated to dryness, and the remaining solid was crystallized from by cooling a saturated warm benzene solution to room temperature. The tan solid was collected by filtration and dried (1.5 g, 57 %). A second crop was obtained by slow evaporation of the mother liquor. X-ray quality crystals were obtained by slow evaporation of a benzene solution.  $^1\text{H}$  NMR ( $\text{C}_6\text{D}_6$ , 500 MHz, 298 K):  $\delta$  -0.84 and -0.56 (s, 3H each,  $\text{AlMe}_2$ ), -0.26 (s, 3H,  $\text{AlMe}$ ), 2.70 (dd, 2H,  $^2J_{\text{PH}} = 1.3$  Hz,  $^2J_{\text{HH}} = 14.5$  Hz, P $\text{CH}_2$ ), 2.83 (d, 2H,  $^2J_{\text{PH}} = 6.8$  Hz, P $\text{CH}_2$ ), 3.56 (dd, 2H,  $^2J_{\text{PH}} = 16.9$  Hz,  $^2J_{\text{HH}} = 14.4$  Hz, P $\text{CH}_2$ ), 7.30 (s, 2H, *p*-H), 7.38 (s, 1H, *p*-H), 7.45 (s, 4H, *o*-H), 7.50 (s, 2H, *o*-H).  $^{13}\text{C}\{^1\text{H}\}$  NMR ( $\text{C}_6\text{D}_6$ , 125.8

MHz, 298 K):  $\delta$  -14.5, -5.6, -1.4 (s, AlMe), -5.16 (s, AlMe), 44.8 (d,  $J_{PC} = 23.1$  Hz, PCH<sub>2</sub>), 50.7 (d,  $J_{PC} = 15.1$  Hz, PCH<sub>2</sub>), 121.1 and 123.4 (s, Ph o-C and m-C), 124.6 (s, Ph p-C), 129.9 (m, PhC-F<sub>3</sub>), 149.4 (s, ipso-C).  $^{31}\text{P}\{^1\text{H}\}$  NMR ( $\text{C}_6\text{D}_6$ , 202.5 MHz, 298 K):  $\delta$  -54.2 (s).  $^{19}\text{F}$  NMR ( $\text{C}_6\text{D}_6$ , 282.1 MHz, 298 K):  $\delta$  14.67 (s). Anal. Calc'd for  $\text{C}_{30}\text{H}_{24}\text{Al}_2\text{F}_{18}\text{N}_3\text{P}$ : C, 42.22; H, 2.84; N, 4.92. Found: C, 41.77; H, 3.30; N, 4.89.

**P(CH<sub>2</sub>NPh)<sub>3</sub>Al<sub>2</sub>Me<sub>3</sub> (25b)**. A solution of AlMe<sub>3</sub> in toluene (1 mL, 2.0 M, 2 mmol) was added to a solution of **1b** (349.4 mg, 1 mmol) in 25 mL toluene. The solution was stirred at room temperature for 24 h. The solution was evaporated to dryness, and the remaining solid was rinsed by pentane prior to crystallization from benzene. The white solid was collected by filtration and dried (328.5 mg, 60 %).  $^1\text{H}$  NMR ( $\text{C}_6\text{D}_6$ , 500 MHz, 298 K):  $\delta$  -0.6, 0.22 and -0.16 (s, 3H each, AlMe), 3.14 (d, 2H,  $J = 14.2$  Hz, PCH), 3.53 (d, 2H,  $J = 6.8$  Hz, PCH<sub>2</sub>), 4.00 (dd, 2H,  $^2J_{\text{HH}} = 14.2$  Hz,  $^2J_{\text{PH}} = 16.6$  Hz PCH), 6.86 and 6.88 (m, 3H total, p-H), 6.96 (dd, 4H,  $J = 7.7$  Hz, m-H), 7.09 (d, 4H,  $J = 7.7$  Hz, o-H), 7.22 (d, 2H,  $J = 8.1$  Hz, o-H), 7.33 (dd, 2H, m-H).  $^{13}\text{C}\{^1\text{H}\}$  NMR ( $\text{C}_6\text{D}_6$ , 125.8 MHz, 298 K):  $\delta$  -11.1, -9.2 and -7.9 (s, AlMe<sub>2</sub>), 49.7 (d,  $J_{PC} = 12.9$  Hz, PCH<sub>2</sub>), 55.5 (d,  $J_{PC} = 27.0$  Hz PCH<sub>2</sub>), 116.8, 118.3, 125.8, 125.9, 129.5, 130.1 (s, Ph o-C, m-C and p-C), 150.6 and 154.6 (s, ipso-C).  $^{31}\text{P}\{^1\text{H}\}$  NMR ( $\text{C}_6\text{D}_6$ , 202.5 MHz, 298 K):  $\delta$  -51.3 (s).  $\text{C}_{24}\text{H}_{30}\text{Al}_2\text{N}_3\text{P}$ : C, 64.71; H, 6.79; N, 9.43. Found: C, 64.51; H, 6.93; N, 9.74.

**P(CH<sub>2</sub>N-3,5-Me<sub>2</sub>C<sub>6</sub>H<sub>3</sub>)<sub>3</sub>Al<sub>2</sub>Me<sub>3</sub> (25c)**. A solution of AlMe<sub>3</sub> in toluene (1 mL, 2.0 M,

2 mmol) was added to a solution of **1c** (433.6 mg, 1 mmol) in 25 mL toluene. The solution was stirred at room temperature for 24 h. The solution was evaporated to dryness, and the remaining solid was rinsed by pentane prior to crystallization from benzene. The white solid was collected by filtration and dried (413.5 mg, 78 %).  $^1\text{H}$  NMR ( $\text{C}_6\text{D}_6$ , 500 MHz, 298 K):  $\delta$  -0.45, -0.1, -0.02 (s, 3H each,  $\text{AlMe}$ ), 2.0 (s, 12H,  $\text{PhCH}_3$ ), 2.33 (s, 6H,  $\text{PhCH}_3$ ), 3.30 (dd, 2H,  $^2J_{\text{PH}} = 1.2$  Hz,  $^2J_{\text{HH}} = 14.3$  Hz,  $\text{PCH}_2$ ), 3.64 (d, 2H,  $^2J_{\text{PH}} = 6.5$  Hz,  $\text{PCH}$ ), 4.16 (dd, 2H,  $^2J_{\text{HH}} = 14.3$  Hz,  $\text{PCH}_2$ ), 6.56 (s, 1H, Ph *o-H*), 6.58 (s, 1H, Ph *o-H*), 6.95 (s, 6H, Ph *p-H*).  $^{13}\text{C}\{^1\text{H}\}$  NMR ( $\text{C}_6\text{D}_6$ , 125.8 MHz, 298 K):  $\delta$  -19.8, -7.3, -5.8 (s,  $\text{AlMe}$ ), 21.4 (s,  $\text{PhCH}_3$ ), 22.3 (s,  $\text{PhCH}_3$ ), 50.5 (d,  $\text{PCH}_2$ ), 56.0 (d,  $\text{PCH}_2$ ), 115.5, 120.5, 124.0, 140.1 (s, Ph *o-C* and *p-C*), 151.1, 155.1 (s, *ipso-C*).  $^{31}\text{P}\{^1\text{H}\}$  NMR ( $\text{C}_6\text{D}_6$ , 202.5 MHz, 298 K):  $\delta$  -50.5 (s).  $\text{C}_{30}\text{H}_{42}\text{Al}_2\text{N}_3\text{P}$ : C, 68.03; H, 7.99; N, 7.93. Found: C, 67.79; H, 7.95; N, 7.63.

**$\text{Me}_3\text{Al-P}(\text{CH}_2\text{NPh})_3\text{Al}_2\text{Me}_3$  (26b)**. A solution of  $\text{AlMe}_3$  in toluene (5.0 mL, 2.0 M, 10.0 mmol) was added to a solution of **1b** (699 mg, 2.0 mmol) in 50 mL toluene. The solution was left for 48 h. The colorless solution was evaporated to dryness, and the remaining solid was rinsed by pentane. The white solid was collected by filtration and dried (558 mg, 54 %). X-ray quality crystals were obtained from slow evaporation of a pentane solution at  $-30$  °C.  $^1\text{H}$  NMR ( $\text{C}_6\text{D}_6$ , 500 MHz, 298 K):  $\delta$  -0.68 and -0.30 and -0.13 (s, 3H each,  $\text{AlMe}$ ), -0.37 (s, 9H,  $\text{P-AlMe}_3$ ), 3.22 (dd, 2H,  $^2J_{\text{PH}} = 4.8$  Hz,  $^2J_{\text{HH}} = 4.8$  Hz,  $\text{PCH}_2$ ), 3.70 (s, 2H,  $\text{PCH}_2$ ), 4.10 (dd, 2H,  $^2J_{\text{PH}} = 8.6$  Hz,

$^2J_{\text{HH}} = 5.6$  Hz,  $\text{PCH}_2$ ), 6.9, 7.1, 7.28 (m, Ph).  $^{13}\text{C}\{^1\text{H}\}$  NMR ( $\text{C}_6\text{D}_6$ , 125.8 MHz, 298 K):  $\delta$  -10.8, -9.0 and -8.5 (s,  $\text{AlMe}_2$ ), -8.0 (s,  $\text{P-AlMe}_3$ ), 47.3 (d,  $J_{\text{PC}} = 10.3$  Hz,  $\text{PCH}_2$ ), 52.7 (s,  $\text{PCH}_2$ ), 117.7, 119.7, 126.0, 126.8, 130.0, 130.6 (s, Ph *o-C*, *m-C* and *p-C*), 149.8 (d,  $J = 3.7$  Hz, *ipso-C*), 153.8 (d,  $J = 6.2$  Hz, *ipso-C*).  $^{31}\text{P}\{^1\text{H}\}$  NMR ( $\text{C}_6\text{D}_6$ , 202.5 MHz, 298 K):  $\delta$  -45.5 (s). Anal. Calc'd for  $\text{C}_{27}\text{H}_{39}\text{Al}_3\text{N}_3\text{P}$ : C, 62.66; H, 7.60; N, 8.12. Found: C, 62.17; H, 6.95; N, 7.72.

**$\text{Me}_3\text{Al-P}(\text{CH}_2\text{N-3,5-Me}_2\text{C}_6\text{H}_3)_3\text{Al}_2\text{Me}_3$  (26c).** A solution of  $\text{AlMe}_3$  in toluene (2.0 mL, 2.0 M, 4.0 mmol) was added to a solution of **1c** (433.6 mg, 1 mmol) in 25 mL toluene. The solution was stirred at room temperature for 24 h. The solution was evaporated to dryness, and the remaining solid was rinsed by pentane. The white solid was collected by filtration and dried (367 mg, 60 %).  $^1\text{H}$  NMR ( $\text{C}_6\text{D}_6$ , 500 MHz, 298 K):  $\delta$  -0.57 and -0.25 and 0.01 (s, 3H each,  $\text{AlMe}$ ), -0.38 (s, 9H,  $\text{P-AlMe}_3$ ), 2.00 (s, 12H,  $\text{PhCH}_3$ ), 2.27 (s, 6H,  $\text{PhCH}_3$ ), 3.45 (dd, 2H,  $^2J_{\text{PH}} = 9.5$  Hz,  $^2J_{\text{HH}} = 5.1$  Hz,  $\text{PCH}_2$ ), 3.87 (s, 2H,  $\text{PCH}_2$ ), 4.29 (dd, 2H,  $^2J_{\text{PH}} = 8.6$  Hz,  $^2J_{\text{HH}} = 6.7$  Hz,  $\text{PCH}_2$ ), 6.87 (s, 3H, Ph *o-H*), 7.00 (s, 6H, Ph *p-H*).  $^{13}\text{C}\{^1\text{H}\}$  NMR ( $\text{C}_6\text{D}_6$ , 125.8 MHz, 298 K):  $\delta$  -14.2, -10.4 (s,  $\text{AlMe}_2$ ), -8.8 (s,  $\text{P-AlMe}_3$ ), -7.4 (s,  $\text{AlMe}$ ), 21.5 (s,  $\text{PhCH}_3$ ), 22.2 (s,  $\text{PhCH}_3$ ), 47.7 (d,  $J_{\text{PC}} = 12.7$  Hz,  $\text{PCH}_2$ ), 52.8 (s,  $\text{PCH}_2$ ), 116.3, 124.0, 139.0 (s, Ph *o-C*, *m-C* and *p-C*), 150.2 (d,  $J = 6.3$  Hz, *ipso-C*).  $^{31}\text{P}\{^1\text{H}\}$  NMR ( $\text{C}_6\text{D}_6$ , 202.5 MHz, 298 K):  $\delta$  -44.5 (s).  $\text{C}_{33}\text{H}_{51}\text{Al}_3\text{N}_3\text{P}$ : C, 65.87; H, 8.54; N, 6.98. Found: C, 65.52; H, 8.21; N, 7.34.

### 4.9.3 Crystal Data and Structure Refinement

**Table 4.5.** Crystallographic data for compounds **22a-c**, **23a**, **23c**, **24b**, **25a**, and **26b**.

	<b>22a</b>	<b>22b</b>	<b>22c</b>
Empirical Formula	C <sub>27</sub> H <sub>18</sub> F <sub>18</sub> N <sub>3</sub> PSe	C <sub>21</sub> H <sub>24</sub> N <sub>3</sub> PSe	C <sub>27</sub> H <sub>36</sub> N <sub>3</sub> PSe
Formula Weight	836.4	428.37	512.53
Crystal System	Triclinic	Triclinic	Monoclinic
<i>a</i>	14.832(2) Å	10.025(3) Å	8.1088(7) Å
<i>b</i>	15.494(2) Å	10.598(3) Å	11.4874(10) Å
<i>c</i>	16.371(3) Å	10.605(3) Å	28.225(3) Å
$\alpha$	73.943(2)°	65.584(3)°	90°
$\beta$	65.716(2)°	86.104(3)°	94.317(2)°
$\gamma$	81.208(2)°	75.794(3)°	90°
V (Å <sup>3</sup> )	3292.3(9)	993.9(5)	2621.6(4)
Space Group	<i>P</i> -1	<i>P</i> -1	<i>P</i> 2(1)/n
Z	4	1	4
Density (calculated)	1.766 mg/m <sup>3</sup>	1.431 mg/m <sup>3</sup>	1.299 mg/m <sup>3</sup>
$\mu$ (MoK $\alpha$ ) (mm <sup>-1</sup> )	1.320	1.979	1.512
Temperature (K)	173	173	173
No. Variables	988	247	307
Total No. of Reflins	37705	11128	20415
Residuals: R; wR <sub>2</sub> (all data)	0.121, 0.151	0.077; 0.126	0.049; 0.112
Residual Density (e <sup>-</sup> /Å <sup>3</sup> )	0.721, -0.503	0.952, -0.492	0.570, -0.327

**Table 4.5 cont'd.**

	<b>23a</b>	<b>23c</b>	<b>24b</b>
Empirical Formula	C <sub>24</sub> H <sub>28</sub> Al <sub>3</sub> F <sub>12</sub> N <sub>2</sub> PSe	C <sub>24</sub> H <sub>40</sub> Al <sub>3</sub> N <sub>2</sub> PSe	C <sub>23</sub> H <sub>41</sub> Al <sub>4</sub> N <sub>2</sub> PSe
Formula Weight	763.35	547.47	563.44
Crystal System	Triclinic	Monoclinic	Orthorhombic
<i>a</i>	9.0018(16) Å	13.118(2) Å	15.679(3) Å
<i>b</i>	13.892(3) Å	8.3825(14) Å	10.954(2) Å
<i>c</i>	13.947(3) Å	28.507(5) Å	8.5522(16) Å
$\alpha$	68.850(2)°	90°	90°
$\beta$	85.035(2)°	90.187(2)°	90°
$\gamma$	88.038(2)°	90°	90°
V (Å <sup>3</sup> )	1620.5(5)	3134.7(9)	1468.8(5)
Space Group	<i>P</i> -1	<i>P</i> 2(1)/n	<i>P</i> m n 21
Z	2	4	2
Density (calculated)	1.564 mg/m <sup>3</sup>	1.256 mg/m <sup>3</sup>	1.274 mg/m <sup>3</sup>
Temperature (K)	173	173	173
2 $\theta$ <sub>max</sub> (degrees)	50.0	55.0	55.0
No. Variables	412	311	151
Total No. of Reflns	18272	34149	10182
Residuals: R; wR <sub>2</sub> (all data)	0.042; 0.101	0.049; 0.115	0.064; 0.096
Residual Density (e/Å <sup>3</sup> )	0.915, -0.507	0.852, -0.596	1.002, -0.398

**Table 4.5 cont'd.**

	<b>25a</b>	<b>26b</b>
Empirical Formula	C <sub>30</sub> H <sub>24</sub> Al <sub>2</sub> F <sub>18</sub> N <sub>3</sub> P	C <sub>27</sub> H <sub>39</sub> Al <sub>3</sub> N <sub>3</sub> P
Formula Weight	853.44	517.54
Crystal System	Triclinic	Orthorhombic
<i>a</i>	11.2709(15) Å	11.8225(13) Å
<i>b</i>	11.6947(15) Å	14.7615(16) Å
<i>c</i>	15.652(2) Å	33.447(4) Å
$\alpha$	68.4510(10)°	90°
$\beta$	86.0640(10)°	90°
$\gamma$	78.9210(10)°	90°
V (Å <sup>3</sup> )	1883.1(4)	5837.1(11)
Space Group	<i>P</i> -1	<i>Pbca</i>
Z value	2	8
Density (calculated)	1.574 mg/m <sup>3</sup>	1.178 mg/m <sup>3</sup>
$\mu$ (MoK $\alpha$ ) (mm <sup>-1</sup> )	0.239	0.204
Temperature (K)	173	173
No. Variables	527	313
Total No. of Reflns	18227	62133
Residuals: R; wR2 (all data)	0.068; 0.175	0.055; 0.119
Residual Density (e-/Å <sup>3</sup> )	0.750, -0.520	0.389, -0.241

#### 4.10 References

- (1) Haagenson, D. C.; Moser, D. F.; Stahl, L.; Staples, R. J. *Inorg. Chem.* **2002**, *41*, 1245-1253.
- (2) Witt, M.; Roesky, H. W.; Stalke, D.; Pauer, F.; Henkel, T.; Sheldrick, G. M. *J. Chem. Soc. Dalton Trans.* **1989**, 2173-2177.
- (3) Straub, B. F.; Eisentrager, F.; Hofmann, P. *Chem. Comm.* **1999**, 2507-2508.
- (4) Roesky, H. W.; Voelker, H.; Witt, M.; Noltemeyer, M. *Angew. Chem.* **1990**, *102*, 712-713.
- (5) Niecke, E.; Frost, M.; Nieger, M.; von der Goenna, V.; Ruban, A.; Schoeller, W. *W. Angew. Chem.* **1994**, *106*, 2170-2172.
- (6) Vollmerhaus, R.; Shao, P.; Taylor, N. J.; Collins, S. *Organometallics* **1999**, *18*, 2731-2733.
- (7) Steiner, A.; Stalke, D. *Inorg. Chem.* **1993**, *32*, 1977-1981.
- (8) Chivers, T.; Parvez, M.; Seay, M. A. *Inorg. Chem.* **1994**, *33*, 2147-2150.
- (9) Briand, G. G.; Chivers, T.; Parvez, M.; Schatte, G. *Inorg. Chem.* **2003**, *42*, 525-531.
- (10) Singh, H. B.; Sudha, N. *Polyhedron* **1996**, *15*, 745-763.
- (11) Paulmier, C. *Selenium Reagents and Intermediates in Organic Synthesis*, 1986.
- (12) Stefan Friedrich. *Angew. Chem. Int. Ed.* **1994**, *33*, 676-678.
- (13) Gysling, H. J.; Luss, H. R.; Gardner, S. A. *J. Organomet. Chem.* **1980**, *184*, 417-431.

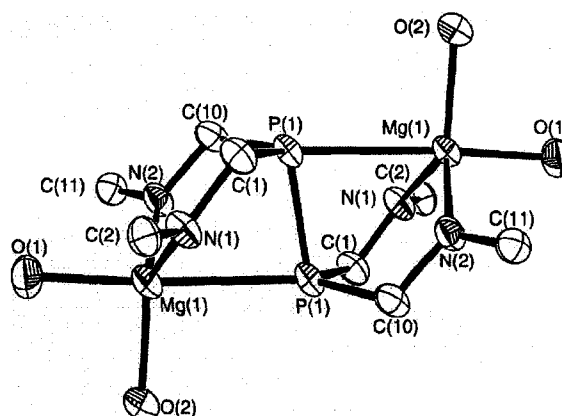
- (14) Steigerwald, M. L. *Polyhedron* **1994**, *13*, 1245-1252.
- (15) Davies, R. P.; Martinelli, M. G. *Inorg. Chem.* **2002**, *41*, 348-352.
- (16) Walther, B. *Coord. Chem. Rev.* **1984**, *60*, 67-105.
- (17) Pilkington, M. J.; Slawin, A. M. Z.; Williams, D. J.; Woollins, J. D. *Polyhedron* **1991**, *10*, 2641-2645.
- (18) Haiduc, I. *J. Organomet. Chem.* **2001**, *623*, 29-42.
- (19) Kuchen, W.; Hertel, H. *Angew. Chem. Int. Ed.* **1969**, *8*, 89-97.
- (20) Keen, A. L.; Doster, M.; Han, H.; Johnson, S. A. *Chem. Commun.* **2006**, 1221-1223.
- (21) Han, H.; Elsmaili, M.; Johnson, S. A. *Inorg. Chem.* **2006**, *45*, 7435-7445.
- (22) Arnold, J. *Inorg. Chem.* **1995**, *43*, 353-417.
- (23) Chivers, T.; Krahn, M.; Schatte, G.; Parvez, M. *Inorg. Chem.* **2003**, *42*, 3994-4005.
- (24) Bochmann, M.; Bwembya, G. C.; Whilton, N.; Song, X.; Hursthouse, M. B.; Coles, S. J.; Karaulov, A. *J. Chem. Soc. Dalton Trans.* **1995**, 1887-1892.
- (25) Lief, G. R.; Carrow, C. J.; Stahl, L.; Staples, R. J. *Organometallics* **2001**, *20*, 1629-1635.
- (26) Lee, W.-Y.; Liang, L.-C. *Dalton Trans.* **2005**, 1952-1956.
- (27) Liang, L.-C.; Huang, M.-H.; Hung, C.-H. *Inorg. Chem.* **2004**, *43*, 2166-2174.
- (28) Fryzuk, M. D.; Giesbrecht, G. R.; Olovsson, G.; Rettig, S. J. *Organometallics* **1996**, *15*, 4832-4841.

- (29) Passarelli, V.; Carta, G.; Rossetto, G.; Zanella, P. *Dalton Trans.* **2003**, 1284-1291.
- (30) Jancik, V.; Pineda, L. W.; Pinkas, J.; Roesky, H. W.; Neculai, D.; Neculai, A. M.; Herbst-Irmer, R. *Angew. Chem. Int. Ed.* **2004**, *43*, 2142-2145.
- (31) Dillingham, M. D. B.; Hill, J. B.; Lee, B.; Schauer, S. J.; Pennington, W. T.; Robinson, G. H.; Hrcir, D. C. *J. Coord. Chem.* **1993**, *28*, 337-346.
- (32) Waggoner, K. M.; Power, P. P. *J. Am. Chem. Soc.* **1991**, *113*, 3385-3393.
- (33) Eisler, D. J.; Chivers, T. *Can. J. Chem.* **2006**, *84*, 443-452.
- (34) Brask, J. K.; Chivers, T.; Yap, G. P. A. *Chem. Commun.* **1998**, 2543-2544.
- (35) Hlavinka, M. L.; Hagadorn, J. R. *Chem. Commun.* **2003**, 2686-2687.
- (36) Bezombes, J.-P.; Gehrhus, B.; Hitchcock, P. B.; Lappert, M. F.; Merle, P. G. *Dalton Trans.* **2003**, 1821-1829.
- (37) Gardinier, J. R.; Gabbai, F. P. *New J. Chem.* **2001**, *25*, 1567-1571.
- (38) Jiang, Z.; Interrante, L. V.; Kwon, D.; Tham, F. S.; Kullnig, R. *Inorg. Chem.* **1991**, *30*, 995-1000.
- (39) Hitchcock, P. B.; Lappert, M. F.; Merle, P. G. *Phosphorus, Sulfur and Silicon and the Related Elements* **2001**, *168-169*, 363-366.
- (40) Gibson, V. C.; Nienhuis, D.; Redshaw, C.; White, A. J. P.; Williams, D. J. *Dalton Trans.* **2004**, 1761-1765.
- (41) Pinkas, J.; Wang, T.; Jacobson, R. A.; Verkade, J. G. *Inorg. Chem.* **1994**, *33*, 5244-5253.

- (42)Sauls, F. C.; Interrante, L. V. *Coord. Chem. Rev.* **1993**, *128*, 193-207.
- (43)Coles, M. P.; Jordan, R. F. *J. Am. Chem. Soc.* **1997**, *119*, 8125-8126.
- (44)Howell, J. A. S.; Fey, N.; Lovatt, J. D.; Yates, P. C.; McArdle, P.; Cunningham, D.; Sadeh, E.; Gottlieb, H. E.; Goldschmidt, Z.; Hursthouse, M. B.; Light, M. E. *J. Chem. Soc. Dalton Trans.* **1999**, 3015-3028.
- (45)Steinberger, H. U.; Ziemer, B.; Meisel, M. *Acta Cryst.* **2001**, *C57*, 323-324.
- (46)Barron, A. R. *J. Chem. Soc. Dalton Trans.* **1988**, 3047-3050.
- (47)Slawin, A. M. Z.; Wheatley, J.; Wheatley, M. V.; Woollins, J. D. *Polyhedron* **2003**, *22*, 1397-1405.
- (48)Allen, D. W.; Taylor, B. F. *J. Chem. Soc. Dalton Trans.* **1982**, 51-54.
- (49)Andersen, N. G.; Keay, B. A. *Chem. Rev.* **2001**, *101*, 997-1030.
- (50)Allen, D. W.; Nowell, I. W.; Taylor, B. F. *J. Chem. Soc. Dalton Trans.* **1985**, 2505-2508.
- (51)Tolman, C. A. *J. Am. Chem. Soc.* **1970**, *92*, 2953-2956.
- (52)Beachley, O. T. Jr.; Tessier-Youngs, C. *Inorg. Chem.* **1979**, *18*, 3188-3191.
- (53)Planas, J. G.; Hampel, F.; Gladysz, J. A. *Chem. A Euro. J.* **2005**, *11*, 1402-1416.
- (54)Beachley, O. T., Jr.; Bueno, C.; Churchill, M. R.; Hallock, R. B.; Simmons, R. G. *Inorg. Chem.* **1981**, *20*, 2423-2428.
- (55)Beachley, O. T., Jr.; Royster, T. L., Jr.; Arhar, J. R.; Rheingold, A. L. *Organometallics* **1993**, *12*, 1976-1980.
- (56)Sauls, F. C.; Czekaj, C. L.; Interrante, L. V. *Inorg. Chem.* **1990**, *29*, 4688-4692.

- (57) Himmel, H.-J.; Vollet, J. *Organometallics* **2002**, *21*, 5972-5977.
- (58) Zhu, H.; Yang, Z.; Magull, J.; Roesky, H. W.; Schmidt, H.-G.; Noltemeyer, M. *Organometallics* **2005**, *24*, 6420-6425.
- (59) Duddeck, H. *NMR Spect.* **1995**, *27*, 1-323.
- (60) Leszczynski, J.; Kwiatkowski, J. S. *J. Phy. Chem.* **1993**, *97*, 1364-1367.
- (61) Lindner, E.; Bosch, E.; Fawzi, R.; Steimann, M.; Mayer, H. A.; Gierling, K. *Chem. Ber.* **1996**, *129*, 945-951.
- (62) Zhang, Q.-F.; Cheung, F. K. M.; Wong, W.-Y.; Williams, I. D.; Leung, W.-H. *Organometallics* **2001**, *20*, 3777-3781.
- (63) Walther, B.; Messbauer, B.; Meyer, H. *Inorg. Chim. Acta* **1979**, *37*, L525-L527.
- (64) Gelmini, L.; Stephan, D. W. *Organometallics* **1987**, *6*, 1515-22.
- (65) Wells, R. L.; Foos, E. E.; Rheingold, A. L.; Yap, G. P. A.; Liable-Sands, L. M.; White, P. S. *Organometallics* **1998**, *17*, 2869-2875.
- (66) Kuczkowski, A.; Schulz, S.; Nieger, M.; Schreiner, P. R. *Organometallics* **2002**, *21*, 1408-1419.
- (67) Almennigen, A.; Halvorsen, S.; Haaland, A. *Acta Chem.* **1971**, *25*, 1937-1945.
- (68) Verevkin, S. P.; Emel'yanenko, V. N. *J. Phy. Chem.* **2004**, *108*, 6575-6580.
- (69) Han, H.; Johnson, S. A. *Organometallics* **2006**, *25*, 5594-5602.

Chapter Five



## A Binuclear Magnesium Complex Bridged by a Bisphosphine Ligand

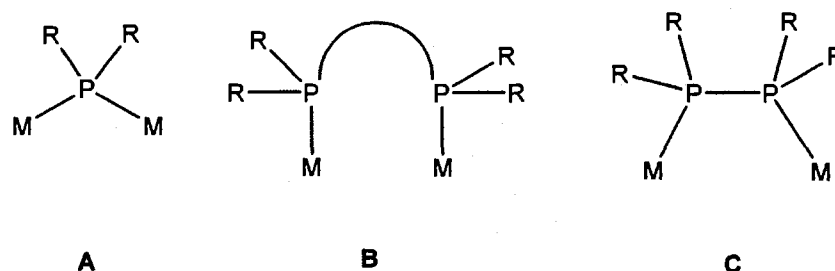
### 5.1-Introduction

There is great interest in binuclear complexes containing bridging ligands, which has been brought about by significant progress in synthetic methodology.

Phosphido groups (Scheme 5.1, **R<sub>2</sub>P<sup>-</sup>**, **A**), biphosphine groups, (Scheme 5.1, **B**), and

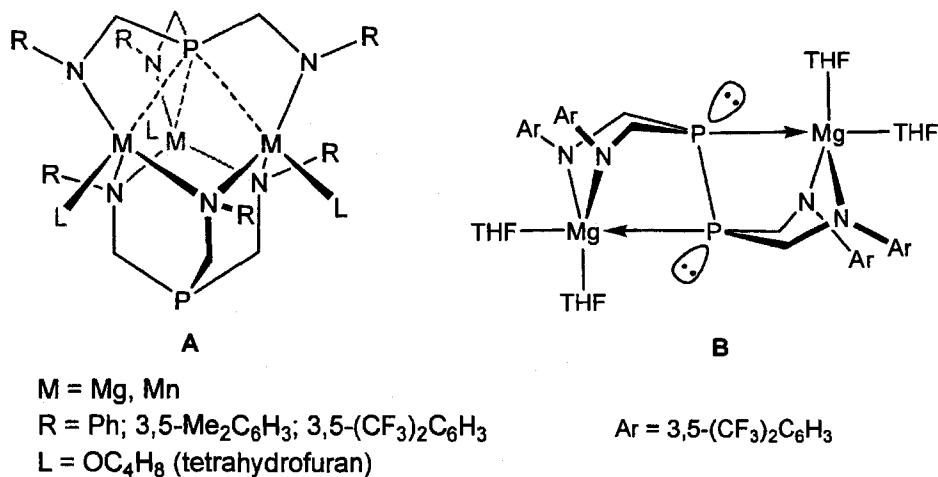
bisphosphine groups with P-P bonds (Scheme 5.1, R<sub>2</sub>P-PR<sub>2</sub>, C), have been widely used as bridging ligands because of their ability to form the stable phosphorus-metal bonds with a variety of metal fragments.<sup>1</sup> In these complexes, metal-metal bonds may exist, with the potential to facilitate the activation and transfer of substrate molecules.<sup>2,3</sup>

### Scheme 5.1



Recently, Hatnean and Johnson reported how trinuclear Mg(II) and Mn(II) complexes could be assembled using the triamidophosphines P(CH<sub>2</sub>NHAr<sup>R</sup>)<sub>3</sub> (**1a-c**, where Ar<sup>R</sup> = 3,5-(CF<sub>3</sub>)<sub>2</sub>C<sub>6</sub>H<sub>3</sub>, Ph, and 3,5-Me<sub>2</sub>C<sub>6</sub>H<sub>3</sub>), as shown in Scheme 5.2 (bonding mode A).<sup>4</sup> These clusters are assembled by two ancillary ligand moieties, with one of the phosphorus donors facing directly towards the centre of the triangle of metal centres.<sup>4</sup>

## Scheme 5.2



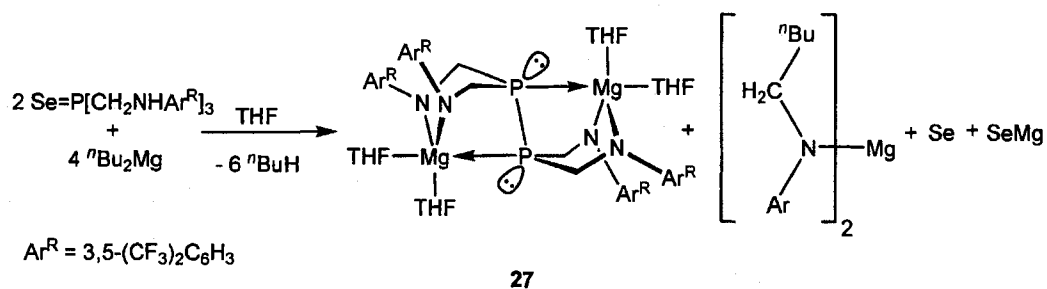
Selenium transfers by the reactions of tertiary phosphine selenides with (carbonyl)metal species provide a simple synthetic route to selenido clusters by taking advantage of the frail P=Se bond.<sup>5,6</sup> The Tiripicchio group found that tertiary phosphine selenides with heterocyclic groups can not only undergo P=Se cleavage but also P-C bond cleavage to afford new clusters. The coordinating ability of the heteroatoms (N atoms in the phosphines) and the short interactions of M...P facilitate P-C bond cleavage.<sup>5,6,7</sup> In Chapter Four, we also report that phosphine selenides Se[P(CH<sub>2</sub>NHAr<sup>R</sup>)<sub>3</sub>] were efficiently reduced to P(III) centres that bind three aluminum metals using the amido and selenium donors by the reactions with AlMe<sub>3</sub>, which were accompanied with P-C bond cleavage under mild conditions.<sup>23</sup> Herein, we report the synthesis, structure and spectroscopy of a *trans*-binuclear magnesium complex bridged by a bisphosphine ligand, as shown in Scheme 5.2 (bonding mode B). The binuclear magnesium complex adopts a  $\kappa^3$ (N, N, P) bonding mode, which is

prepared by the reaction of the phosphine selenide  $\text{Se}=\text{P}(\text{CH}_2\text{NHAr}^{\text{R}})_3$  (where  $\text{Ar}^{\text{R}} = 3,5\text{-(CF}_3)_2\text{C}_6\text{H}_3$ ) with *n*-butylmagnesium, as well as the coordination chemistry of the phosphine selenides with the zirconium metal compounds.

## 5.2 Synthesis and Structure of a Binuclear Magnesium Complex Bridged by a Bisphosphine Ligand

The treatment of  $\text{Se}=\text{P}[\text{CH}_2\text{NH-}3,5\text{-(CF}_3)_2\text{C}_6\text{H}_3]_3$  (**22a**) with *n*-butylmagnesium in THF provided the *trans*-binuclear magnesium complex bridged by a bisphosphine ligand  $\{\text{P}[\text{CH}_2\text{N-}3,5\text{-(CF}_3)_2\text{C}_6\text{H}_3]_2\text{MgTHF}_2\}_2$  (**27**). Both the P-C and the Se=P bond cleave easily to form P-P bond thereby producing a binuclear magnesium complex, as shown in Scheme 5.3. Upon dropwise addition of the 1.0 M heptane solution of  ${}^n\text{Bu}_2\text{Mg}$  to a solution of  $\text{Se}=\text{P}[\text{CH}_2\text{NH-}3,5\text{-(CF}_3)_2\text{C}_6\text{H}_3]_3$  (**22a**) in THF at  $-30\text{ }^\circ\text{C}$ , the color gradually turned from colorless to yellow at room temperature. After 4 h the solvent was removed to give a brown oil that was triturated with toluene and pentane. The white solid was collected and recrystallized from a 1:1 mixture of toluene and THF. The complex is not soluble in toluene, benzene and pentane, but is soluble in THF. The  ${}^{31}\text{P}\{^1\text{H}\}$  NMR and  ${}^{19}\text{F}\{^1\text{H}\}$  NMR spectra of  $\{\text{P}[\text{CH}_2\text{N-}3,5\text{-(CF}_3)_2\text{C}_6\text{H}_3]_2\text{MgTHF}_2\}_2$  (**27**) reveal single resonances at  $\delta -63.6$  and  $\delta 14.19$ , respectively.

## Scheme 5.3



The solid-state structure of  $\{\text{P}[\text{CH}_2\text{N-3,5-(CF}_3)_2\text{C}_6\text{H}_3]_2\text{MgTHF}_2\}_2$  **27** was determined by X-ray crystallography. An ORTEP depiction of the solid-state molecular structure of **27** is shown in Figure 5.1 and the pertinent crystallographic data is summarized in Table 5.1. The  $^1\text{H}$  and  $^{13}\text{C}\{^1\text{H}\}$  spectra of **27** in  $d_8$ -THF are consistent with an identical solution structure. The complex  $\{\{\text{PCH}_2\text{N-3,5-(CF}_3)_2\text{C}_6\text{H}_3\}_2\text{MgTHF}_2\}_2$  **27** crystallizes in the triclinic space group  $P-1$  with an inversion center in the middle of the bridging P-P bond. The binuclear complex consists of two distorted trigonal bipyramidal Mg units, where a THF donor resides in the axial sites *trans* to the phosphine. The two magnesium centers bind the bisphosphine ligand via one phosphine and two amido donors, all of which act as bridging ligands. The donors along with the magnesium atom form a five-membered  $\text{P}_2\text{MgNC}$  ring and a six-membered  $\text{PC}_2\text{N}_2\text{Mg}$  ring. The average Mg-N bond length of 2.023(4) Å is typical of previously structurally characterized Mg amido compounds.<sup>8-10</sup> The sum of N(1)-Mg(1)-N(2), N(1)-Mg(1)-O(2) and N(2)-Mg(1)-O(2) bond angles is 356.63(26)°, which is close to 360° expected for a planar arrangement of these atoms. However, the N(1)-Mg(1)-N(2) angle of 108.18(15)° is smaller than

that of N(1)-Mg(1)-O(2) ( $123.49(15)^\circ$ ) and N(2)-Mg(1)-O(2) ( $124.96(15)^\circ$ ) angles. The nearly linear O(1)-Mg(1)-P(1) angle of  $176.47(11)^\circ$  is further evidence that the geometry around the Mg(1) atom is best described as trigonal bipyramidal.<sup>11,12,13</sup>

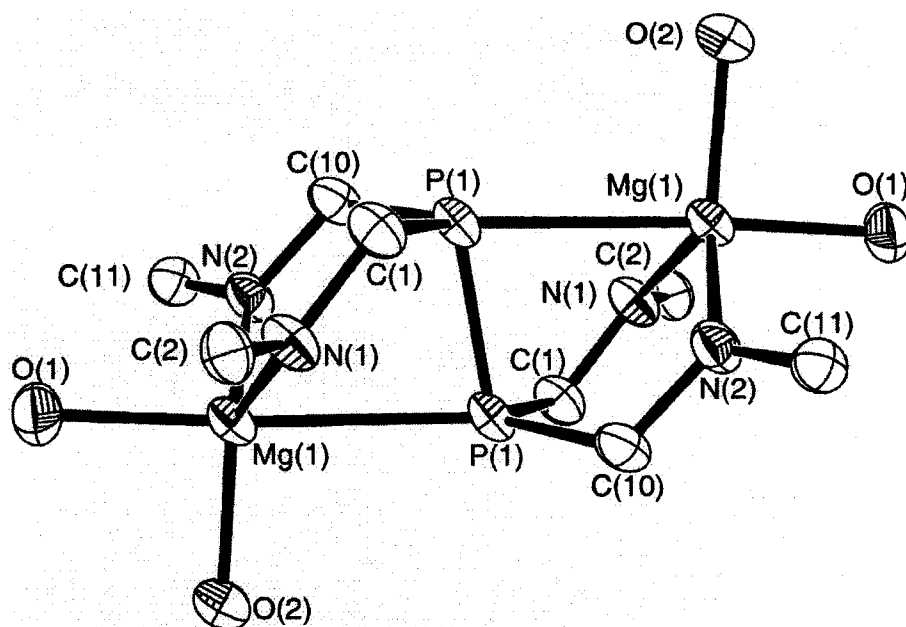


**Figure 5.1.** Solid-state molecular structure of **27** obtained by X-ray crystallography.

Selected bond lengths, in Å: P(1)-Mg(1), 2.8492(18); Mg(1)-N(1), 2.023(4); Mg(1)-N(2), 2.030(4); Mg(1)-O(1), 2.063(3); Mg(1)-O(2), 2.036(3); P(1)-P(1), 2.192(2). Selected bond angles (deg): P(1)-P(1)-Mg(1), 79.00(7); N(1)-Mg(1)-N(2), 108.18(15); N(1)-Mg(1)-O(2), 123.49(15); N(2)-Mg(1)-O(2), 124.96(15); N(1)-Mg(1)-O(1), 98.85(15); N(2)-Mg(1)-O(1), 99.40(15); O(2)-Mg(1)-O(1), 90.77(14); N(1)-Mg(1)-P(1), 78.76(11); N(2)-Mg(1)-P(1), 79.02(11); O(2)-Mg(1)-P(1), 92.72(10); O(1)-Mg(1)-P(1), 176.47(11).

A significant criticism against the existence of the P-Mg bonds in the complex **27** is that the lone pairs are not directed towards the Mg metal centers. The P-Mg distance of 2.8492(18) Å is slightly larger in comparison with the P-Mg bond lengths of 2.65-2.77 Å of the few crystallographically characterized magnesium phosphine complexes.<sup>14,15</sup> The geometry at the metal centers in the complex **27** is approximately distorted trigonal bipyramidal, where a THF donor resides in the axial sites *trans* to the phosphine. In comparison to the trinuclear Mg(II) complexes<sup>4</sup> assembled using the triamidophosphines  $\text{P}(\text{CH}_2\text{NHAr}^{\text{R}})_3$  (where  $\text{Ar}^{\text{R}} = 3,5\text{-(CF}_3)_2\text{C}_6\text{H}_3$ , Ph, and 3,5-Me<sub>2</sub>C<sub>6</sub>H<sub>3</sub>) (as shown in Scheme 5.2, bonding mode A), one of the phosphorus donors faces directly towards the centre of the triangle of metal centres in these clusters. The geometries at the metal centers in these clusters also are approximately distorted trigonal bipyramidal. However, even the shortest Mg-P distances in these complexes are significantly longer than typical bonding distances.<sup>14</sup> Although phosphines are known to be capable of bridging two or three late transition metal complexes, similar bonding in main group metal complexes, where the bonding is undoubtedly significantly more ionic than covalent, lacks precedent.

### 5.3 Characterization of the Byproducts and the Mechanism of the Reaction of $\text{Se}=\text{P}[\text{CH}_2\text{NH-3,5-(CF}_3)_2\text{C}_6\text{H}_3]_3$ with *n*-Butylmagnesium .

#### 5.3.1 Characterization of the Byproducts

The byproducts are much more soluble in toluene than the scarcely soluble **27**,

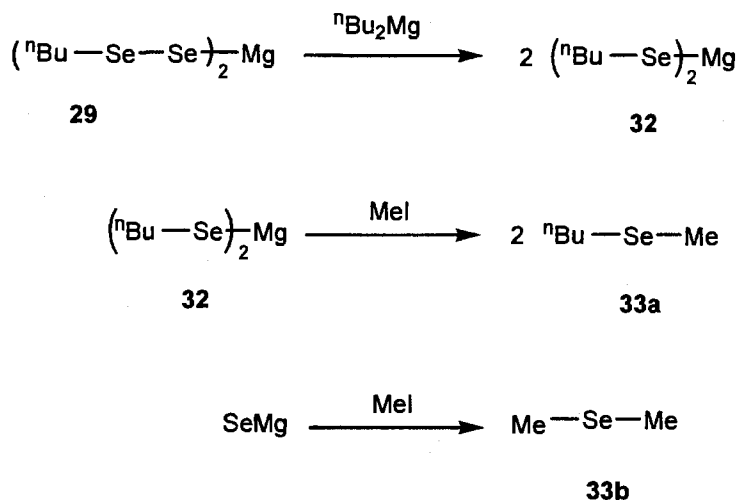
and were easily rinsed from the crude product mixtures. The overall reaction involves the loss of 2 ligand  $-\text{CH}_2\text{NHAr}^{\text{R}}$  arms ( $\text{Ar}^{\text{R}} = 3,5\text{-(CF}_3)_2\text{C}_6\text{H}_3$ ), which makes the use of 4 equiv of  ${}^n\text{Bu}_2\text{Mg}$  be necessary for every 2 equiv of ligand. As shown in Scheme 5.3, the byproducts are believed to be 1 equiv of  $[{}^n\text{BuCH}_2\text{N}(\text{Ar}^{\text{R}})]_2\text{Mg}$ , 1 equiv of elemental selenium and  $\text{SeMg}$ . Definitive proof regarding the nature of  $[{}^n\text{BuCH}_2\text{N}(\text{Ar}^{\text{R}})]_2\text{Mg}$  was obtained by the hydrolysis of the toluene fraction used to rinse the crude product mixture in the synthesis of **27**. The hydrolysis product was identified as  ${}^n\text{BuCH}_2\text{N}(\text{H})\text{-}3,5\text{-(CF}_3)_2\text{C}_6\text{H}_3$  (**28**) by  ${}^1\text{H}$  NMR and GC/MS.

The elemental selenium insertion reactions along with the reactions of selenium with organic selenolates are poorly described. Recently, Krief's group investigated these reactions systematically through the use of *n*-butyllithium and treated it stepwise with elemental selenium. They not only found that selenium can react with *n*-butyllithium rapidly to produce *n*-butyl diselenolate or *n*-butyl selenolate, but also proved the existence of these species. The study implies the selective insertion of two Se atoms into carbon-metal bonds or one Se atom into selenolates,<sup>16</sup> affording the most valuable method to characterize the byproducts in the reaction of phosphine selenide  $\text{Se}=\text{P}[\text{CH}_2\text{NH-}3,5\text{-(CF}_3)_2\text{C}_6\text{H}_3]_3$  with *n*-butylmagnesium .

When 1 equiv of  $\text{Se}=\text{P}[\text{CH}_2\text{NH-}3,5\text{-(CF}_3)_2\text{C}_6\text{H}_3]_3$  (**22a**) reacts with 4.25 equiv of  ${}^n\text{Bu}_2\text{Mg}$  in THF, a dark-red clear solution is produced.<sup>16</sup> This is because 2 equiv of elemental selenium reacts with 0.5 equiv of  ${}^n\text{Bu}_2\text{Mg}$  rapidly producing the dark-red clear solution of *n*-butyl diselenolate salt **29**, as shown in Scheme 5.4. The byproducts were easily rinsed by toluene from the crude product mixtures and filtrate was



## Scheme 5.5



Although the exact mechanism by which P=Se and P-C bond cleavages occur is not clear, and the mixtures of byproducts are too complicated to be isolated, we have presented some evidence that byproducts include elemental selenium and SeMg.

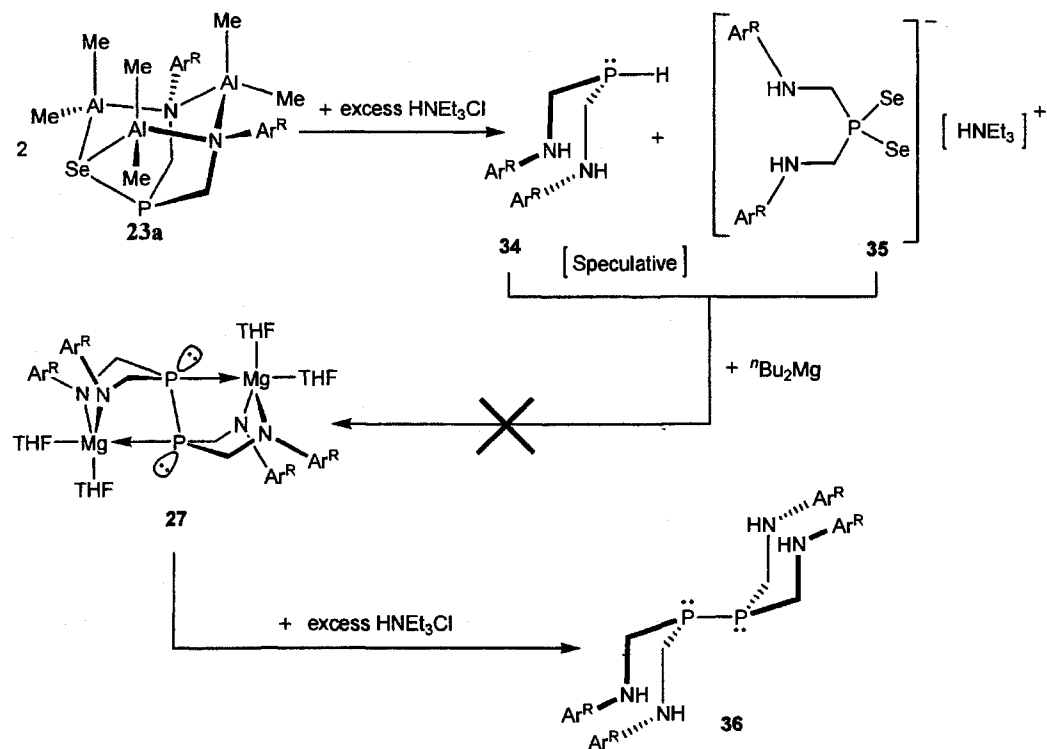
### 5.3.2 The Study of the Mechanism of the Reaction of Phosphine Selenide $\text{Se}=\text{P}[\text{CH}_2\text{NH}-3,5\text{-(CF}_3)_2\text{C}_6\text{H}_3]_3$ with *n*-Butylmagnesium

We propose that the cleavage of the P-C bond occurs before the Se=P bond and the intermediate maybe similar to the biamido-selenophosphine(III) (N, N, Se) aluminum complexes. In agreement with proposal, the binuclear magnesium complex  $\{\text{P}[\text{CH}_2\text{N}-3,5\text{-(CF}_3)_2\text{C}_6\text{H}_3]_2\text{MgTHF}_2\}_2$  **27** is not observed in the reaction of  $\text{P}[\text{CH}_2\text{NH}-3,5\text{-(CF}_3)_2\text{C}_6\text{H}_3]_3$  with  ${}^n\text{Bu}_2\text{Mg}$ . In an attempt to prove that the magnesium salt with the biamido-selenophosphine(III) (N, N, Se) ligand is a viable intermediate, we treated the biamido-selenophosphine(III) aluminum complex **23a** with excess

HNEt<sub>3</sub>Cl, in the hope of isolating HSe[CH<sub>2</sub>NH-3,5-(CF<sub>3</sub>)<sub>2</sub>C<sub>6</sub>H<sub>3</sub>]<sub>2</sub>, which could then be converted to **27** by treatment with <sup>n</sup>Bu<sub>2</sub>Mg. Unfortunately, in the <sup>31</sup>P{<sup>1</sup>H} NMR spectrum of the mixture, two phosphorus signals were observed at δ 30.1 (satellite, *J* = 615.9 Hz) and δ -73.9 (singlet). Although we did not separate the mixture, crystals of a new complex **35** was collected from the oily mixture, as shown in Scheme 5.6. The solid-state structure of **35** has been determined by X-ray diffraction study, <sup>1</sup>H NMR, <sup>31</sup>P{<sup>1</sup>H} NMR [δ 30.1 (satellite, *J* = 615.9 Hz)] and <sup>13</sup>C{<sup>1</sup>H} NMR spectra. The singlet at δ -73.9 in the <sup>31</sup>P{<sup>1</sup>H} NMR spectrum of the mixture may be speculatively attributed to **34**, which could be responsible to the formation of the binuclear magnesium complex {P[CH<sub>2</sub>N-3,5-(CF<sub>3</sub>)<sub>2</sub>C<sub>6</sub>H<sub>3</sub>]<sub>2</sub>MgTHF<sub>2</sub>}<sub>2</sub> **27**. However, the addition of <sup>n</sup>Bu<sub>2</sub>Mg into the mixture did not afford the binuclear magnesium complex {P[CH<sub>2</sub>N-3,5-(CF<sub>3</sub>)<sub>2</sub>C<sub>6</sub>H<sub>3</sub>]<sub>2</sub>MgTHF<sub>2</sub>}<sub>2</sub> **27** by <sup>31</sup>P{<sup>1</sup>H} NMR spectroscopy. Thus, this study fails to explain the mechanism of the reaction of phosphine selenide Se=P[CH<sub>2</sub>NH-3,5-(CF<sub>3</sub>)<sub>2</sub>C<sub>6</sub>H<sub>3</sub>]<sub>3</sub> with *n*-butyl-magnesium.

We also considered the possibility that the byproduct **34** in the reaction of **23a** with HNEt<sub>3</sub>Cl could be the precursor to complex **27**, shown as species **36** in Scheme 5.6. However, the hydrolysis of **27** with HNEt<sub>3</sub>Cl to produce **36** shows that the <sup>31</sup>P{<sup>1</sup>H} NMR shifts are distinct. The <sup>31</sup>P{<sup>1</sup>H} NMR spectrum of **36** obtained from the reaction of **27** with HNEt<sub>3</sub>Cl displays a singlet at δ -46.9.

## Scheme 5.6



An ORTEP depiction of the solid-state molecular structure of **35** is shown in Figure 5.2 and the pertinent crystallographic data is summarized in Table 5.1. The complex  $\{P[CH_2NH-3,5-(CF_3)_2C_6H_3]_2Se_2\} [HNEt_3]^+$  **35** crystallizes in the monoclinic space group  $P 1 21/n 1$ . The P-Se bond lengths of 2.133(4) Å and 2.137(4) Å are intermediate between those of P-Se single bonds (2.26 Å) and double bonds (2.09 Å).<sup>21</sup> The  $^{31}P\{^1H\}$  NMR spectrum of **35** consists of singlet at  $\delta$  30.1, with selenium satellites  $J_{PSe} = 615.9$  Hz, which also indicates a P-Se bond order of 1.5.<sup>21</sup>

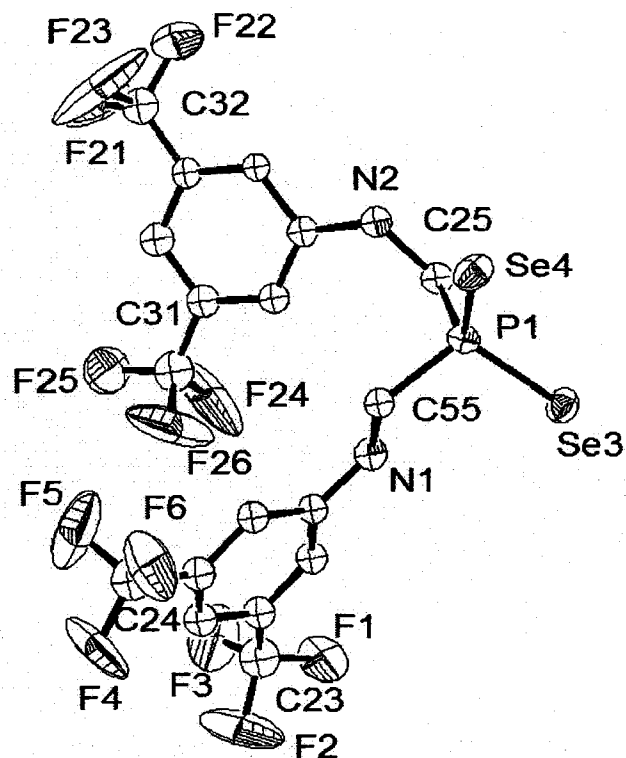
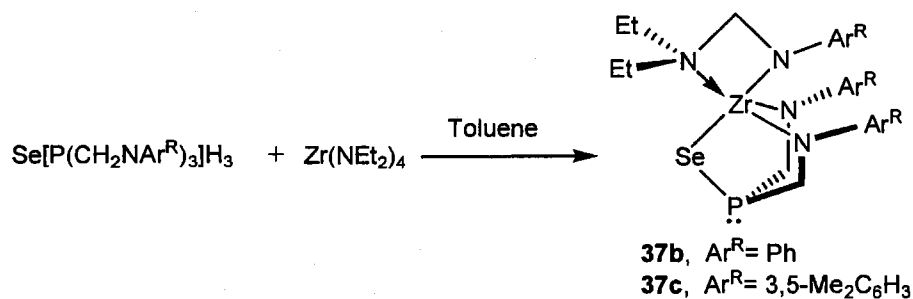


**Figure 5.2.** Solid-state molecular structure of the anionic fragment of **35** determined by X-ray crystallography. Hydrogen atoms and  $[\text{HNEt}_3]^+$  are omitted for clarity. Selected distances ( $\text{\AA}$ ): P(1)-C(25), 1.848(15); P(1)-C(55), 1.812(14); P(1)-Se(3), 2.133(4); P(1)-Se(4), 2.137(4); N(1)-C(55), 1.463(18); N(2)-C(25), 1.466(17). Selected bond angles (deg): C(25)-P(1)-C(55), 105.3(7); C(25)-P(1)-Se(3), 105.5(5); C(55)-P(1)-Se(3), 109.3(5); C(25)-P(1)-Se(4), 111.9(5); C(55)-P(1)-Se(3), 105.2(5); Se(3)-P(1)-Se(4), 118.8(2).

## 5.4 Synthesis and Structures of Zirconium Compounds with Tripodal Diamido-selenophosphinito ligands

The treatment of  $\text{SeP}[\text{CH}_2\text{NAr}^{\text{R}}]_3\text{H}_3$  (where **22b**,  $\text{Ar}^{\text{R}} = \text{Ph}$ , and **22c**,  $3,5\text{-Me}_2\text{C}_6\text{H}_3$ ) with 1 equiv of  $\text{Zr}(\text{NEt}_2)_4$  in toluene at room temperature produced the mononuclear amido-seleno-phosphinito  $\kappa^3(\text{N}, \text{N}, \text{Se})$  zirconium compounds **37b-c** accompanied with P-C bond cleavage, as shown in Scheme 5.6. The phosphorus (V) centre was formally reduced to phosphorus (III), and P=Se double bond was changed into P-Se single bond. The coordinating ability of the amido donors and the short interaction of  $\text{Zr}\cdots\text{P}$  facilitate P-C bond cleavage. Dissociation of  $-\text{CH}_2\text{NAr}^{\text{R}}$  from phosphorus generates the new  $\text{Et}_2\text{NCH}_2\text{NAr}^{\text{R}}$  moiety. The reaction requires 2 h to go to completion. No intermediates were observed by  $^1\text{H}$  or  $^{31}\text{P}\{^1\text{H}\}$  NMR spectroscopy and the resultant products were all obtained in high yields as orange crystalline solids. The  $^{31}\text{P}\{^1\text{H}\}$  NMR spectra of the zirconium compounds **37b** and **37c** consisted of singlets at  $\delta$  -90.8 and -92.9, with selenium satellites  $J_{\text{PSe}} = 256.2$  Hz and  $J_{\text{PSe}} = 253.9$  Hz, respectively, which are well within the range expected for the P-Se single bond.<sup>21</sup>

**Scheme 5.7**



The solid-state structure of **37c** was determined by X-ray crystallography, and an ORTEP depiction of the solid-state molecular structure of **37c** is shown in Figure 5.3. The pertinent crystallographic data is summarized in Table 5.1. The geometry of the Zr centre is best described as a distorted trigonal bipyramidal, in which the seleno donor and N(3) occupy the axial positions with a N(3)-Zr(1)-Se(1) angle of 145.39(8)°. The -NEt<sub>2</sub> ligand and the two amido donors of the ligand are in three equatorial sites. The Zr(1)-Se(1)-P(1) bond angle (73.11(4)°) is quite narrow. The chelate amido-seleno-phosphinito ligand bite angles of N(1)-Zr(1)-Se(1), N(2)-Zr(1)-Se(1) and N(2)-Zr(1)-N(1) are 93.52(8)°, 96.00(9)° and 104.50(12)° respectively, which are more compressed than those of tripodal-amido zirconium compounds. The Zr-N<sub>amido</sub> bond lengths (from 2.062(3) to 2.092(3) Å) are within the normal range,<sup>22</sup> and are much shorter than the Zr-N(4) bond length (2.397(3) Å). The Zr-Se bond length of 2.6534(8) Å is a typical single bond length.<sup>23,24</sup> The P...Zr distances of 2.9390(15) Å is under the sum of Van der Waals radii of these elements. Both the P-Se bond lengths (2.2513(15) Å) and the <sup>1</sup>J<sub>PSe</sub> values (253.9 Hz) are within the ranges expected for P-Se single bonds.<sup>21</sup>

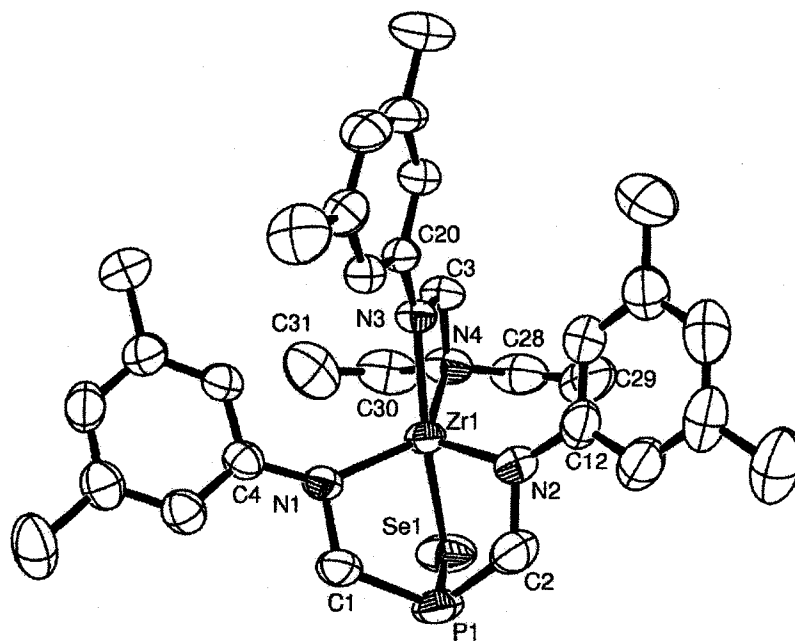


**Figure 5.3** Solid-state molecular structure of **37c** as determined by X-ray crystallography. Hydrogen atoms are omitted for clarity. Selected distances (Å): Zr(1)–P(1), 2.9390(15); Zr(1)–N(1), 2.075(3); Zr(1)–N(2), 2.062(3); Zr(1)–N(3), 2.092(3); Zr(1)–N(4), 2.397(3); Zr(1)–Se(1), 2.6534(8); P(1)–C(1), 1.874(4); P(1)–C(2), 1.860(5); P(1)–Se(1), 2.2513(15). Selected bond angles (deg): C(1)–P(1)–C(2), 104.5(2); C(1)–P(1)–Se(1), 102.68(14); C(2)–P(1)–Se(1), 104.17(15); Zr(1)–N(1)–C(1), 105.5(2); Zr(1)–N(1)–C(4), 139.5(2); Zr(1)–N(2)–C(2), 105.5(3); Zr(1)–N(2)–C(12), 138.1(3); Zr(1)–Se(1)–P(1), 73.11(4); Zr(1)–N(3)–C(3), 104.7(2); N(1)–Zr(1)–N(2), 105.49(13); N(1)–Zr(1)–N(3), 107.11(11); N(1)–Zr(1)–N(4), 132.52(12); N(1)–Zr(1)–Se(1), 93.52(8); N(2)–Zr(1)–N(3), 104.50(12); N(2)–Zr(1)–Se(1), 96.00(9); N(3)–Zr(1)–Se(1), 145.39(8); N(4)–Zr(1)–Se(1), 84.30(8); N(3)–Zr(1)–N(4), 61.22(10); N(3)–C(3)–N(4), 102.8(3).

## 5.5 Summary and Conclusions

The reaction of the ligand precursors  $\text{Se}=\text{P}[\text{CH}_2\text{NH}-3,5\text{-(CF}_3)_2\text{C}_6\text{H}_3]_3$  (**22a**) with *n*-butylmagnesium affords the binuclear magnesium complex bridged by a biamido bisphosphine ligand  $\{\text{P}[\text{CH}_2\text{N}-3,5\text{-(CF}_3)_2\text{C}_6\text{H}_3]_2\text{MgTHF}_2\}_2$  (**27**), with concomitant loss of one equiv of  $[\text{}^n\text{BuCH}_2\text{N}(\text{Ar}^{\text{R}})]_2\text{Mg}$ . A P-P bond is formed through P=Se and P-C bond cleavages. Although the mixtures of byproducts are too complicated to be isolated, the by-products are identified to include elemental selenium, *n*-butyl diselenolate salt (**29**), or *n*-butyl selenolate salt (**32**) depending on the number of equivalent of  ${}^n\text{Bu}_2\text{Mg}$  added.

Ligands  $\text{Se}[\text{P}(\text{CH}_2\text{NAr}^{\text{R}})_3]$  are efficiently reduced by  $\text{Zr}(\text{NEt}_2)_4$  to produce mononuclear zirconium complexes  $\text{P}(\text{CH}_2\text{NAr}^{\text{R}})_2\text{SeZrNAr}^{\text{R}}\text{CH}_2\text{NEt}_2$  (**37 b-c**), which are accompanied with P-C bond cleavage.

## 5.6 Experimental

### 5.6.1 General procedures

Unless otherwise stated, general procedures were performed according to Section 2.11.1.

The compounds and 1.0 M dibutylmagnesium in heptane were purchased from Aldrich, and used as received. The ligands were prepared as previously reported in

Chapter 2 &amp; 4.

## 5.6.2 Synthesis and Characterization of Complexes

**{P[CH<sub>2</sub>N-3,5-(CF<sub>3</sub>)<sub>2</sub>C<sub>6</sub>H<sub>3</sub>]<sub>2</sub>MgTHF<sub>2</sub>}<sub>2</sub> (27).** A 1.0 M heptane solution of <sup>n</sup>Bu<sub>2</sub>Mg (3.25 mL, 3.25 mmol, 3.25 equiv) was added to a solution of SeP[CH<sub>2</sub>N-3,5-(CF<sub>3</sub>)<sub>2</sub>C<sub>6</sub>H<sub>3</sub>]<sub>3</sub>H<sub>3</sub> (1.672 g, 2.0 mmol) in 50 mL THF at -78 °C. The solution was stirred for 4.5 h and the solvent was removed under vacuum. The addition of toluene and pentane (1:1) to the remaining oil and triturating removed brown solution. Single crystals were grown from a mixture of ethanol (50 %) and acetone (50 %) at -30 °C. (0.410 g, 30 %) and rinsed by toluene. <sup>1</sup>H NMR (THF-*d*<sub>8</sub>, 300 MHz, 298 K): δ 1.78 (m, 16H, MgOCH<sub>2</sub>CH<sub>2</sub>), 3.33 (d, 4H, *J* = 15.2 Hz, PCH<sub>2</sub>), 3.62 (m, 16H, MgOCH<sub>2</sub>CH<sub>2</sub>), 3.67 (dd, 4H, *J* = 7.0 Hz, PCH<sub>2</sub>), 6.63 (s, 8H, Ph *o*-H), 6.65 (s, 4H, Ph *p*-H). <sup>13</sup>C{<sup>1</sup>H} NMR (THF-*d*<sub>8</sub>, 300 MHz, 298 K): δ 26.4 (s, MgOCH<sub>2</sub>CH<sub>2</sub>), 41.6 (d, *J*<sub>PC</sub> = 20.8 Hz, PCH<sub>2</sub>), 43.0 (d, *J*<sub>PC</sub> = 18.5 Hz, PCH<sub>2</sub>), 103.0 (m, MgOCH<sub>2</sub>CH<sub>2</sub>), 120.1 and 123.7 (s, Ph *o*-C and *m*-C), 127.1 (s, Ph *p*-C), 132.3 (m, Ph C-F<sub>3</sub>), 160.6 (s, Ph *ipso*-C). <sup>31</sup>P{<sup>1</sup>H} NMR (THF-*d*<sub>8</sub>, 300 MHz, 298 K): δ -63.6 (s). <sup>19</sup>F{<sup>1</sup>H} NMR (THF-*d*<sub>8</sub>, 300 MHz, 298 K): δ 14.19 (s). Anal. Calc'd for C<sub>52</sub>H<sub>52</sub>F<sub>24</sub>Mg<sub>2</sub>N<sub>4</sub>O<sub>4</sub>P<sub>2</sub>: F.W. 1363.52; C, 45.80; H, 3.84; N, 4.11. Found: C, 45.85; H, 3.78; N, 3.93.

**<sup>n</sup>BuCH<sub>2</sub>N(H)-3,5-(CF<sub>3</sub>)<sub>2</sub>C<sub>6</sub>H<sub>3</sub> (28).** The toluene rinse was hydrolyzed with water.

The sample was extracted into C<sub>6</sub>D<sub>6</sub> and passed through a short plug of alumina.

Mass spectrum m/z: (<sup>18</sup>BuCH<sub>2</sub>NH-3,5-(CF<sub>3</sub>)<sub>2</sub>C<sub>6</sub>H<sub>3</sub>): 299.1 (100.0%), 300.1 (14.4%).

<sup>1</sup>H NMR (C<sub>6</sub>D<sub>6</sub>, 300 MHz, 298 K): δ 0.8 (t, 3H, CH<sub>2</sub>(CH<sub>2</sub>)<sub>3</sub>CH<sub>3</sub>), 1.4 (m, 6H, CH<sub>2</sub>(CH<sub>2</sub>)<sub>3</sub>CH<sub>3</sub>), 3.07 (m, 2H, NHCH<sub>2</sub>CH<sub>3</sub>), 4.8 (br, 1H, NH), 6.5 (s, 2H, Ph *o*-H), 6.7 (s, 1H, Ph *p*-H), consistent with <sup>18</sup>BuCH<sub>2</sub>NH-3,5-(CF<sub>3</sub>)<sub>2</sub>C<sub>6</sub>H<sub>3</sub>.

<sup>18</sup>BuSeSeH (30). Mass spectrum m/z: (<sup>18</sup>BuSe<sub>2</sub>H): 217.9(100.0%), 215.9(87.7%), 213.9(52.0%), 219.9(30.1%), 214.9(26.3%), 211.91(15.5%), 212.9(13.5%), 211.92(5.3%), 210.9(5.2%), 216.91(4.6%), 209.9(4.5%), 216.92(3.9%), 218.91(3.7%), 221.91(2.6%).

<sup>18</sup>BuSeSe<sup>18</sup>Bu (31). Mass spectrum m/z: (<sup>18</sup>Bu<sub>2</sub>Se<sub>2</sub>): 273.9(100.0%), 271.9(82.0%), 269.98(53.7%), 270.98(31.0%), 275.97(30.1%), 267.98(21.0%), 268.98(14.4%), 272.98(12.5%), 274.98(8.9%), 271.98(8.2%), 266.98(5.4%), 265.98(4.5%), 276.98(2.7%), 277.97(2.6%).

{P[CH<sub>2</sub>NH-3,5-(CF<sub>3</sub>)<sub>2</sub>C<sub>6</sub>H<sub>3</sub>]<sub>2</sub>Se<sub>2</sub>}<sup>+</sup>{HNEt<sub>3</sub>}<sup>-</sup> (35). Excess HNEt<sub>3</sub>Cl (635.4 mg, 3.6 mmol, 12 equiv) was added to a solution of P[CH<sub>2</sub>N-3,5-(CF<sub>3</sub>)<sub>2</sub>C<sub>6</sub>H<sub>3</sub>]<sub>2</sub>Se(AlMe<sub>2</sub>)<sub>3</sub> (232.5 mg, 0.3 mmol) in 50 mL toluene. The solid was filtered and the remaining pale yellow solution was collected, and then dried under vacuum. The white oily products were obtained. Single crystals were grown from a 1:1 mixture of toluene and pentane at -30 °C. <sup>1</sup>H NMR (C<sub>6</sub>D<sub>6</sub>, 300 MHz, 298 K): δ 0.80 (t, 9H, -CH<sub>2</sub>CH<sub>3</sub>), 2.38 (dd, 6H,

- $\underline{\text{CH}_2\text{CH}_3}$ ), 3.65 (t, 4H,  $J = 5.2$  Hz,  $\text{P}\underline{\text{CH}_2}$ ), 5.1 (b, 2H,  $\text{NH}$ ), 6.81 (s, 4H, Ph  $o$ - $\underline{\text{H}}$ ), 7.17 (s, 2H, Ph  $p$ - $\underline{\text{H}}$ ).  $^{13}\text{C}\{^1\text{H}\}$  NMR ( $\text{C}_6\text{D}_6$ , 300 MHz, 298 K):  $\delta$  8.71 (s,  $-\underline{\text{CH}_2\text{CH}_3}$ ), 46.7 (s,  $-\underline{\text{CH}_2\text{CH}_3}$ ), 50.8 (d,  $J_{\text{PC}} = 37.8$  Hz,  $\text{P}\underline{\text{CH}_2}$ ), 111.1, 123.7 and 127.1 (s, Ph  $o$ - $\underline{\text{C}}$   $m$ - $\underline{\text{C}}$  and  $p$ - $\underline{\text{C}}$ ) 133.1 (m, Ph  $\underline{\text{C}}\text{-F}_3$ ), 148.9 (d, Ph  $ipso$ - $\underline{\text{C}}$ ).  $^{31}\text{P}\{^1\text{H}\}$  NMR ( $\text{C}_6\text{D}_6$ , 300 MHz, 298 K):  $\delta$  30.12 (s,  $J_{\text{PSe}} = 615.9$  Hz).  $^{19}\text{F}\{^1\text{H}\}$  NMR ( $\text{C}_6\text{D}_6$ , 300 MHz, 298 K):  $\delta$  14.5 (s).

**$\{\text{P}[\underline{\text{CH}_2\text{N}}\text{-}3,5\text{-}(\text{CF}_3)_2\text{C}_6\text{H}_3]_2\}_2$  (36)**. Excess  $\text{HNEt}_3\text{Cl}$  (16.5 mg, 0.12 mmol, 6 equiv) was added to a solution of  $\{\text{P}[\underline{\text{CH}_2\text{N}}\text{-}3,5\text{-}(\text{CF}_3)_2\text{C}_6\text{H}_3]_2\text{MgTHF}_2\}_2$  (27.5 mg, 0.02 mmol) in 0.7 mL  $\text{THF-}d_8$ . The brown solution was obtained.  $^1\text{H}$  NMR ( $\text{THF-}d_8$ , 300 MHz, 298 K):  $\delta$  2.90 (m, 4H,  $J = 5.7$  Hz,  $\text{P}\underline{\text{CH}_2}$ ), 3.9 (m, 2H,  $-\text{NH}$ ), 7.12 (s, 4H, Ph  $o$ - $\underline{\text{H}}$ ), 7.16 (s, 4H, Ph  $p$ - $\underline{\text{H}}$ ).  $^{31}\text{P}\{^1\text{H}\}$  NMR ( $\text{THF-}d_8$ , 300 MHz, 298 K):  $\delta$  -46.9 (s).

**$\text{P}[\underline{\text{CH}_2\text{N}}\text{-}3,5\text{-}\text{Me}_2\text{C}_6\text{H}_3]_2\text{SeZrN}(\text{-}3,5\text{-}\text{Me}_2\text{C}_6\text{H}_3)\underline{\text{CH}_2\text{NEt}_2}$  (37b)**.  $\text{Zr}(\text{NEt}_2)_4$  (380 mg, 1 mmol) was added to a solution of  $\text{SeP}[\underline{\text{CH}_2\text{N}}\text{-}3,5\text{-}\text{Me}_2\text{C}_6\text{H}_3]_3\text{H}_3$  (509 mg, 1 mmol) in 50 mL of toluene. The solution was stirred for 2 h and stored at  $-40$  °C for several days. The compound precipitated as an orange crystalline solid (0.54g, 80%).  $^1\text{H}$  NMR ( $\text{C}_6\text{D}_6$ , 300 MHz, 298 K):  $\delta$  0.96(t,  $J = 7.2$  Hz, 6H), 2.06 (s, 6H), 2.08 (s, 12H), 2.40 (m, 2H), 2.60 (m, 2H), 3.78 (t,  $J = 11.3$  Hz, 2H), 4.01 (t,  $J = 12.7$  Hz, 2H), 4.58 (s, 2H), 6.23 (s, 3H), 6.51 (s, 2H), 6.65 (s, 4H).  $^{13}\text{C}\{^1\text{H}\}$  NMR ( $\text{C}_6\text{D}_6$ , 125.8 MHz, 298 K):  $\delta$  11.0 (s,  $\text{NCH}_2\text{CH}_3$ ),  $\delta$  22.0 (s,  $\text{Ph}\underline{\text{CH}_3}$ ), 44.4 (d,  $J_{\text{PC}} = 36.2$  Hz,  $\text{P}\underline{\text{CH}_2}$ ), 52.9 (s,  $\text{NCH}_2\text{CH}_3$ ), 69.9 (s), 113.8 (s), 114.6 (s), 122.3 (s), 122.6 (s), 138.6 (d,  $J =$

24.7 Hz), 149.0 (s), 152.2 (s).  $^{31}\text{P}\{^1\text{H}\}$  NMR ( $\text{C}_6\text{D}_6$ , 121.5 MHz, 298 K):  $\delta$  -92.9 (s with satellites,  $J_{\text{PSe}} = 253.9$  Hz.).  $^{77}\text{Se}\{^1\text{H}\}$  NMR ( $\text{C}_6\text{D}_6$ , 57.2 MHz, 298 K) :  $\delta$  88.6 (d,  $J_{\text{PSe}} = 254.3$  Hz). Anal. Calc'd for  $\text{C}_{31}\text{H}_{43}\text{N}_4\text{PSeZr}$ : F.W.: 672.86; C, 55.34; H, 6.44; N, 8.33. Found: C, 55.80; H, 6.52; N, 7.93.

**$\text{P}[\text{CH}_2\text{NPh}]_2\text{SeZrNPhCH}_2\text{NEt}_2$  (37c).**  $\text{Zr}(\text{NEt}_2)_4$  (0.380g, 1mmol) was added to a solution of  $\text{Se}[\text{CH}_2\text{NPh}]_3\text{H}_3$  (0.43 g, 1 mmol) in 50 mL of toluene. The solution was stirred for 2 h and the solvent was removed under vacuum. The remaining yellow solid was rinsed with a small portion of pentane, and then dried under vacuum (0.53 g, 89%).  $^1\text{H}$  NMR ( $\text{C}_6\text{D}_6$ , 300 MHz, 298 K):  $\delta$  0.844 (t,  $J = 7.2$  Hz, 6H), 2.36 (m, 2H), 2.51 (m, 2H), 3.71 (t,  $J = 11.2$  Hz, 2H), 4.00 (t,  $J = 12.8$  Hz, 2H), 4.51 (s, 2H), 6.70 (m, 5H), 6.88 (d,  $J = 8.0$  Hz, 4H), 7.0 (m, 6H).  $^{13}\text{C}\{^1\text{H}\}$  NMR ( $\text{C}_6\text{D}_6$ , 125.8 MHz, 298 K):  $\delta$  10.7 (s,  $\text{NCH}_2\text{CH}_3$ ), 44.2 (d,  $J_{\text{PC}} = 36.2$  Hz,  $\text{PCH}_2$ ), 52.2 (s,  $\text{NCH}_2\text{CH}_3$ ), 69.4 (s), 115.5 (s), 116.2 (s), 120.4 (s), 120.9 (s), 129.5 (s), 129.7 (s), 148.6 (s), 152.1 (s).  $^{31}\text{P}\{^1\text{H}\}$  NMR ( $\text{C}_6\text{D}_6$ , 121.5 MHz, 298 K):  $\delta$  -93.6 (s with satellites,  $J_{\text{PSe}} = 256.2$  Hz.).  $^{77}\text{Se}\{^1\text{H}\}$  NMR ( $\text{C}_6\text{D}_6$ , 121.5 MHz, 298 K):  $\delta$  -90.8 (d,  $J_{\text{PSe}} = 256.7$  Hz). Anal. Calc'd for  $\text{C}_{25}\text{H}_{31}\text{N}_4\text{P}$ : F.W.: 588.70; C, 51.01; H, 5.31; N, 9.52. Found: C, 51.14; H, 5.63; N, 9.38.

## 5.6.3 Crystal Data and Structure Refinement

Table 5.1. Crystallographic data for compounds 27, 35 and 37c

	27	35	37c
Empirical formula	C <sub>52</sub> H <sub>52</sub> F <sub>24</sub> Mg <sub>2</sub> N <sub>4</sub> O <sub>4</sub> P <sub>2</sub>	C <sub>33</sub> H <sub>42</sub> F <sub>12</sub> N <sub>3</sub> PSe <sub>2</sub>	C <sub>34.5</sub> H <sub>47</sub> N <sub>4</sub> PSeZr
Formula weight	1363.54	845.61	718.91
Temperature	253(2) K	173(2) K	173(2) K
Crystal system	Triclinic	Monoclinic	Orthorhombic
a	11.025(2) Å	13.875(3) Å	11.816(5) Å
b	12.542(2) Å	28.958(7) Å	15.950(6) Å
c	12.674(2) Å	18.386(5) Å	37.747(15) Å
α	62.374(2)°	90°	90°
β	82.161(2)°	96.046(3)°	90°
γ	77.708(2)°	90°	90°
Volume Å <sup>3</sup>	1515.6(5)	7346(3)	7114(5)
Z	1	8	8
Density (calculated)	1.494 mg/m <sup>3</sup>	1.529 mg/m <sup>3</sup>	1.342 mg/m <sup>3</sup>
Absorption coefficient	0.213 mm <sup>-1</sup>	1.180 mm <sup>-1</sup>	0.455 mm <sup>-1</sup>
No. Variables	397	365	551
Crystal size mm <sup>3</sup>	0.40 x 0.40 x 0.38	0.20 x 0.20 x 0.20	0.40 x 0.40 x 0.20
Total No. of Reflins	14155	30565	65696
No. of Unique Reflins	5314 ( <i>R</i> <sub>int</sub> = 0.0429)	6822 ( <i>R</i> <sub>int</sub> = 0.1587)	8151 ( <i>R</i> <sub>int</sub> = 0.066)

## 5.7 References

- (1) Tsutomu, M.; Satoru, K.; Katsuhiko, M. *J. Organomet. Chem.* **2004**, *689*, 2624-2632.
- (2) Puddephatt, R. *J. Chem. Soc. Rev.* **1983**, *12*, 99 - 127.
- (3) Wheatley, N.; Kalck, P. *Chem. Rev.* **1999**, *99*, 3379-3420.
- (4) Hatnean, J. A.; Raturi, R.; Lefebvre, J.; Leznoff, D. B.; Lawes, G.; Johnson, S. A. *J. Am. Chem. Soc.* **2006**, *128*
- (5) Graiff, C.; Predieri, G.; Tiripicchio, A. *Eur. J. Inorg. Chem.* **2003**, 1659-1668.
- (6) Belletti, D.; Graiff, C.; Massera, C.; Predieri, G.; Tiripicchio, A. *Inorg. Chim. Acta* **2003**, *350*, 421-427.
- (7) Fryzuk, M. D.; Kozak, C. M.; Bowdridge, M. R.; Jin, W.; Tung, D.; Patrick, B. O.; Rettig, S. J. *Organometallics* **2001**, *20*, 3752-3761.
- (8) Tang, Y.; Zakharov, L. N.; Rheingold, A. L.; Kemp, R. A. *Organometallics* **2005**, *24*, 836-841.
- (9) Sebestl, J. L.; Nadasdi, T. T.; Heeg, M. J.; Winter, C. H. *Inorg. Chem.* **1998**, *37*, 1289-1294.
- (10) Vargas, W.; Englich, U.; Ruhlandt-Senge, K. *Inorg. Chem.* **2002**, *41*, 5602-5608.
- (11) Heyn, R. H.; Goerbitz, C. H. *Organometallics* **2002**, *21*, 2781-2784.
- (12) Magistrato, A.; Merlin, M.; Pregosin, P. S.; Rothlisberger, U.; Albinati, A. *Organometallics* **2000**, *19*, 3591-3596.
- (13) Magistrato, A.; Pregosin, P. S.; Albinati, A.; Rothlisberger, U. *Organometallics* **2001**, *20*, 4178-4184.

- (14) Gindelberger, D. E.; Arnold, J. *Inorg. Chem.* **1994**, *33*, 6293-6299.
- (15) Becker, G.; Golla, W.; Grobe, J.; Klinkhammer, K. W.; Le Van, D.; Maulitz, A. H.; Mundt, O.; Oberhammer, H.; Sachs, M. *Inorg. Chem.* **1999**, *38*, 1099-1107.
- (16) Krief, A.; Van Wemmel, T.; Redon, M.; Dumont, W.; Delmotte, C. *Angew. Chem. Int. Ed.* **1999**, *38*, 2245-2247.
- (17) Krief, A.; Dumont, W.; Delmotte, C. *Angew. Chem. Int. Ed.* **2000**, *39*, 1669-1672.
- (18) Krief, A.; Delmotte, C.; Dumont, W. *Tetrahedron* **1997**, *53*, 12147-12158.
- (19) Anderson, J. A.; Odom, J. D.; Zozulin, A. J. *Organometallics* **1984**, *3*, 1458-65.
- (20) Anderson, J. A.; Odom, J. D. *Organometallics* **1988**, *7*, 267-71.
- (21) Davies, R. P.; Martinelli, M. G. *Inorg. Chem.* **2002**, *41*, 348-352.
- (22) Jeon, Y.-M.; Heo, J.; Lee, W. M.; Chang, T.; Kim, K. *Organometallics* **1999**, *18*, 4107-4113.
- (23) Howard, W. A.; Trnka, T. M.; Parkin, G. *Inorg. Chem.* **1995**, *34*, 5900-9.
- (24) Howard, W. A.; Parkin, G. *J. Am. Chem. Soc.* **1994**, *116*, 606-15.
- (25) Pangborn, A. B.; Giardello, M. A.; Grubbs, R. H.; Rosen, R. K.; Timmers, F. J. *Organometallics* **1996**, *15*, 1518-20.

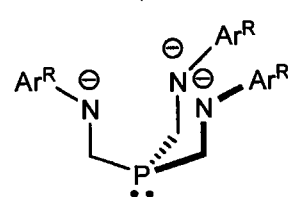
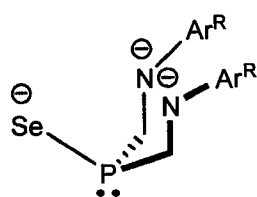
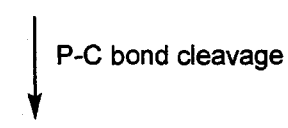
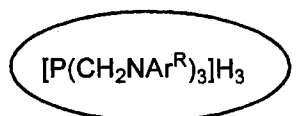
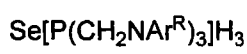
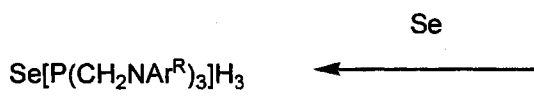
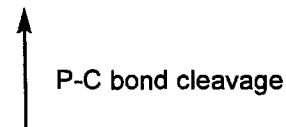
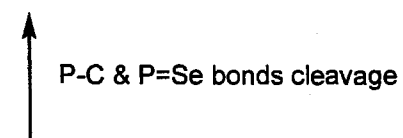
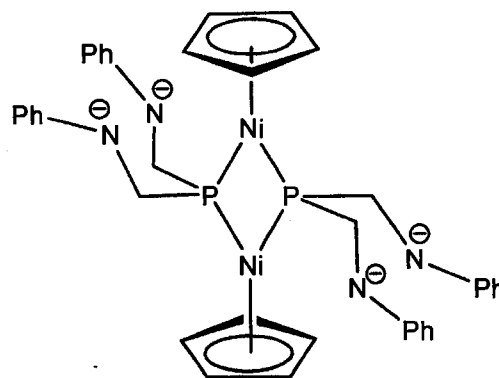
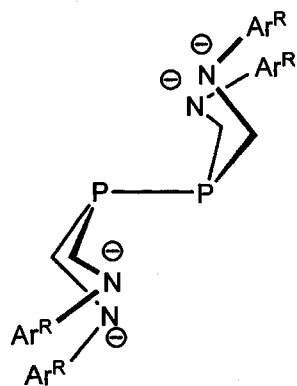
## Chapter 6

### Summary and Future Work

#### 6.1 Summary

This thesis begins with the tripodal amido ligands  $[P(CH_2NHA r^R)_3]$  for mononuclear early transition metal complexes, where  $Ar^R = 3,5-(CF_3)_2C_6H_3$ , Ph, and 3,5-Me<sub>2</sub>C<sub>6</sub>H<sub>3</sub>. These ligands are used to synthesize early-late polynuclear or heterobimetallic complexes, as well as the bridged binuclear complexes. Based on these tripodal amido ligands  $[P(CH_2NHA r^R)_3]$ , the ligands  $Se=P(CH_2NHA r^R)_3$  are designed to prepare polynuclear complexes, which provide the unanticipated diamidoselenophosphinito ligands by the cleavage of P-C bonds, as shown in Scheme 6.1. By the cleavage of the P-C bond and the P=Se bond, a diamido bisphosphine ligand with a stable P-P bond is synthesized.<sup>1,2</sup> A Ni(II) dimer with a bridging diamido-phosphido ligand is prepared by the cleavage of the P-C bond in the phosphine ligand  $[P(CH_2NHPh)_3]$ , which was used as a ligand to give early-late transition tetranuclear heterometallic complexes.

Scheme 6.1

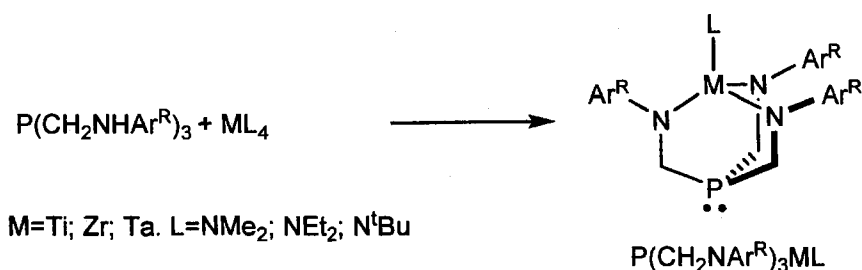


Ligands used in the thesis:

$[\text{PNNN}]^{3-}$ ;  $[\text{PNNSe}]^{3-}$ ;  $[\text{Ar}^{\text{R}}\text{NP-PNAr}^{\text{R}}]^{4-}$ ;  $[\text{CpNiP}(\text{CH}_2\text{NPh})_2]^{4-}$

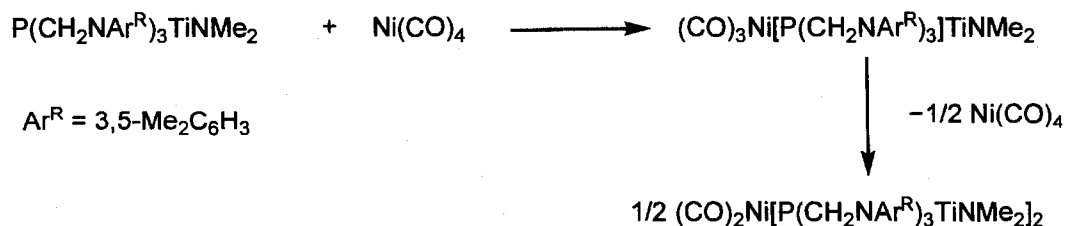
The reactions of the ligand precursors  $P(\text{CH}_2\text{NHA}r^R)_3$  with  $\text{ML}_4$  ( $M = \text{Ti}; \text{Zr}; \text{Ta}$ ) produce the mononuclear early transition metal complexes  $P(\text{CH}_2\text{NA}r^R)_3\text{ML}$ .<sup>2</sup> The ligands  $P(\text{CH}_2\text{NHA}r^R)_3$  chelate metal centres via three amido donors, and the lone-pair of the phosphine donor is directed away from the metal centres.<sup>1</sup>

### Scheme 6.2



These mononuclear early transition metal complexes  $P(\text{CH}_2\text{NA}r^R)_3\text{ML}$  can be used to prepare the early-late heterobimetallic and polynuclear complexes. The mononuclear titanium compound  $P(\text{CH}_2\text{NA}r^R)_3\text{TiNMe}_2$  ( $\text{Ar}^R = 3,5\text{-Me}_2\text{C}_6\text{H}_3$ ) reacts instantaneously with excess  $\text{Ni}(\text{CO})_4$  to afford an early-late heterobimetallic complex  $(\text{CO})_3\text{Ni}[P(\text{CH}_2\text{NA}r^R)_3\text{TiNMe}_2]$ , which is not stable at room temperature, and solutions undergo ligand redistribution over the course of 48 h to form a stable trinuclear early-late transition metal complex  $(\text{CO})_2\text{Ni}[P(\text{CH}_2\text{NA}r^R)_3\text{TiNMe}_2]_2$ , as shown in Scheme 6.3.<sup>2</sup>

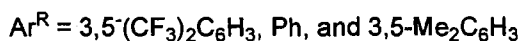
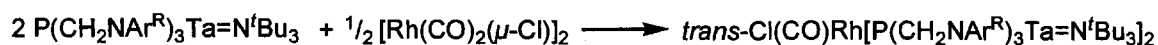
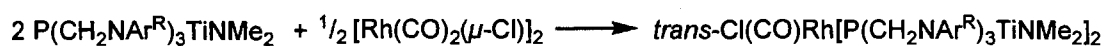
### Scheme 6.3



The reactions of 4 equiv of mononuclear early transition metal complexes  $P(\text{CH}_2\text{NA}r^R)_3\text{ML}$  with  $[\text{Rh}(\text{CO})_2(\mu\text{-Cl})]_2$  allow for the facile preparation of trinuclear

*trans*-rhodiumcarbonylchlorobisphosphine complexes, where  $\text{Ar}^{\text{R}} = 3,5\text{-(CF}_3)_2\text{C}_6\text{H}_3$ , Ph, and  $3,5\text{-Me}_2\text{C}_6\text{H}_3$ , as shown in Scheme 6.4.<sup>2</sup> The early transition metal centre affects the property of the phosphine donor in the heterometallic complexes, despite the fact that the phosphine lone-pair is not coordinated to the metal center. Although the lone pair of the phosphine donor is aimed away from early transition metal centres, the donor abilities of phosphines are affected by the direct interactions between the early transition metals and the phosphine donor.

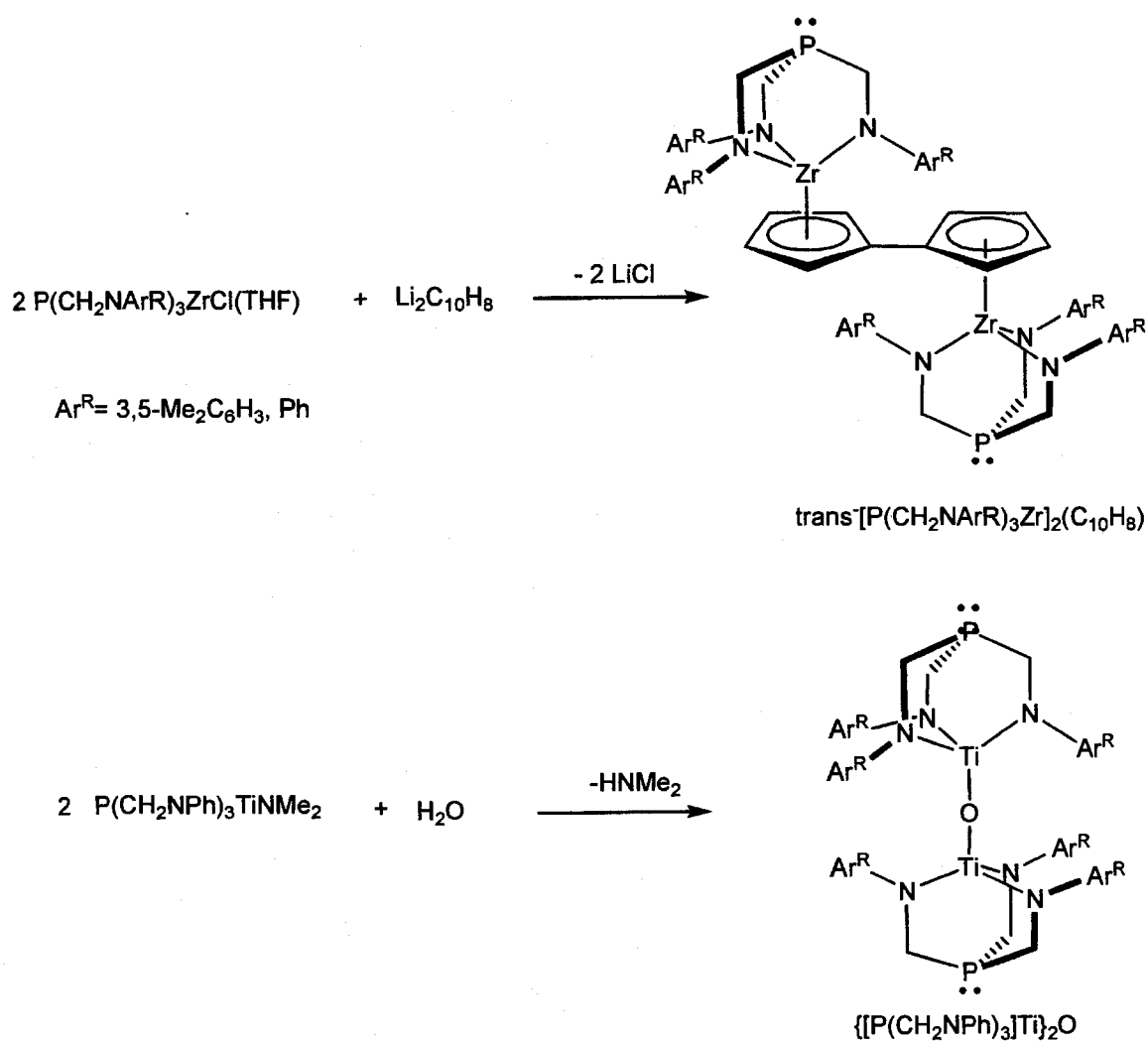
#### Scheme 6.4



In this thesis, the ligands  $\text{P}(\text{CH}_2\text{NHAr}^{\text{R}})_3$  have been demonstrated to stabilize the mononuclear early transition metal complexes to be suited for the bridged early transition homobimetallic complexes, which provide a facile route to linear rigid metal-containing polymers. Due to ring strain, the phosphine lone-pair cannot chelate to early transition metal centers, but there are through-space interactions between them. With suitable building-blocks, the interactions could be used to create 1-D wires, or 2-D or 3-D networks with properties that result from through-space exchange-coupling, or through-space electron-transfer. The reactions of the lithium salts of the fulvalene dianion

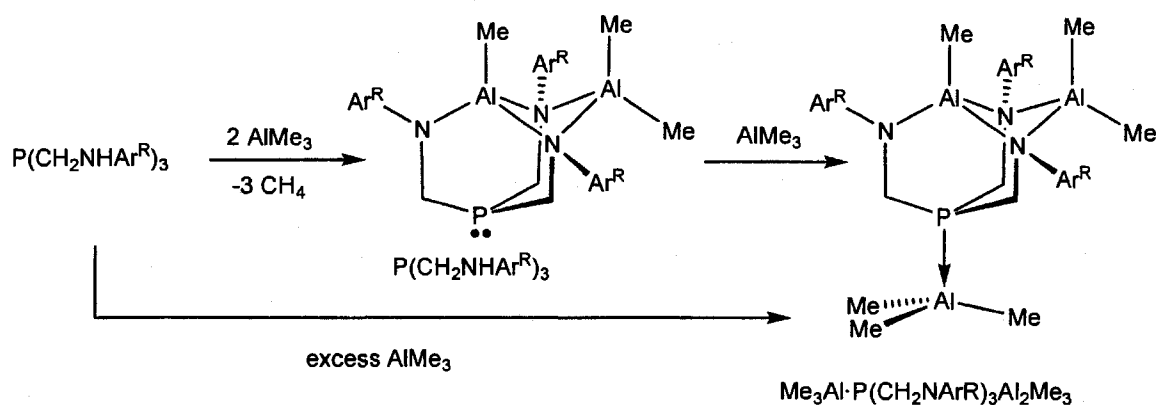
( $\text{Li}_2\text{C}_{10}\text{H}_8$ ) with the zirconium chloride complexes  $\text{P}[\text{CH}_2\text{NAr}^{\text{R}}]_3\text{ZrCl}(\text{THF})$  produce the binuclear complexes *trans*- $[\text{P}(\text{CH}_2\text{NAr}^{\text{R}})_3\text{Zr}]_2(\eta^5:\eta^5\text{-C}_{10}\text{H}_8)$ , as shown in Scheme 6.5, where  $\text{Ar}^{\text{R}} = \text{Ph}$  and 3,5- $\text{Me}_2\text{C}_6\text{H}_3$ . The binuclear titanium complex  $\{[\text{P}(\text{CH}_2\text{NPh})_3]\text{Ti}\}_2(\mu\text{-O})$  can be prepared from  $[\text{P}(\text{CH}_2\text{NAr}^{\text{R}})_3]\text{TiNMe}_2$ .

Scheme 6.5



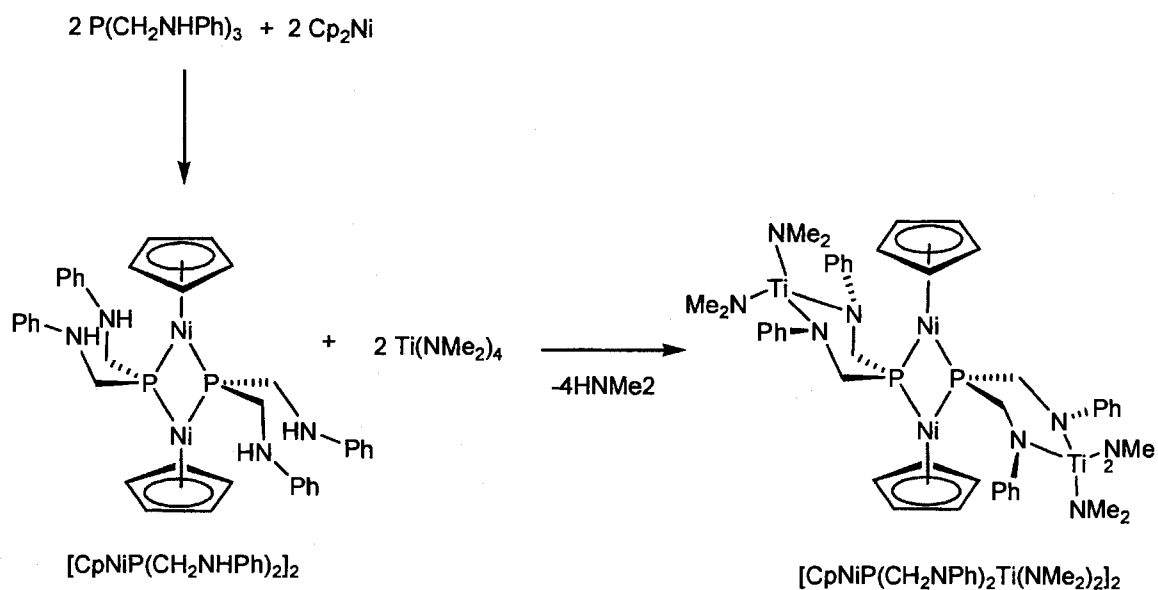
The reactions of  $P(\text{CH}_2\text{NAr}^R)_3$  with 2 equiv of  $\text{AlMe}_3$  produce the dinuclear aluminum complexes  $P(\text{CH}_2\text{NAr}^R)_3\text{Al}_2\text{Me}_3$ , where  $\text{Ar}^R = 3,5\text{-(CF}_3)_2\text{C}_6\text{H}_3$ , Ph, and 3,5- $\text{Me}_2\text{C}_6\text{H}_3$ , which react with excess  $\text{AlMe}_3$  to produce the Lewis acid-base adducts  $\text{Me}_3\text{Al}\cdot P(\text{CH}_2\text{NAr}^R)_3\text{Al}_2\text{Me}_3$ .

Scheme 6.6



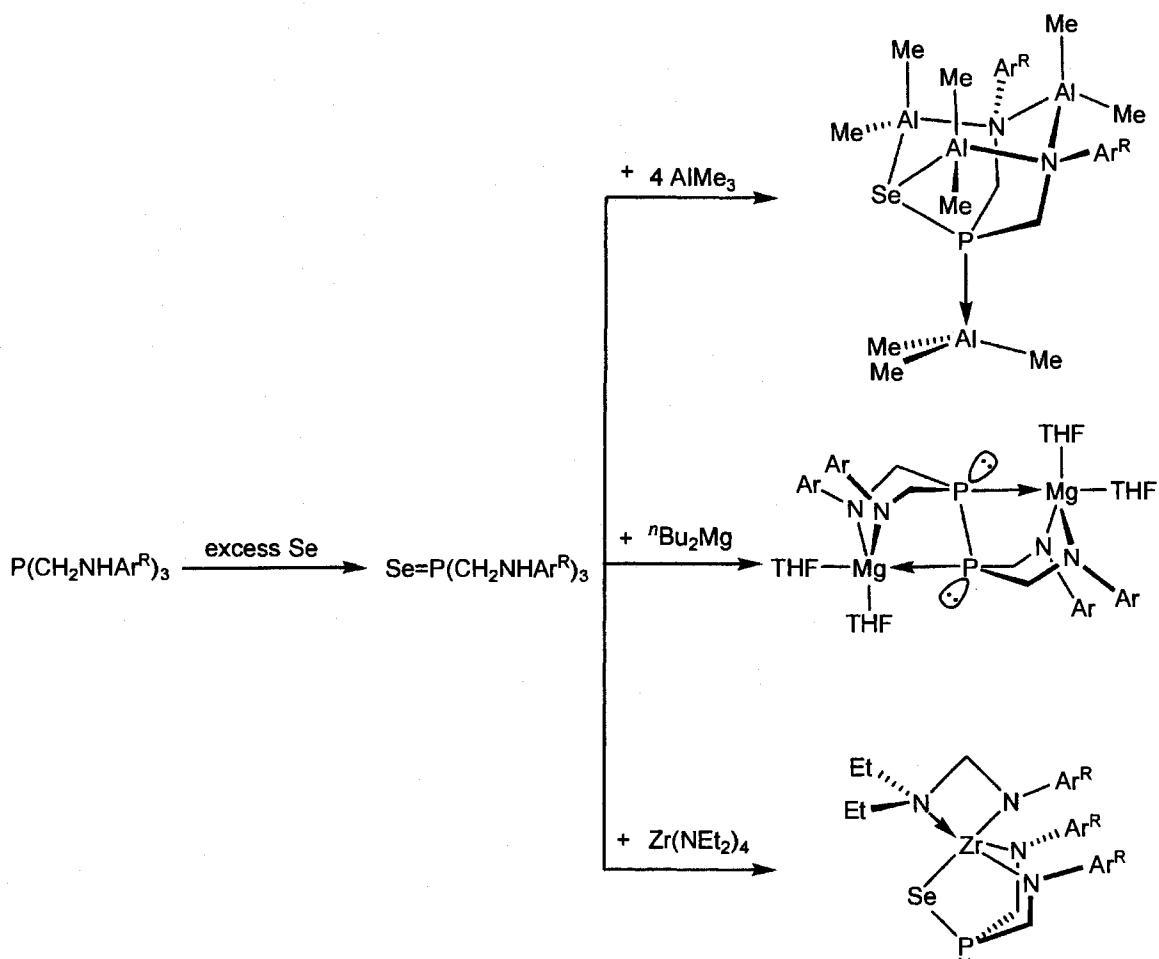
The reaction of phosphine ligand  $[P(\text{CH}_2\text{NHPH})_3]$  and 2 equiv of nickelocene,  $\text{Cp}_2\text{Ni}$ , occurs with cleavage of the P-C bond under mild conditions, which provides access to the phosphido-bridged Ni(II) dimer complex and allows the achievement of the favored 18-electron complex when the resulting  $-P[\text{CH}_2\text{NHPH}]_2$  ligand is considered to act as a three electron donor. The Ni dimer readily binds titanium metal centers using amido donors, which leads to the facile synthesis of an early-late tetranuclear heterometallic complex  $[\text{CpNiP}(\text{CH}_2\text{NPh})_2\text{Ti}(\text{NMe}_2)_2]_2$ , as shown in Scheme 6.7. The binding of Ti metal center to the amido donors has a slight effect on the Ni metal center in the Ni(II) dimer  $[\text{CpNiP}(\text{CH}_2\text{NHPH})_2]_2$ .

## Scheme 6.7



Phosphine selenides  $\text{SeP}(\text{CH}_2\text{NHAr}^{\text{R}})_3$  can be prepared by the treatments of the ligands  $\text{P}(\text{CH}_2\text{NHAr}^{\text{R}})_3$  with excess elemental selenium, as shown in Scheme 7.8.<sup>2</sup> Ligands  $\text{Se}[\text{P}(\text{CH}_2\text{NHAr}^{\text{R}})_3]$  are efficiently reduced to P(III) centres that stabilize main group and early transition metal centers to produce polynuclear, binuclear or mononuclear metal complexes.

## Scheme 6.8



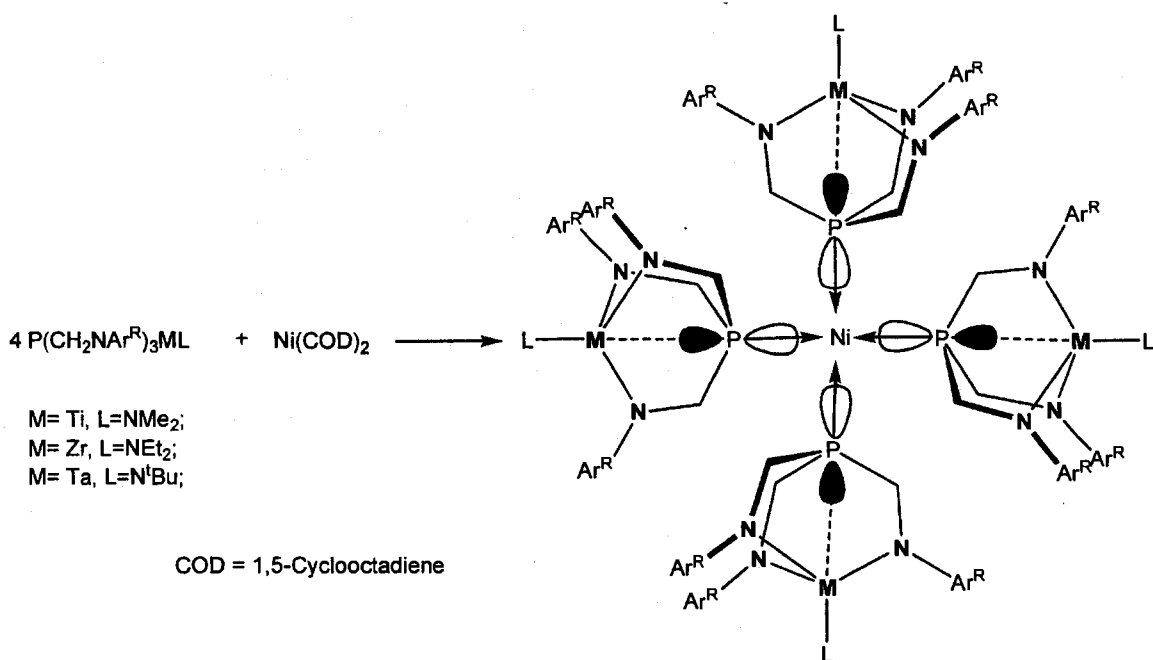
## 6.2 Future work

### 6.2.1 Further Study of the Mononuclear Early Transition Metal Complexes as Building Blocks for Clusters or Polymer Synthesis

This chapter describes some reactions that may yield new chemistry based on the tripodal amido ligands, and provides clues to fulfill the long-term goals of our research, which are to develop the synthetic methodology to prepare polynuclear clusters and assemblies of metals with specific molecular properties including magnetic interactions and novel catalytic reactivities.<sup>3-14</sup>

The mononuclear early transition metal complexes with ligands  $P(\text{CH}_2\text{NHAr}^R)_3$  have been demonstrated to be ideal starting materials to synthesize clusters.<sup>15-18</sup> For example, the reactions of  $P[\text{CH}_2\text{NAr}^R]_3\text{TiNMe}_2$  with  $\text{Ni}(\text{COD})_2$  [COD = 1,5-cyclooctadiene] provide the cluster of  $\text{Ni}\{P[\text{CH}_2\text{NAr}^R]_3\text{TiNMe}_2\}_4$ , as shown in Scheme 6.9. Some initial experimental results are reported here without elemental analysis.

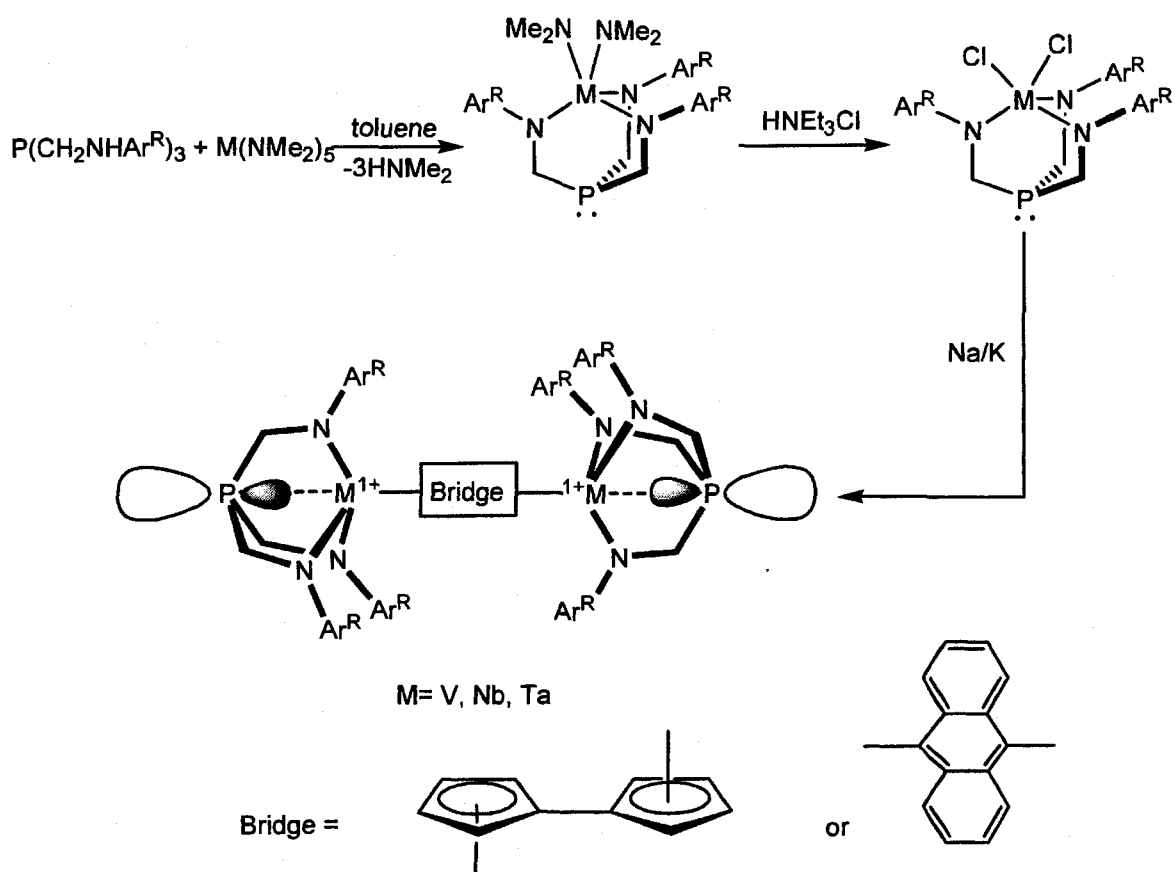
Scheme 6.9



The ligand precursors  $P(\text{CH}_2\text{NHAr}^R)_3$  are expected to react with group-5 transition metal centers to form the mononuclear complexes type  $P(\text{CH}_2\text{NAr}^R)_3\text{MCl}_2$ , which may be reduced into paramagnetic  $d^1$  transition metal complexes, as shown in Scheme 6.10. The phosphine lone-pair will not be coordinated to the metal centers, but affected by through-space interaction between phosphine donor and metal centers. With suitable bridges, the mononuclear paramagnetic  $d^1$  transition metal complexes may be used to make bridged

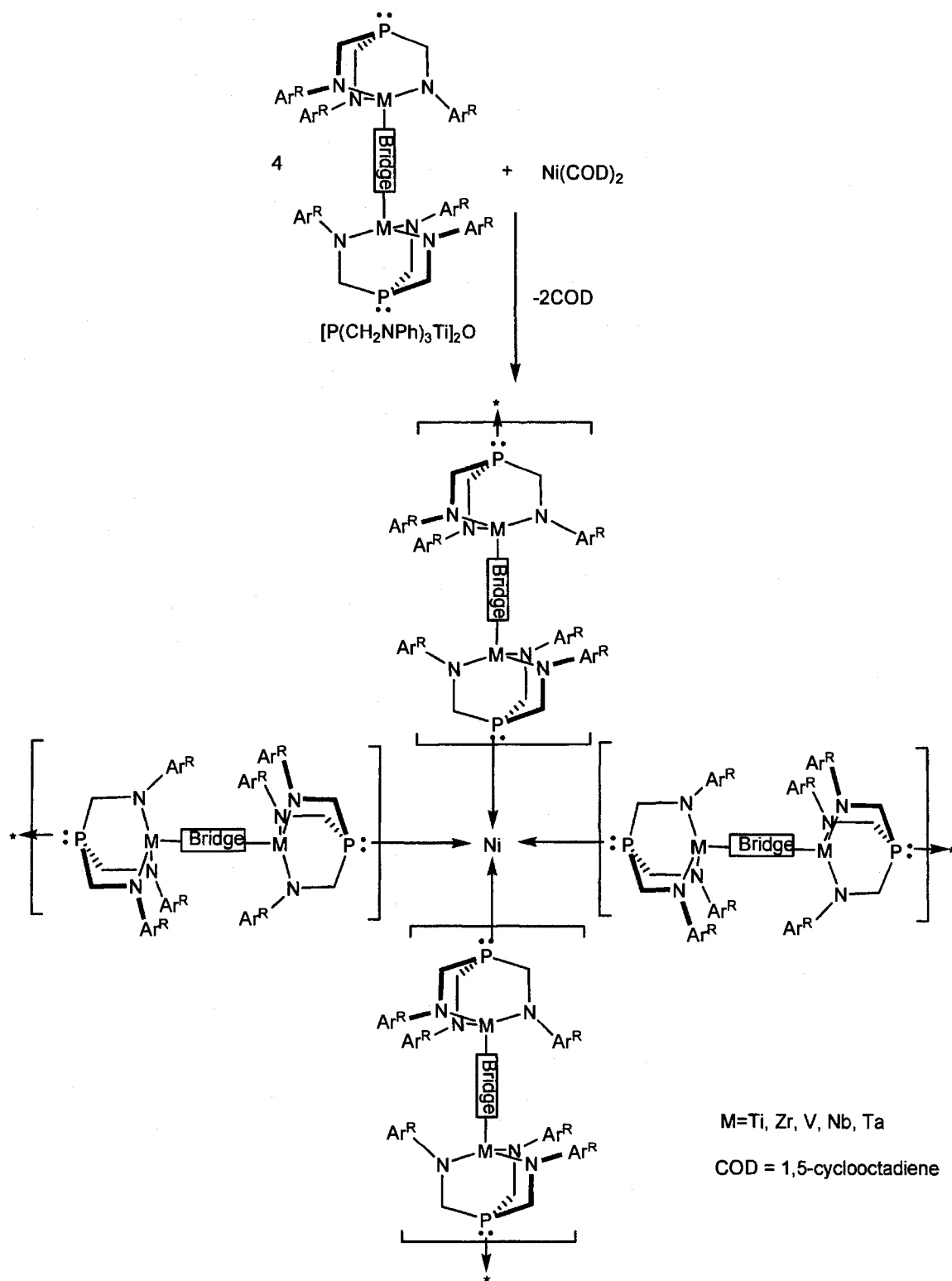
binuclear complexes. The bridges could be fulvalene or anthracene ligands. These paramagnetic bridged binuclear complexes could be utilized to create paramagnetic 1-D wires, or 2-D or 3-D networks that could have the properties resulting from through-space exchange-coupling, or through-space electron-transfer.

Scheme 6.10



Both the paramagnetic and diamagnetic bridging binuclear complexes should provide a facile route to the polymeric materials that contain early transition metals along the main polymer chains, as shown in Scheme 6.11.<sup>19-24</sup>

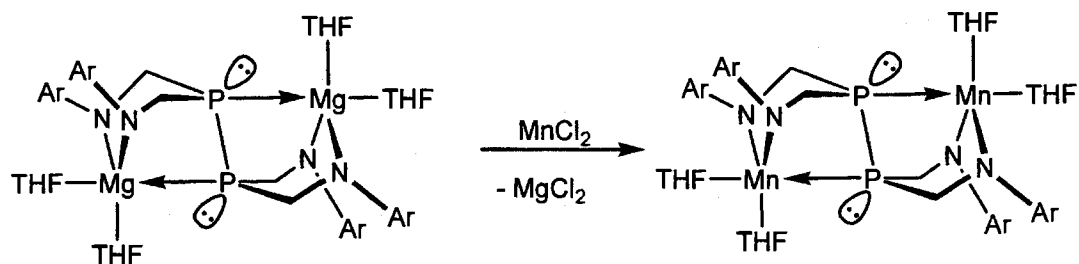
Scheme 6.11



### 6.2.2 Further Study of $\text{Se}=\text{P}(\text{CH}_2\text{NHA}r^R)_3$ and the Ni(II) Dimer as the Ligands

The ligands  $\text{Se}=\text{P}(\text{CH}_2\text{NHA}r^R)_3$  are demonstrated to be well suited for the facile synthesis of polynuclear or binuclear main group metal complexes.<sup>25-32</sup> The ligands  $\text{Se}=\text{P}(\text{CH}_2\text{NHA}r^R)_3$  may react with other metal complexes to afford the polynuclear complexes with magnetic interactions. For example, the reaction of  $\{\text{P}[\text{CH}_2\text{N}-3,5-(\text{CF}_3)_2\text{C}_6\text{H}_3]_2\text{MgTHF}_2\}_2$  (27) with  $\text{MnCl}_2$  may provide the binuclear magnesium complex bridged by a bisphosphine ligand.

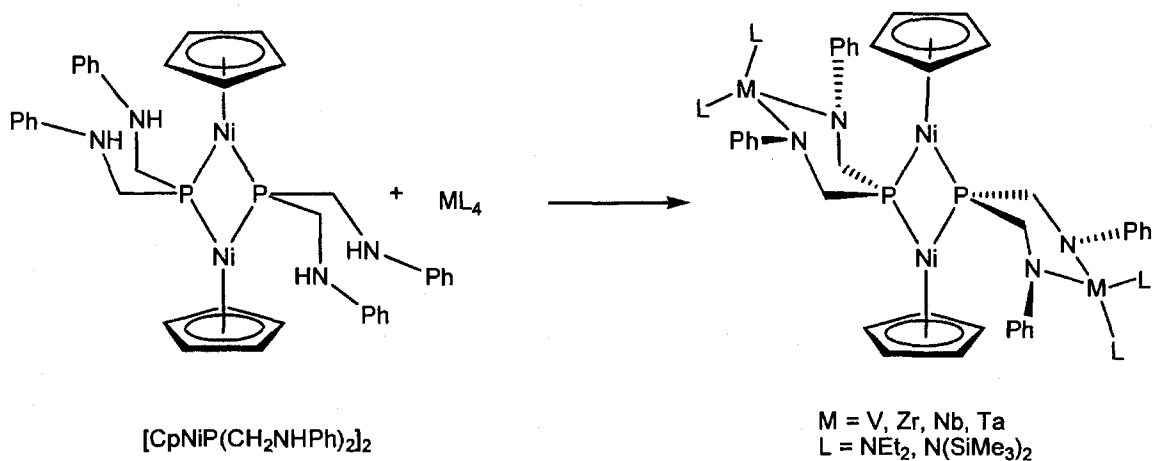
**Scheme 6.12**



The Ni(II) dimer  $[\text{CpNiP}(\text{CH}_2\text{NHPH})_2]_2$  can bind the titanium metal center using amido donors to allow for the synthesis of the early-late tetranuclear heterometallic complex  $[\text{CpNiP}(\text{CH}_2\text{NPh})_2\text{Ti}(\text{NMe}_2)_2]_2$ .<sup>33-36</sup> However, many aspects of the study of the Ni(II) dimer  $[\text{CpNiP}(\text{CH}_2\text{NHPH})_2]_2$  as a ligand and the communication between different metal centers remain unstudied.<sup>37,38</sup> In particular, only the Ti-Ni tetranuclear heterometallic complex was performed. It is necessary to study the reactions of the Ni(II) dimer  $[\text{CpNiP}(\text{CH}_2\text{NHPH})_2]_2$  with other transition metal complexes and the

communication between metal centers, including the lanthanides with unique chemical and magnetic properties.

**Scheme 6.13**



## 6.3 Experimental

### 6.3.1 General procedures

Unless otherwise stated, general procedures were performed according to Section 2.11.1.

### 6.3.2 Synthesis and Characterization of Complexes

$Ni[P(CH_2N-3,5-CF_3C_6H_3)_3TiNMe_2]_4$ .  $P(CH_2N-3,5-CF_3C_6H_3)_3TiNMe_2$  (170 mg, 0.2 mmol) was added to a solution of  $Ni(COD)_2$  (13.8 mg, 0.05mmol) in 30 mL of toluene.

The dark red solution was stirred 5 h. The solvent was removed under vacuum and the remaining yellow solid was rinsed with a small portion of pentane, and then dried under vacuum (136 mg, 80 %).  $^1\text{H}$  NMR ( $\text{C}_6\text{D}_6$ , 300 MHz, 298 K):  $\delta$  2.77 (s, 3H,  $\text{NCH}_3$ ), 4.56 (s, 6H,  $\text{PCH}_2$ ), 7.03 (s, 6H, Ph *o-H*), 7.27 (s, 3H, Ph *p-H*).  $^{13}\text{C}\{^1\text{H}\}$  NMR ( $\text{C}_6\text{D}_6$ , 125.8 MHz, 298 K):  $\delta$  42.6 (s,  $\text{TiNCH}_3$ ), 56.4 (p,  $J_{\text{PC}} = 8.8$  Hz,  $\text{PCH}_2$ ), 116.2 and 125.6 (s, Ph *o-C* and *m-C*), 122.0 (s, Ph *p-C*), 134.0 (q,  $J = 33.2$  Hz,  $\text{PhC-F}_3$ ), 152.9 (d, *ipso-C*).  $^{31}\text{P}\{^1\text{H}\}$  NMR ( $\text{C}_6\text{D}_6$ , 121.5 MHz, 298 K):  $\delta$  5.2 (s).  $^{19}\text{F}\{^1\text{H}\}$  NMR ( $\text{C}_6\text{D}_6$ , 282.1 MHz, 298 K):  $\delta$  14.07 (s).

**$\text{Ni}[\text{P}(\text{CH}_2\text{N-3,5-Me}_2\text{C}_6\text{H}_3)_3\text{TiNMe}_2]_4$ .**  $\text{P}(\text{CH}_2\text{N-3,5-Me}_2\text{C}_6\text{H}_3)_3\text{TiNMe}_2$  (105 mg, 0.2 mmol) was added to a solution of  $\text{Ni}(\text{COD})_2$  (13.8 mg, 0.05 mmol) in 30 mL of toluene. The dark red solution was stirred 5 h. The solvent was removed under vacuum and the remaining yellow solid was rinsed with a small portion of pentane, and then dried under vacuum (95 mg, 90 %).  $^1\text{H}$  NMR ( $\text{C}_6\text{D}_6$ , 300 MHz, 298 K):  $\delta$  2.10 (s, 18H,  $\text{PhCH}_3$ ), 3.11 (s, 6H,  $\text{NCH}_3$ ), 4.77 (s, 6H,  $\text{PCH}_2$ ), 6.49 (s, 6H, Ph *o-H*), 6.54 (s, 3H, Ph *p-H*).  $^{13}\text{C}\{^1\text{H}\}$  NMR ( $\text{C}_6\text{D}_6$ , 125.8 MHz, 298 K):  $\delta$  22.0 (s,  $\text{PhCH}_3$ ), 43.1 (s,  $\text{ZrNCH}_3$ ), 57.2 (p,  $J_{\text{PC}} = 8.2$  Hz,  $\text{PCH}_2$ ), 116.0 and 123.1 (s, Ph *o-C* and *m-C*), 138.9 (s, Ph *p-C*), 154.1 (d, *ipso-C*).  $^{31}\text{P}\{^1\text{H}\}$  NMR ( $\text{C}_6\text{D}_6$ , 121.5 MHz, 298 K):  $\delta$  9.20 (s).

**$\text{Ni}[\text{P}(\text{CH}_2\text{N-3,5-Me}_2\text{C}_6\text{H}_3)_3\text{ZrNEt}_2]_4$ .**  $\text{P}[\text{CH}_2\text{N-3,5-Me}_2\text{C}_6\text{H}_3]_3\text{ZrNEt}_2$  (1.19 g, 2.0 mmol) was added to a solution of  $\text{Ni}(\text{COD})_2$  (138 mg, 0.5 mmol) in 30 mL of toluene. The pale yellow solution was stirred 5 h. The solvent was removed under vacuum and the remaining yellow solid was rinsed with a small portion of pentane, and then dried under

vacuum (1.00 g, 83 %).  $^1\text{H}$  NMR ( $\text{C}_6\text{D}_6$ , 300 MHz, 298 K):  $\delta$  1.04 (t,  $^3J = 7.0$  Hz, 6H,  $\text{NCH}_2\text{CH}_3$ ), 2.05 (s, 18H,  $\text{PhCH}_3$ ), 3.34 (q, 4H,  $^3J = 7.0$  Hz,  $\text{NCH}_2\text{CH}_3$ ), 4.91 (s, 6H,  $\text{PCH}_2$ ), 6.44 (s, 6H, Ph *o-H*), 6.60 (s, 3H, Ph *p-H*).  $^{13}\text{C}\{^1\text{H}\}$  NMR ( $\text{C}_6\text{D}_6$ , 125.8 MHz, 298 K):  $\delta$  14.7 (s,  $\text{NCH}_2\text{CH}_3$ ), 21.9 (s,  $\text{PhCH}_3$ ), 42.3 (s,  $\text{ZrNCH}_2\text{CH}_3$ ), 55.3 (d,  $J_{\text{PC}} = 8.8$  Hz,  $\text{PCH}_2$ ), 115.7 and 122.6 (s, Ph *o-C* and *m-C*), 138.9 (s, Ph *p-C*), 153.4 (d, *ipso-C*).  $^{31}\text{P}\{^1\text{H}\}$  NMR ( $\text{C}_6\text{D}_6$ , 121.5 MHz, 298 K):  $\delta$  -7.57 (s).

$\text{Ni}[\text{P}(\text{CH}_2\text{NPh})_3\text{ZrNEt}_2]_4$ .  $\text{P}(\text{CH}_2\text{NPh})_3\text{ZrNEt}_2$  (1.17 g, 2.0 mmol) was added to a solution of  $\text{Ni}(\text{COD})_2$  (138 mg, 0.5 mmol) in 30 mL of toluene. The pale yellow solution was stirred 5 h. The solvent was removed under vacuum and the remaining yellow solid was rinsed with a small portion of pentane, and then dried under vacuum (0.90 g, 80 %).  $^1\text{H}$  NMR ( $\text{C}_6\text{D}_6$ , 300 MHz, 298 K):  $\delta$  1.07 (t,  $^3J = 7.0$  Hz, 6H,  $\text{NCH}_2\text{CH}_3$ ), 3.32 (q, 4H,  $^3J = 7.0$  Hz,  $\text{NCH}_2\text{CH}_3$ ), 4.43 (s, 6H,  $\text{PCH}_2$ ), 6.96 (m, 6H, Ph *o-H*, 3H, Ph *p-H*), 7.38 (m, 6H, Ph *m-H*).  $^{13}\text{C}\{^1\text{H}\}$  NMR ( $\text{C}_6\text{D}_6$ , 125.8 MHz, 298 K):  $\delta$  14.8 (s,  $\text{NCH}_2\text{CH}_3$ ), 42.4 (s,  $\text{ZrNCH}_2\text{CH}_3$ ), 54.8 (p,  $J_{\text{PC}} = 8.8$  Hz,  $\text{PCH}_2$ ), 117.9 and 129.9 (s, Ph *o-C* and *m-C*), 120.4 (s, Ph *p-C*), 153.6 (d, *ipso-C*).  $^{31}\text{P}\{^1\text{H}\}$  NMR ( $\text{C}_6\text{D}_6$ , 121.5 MHz, 298 K):  $\delta$  -11.0 (s).

## 6.4 References

- (1) Keen, A. L.; Doster, M.; Han, H.; Johnson, S. A. *Chem. Commun.* **2006**, 1221-1223.
- (2) Fryzuk, M. D.; Kozak, C. M.; Bowdridge, M. R.; Jin, W.; Tung, D.; Patrick, B. O.; Rettig, S. J. *Organometallics* **2001**, *20*, 3752-3761.

- (3) Memmler, H.; Gade, L. H.; Lauher, J. W. *Inorg. Chem.* **1994**, *33*, 3064-71.
- (4) Hellmann, K. W.; Steinert, P.; Gade, L. H. *Inorg. Chem.* **1994**, *33*, 3859-60.
- (5) Hellmann, K. W.; Gade, L. H.; Li, W.-S.; McPartlin, M. *Inorg. Chem.* **1994**, *33*, 5974-7.
- (6) Beer, P. D.; Hopkins, P. K.; McKinney, J. D. *Chem. Commun.* **1999**, 1253-1254.
- (7) Renner, P.; Galka, C.; Memmler, H.; Kauper, U.; Gade, L. H. *J. Organomet. Chem.* **1999**, *591*, 71-77.
- (8) Gade, L. H.; Memmler, H.; Kauper, U.; Schneider, A.; Fabre, S.; Bezougli, I.; Lutz, M.; Galka, C.; Scowen, I. J.; McPartlin, M. *Chem. Eur. J.* **2000**, *6*, 692-708.
- (9) Ballester, P.; Capo, M.; Costa, A.; Deya, P. M.; Gomila, R.; Decken, A.; Deslongchamps, G. *Org. Lett.* **2001**, *3*, 267-270.
- (10) Gade, L. H.; Renner, P.; Memmler, H.; Fecher, F.; Galka, C. H.; Laubender, M.; Radojevic, S.; McPartlin, M.; Lauher, J. W. *Chem. Eur. J.* **2001**, *7*, 2563-2580.
- (11) Jia, L.; Zhao, J.; Ding, E.; Brennessel, W. W. *J. Chem. Soc. Dalton Trans.* **2002**, 2608-2615.
- (12) Turculet, L.; Tilley, T. D. *Organometallics* **2002**, *21*, 3961-3972.
- (13) Porter, R. M.; Danopoulos, A. A. *J. Chem. Soc. Dalton Trans.* **2004**, 2556-2562.
- (14) Zhu, H.; Chen, E. Y. X. *Inorg. Chem.* **2007**, *46*, 1481-1487.
- (15) Alvarez-Vergara, M. C.; Casado, M. A.; Martin, M. L.; Lahoz, F. J.; Oro, L. A.; Perez-Torrente, J. J. *Organometallics* **2005**, *24*, 5929-5936.
- (16) Stang, P. J.; Persky, N. E. *Chem. Commun.* **1997**, 77-78.
- (17) Mokuolu, Q. F.; Avent, A. G.; Hitchcock, P. B.; Love, J. B. *Journal of the Chemical Society, Dalton Trans.* **2001**, 2551-2553.

- (18) Mokuolu, Q. F.; Duckmanton, P. A.; Hitchcock, P. B.; Wilson, C.; Blake, A. J.; Shukla, L.; Love, J. B. *J. Chem. Soc. Dalton Trans.* **2004**, 1960-1970.
- (19) Alder, R. W.; Butts, C. P.; Orpen, A. G.; Read, D.; Oliva, J. M. *J. Chem. Soc. Perkin Trans.* **2001**, 282-287.
- (20) Alder, R. W.; Ellis, D. D.; Gleiter, R.; Harris, C. J.; Lange, H.; Orpen, A. G.; Read, D.; Taylor, P. N. *J. Chem. Soc. Perkin Trans.* **1998**, 1657-1668.
- (21) Alder, R. W.; Ellis, D. D.; Orpen, A. G.; Taylor, P. N. *Chem. Commun.* **1996**, 539-40.
- (22) Diel, B. N.; Norman, A. D. *Phosphorus and Sulfur and the Related Elements* **1982**, *12*, 227-35.
- (23) Kisanga, P.; Verkade, J. *Heteroatom Chem.* **2001**, *12*, 114-117.
- (24) Keller, H.; Regitz, M. *Tetrahedron Lett.* **1988**, *29*, 925-8.
- (25) Konrad W. Hellmann. *Angew. Chem. Int. Ed.* **1997**, *36*, 160-163.
- (26) Gysling, H. J.; Luss, H. R.; Gardner, S. A. *J. Organomet. Chem.* **1980**, *184*, 417-31.
- (27) Steigerwald, M. L. *Polyhedron* **1994**, *13*, 1245-52.
- (28) Davies, R. P.; Martinelli, M. G. *Inorg. Chem.* **2002**, *41*, 348-352.
- (29) Walther, B. *Coord. Chem. Rev.* **1984**, *60*, 67-105.
- (30) Pilkington, M. J.; Slawin, A. M. Z.; Williams, D. J.; Woollins, J. D. *Polyhedron* **1991**, *10*, 2641-5.
- (31) Haiduc, I. *J. Organomet. Chem.* **2001**, *623*, 29-42.
- (32) Kuchen, W.; Hertel, H. *Angew. Chem. Int. Ed.* **1969**, *8*, 89-97.

- (33) Baker, R. T.; Fultz, W. C.; Marder, T. B.; Williams, I. D. *Organometallics* **1990**, *9*, 2357-67.
- (34) Lindenberg, F.; Shribman, T.; Sieler, J.; Hey-Hawkins, E.; Eisen, M. S. *J. Organomet. Chem.* **1996**, *515*, 19-25.
- (35) Amor, I.; Garcia-Vivo, D.; Garcia, M. E.; Ruiz, M. A.; Saez, D.; Hamidov, H.; Jeffery, J. C. *Organometallics* **2007**, *26*, 466-468.
- (36) Zheng, P. Y.; Nadasdi, T. T.; Stephan, D. W. *Organometallics* **1989**, *8*, 1393-8.
- (37) Han, H.; Elsmaili, M.; Johnson, S. A. *Inorg. Chem.* **2006**, *45*, 7435-7445.
- (38) Han, H.; Johnson, S. A. *Organometallics* **2006**, *25*, 5594-5602.

## Appendix One: X-ray Crystal Structure Data

Table A 1.1. Positional parameters and U(eq) for P[CH<sub>2</sub>NH-3,5-(CF<sub>3</sub>)<sub>2</sub>C<sub>6</sub>H<sub>3</sub>]<sub>3</sub> (1a)

	x	y	z	U(eq)
C(1)	9287(2)	-276(2)	5757(1)	36(1)
C(2)	10710(1)	728(1)	5995(1)	28(1)
C(3)	9171(2)	915(2)	6659(2)	59(1)
C(4)	7964(2)	-1033(2)	5490(1)	34(1)
C(5)	7081(2)	-991(2)	5372(1)	33(1)
C(6)	6603(1)	-1692(2)	5341(1)	28(1)
C(7)	6976(2)	-2453(2)	5421(1)	28(1)
C(8)	7845(2)	-2489(1)	5530(1)	27(1)
C(9)	8344(2)	-1794(2)	5566(1)	29(1)
C(10)	5652(2)	-1642(2)	5245(1)	34(1)
C(11)	8271(2)	-3303(2)	5583(1)	34(1)
C(12)	11918(2)	1681(1)	6135(1)	26(1)
C(13)	12477(2)	1050(1)	6274(1)	28(1)
C(14)	13335(2)	1218(2)	6385(1)	31(1)
C(15)	13656(2)	2003(2)	6360(1)	30(1)
C(16)	13091(2)	2623(1)	6214(1)	28(1)
C(17)	12237(2)	2475(1)	6101(1)	27(1)
C(18)	13918(2)	516(2)	6525(2)	44(1)
C(19)	13414(2)	3482(2)	6160(1)	37(1)
C(20)	8615(2)	2289(3)	6966(2)	29(1)
C(21)	8832(2)	3117(3)	6991(1)	29(1)
C(22)	8214(3)	3696(3)	7119(2)	31(1)
C(23)	7371(3)	3481(4)	7218(3)	33(1)
C(24)	7162(3)	2659(3)	7208(2)	28(1)
C(25)	7769(3)	2065(2)	7081(2)	28(1)
C(26)	8483(3)	4575(3)	7116(2)	43(1)
C(27)	6252(2)	2444(2)	7330(2)	33(1)
C(20B)	8218(8)	1990(6)	7023(4)	28(2)
C(21B)	8727(6)	2687(9)	6974(4)	28(2)
C(22B)	8383(9)	3465(8)	7059(6)	27(3)
C(23B)	7499(11)	3548(11)	7201(8)	33(1)

Appendix One: X-ray Crystal Structure Data

C(24B)	7026(8)	2859(8)	7227(5)	29(3)
C(25B)	7348(8)	2095(7)	7151(4)	32(2)
C(26B)	8906(9)	4195(9)	7006(6)	52(3)
C(27B)	6053(7)	2960(7)	7372(5)	39(2)
N(1)	8425(2)	-325(2)	5520(2)	53(1)
N(2)	11050(1)	1548(1)	6041(1)	30(1)
N(3)	9252(2)	1733(2)	6841(2)	50(1)
N(3B)	8509(5)	1195(5)	6948(5)	41(2)
F(1)	5217(1)	-1740(2)	5748(1)	63(1)
F(2)	5369(1)	-2242(1)	4892(1)	57(1)
F(3)	5413(1)	-958(1)	4994(1)	66(1)
F(4)	8522(1)	-3593(1)	5056(1)	57(1)
F(5)	7747(1)	-3864(1)	5820(1)	54(1)
F(6)	8962(1)	-3295(1)	5924(1)	45(1)
F(7)	13917(2)	-35(2)	6098(1)	83(1)
F(8)	13664(2)	112(1)	7008(1)	70(1)
F(9)	14705(1)	743(2)	6626(2)	106(1)
F(10)	13486(2)	3729(1)	5611(1)	101(1)
F(11)	14160(2)	3592(1)	6429(2)	89(1)
F(12)	12911(2)	4012(1)	6429(1)	70(1)
F(13)	8609(7)	4848(6)	6602(4)	119(3)
F(14)	9211(3)	4684(2)	7429(2)	71(1)
F(15)	7931(3)	5049(2)	7396(3)	131(2)
F(13B)	8836(17)	4664(18)	6555(11)	117(11)
F(14B)	9721(7)	4039(7)	7024(9)	132(6)
F(15B)	8715(8)	4750(6)	7447(5)	63(3)
F(16)	6121(2)	1650(1)	7370(1)	55(1)
F(17)	5721(2)	2736(2)	6913(1)	50(1)
F(18)	5974(2)	2773(2)	7847(2)	41(1)
F(16B)	5598(5)	2286(7)	7261(6)	85(4)
F(17B)	5693(6)	3539(8)	7052(5)	86(4)
F(18B)	5928(7)	3160(9)	7934(5)	66(3)
P(1)	9542(1)	809(1)	5879(1)	34(1)

**Table A 1.2.** Positional parameters and U(eq) for P(CH<sub>2</sub>NAr<sup>CF<sub>3</sub></sup>)<sub>3</sub>TiNMe<sub>2</sub> (**2a**)

	x	y	z	U(eq)
F(1)	3207(4)	490(19)	621(6)	128(7)
F(1B)	2542(6)	1070(20)	288(4)	158(7)
F(2)	2563(4)	219(12)	371(5)	86(3)
F(2B)	3180(5)	1161(13)	562(7)	107(5)
F(3)	2783(6)	1594(6)	389(4)	94(4)
F(3B)	2883(8)	-142(6)	563(6)	121(4)
F(4)	3134(4)	1987(10)	4060(8)	103(5)
F(4B)	3588(7)	800(20)	3549(16)	98(9)
F(5)	3603(3)	1813(16)	3200(7)	125(7)
F(5B)	3153(6)	1440(40)	4230(10)	136(15)
F(6)	3390(6)	640(8)	3844(9)	116(5)
F(6B)	3461(11)	2225(15)	3354(18)	119(12)
F(10)	540(8)	-4216(10)	2431(10)	129(7)
F(10B)	871(7)	-4908(11)	1350(12)	125(9)
F(11)	938(5)	-4934(11)	1695(15)	127(9)
F(11B)	343(3)	-4169(8)	1772(17)	133(9)
F(12)	403(6)	-4284(13)	1262(13)	161(8)
F(12B)	853(8)	-4539(11)	2502(10)	145(6)
C(1)	1707(1)	395(3)	3707(2)	39(1)
C(2)	1058(1)	-1046(3)	3313(2)	42(1)
C(3)	819(1)	942(3)	3743(2)	36(1)
C(4)	2187(1)	817(3)	2646(2)	35(1)
C(5)	2300(1)	730(3)	1851(2)	37(1)
C(6)	2715(1)	876(3)	1608(2)	39(1)
C(7)	3037(1)	1103(3)	2136(2)	43(1)
C(8)	2928(1)	1197(3)	2915(2)	42(1)
C(9)	2511(1)	1059(3)	3174(2)	39(1)
C(10)	2820(1)	759(4)	752(2)	54(1)
C(11)	3270(1)	1420(4)	3501(2)	57(1)
C(12)	1135(1)	-1646(3)	1976(2)	40(1)
C(13)	1367(1)	-1564(3)	1282(2)	49(1)
C(14)	1385(2)	-2314(3)	752(3)	60(1)
C(15)	1182(2)	-3180(3)	905(3)	64(1)

Appendix One: X-ray Crystal Structure Data

C(16)	961(1)	-3275(3)	1602(3)	55(1)
C(17)	936(1)	-2517(3)	2132(2)	47(1)
C(18)	1625(2)	-2181(4)	4(3)	89(2)
C(19)	738(2)	-4199(4)	1785(4)	75(2)
C(20)	548(1)	2011(2)	2733(2)	29(1)
C(21)	439(1)	2197(2)	1949(2)	33(1)
C(22)	214(1)	3005(3)	1737(2)	36(1)
C(23)	78(1)	3673(3)	2291(2)	37(1)
C(24)	173(1)	3481(3)	3068(2)	36(1)
C(25)	397(1)	2667(2)	3291(2)	33(1)
C(26)	109(1)	3151(3)	887(2)	51(1)
C(27)	35(1)	4164(3)	3697(2)	52(1)
C(28)	1061(1)	580(3)	554(2)	52(1)
C(29)	1435(1)	1874(3)	1216(2)	50(1)
N(1)	1770(1)	635(2)	2870(2)	36(1)
N(2)	1115(1)	-852(2)	2475(2)	36(1)
N(3)	799(1)	1215(2)	2912(1)	30(1)
N(4)	1242(1)	922(2)	1289(2)	37(1)
F(7)	1908(2)	-1501(3)	23(2)	138(2)
F(8)	1352(2)	-1930(3)	-590(2)	134(2)
F(9)	1796(1)	-2972(3)	-267(2)	108(1)
F(13)	427(1)	2973(3)	424(2)	122(2)
F(14)	-45(1)	4013(2)	721(1)	72(1)
F(15)	-209(1)	2560(3)	661(2)	99(1)
F(16)	-228(1)	3744(2)	4213(2)	97(1)
F(17)	-179(1)	4918(2)	3430(1)	66(1)
F(18)	358(1)	4500(3)	4101(2)	110(1)
P(2)	1176(1)	-65(1)	4019(1)	34(1)
Ti(1)	1227(1)	495(1)	2324(1)	30(1)
C(30)	2500	7500	8301(11)	450(20)
C(31)	2772(4)	6818(10)	7939(7)	251(7)
C(32)	2754(5)	6802(10)	7120(7)	264(8)
C(33)	2500	7500	6748(10)	361(17)

**Table A 1.3.** Positional parameters and U(eq) for P(CH<sub>2</sub>NPh)<sub>3</sub>TiNMe<sub>2</sub> (**2b**)

	x	y	z	U(eq)
C(1)	9199(1)	3674(1)	6443(1)	33(1)
C(2)	7786(1)	2068(1)	7038(1)	31(1)
C(3)	9973(1)	1798(1)	6099(1)	33(1)
C(4)	8074(1)	4630(1)	5272(1)	33(1)
C(5)	7017(1)	4703(1)	4818(1)	46(1)
C(6)	6561(2)	5561(2)	4591(2)	66(1)
C(7)	7145(2)	6358(1)	4825(2)	68(1)
C(8)	8190(2)	6297(1)	5276(1)	56(1)
C(9)	8659(1)	5446(1)	5495(1)	41(1)
C(10)	6148(1)	1621(1)	5997(1)	29(1)
C(11)	5436(1)	1797(1)	5148(1)	33(1)
C(12)	4415(1)	1357(1)	5057(1)	37(1)
C(13)	4056(1)	748(1)	5813(1)	41(1)
C(14)	4726(1)	592(1)	6673(1)	43(1)
C(15)	5757(1)	1025(1)	6774(1)	36(1)
C(16)	10250(1)	1422(1)	4274(1)	29(1)
C(17)	10134(1)	1649(1)	3213(1)	34(1)
C(18)	10760(1)	1203(1)	2457(1)	38(1)
C(19)	11536(1)	536(1)	2732(1)	40(1)
C(20)	11687(1)	328(1)	3776(1)	42(1)
C(21)	11056(1)	760(1)	4539(1)	36(1)
C(22)	7474(2)	3183(1)	2830(1)	59(1)
C(23)	7298(2)	1562(1)	3268(1)	49(1)
N(1)	8505(1)	3755(1)	5507(1)	32(1)
N(2)	7213(1)	2026(1)	6024(1)	30(1)
N(3)	9591(1)	1875(1)	5019(1)	30(1)
N(4)	7602(1)	2481(1)	3621(1)	34(1)
P(1)	9244(1)	2517(1)	7084(1)	31(1)

**Table A 1.4.** Positional parameters and U(eq) for P(CH<sub>2</sub>NAr<sup>Me</sup>)<sub>3</sub>TiNMe<sub>2</sub> (**2c**)

	x	y	z	U(eq)
Ti(2)	8808(1)	2422(1)	3758(1)	23(1)
P(2)	9693(2)	2635(2)	2296(1)	34(1)
N(24)	8503(5)	2317(4)	4732(3)	28(1)
N(25)	10439(5)	2305(4)	3794(3)	29(2)
N(26)	8687(5)	3585(4)	3331(3)	24(1)
N(27)	7877(5)	1498(4)	2968(3)	29(2)
C(35)	8169(10)	6758(6)	2914(6)	63(3)
C(41)	12511(7)	2325(7)	4387(5)	46(2)
C(42)	13295(9)	2056(8)	4971(6)	62(3)
C(43)	12837(10)	1529(8)	5496(6)	63(3)
C(44)	11621(9)	1243(6)	5487(5)	47(3)
C(46)	14634(9)	2412(10)	5001(7)	97(5)
C(47)	11129(11)	661(7)	6067(6)	74(4)
C(50)	6894(7)	747(5)	2955(4)	35(2)
C(51)	6067(7)	779(5)	3404(4)	29(2)
C(52)	5103(9)	43(6)	3425(6)	52(3)
C(53)	4971(11)	-744(7)	2950(7)	73(4)
C(54)	5762(12)	-803(7)	2493(7)	68(4)
C(55)	6724(9)	-62(6)	2481(5)	51(3)
C(56)	4232(9)	89(7)	3929(6)	67(3)
C(57)	5612(14)	-1683(8)	1994(8)	117(6)
C(90)	8298(6)	4352(5)	3545(4)	23(2)
C(91)	8411(7)	5146(5)	3137(4)	34(2)
C(92)	8010(7)	5909(5)	3369(5)	38(2)
C(93)	7492(7)	5885(5)	3984(5)	38(2)
C(94)	7348(8)	5104(6)	4407(6)	49(2)
C(95)	7739(7)	4355(5)	4160(5)	35(2)
C(97)	6800(12)	5085(8)	5093(7)	90(4)
C(100)	9127(7)	3610(5)	2630(4)	32(2)
C(102)	10870(7)	2566(6)	3107(5)	40(2)
C(109)	8507(7)	1561(6)	2343(4)	38(2)
C(124)	7824(8)	1623(6)	5140(4)	41(2)
C(125)	9320(7)	3077(6)	5217(5)	42(2)

Appendix One: X-ray Crystal Structure Data

C(130)	11265(7)	2049(6)	4361(4)	35(2)
C(131)	10855(8)	1498(6)	4915(5)	42(2)
Ti(1)	3344(1)	3013(1)	1400(1)	21(1)
P(1)	5083(2)	2932(1)	2815(1)	30(1)
N(1)	5004(5)	3155(4)	1262(3)	25(1)
N(2)	3427(5)	3952(4)	2187(3)	26(1)
N(3)	2876(5)	1885(4)	1883(3)	23(1)
N(4)	2414(5)	3033(4)	453(3)	27(1)
C(1)	5753(7)	3017(6)	1963(4)	35(2)
C(2)	4407(7)	3944(5)	2812(4)	30(2)
C(3)	3799(6)	1904(5)	2559(4)	27(2)
C(4)	5540(6)	3303(5)	624(4)	24(2)
C(5)	5009(7)	3715(5)	21(4)	30(2)
C(6)	5468(7)	3830(5)	-624(4)	30(2)
C(7)	6497(8)	3551(5)	-675(5)	37(2)
C(8)	7073(8)	3152(5)	-82(5)	40(2)
C(9)	6591(7)	3029(5)	557(5)	33(2)
C(10)	4813(8)	4245(6)	-1279(5)	46(2)
C(11)	8177(9)	2815(7)	-160(6)	64(3)
C(12)	2773(7)	4618(5)	2235(4)	25(2)
C(13)	3151(7)	5396(5)	2750(4)	32(2)
C(14)	2472(8)	6046(5)	2752(4)	35(2)
C(15)	1441(8)	5948(5)	2236(4)	37(2)
C(16)	1022(7)	5177(5)	1720(4)	33(2)
C(17)	1692(6)	4527(5)	1735(4)	28(2)
C(18)	2907(10)	6871(6)	3319(5)	56(3)
C(19)	-122(8)	5053(6)	1162(5)	47(2)
C(20)	1922(6)	1101(5)	1758(4)	24(2)
C(21)	872(7)	1122(5)	1255(4)	27(2)
C(22)	-110(7)	371(5)	1099(4)	34(2)
C(23)	-60(8)	-421(6)	1470(5)	42(2)
C(24)	957(9)	-470(6)	1964(5)	46(2)
C(25)	1929(8)	286(5)	2109(5)	39(2)
C(26)	-1214(7)	424(6)	547(5)	43(2)
C(27)	1023(11)	-1351(7)	2352(7)	93(5)
C(120)	2351(8)	2187(6)	-2(4)	40(2)

Appendix One: X-ray Crystal Structure Data

C(121)	1897(8)	3686(7)	15(5)	46(2)
C(151)	5716(19)	9651(15)	9034(12)	152(7)
C(153)	4940(30)	10570(20)	9860(20)	111(10)

**Table A 1.5.** Positional parameters and U(eq) for P(CH<sub>2</sub>NPh)<sub>3</sub>Ta=N<sup>t</sup>Bu (**3b**)

	x	y	z	U(eq)
C(1)	12303(1)	11080(2)	13079(2)	37(1)
C(2)	12988(1)	11371(2)	12424(2)	36(1)
C(3)	12048(1)	9505(2)	11669(2)	39(1)
C(4)	11627(1)	12683(2)	12782(2)	28(1)
C(5)	11226(1)	13597(2)	12243(2)	30(1)
C(6)	10992(1)	14298(2)	12530(2)	36(1)
C(7)	11159(1)	14135(3)	13373(2)	45(1)
C(8)	11563(2)	13248(3)	13917(2)	48(1)
C(9)	11796(1)	12520(3)	13634(2)	40(1)
C(10)	12777(1)	12874(2)	11372(2)	31(1)
C(11)	12357(1)	13461(2)	10542(2)	34(1)
C(12)	12580(2)	14167(2)	10240(2)	43(1)
C(13)	13229(2)	14326(3)	10764(2)	48(1)
C(14)	13648(2)	13758(3)	11588(2)	51(1)
C(15)	13427(1)	13035(2)	11895(2)	41(1)
C(16)	10975(1)	9559(2)	10147(2)	36(1)
C(17)	10379(2)	10052(3)	9574(2)	62(1)
C(18)	9865(2)	9513(3)	8765(3)	77(1)
C(19)	9949(2)	8469(3)	8531(3)	65(1)
C(20)	10517(2)	7959(4)	9115(3)	77(1)
C(21)	11036(2)	8489(3)	9924(3)	62(1)
C(22)	10544(1)	13377(2)	9634(2)	28(1)
C(23)	10745(1)	14628(2)	9830(2)	37(1)
C(24)	9962(1)	13211(2)	9542(2)	39(1)
C(25)	10388(1)	13004(2)	8745(2)	39(1)
N(1)	11843(1)	11981(2)	12454(1)	29(1)
N(2)	12528(1)	12138(2)	11644(1)	29(1)
N(3)	11486(1)	10171(2)	10931(1)	31(1)
N(4)	11067(1)	12681(2)	10391(1)	25(1)
P(1)	12698(1)	10253(1)	12757(1)	37(1)
Ta(1)	11692(1)	11805(1)	11293(1)	25(1)

**Table A 1.6.** Positional parameters and U(eq) for (CO)<sub>2</sub>Ni[P(CH<sub>2</sub>NAr<sup>Me</sup>)<sub>3</sub>TiNMe<sub>2</sub>]<sub>2</sub> (**5**)

	x	y	z	U(eq)
C(1)	4221(3)	5848(3)	14841(3)	38(1)
C(2)	3988(3)	6940(3)	13738(3)	35(1)
C(3)	4471(3)	5156(3)	13081(3)	34(1)
C(4)	5236(4)	7202(3)	16363(4)	41(1)
C(5)	4475(4)	7537(3)	16528(4)	56(2)
C(6)	4601(7)	8194(4)	17404(6)	80(2)
C(7)	5469(7)	8525(4)	18120(6)	82(2)
C(8)	6266(6)	8228(4)	18012(4)	74(2)
C(9)	6125(4)	7525(3)	17108(4)	51(1)
C(10)	3772(6)	8553(5)	17577(6)	120(3)
C(11)	7250(6)	8570(5)	18781(5)	117(3)
C(12)	5224(3)	8133(3)	13871(3)	35(1)
C(13)	4610(4)	8725(3)	13784(3)	44(1)
C(14)	4876(4)	9539(3)	13691(4)	49(1)
C(15)	5745(4)	9756(4)	13671(4)	53(2)
C(16)	6362(4)	9177(4)	13727(4)	48(1)
C(17)	6089(3)	8365(3)	13813(3)	42(1)
C(18)	4219(4)	10191(4)	13645(4)	62(2)
C(19)	7307(4)	9395(4)	13661(5)	71(2)
C(20)	6069(3)	4918(3)	13432(3)	30(1)
C(21)	5816(3)	4265(3)	12503(3)	36(1)
C(22)	6433(3)	3753(3)	12235(4)	40(1)
C(23)	7319(4)	3898(4)	12927(4)	47(1)
C(24)	7599(3)	4533(3)	13870(4)	39(1)
C(25)	6971(3)	5028(3)	14116(3)	34(1)
C(26)	6133(4)	3081(4)	11207(4)	67(2)
C(27)	8581(4)	4698(4)	14611(4)	65(2)
C(28)	7379(4)	8349(4)	16111(4)	57(2)
C(29)	7802(4)	7294(4)	14924(4)	63(2)
C(30)	644(3)	4239(3)	10453(3)	35(1)
C(31)	2276(3)	5698(3)	11061(3)	37(1)
C(32)	2438(3)	3790(3)	10703(3)	36(1)
C(33)	-177(3)	2859(3)	8884(4)	40(1)

## Appendix One: X-ray Crystal Structure Data

C(34)	-232(4)	2213(4)	9286(5)	56(2)
C(35)	-825(6)	1323(4)	8720(7)	81(2)
C(36)	-1355(5)	1074(4)	7769(7)	90(3)
C(37)	-1319(4)	1695(5)	7351(5)	74(2)
C(38)	-717(3)	2595(4)	7933(4)	49(1)
C(39)	-854(7)	623(5)	9159(7)	132(4)
C(40)	-1871(5)	1419(5)	6296(5)	112(3)
C(41)	1899(3)	6348(3)	9871(3)	32(1)
C(42)	2566(3)	7208(3)	10518(4)	38(1)
C(43)	2605(4)	7961(3)	10277(4)	47(1)
C(44)	1979(4)	7867(4)	9393(4)	50(1)
C(45)	1301(4)	7025(4)	8733(4)	45(1)
C(46)	1270(3)	6283(3)	8990(3)	37(1)
C(47)	3350(4)	8884(4)	10977(5)	74(2)
C(48)	605(4)	6928(4)	7778(5)	70(2)
C(49)	3138(3)	3376(3)	9504(3)	33(1)
C(50)	3261(3)	2521(3)	9509(3)	43(1)
C(51)	3852(4)	2079(3)	9122(4)	45(1)
C(52)	4352(3)	2530(4)	8760(3)	44(1)
C(53)	4257(3)	3383(3)	8765(3)	39(1)
C(54)	3649(3)	3807(3)	9145(3)	37(1)
C(55)	3969(5)	1138(4)	9109(5)	71(2)
C(56)	4810(4)	3868(4)	8398(4)	54(1)
C(57)	1172(4)	2829(4)	7367(4)	63(2)
C(58)	1732(4)	4361(4)	7468(4)	60(2)
C(59)	1436(4)	5675(4)	13185(4)	50(1)
C(60)	1967(3)	3902(4)	12876(4)	52(1)
N(1)	5131(3)	6548(3)	15450(3)	34(1)
N(2)	5001(3)	7327(2)	14011(3)	35(1)
N(3)	5489(2)	5476(2)	13723(3)	32(1)
N(4)	7073(3)	7455(3)	15291(3)	39(1)
N(5)	448(3)	3761(3)	9430(3)	35(1)
N(6)	1843(3)	5563(2)	10064(3)	34(1)
N(7)	2490(3)	3814(3)	9841(3)	36(1)
N(8)	1407(3)	3828(3)	7924(3)	40(1)
O(1)	951(3)	6094(4)	13454(3)	92(2)

Appendix One: X-ray Crystal Structure Data

O(2)	1808(3)	3213(3)	12939(4)	90(2)
P(1)	3670(1)	5720(1)	13591(1)	31(1)
P(2)	1902(1)	4692(1)	11297(1)	32(1)
Ti(1)	5812(1)	6731(1)	14700(1)	31(1)
Ti(2)	1483(1)	4253(1)	9173(1)	32(1)
Ni(1)	2163(1)	4977(1)	12788(1)	32(1)
C(61)	740(14)	-2270(14)	5574(15)	136(7)
C(62)	460(20)	-1400(20)	5890(20)	195(10)
C(63)	955(16)	-1077(15)	6879(18)	148(8)
C(64)	690(20)	-530(30)	7640(30)	243(14)
C(65)	890(20)	330(20)	7650(20)	210(40)
C(66)	1158	111	8502	110(5)
C(67)	829	229	7615	310(70)
C(68)	473	-543	6716	185(10)
C(69)	18	-147	5957	258(16)

## Appendix One: X-ray Crystal Structure Data

**Table A 1.7.** Positional parameters and U(eq) for *trans*-RhCl(CO)(3c)<sub>2</sub> (**8c**)

	x	y	z	U(eq)
C(10)	6667	3333	4184(5)	38(3)
C(11)	6904(7)	2453(8)	3996(4)	53(2)
Cl(1)	6401(10)	1687(7)	7500	57(3)
O(1)	8670(40)	2900(40)	7500	105(13)
C(12)	7860(40)	3020(40)	7500	62(11)
Ta(1)	6667	3333	5454(1)	24(1)
Rh(1)	6667	3333	7500	37(1)
P(1)	6667	3333	6605(1)	29(1)
N(1)	6757(4)	4662(4)	5763(2)	27(1)
C(1)	6875(6)	4620(6)	6326(3)	32(1)
N(2)	6667	3333	4758(4)	33(2)
C(7)	7238(6)	6584(6)	5853(3)	36(2)
C(3)	6452(5)	5599(5)	5058(3)	30(1)
C(5)	7005(6)	7494(6)	5115(3)	42(2)
C(4)	6563(6)	6536(6)	4827(3)	37(2)
C(8)	6181(7)	6490(7)	4274(3)	44(2)
C(2)	6817(5)	5624(6)	5561(2)	29(1)
C(9)	7819(10)	8559(8)	5942(4)	73(3)

**Table A 1.8** Positional parameters and U(eq) for [CpNiP(CH<sub>2</sub>NHPh)<sub>2</sub>]<sub>2</sub> (**9**)

	x	y	z	U(eq)
C(57)	2517(3)	4345(3)	612(2)	34(1)
C(56)	3896(3)	4976(3)	806(2)	34(1)
C(55)	4741(3)	4321(3)	550(2)	38(1)
C(48)	1738(4)	1279(3)	2593(2)	45(1)
C(53)	2525(4)	3328(3)	197(2)	41(1)
C(51)	4011(4)	1439(3)	2740(2)	49(1)
C(54)	3898(4)	3307(3)	168(2)	43(1)
C(52)	2773(4)	816(3)	2343(2)	45(1)
C(49)	2336(4)	2188(3)	3152(2)	47(1)
C(50)	3726(4)	2253(3)	3251(2)	49(1)
C(59)	101(9)	134(5)	-586(4)	93(2)
C(58)	-1178(7)	-293(5)	-414(5)	113(3)
C(60)	1304(8)	437(5)	-163(5)	116(3)
C(61)	273(16)	401(11)	-1055(7)	111(5)
Ni(2)	3256(1)	2390(1)	2301(1)	27(1)
Ni(3)	3452(1)	3635(1)	1160(1)	24(1)
Ni(1)	-836(1)	699(1)	4716(1)	26(1)
P(2)	2331(1)	3410(1)	1983(1)	25(1)
P(1)	872(1)	31(1)	4536(1)	25(1)
P(3)	4668(1)	3012(1)	1672(1)	27(1)
N(3)	2331(3)	5501(2)	2390(1)	32(1)
N(2)	2704(3)	1913(2)	5156(1)	33(1)
N(1)	-680(3)	-1606(2)	3538(1)	34(1)
C(24)	2958(3)	6579(3)	2705(2)	31(1)
N(6)	6779(3)	3654(2)	2638(1)	35(1)
C(2)	2533(3)	1016(2)	4559(2)	30(1)
C(21)	402(3)	2878(3)	1898(2)	35(1)
C(9)	3789(3)	2825(2)	5266(2)	28(1)
C(3)	-1268(3)	-2137(2)	2890(2)	29(1)
N(4)	-371(3)	3530(3)	1747(2)	38(1)
C(10)	4992(3)	2831(3)	4945(2)	28(1)
C(13)	4781(4)	4672(3)	5876(2)	40(1)
C(4)	-2691(3)	-2626(3)	2781(2)	34(1)

Appendix One: X-ray Crystal Structure Data

C(20)	2622(3)	4706(2)	2644(1)	31(1)
C(18)	-948(4)	1401(3)	3999(2)	51(1)
C(1)	682(3)	-863(2)	3674(2)	32(1)
C(30)	-719(3)	3509(3)	1113(2)	30(1)
C(42)	7920(3)	4275(2)	3080(2)	28(1)
C(43)	8374(3)	3879(3)	3544(2)	36(1)
C(47)	8674(3)	5268(2)	3065(2)	31(1)
C(14)	3700(3)	3762(3)	5736(2)	35(1)
C(11)	6064(3)	3755(3)	5090(2)	35(1)
C(23)	6146(3)	4056(2)	2196(2)	30(1)
N(5)	6477(3)	1727(2)	1381(2)	47(1)
C(36)	6139(4)	701(3)	1399(2)	37(1)
C(7)	-1125(4)	-2774(3)	1708(2)	47(1)
C(22)	5601(3)	2162(3)	1081(2)	35(1)
C(31)	-988(3)	4406(3)	1032(2)	35(1)
C(37)	5089(4)	-116(3)	988(2)	46(1)
C(5)	-3298(4)	-3179(3)	2144(2)	42(1)
C(44)	9534(4)	4455(3)	3973(2)	46(1)
C(46)	9853(3)	5840(3)	3497(2)	35(1)
C(27)	4170(4)	8759(3)	3295(2)	43(1)
C(8)	-485(4)	-2217(3)	2349(2)	38(1)
C(15)	-2792(3)	888(3)	4533(2)	42(1)
C(25)	3585(3)	6989(3)	3356(2)	34(1)
C(26)	4180(3)	8065(3)	3636(2)	39(1)
C(28)	3548(4)	8359(3)	2653(2)	44(1)
C(12)	5965(4)	4679(3)	5557(2)	40(1)
C(41)	6934(4)	463(3)	1835(2)	53(1)
C(29)	2947(4)	7286(3)	2360(2)	38(1)
C(34)	-1323(4)	2620(3)	-55(2)	47(1)
C(6)	-2514(4)	-3254(3)	1604(2)	46(1)
C(35)	-888(3)	2614(3)	560(2)	37(1)
C(32)	-1415(3)	4403(3)	419(2)	42(1)
C(38)	4860(4)	-1130(3)	1004(2)	58(1)
C(19)	-2220(4)	623(3)	3930(2)	48(1)
C(45)	10283(4)	5436(3)	3950(2)	43(1)
C(39)	5644(5)	-1369(3)	1415(2)	58(1)

Appendix One: X-ray Crystal Structure Data

C(40)	6682(5)	-578(4)	1841(2)	62(1)
C(33)	-1595(4)	3514(3)	-126(2)	49(1)
C(17)	-796(4)	2182(3)	4626(2)	48(1)
C(16)	-1918(4)	1851(3)	4959(2)	41(1)

**Table A 1.9** Positional parameters and U(eq) for [CpNiP(CH<sub>2</sub>NPh)<sub>2</sub>Ti(NMe<sub>2</sub>)<sub>2</sub>]<sub>2</sub> (**11**)

	x	y	z	U(eq)
Ni(1)	4338(1)	4198(1)	1581(1)	27(1)
Ti(1)	8021(1)	1726(1)	1503(1)	27(1)
P(1)	5948(1)	4178(1)	130(1)	26(1)
N(1)	6495(3)	1451(3)	909(3)	27(1)
N(2)	7963(3)	3478(3)	1561(3)	30(1)
N(3)	9454(3)	1813(3)	214(3)	37(1)
N(4)	8210(3)	436(3)	3087(3)	34(1)
C(1)	6248(4)	2639(4)	-177(4)	30(1)
C(2)	7577(4)	4457(4)	398(4)	31(1)
C(3)	5520(4)	443(4)	1496(4)	28(1)
C(4)	4230(4)	639(4)	1418(4)	40(1)
C(5)	3306(5)	-387(5)	2101(5)	53(1)
C(6)	3647(5)	-1615(5)	2869(5)	55(1)
C(7)	4931(5)	-1832(5)	2921(5)	54(1)
C(8)	5855(5)	-826(4)	2250(4)	42(1)
C(9)	8133(4)	3912(4)	2510(3)	29(1)
C(10)	7511(4)	5003(4)	2680(4)	34(1)
C(11)	7741(4)	5386(4)	3621(4)	41(1)
C(12)	8576(4)	4714(5)	4420(4)	42(1)
C(13)	9173(4)	3635(5)	4278(4)	39(1)
C(14)	8964(4)	3241(4)	3337(4)	34(1)
C(15)	9535(5)	1600(5)	-968(4)	55(1)
C(16)	10689(5)	2358(6)	230(5)	74(2)
C(17)	7076(5)	425(5)	4054(4)	49(1)
C(18)	9131(5)	-555(5)	3618(5)	58(1)
C(37)	2697(5)	4166(5)	2941(4)	47(1)
C(38)	3802(5)	4409(4)	3362(4)	43(1)
C(39)	4584(4)	3325(4)	3525(3)	35(1)
C(40)	3969(4)	2403(4)	3219(3)	35(1)
C(41)	2785(4)	2899(5)	2902(4)	40(1)

**Table A 1.10** Positional parameters and U(eq) for P[CH<sub>2</sub>N-3,5-Me<sub>2</sub>C<sub>6</sub>H<sub>3</sub>]<sub>3</sub>ZrCp (**14c**)

	x	y	z	U(eq)
zr(1)	4407(1)	3074(1)	1418(1)	22(1)
zr(2)	-1746(1)	289(1)	-2836(1)	21(1)
p(2)	-4218(1)	487(1)	-3905(1)	26(1)
p(1)	6962(1)	4499(1)	1776(1)	29(1)
n(1)	4625(2)	3466(1)	462(1)	29(1)
n(4)	-1522(2)	924(1)	-3684(1)	26(1)
n(2)	6025(2)	2692(1)	1907(1)	27(1)
n(3)	4659(2)	4373(1)	2154(1)	29(1)
n(5)	-2640(2)	1077(1)	-2268(1)	27(1)
c(37)	-455(2)	2377(2)	-3868(1)	30(1)
n(6)	-3142(2)	-961(1)	-3511(1)	26(1)
c(28)	3222(2)	1670(1)	1695(1)	30(1)
c(31)	2010(2)	2384(2)	933(1)	31(1)
c(35)	-4323(2)	-708(2)	-3835(1)	33(1)
c(12)	6328(2)	1917(1)	2142(1)	27(1)
c(39)	1336(2)	2494(2)	-4286(1)	32(1)
c(63)	642(2)	788(2)	-2239(1)	33(1)
c(9)	2690(2)	3436(1)	-563(1)	30(1)
c(36)	-548(2)	1459(1)	-3880(1)	26(1)
c(30)	2423(2)	1800(2)	450(1)	32(1)
c(44)	-2365(2)	1664(2)	-1508(1)	28(1)
c(3)	5961(2)	4931(2)	2296(2)	38(1)
c(15)	6847(2)	383(2)	2591(2)	37(1)
c(41)	330(2)	1072(2)	-4093(1)	28(1)
c(52)	-3318(2)	-1920(1)	-3686(1)	28(1)
c(4)	3906(2)	3313(1)	-343(1)	27(1)
c(29)	3167(2)	1354(1)	918(1)	31(1)
c(53)	-4479(2)	-2552(2)	-3802(1)	32(1)
c(6)	3651(2)	2879(1)	-1720(1)	30(1)
c(32)	2516(2)	2312(2)	1708(1)	31(1)
c(17)	6037(2)	1083(2)	1581(1)	33(1)
c(64)	276(2)	-173(2)	-2588(1)	31(1)
c(7)	2450(2)	3014(1)	-1922(1)	31(1)

Appendix One: X-ray Crystal Structure Data

c(61)	-411(2)	67(2)	-1559(1)	33(1)
c(40)	1280(2)	1585(2)	-4298(1)	30(1)
c(33)	-2822(2)	857(2)	-4197(1)	33(1)
c(5)	4378(2)	3036(1)	-930(1)	29(1)
c(25)	2633(2)	4540(2)	2212(1)	32(1)
c(24)	1910(2)	4975(2)	2545(2)	35(1)
c(47)	-1722(2)	2808(2)	-4(1)	39(1)
c(21)	4562(2)	5677(1)	3122(1)	31(1)
c(60)	-379(2)	-618(2)	-2171(1)	31(1)
c(45)	-2303(2)	2596(2)	-1389(1)	31(1)
c(57)	-2324(2)	-2271(2)	-3762(1)	31(1)
c(54)	-4639(2)	-3501(2)	-3976(1)	37(1)
c(22)	3845(2)	6130(2)	3458(1)	33(1)
c(8)	1950(2)	3286(2)	-1353(1)	31(1)
c(38)	481(2)	2902(2)	-4067(1)	32(1)
c(2)	7169(2)	3455(2)	2081(2)	34(1)
c(48)	-1799(2)	1879(2)	-104(1)	39(1)
c(26)	4527(3)	7003(2)	4133(2)	44(1)
c(56)	-2457(3)	-3214(2)	-3917(1)	38(1)
c(13)	6931(2)	1979(2)	2931(1)	32(1)
c(20)	3974(2)	4863(1)	2499(1)	28(1)
c(49)	-2133(2)	1313(2)	-859(1)	34(1)
c(14)	7198(2)	1217(2)	3160(1)	36(1)
c(34)	-3694(2)	1206(2)	-2883(1)	42(1)
c(10)	4159(3)	2537(2)	-2346(2)	43(1)
c(46)	-1979(2)	3175(2)	-637(1)	36(1)
c(11)	639(2)	3423(2)	-1586(2)	44(1)
c(62)	218(2)	938(2)	-1603(1)	35(1)
c(1)	5944(2)	4063(2)	717(1)	41(1)
c(16)	6277(2)	306(2)	1799(2)	38(1)
c(55)	-3624(3)	-3822(2)	-4022(1)	41(1)
c(43)	2210(2)	1148(2)	-4537(2)	39(1)
c(23)	2525(2)	5775(2)	3171(1)	36(1)
c(50)	-1894(3)	4187(2)	-529(2)	52(1)
c(18)	7865(3)	1305(2)	4018(2)	58(1)
c(58)	-5927(3)	-4156(2)	-4120(2)	51(1)

Appendix One: X-ray Crystal Structure Data

c(42)	566(3)	3899(2)	-4044(2)	48(1)
c(59)	-1353(3)	-3565(2)	-3976(2)	54(1)
c(27)	469(2)	4579(2)	2213(2)	49(1)
c(19)	5932(3)	-597(2)	1177(2)	61(1)
c(51)	-1525(3)	1485(2)	593(2)	56(1)

**Table A 1.11** Positional parameters and U(eq) for P[CH<sub>2</sub>NPh]<sub>3</sub>Li<sub>3</sub>(Et<sub>2</sub>O)<sub>1.5</sub> (**15d**)

	x	y	z	U(eq)
Li(1)	1861(3)	535(5)	393(10)	57(2)
Li(2)	1074(3)	2996(5)	452(11)	66(2)
Li(3)	1004(2)	1326(5)	-334(10)	53(2)
P(1)	1857(1)	2197(1)	-1884(9)	62(1)
N(2)	1490(1)	445(2)	-1271(9)	55(1)
N(3)	798(1)	2511(2)	-1174(9)	56(1)
O(1)	2642(1)	368(2)	163(9)	73(1)
O(2)	1813(1)	-377(2)	1743(9)	76(1)
O(3)	1418(1)	4215(2)	267(9)	72(1)
O(4)	574(1)	3475(2)	1798(10)	81(1)
O(5)	360(1)	725(2)	369(9)	66(1)
C(1)	1997(2)	2306(3)	-234(9)	53(1)
C(4)	1787(1)	2018(2)	1854(10)	44(1)
C(5)	2262(2)	2387(3)	2255(10)	58(1)
C(6)	2387(2)	2402(3)	3488(10)	71(1)
C(7)	2071(2)	2091(3)	4359(10)	73(1)
C(8)	1589(2)	1744(3)	4002(10)	71(1)
C(9)	1454(2)	1702(3)	2789(9)	64(1)
C(2)	1785(2)	977(3)	-2129(10)	64(1)
C(10)	1390(2)	-419(3)	-1666(9)	52(1)
C(11)	1093(2)	-1000(3)	-908(10)	65(1)
C(12)	971(2)	-1841(3)	-1246(10)	81(1)
C(13)	1122(2)	-2199(3)	-2356(10)	85(2)
C(14)	1418(2)	-1667(4)	-3083(10)	78(1)
C(15)	1539(2)	-800(3)	-2757(10)	67(1)
C(3)	1182(2)	2598(3)	-2150(10)	66(1)
C(16)	308(2)	2743(3)	-1523(10)	60(1)
C(17)	159(2)	3007(3)	-2716(10)	77(1)
C(18)	-368(3)	3234(4)	-2937(10)	96(2)
C(19)	-736(2)	3224(4)	-2062(11)	104(2)
C(20)	-591(2)	2959(4)	-914(11)	93(2)
C(21)	-92(2)	2737(3)	-643(10)	71(1)
C(22)	2775(3)	-410(6)	-453(12)	173(4)

Appendix One: X-ray Crystal Structure Data

C(23)	3334(3)	-634(6)	-175(12)	151(3)
C(24)	3514(2)	86(5)	516(14)	170(4)
C(25)	3103(2)	780(5)	638(12)	149(3)
C(30)	1703(3)	4645(4)	1202(11)	103(2)
C(31)	1877(3)	5531(5)	747(11)	114(2)
C(32)	1565(3)	5691(5)	-314(11)	126(2)
C(33)	1384(2)	4808(4)	-748(10)	103(2)
C(34)	401(2)	3168(5)	2946(11)	111(2)
C(35)	124(3)	3878(7)	3575(12)	160(3)
C(36)	-82(3)	4402(5)	2506(14)	181(4)
C(37)	320(3)	4312(4)	1527(12)	127(2)
C(38)	42(2)	421(4)	-625(10)	91(2)
C(39)	-330(3)	-245(6)	-97(11)	144(3)
C(40)	-220(2)	-311(4)	1192(10)	108(2)
C(41)	121(2)	455(4)	1476(10)	97(2)
C(27)	1700(4)	-1487(6)	3234(12)	173(4)
C(28)	1996(3)	-776(6)	3800(11)	147(3)
C(29)	2210(3)	-304(5)	2696(11)	130(2)
C(26A)	1513	-1138	2060	199(4)
C(26B)	1438	-963	2194	199(4)
N(1)	1629(1)	1933(2)	659(9)	50(1)

**Table A 1.12** Positional parameters and U(eq) for [P(CH<sub>2</sub>N-3,5-Me<sub>2</sub>C<sub>6</sub>H<sub>3</sub>)<sub>3</sub>Zr]<sub>2</sub>(η<sup>5</sup>:η<sup>5</sup>-C<sub>10</sub>H<sub>8</sub>) (**16c**)

	x	y	z	U(eq)
C(33)	5897(7)	5672(6)	1459(9)	129(3)
C(36)	7625(6)	6502(6)	1825(8)	129(3)
C(34)	6106(8)	6029(7)	880(6)	145(4)
C(35)	6991(10)	6452(8)	1046(7)	155(4)
C(38)	6546(15)	5695(9)	2206(9)	189(7)
C(37)	7406(12)	6120(9)	2394(7)	176(5)
C(1)	2569(2)	3370(2)	2085(2)	33(1)
C(2)	2530(2)	4519(2)	3427(2)	32(1)
C(3)	3504(2)	5281(2)	2463(2)	35(1)
C(4)	1011(2)	2878(2)	1128(2)	26(1)
C(5)	1308(2)	2442(2)	577(2)	33(1)
C(6)	771(3)	1698(2)	75(2)	36(1)
C(7)	-50(3)	1382(2)	159(2)	40(1)
C(8)	-362(2)	1787(2)	707(2)	36(1)
C(9)	176(2)	2543(2)	1190(2)	30(1)
C(10)	1079(3)	1294(3)	-554(2)	53(1)
C(11)	-1264(3)	1433(3)	790(3)	55(1)
C(12)	1412(2)	5691(2)	3536(2)	29(1)
C(13)	1528(2)	5305(3)	4282(2)	37(1)
C(14)	1203(3)	5786(3)	4799(2)	44(1)
C(15)	741(3)	6663(3)	4564(2)	47(1)
C(16)	607(3)	7072(3)	3828(2)	41(1)
C(17)	948(2)	6585(2)	3325(2)	33(1)
C(18)	1377(4)	5338(4)	5606(3)	66(1)
C(19)	123(4)	8044(3)	3576(3)	62(1)
C(20)	3020(2)	6212(2)	1242(2)	30(1)
C(21)	3700(2)	6939(2)	1580(2)	36(1)
C(22)	4041(3)	7491(3)	1111(2)	42(1)
C(23)	3674(3)	7325(3)	291(3)	47(1)
C(24)	3004(3)	6604(3)	-66(2)	45(1)
C(25)	2690(2)	6046(3)	417(2)	36(1)
C(26)	4817(3)	8242(3)	1514(3)	61(1)

Appendix One: X-ray Crystal Structure Data

C(27)	2640(3)	6404(4)	-963(3)	65(1)
C(28)	39(2)	5280(2)	356(2)	25(1)
C(29)	496(2)	6186(2)	597(2)	27(1)
C(30)	345(2)	6503(2)	1275(2)	29(1)
C(31)	-179(2)	5785(2)	1480(2)	30(1)
C(32)	-351(2)	5027(2)	923(2)	27(1)
N(1)	1548(2)	3639(2)	1631(2)	26(1)
N(2)	1755(2)	5225(2)	3011(2)	27(1)
N(3)	2706(2)	5620(2)	1723(2)	27(1)
P(1)	3334(1)	4148(1)	2934(1)	28(1)
Zr(1)	1451(1)	5098(1)	1782(1)	20(1)

**Table A 1.13** Positional parameters and U(eq) for P[CH<sub>2</sub>N-3,5-Me<sub>2</sub>C<sub>6</sub>H<sub>3</sub>]<sub>3</sub>TiO[4-*t*-BuC<sub>6</sub>H<sub>3</sub>] (17c)

	x	y	z	U(eq)
C(75)	3173(7)	7305(7)	2645(5)	87(3)
C(76)	3480(13)	7397(13)	1902(8)	170(6)
C(77)	3672(9)	8326(9)	1449(6)	113(4)
C(78)	4035(14)	8279(14)	651(9)	189(7)
C(79)	4319(12)	9076(12)	423(8)	155(5)
C(1)	3668(4)	7094(4)	5583(3)	31(1)
C(2)	4729(4)	6804(3)	4239(3)	28(1)
C(3)	2605(4)	6908(4)	4586(3)	30(1)
C(4)	3605(3)	8733(4)	5725(2)	24(1)
C(5)	3477(4)	8378(4)	6453(3)	31(1)
C(6)	3470(4)	8971(4)	6872(3)	37(1)
C(7)	3606(4)	9926(4)	6555(3)	34(1)
C(8)	3740(3)	10294(4)	5841(3)	30(1)
C(9)	3756(3)	9689(4)	5435(3)	25(1)
C(10)	3289(6)	8594(6)	7659(3)	63(2)
C(11)	3855(4)	11345(4)	5497(3)	36(1)
C(12)	4959(3)	8235(4)	3238(2)	24(1)
C(13)	5990(4)	7697(4)	3100(3)	27(1)
C(14)	6569(4)	8103(4)	2521(3)	32(1)
C(15)	6110(4)	9034(4)	2066(3)	35(1)
C(16)	5082(4)	9587(4)	2184(3)	31(1)
C(17)	4520(4)	9171(4)	2768(3)	27(1)
C(18)	7695(4)	7538(5)	2406(3)	46(2)
C(19)	4596(5)	10606(5)	1684(3)	47(2)
C(20)	1161(3)	8458(4)	4226(2)	23(1)
C(21)	660(4)	7892(4)	4076(3)	30(1)
C(22)	-330(4)	8348(4)	3900(3)	35(1)
C(23)	-842(4)	9378(4)	3881(3)	33(1)
C(24)	-371(3)	9965(4)	4029(2)	26(1)
C(25)	622(3)	9496(3)	4203(2)	21(1)
C(26)	-847(5)	7724(6)	3731(4)	57(2)
C(27)	-934(4)	11083(4)	4008(3)	33(1)

Appendix One: X-ray Crystal Structure Data

C(28)	2643(4)	11017(3)	3947(2)	25(1)
C(29)	1792(4)	11598(4)	4282(3)	35(1)
C(30)	1697(5)	12602(4)	4246(4)	46(2)
C(31)	2441(5)	13032(4)	3892(3)	45(2)
C(32)	3283(6)	12436(5)	3554(3)	53(2)
C(33)	3383(5)	11440(5)	3575(3)	46(2)
C(34)	2355(6)	14123(5)	3896(4)	58(2)
C(35)	1841(9)	14896(6)	3294(5)	102(3)
C(36)	3327(11)	14176(11)	3928(8)	153(5)
C(37)	1598(11)	14466(11)	4508(7)	151(5)
C(38)	10676(4)	2091(4)	2504(3)	26(1)
C(39)	11848(3)	1595(4)	1243(2)	26(1)
C(40)	10894(4)	157(4)	2203(3)	28(1)
C(41)	8930(4)	3264(3)	2553(2)	25(1)
C(42)	7915(4)	3584(4)	2417(2)	25(1)
C(43)	7151(4)	4321(4)	2701(3)	30(1)
C(44)	7399(4)	4739(4)	3140(3)	34(1)
C(45)	8386(4)	4431(4)	3294(3)	31(1)
C(46)	9152(4)	3703(4)	2999(2)	28(1)
C(47)	6062(4)	4638(5)	2542(3)	42(1)
C(48)	8658(5)	4887(5)	3771(3)	47(2)
C(49)	11141(4)	2871(3)	193(2)	23(1)
C(50)	10322(4)	3679(4)	-128(2)	26(1)
C(51)	10447(4)	4272(3)	-802(2)	26(1)
C(52)	11416(4)	4076(4)	-1167(2)	28(1)
C(53)	12240(4)	3303(4)	-861(3)	29(1)
C(54)	12102(4)	2691(4)	-181(3)	27(1)
C(55)	9548(4)	5130(4)	-1135(3)	33(1)
C(56)	13302(4)	3110(5)	-1247(3)	40(1)
C(57)	9847(4)	-131(4)	1529(2)	24(1)
C(58)	10228(4)	-1195(4)	1828(3)	28(1)
C(59)	10051(4)	-1889(4)	1562(3)	32(1)
C(60)	9472(4)	-1511(4)	1004(3)	34(1)
C(61)	9055(4)	-454(4)	721(3)	39(1)
C(62)	9249(4)	217(4)	985(3)	33(1)
C(63)	10485(5)	-3030(4)	1884(4)	49(2)

Appendix One: X-ray Crystal Structure Data

C(64)	8396(6)	-55(5)	132(4)	57(2)
C(65)	7976(4)	3427(4)	519(2)	26(1)
C(66)	7771(5)	3180(4)	-16(3)	43(1)
C(67)	7141(5)	3934(5)	-503(3)	47(2)
C(68)	6723(4)	4953(4)	-474(3)	33(1)
C(69)	6953(4)	5178(4)	70(3)	40(1)
C(70)	7562(4)	4431(4)	565(3)	36(1)
C(71)	6083(5)	5806(5)	-1033(3)	44(1)
C(72)	5664(8)	5386(6)	-1447(5)	108(4)
C(73)	6761(6)	6398(6)	-1525(4)	67(2)
C(74)	5201(6)	6552(7)	-712(4)	98(3)
N(1)	3571(3)	8181(3)	5282(2)	24(1)
N(2)	4352(3)	7876(3)	3838(2)	23(1)
N(3)	2164(3)	8036(3)	4402(2)	22(1)
N(4)	9675(3)	2516(3)	2252(2)	24(1)
N(5)	10957(3)	2273(3)	876(2)	24(1)
N(6)	10085(3)	582(3)	1739(2)	24(1)
O(1)	2781(3)	10003(2)	4019(2)	28(1)
O(2)	8639(3)	2717(3)	978(2)	30(1)
P(1)	3842(1)	6323(1)	4968(1)	28(1)
P(2)	11623(1)	995(1)	2189(1)	25(1)
Ti(1)	3184(1)	8632(1)	4355(1)	21(1)
Ti(2)	9746(1)	2059(1)	1440(1)	23(1)

**Table A 1.14** Positional parameters and U(eq) for P[CH<sub>2</sub>NPh]<sub>3</sub>Ti-μ-O-Ti[PhNCH<sub>2</sub>]<sub>3</sub>P (19)

	x	y	z	U(eq)
C(1)	2578(3)	5197(3)	-306(1)	43(1)
C(2)	2587(2)	4099(2)	668(1)	31(1)
C(3)	3264(3)	4080(3)	1191(1)	37(1)
C(4)	2976(3)	3027(3)	1496(2)	46(1)
C(5)	2036(3)	1981(3)	1285(2)	48(1)
C(6)	1376(3)	1999(3)	766(2)	48(1)
C(7)	1642(3)	3036(3)	457(2)	39(1)
N(1)	2872(2)	5182(2)	386(1)	33(1)
O(1)	3333	6667	1667	28(1)
P(2)	3333	6667	-706(1)	42(1)
Ti(1)	3333	6667	786(1)	25(1)

**Table A 1.15** Positional parameters and U(eq) for P[CH<sub>2</sub>N-3,5-Me<sub>2</sub>C<sub>6</sub>H<sub>3</sub>]<sub>3</sub>Ti-μ-O-Ti(NMe<sub>2</sub>)<sub>3</sub> (**20**)

	x	y	z	U(eq)
C(1)	2218(2)	108(2)	1005(2)	32(1)
O(1)	2722(1)	2722(1)	2722(1)	25(1)
Ti(2)	3492(1)	3492(1)	3492(1)	25(1)
N(2)	4896(2)	3778(2)	2721(2)	35(1)
C(10)	5932(2)	3777(3)	3159(3)	52(1)
C(11)	4987(3)	4139(3)	1526(3)	50(1)
Ti(1)	2005(1)	2005(1)	2005(1)	22(1)
P(1)	794(1)	794(1)	794(1)	36(1)
N(1)	2925(2)	709(2)	1470(2)	27(1)
C(2)	4024(2)	184(2)	1525(2)	25(1)
C(3)	4801(2)	744(2)	1841(2)	29(1)
C(6)	5475(2)	-1412(2)	1350(2)	32(1)
C(7)	4392(2)	-900(2)	1275(2)	30(1)
C(5)	6209(2)	-837(2)	1685(2)	34(1)
C(4)	5880(2)	248(2)	1923(2)	32(1)
C(9)	5829(3)	-2579(2)	1057(3)	44(1)
C(8)	6701(2)	878(3)	2264(3)	48(1)

**Table A 1.16** Positional parameters and U(eq) for Se=P[CH<sub>2</sub>NH-3,5-(CF<sub>3</sub>)<sub>2</sub>C<sub>6</sub>H<sub>3</sub>]<sub>3</sub> (**22a**)

	x	y	z	U(eq)
N(1)	2447(2)	8176(1)	3357(1)	22(1)
N(2)	1128(2)	6926(1)	2148(1)	24(1)
Se(1)	1791(1)	5698(1)	4563(1)	25(1)
P(1)	-103(1)	6868(1)	4124(1)	24(1)
C(1)	904(2)	8079(2)	3876(2)	24(1)
C(2)	-282(2)	6961(2)	2783(2)	25(1)
C(3)	3142(2)	9131(2)	3288(2)	24(1)
C(4)	2402(2)	9881(2)	3595(2)	28(1)
C(5)	3170(3)	10747(2)	3557(2)	32(1)
C(6)	4655(3)	10895(2)	3211(2)	32(1)
C(7)	5379(3)	10151(2)	2897(2)	31(1)
C(8)	4645(2)	9280(2)	2934(2)	27(1)
C(9)	2340(3)	11511(2)	3943(2)	48(1)
C(10)	6985(3)	10284(2)	2491(2)	41(1)
C(11)	819(3)	6925(2)	1135(2)	26(1)
C(12)	-582(3)	7110(2)	759(2)	32(1)
C(13)	-802(3)	7036(2)	-185(2)	36(1)
C(14)	353(3)	6787(2)	-773(2)	37(1)
C(15)	1751(3)	6609(2)	-402(2)	33(1)
C(16)	1992(3)	6686(2)	537(2)	30(1)
C(17)	-2339(3)	7222(3)	-560(2)	51(1)
C(18)	3014(3)	6300(3)	-1004(2)	45(1)
C(19)	4053(3)	5226(2)	2504(2)	44(1)
C(20)	468(3)	4538(2)	2838(2)	39(1)
C(21)	5587(3)	6717(2)	3900(2)	44(1)
C(22)	3394(3)	7355(2)	5643(2)	44(1)
C(23)	4258(3)	8206(2)	1188(2)	38(1)
C(24)	1023(3)	9381(2)	1242(2)	40(1)
Al(1)	1975(1)	5509(1)	2850(1)	27(1)
Al(2)	3605(1)	7069(1)	4366(1)	27(1)
Al(3)	2303(1)	8207(1)	1913(1)	24(1)
F(1)	968(2)	11680(2)	3655(3)	99(1)
F(2)	2969(2)	12428(1)	3593(2)	66(1)

Appendix One: X-ray Crystal Structure Data

F(3)	2234(5)	11199(2)	4941(2)	134(1)
F(4)	7155(2)	10758(2)	1489(2)	81(1)
F(5)	7694(2)	9377(1)	2711(2)	67(1)
F(6)	7743(2)	10815(2)	2905(2)	84(1)
F(7)	-3408(2)	6820(2)	200(2)	72(1)
F(8)	-2544(2)	6794(3)	-1229(2)	107(1)
F(9)	-2680(3)	8200(2)	-943(3)	139(2)
F(10)	2635(5)	5808(9)	-1580(7)	109(4)
F(11)	3974(6)	5636(5)	-401(3)	63(2)
F(12)	3908(7)	7050(3)	-1562(6)	101(3)
F(10A)	4183(7)	6590(20)	-879(14)	176(10)
F(11A)	2829(10)	6776(10)	-1998(4)	84(3)
F(12A)	2940(20)	5386(6)	-863(15)	157(9)

**Table A 1.17** Positional parameters and U(eq) for Se=P(CH<sub>2</sub>NHPh)<sub>3</sub> (**22b**)

	x	y	z	U(eq)
C(1)	7458(4)	1203(4)	3647(4)	28(1)
C(2)	8368(4)	3318(4)	4385(4)	26(1)
C(3)	7675(4)	4056(4)	1564(4)	28(1)
C(4)	5117(4)	1888(4)	4495(4)	26(1)
C(5)	3700(4)	2121(4)	4298(4)	31(1)
C(6)	2815(4)	2362(4)	5249(5)	34(1)
C(7)	3270(4)	2398(5)	6419(5)	38(1)
C(8)	4664(5)	2150(5)	6643(5)	40(1)
C(9)	5600(4)	1885(4)	5694(4)	32(1)
C(10)	9267(4)	2638(4)	6736(4)	25(1)
C(11)	8826(4)	4020(4)	6643(4)	29(1)
C(12)	9169(4)	4350(5)	7693(4)	32(1)
C(13)	9913(4)	3329(5)	8860(4)	33(1)
C(14)	10349(4)	1943(5)	8967(4)	32(1)
C(15)	10033(4)	1588(4)	7925(4)	29(1)
C(16)	5601(4)	6074(4)	919(4)	27(1)
C(17)	6271(4)	7087(4)	15(4)	31(1)
C(18)	5538(5)	8474(5)	-702(5)	37(1)
C(19)	4131(5)	8872(5)	-573(5)	38(1)
C(20)	3460(4)	7866(5)	287(5)	38(1)
C(21)	4185(4)	6480(5)	1022(5)	34(1)
N(1)	5977(3)	1749(4)	3453(4)	30(1)
N(2)	8948(4)	2263(4)	5715(4)	29(1)
N(3)	6281(3)	4688(4)	1775(4)	31(1)
P(1)	8487(1)	2550(1)	3118(1)	23(1)
Se(1)	10533(1)	1631(1)	2837(1)	28(1)

**Table A 1.18** Positional parameters and U(eq) for Se=P(CH<sub>2</sub>NH-3,5-Me<sub>2</sub>C<sub>6</sub>H<sub>3</sub>)<sub>3</sub> (**22c**)

	x	y	z	U(eq)
Se(1)	2940(1)	7771(1)	2422(1)	78(1)
P(1)	530(1)	7701(1)	2098(1)	47(1)
N(3)	1698(3)	7805(2)	1245(1)	54(1)
C(3)	448(3)	7192(2)	1486(1)	48(1)
C(20)	2131(3)	7394(2)	803(1)	45(1)
C(21)	945(3)	7032(2)	455(1)	51(1)
N(2)	-2234(3)	9088(2)	1983(1)	60(1)
C(9)	-1685(3)	4518(2)	1867(1)	49(1)
C(4)	-2759(3)	5445(2)	1905(1)	50(1)
C(23)	3050(3)	6624(2)	-63(1)	63(1)
C(8)	-2211(3)	3519(2)	1624(1)	51(1)
C(14)	-5332(3)	10336(2)	1110(1)	56(1)
C(25)	3783(3)	7377(2)	707(1)	52(1)
N(1)	-2354(3)	6441(2)	2166(1)	70(1)
C(13)	-4584(3)	9877(2)	1522(1)	54(1)
C(6)	-4887(3)	4380(2)	1450(1)	58(1)
C(15)	-4418(3)	10420(2)	717(1)	60(1)
C(12)	-2940(3)	9528(2)	1552(1)	48(1)
C(7)	-3800(3)	3462(2)	1419(1)	57(1)
C(5)	-4357(3)	5362(2)	1692(1)	57(1)
C(22)	1397(3)	6657(2)	20(1)	57(1)
C(17)	-2061(3)	9602(2)	1150(1)	51(1)
C(24)	4248(3)	6980(2)	280(1)	60(1)
C(16)	-2794(3)	10055(2)	735(1)	55(1)
C(1)	-789(4)	6705(2)	2405(1)	64(1)
C(2)	-479(3)	9117(2)	2107(1)	57(1)
C(19)	-1803(4)	10165(3)	307(1)	75(1)
C(18)	-7101(3)	10743(3)	1090(1)	79(1)
C(27)	6053(4)	6921(4)	189(2)	94(1)
C(11)	-1058(4)	2504(2)	1587(1)	70(1)
C(26)	96(4)	6313(4)	-365(1)	87(1)
C(10)	-6632(4)	4310(3)	1229(1)	92(1)

**Table A 1.19** Positional parameters and  $U(\text{eq})$  for  $\text{P}[\text{CH}_2\text{N}-3,5\text{-(CF}_3)_2\text{C}_6\text{H}_3]_2\text{Se(AlMe}_2)_3$  (**23a**)

	x	y	z	$U(\text{eq})$
N(1)	2447(2)	8176(1)	3357(1)	22(1)
N(2)	1128(2)	6926(1)	2148(1)	24(1)
Se(1)	1791(1)	5698(1)	4563(1)	25(1)
P(1)	-103(1)	6868(1)	4124(1)	24(1)
C(1)	904(2)	8079(2)	3876(2)	24(1)
C(2)	-282(2)	6961(2)	2783(2)	25(1)
C(3)	3142(2)	9131(2)	3288(2)	24(1)
C(4)	2402(2)	9881(2)	3595(2)	28(1)
C(5)	3170(3)	10747(2)	3557(2)	32(1)
C(6)	4655(3)	10895(2)	3211(2)	32(1)
C(7)	5379(3)	10151(2)	2897(2)	31(1)
C(8)	4645(2)	9280(2)	2934(2)	27(1)
C(9)	2340(3)	11511(2)	3943(2)	48(1)
C(10)	6985(3)	10284(2)	2491(2)	41(1)
C(11)	819(3)	6925(2)	1135(2)	26(1)
C(12)	-582(3)	7110(2)	759(2)	32(1)
C(13)	-802(3)	7036(2)	-185(2)	36(1)
C(14)	353(3)	6787(2)	-773(2)	37(1)
C(15)	1751(3)	6609(2)	-402(2)	33(1)
C(16)	1992(3)	6686(2)	537(2)	30(1)
C(17)	-2339(3)	7222(3)	-560(2)	51(1)
C(18)	3014(3)	6300(3)	-1004(2)	45(1)
C(19)	4053(3)	5226(2)	2504(2)	44(1)
C(20)	468(3)	4538(2)	2838(2)	39(1)
C(21)	5587(3)	6717(2)	3900(2)	44(1)
C(22)	3394(3)	7355(2)	5643(2)	44(1)
C(23)	4258(3)	8206(2)	1188(2)	38(1)
C(24)	1023(3)	9381(2)	1242(2)	40(1)
Al(1)	1975(1)	5509(1)	2850(1)	27(1)
Al(2)	3605(1)	7069(1)	4366(1)	27(1)
Al(3)	2303(1)	8207(1)	1913(1)	24(1)
F(1)	968(2)	11680(2)	3655(3)	99(1)

Appendix One: X-ray Crystal Structure Data

F(2)	2969(2)	12428(1)	3593(2)	66(1)
F(3)	2234(5)	11199(2)	4941(2)	134(1)
F(4)	7155(2)	10758(2)	1489(2)	81(1)
F(5)	7694(2)	9377(1)	2711(2)	67(1)
F(6)	7743(2)	10815(2)	2905(2)	84(1)
F(7)	-3408(2)	6820(2)	200(2)	72(1)
F(8)	-2544(2)	6794(3)	-1229(2)	107(1)
F(9)	-2680(3)	8200(2)	-943(3)	139(2)
F(10)	2635(5)	5808(9)	-1580(7)	109(4)
F(11)	3974(6)	5636(5)	-401(3)	63(2)
F(12)	3908(7)	7050(3)	-1562(6)	101(3)
F(10A)	4183(7)	6590(20)	-879(14)	176(10)
F(11A)	2829(10)	6776(10)	-1998(4)	84(3)
F(12A)	2940(20)	5386(6)	-863(15)	157(9)

**Table A 1.20** Positional parameters and U(eq) for P(CH<sub>2</sub>N-3,5-Me<sub>2</sub>C<sub>6</sub>H<sub>3</sub>)<sub>2</sub>Se(AlMe<sub>2</sub>)<sub>3</sub> (**23c**)

	x	y	z	U(eq)
N(1)	7978(1)	5681(2)	1002(1)	20(1)
N(2)	9654(1)	4617(2)	1719(1)	21(1)
Al(1)	9478(1)	5315(1)	1051(1)	23(1)
Al(2)	9377(1)	6132(1)	2241(1)	24(1)
Al(3)	7236(1)	7369(1)	1344(1)	24(1)
P(1)	7567(1)	3632(1)	1776(1)	23(1)
Se(1)	7494(1)	6076(1)	2125(1)	25(1)
C(1)	7456(2)	4183(3)	1149(1)	23(1)
C(2)	8949(2)	3239(3)	1803(1)	24(1)
C(3)	10726(2)	4129(3)	1762(1)	23(1)
C(4)	11036(2)	2546(3)	1731(1)	26(1)
C(5)	12060(2)	2141(3)	1767(1)	28(1)
C(6)	12778(2)	3341(3)	1839(1)	28(1)
C(7)	12481(2)	4928(3)	1874(1)	26(1)
C(8)	11461(2)	5307(3)	1830(1)	25(1)
C(9)	12385(2)	420(3)	1736(1)	39(1)
C(10)	13262(2)	6229(3)	1954(1)	33(1)
C(11)	7793(2)	6048(3)	503(1)	24(1)
C(12)	7351(2)	4978(3)	192(1)	31(1)
C(13)	7202(2)	5394(4)	-275(1)	39(1)
C(14)	7494(2)	6895(4)	-427(1)	40(1)
C(15)	7936(2)	7990(3)	-122(1)	35(1)
C(16)	8086(2)	7546(3)	342(1)	28(1)
C(17)	6726(3)	4223(5)	-611(1)	59(1)
C(18)	8267(3)	9617(4)	-287(1)	48(1)
C(19)	10287(2)	7222(3)	917(1)	34(1)
C(20)	9741(2)	3448(3)	654(1)	37(1)
C(21)	9665(2)	5000(4)	2825(1)	40(1)
C(22)	9818(2)	8349(3)	2193(1)	34(1)
C(23)	5794(2)	7098(4)	1187(1)	39(1)
C(24)	7819(2)	9511(3)	1370(1)	36(1)
C(26)	4751(3)	8227(3)	9629(1)	216(9)

Appendix One: X-ray Crystal Structure Data

C(27)	5039(3)	8239(3)	9090(1)	99(3)
C(30)	5285(3)	9695(3)	9700(1)	75(2)
C(29)	5000(3)	10000(3)	10000(1)	153(4)
C(28)	4492(3)	8838(3)	9546(1)	100(3)
C(31)	4774(3)	8445(3)	9308(1)	102(3)

**Table A 1.21** Positional parameters and U(eq) for Me<sub>3</sub>Al·P(CH<sub>2</sub>NPh)<sub>2</sub>Se(AlMe<sub>2</sub>)<sub>3</sub> (**24b**)

	x	y	z	U(eq)
Se(1)	0	9969(1)	68(1)	26(1)
P(1)	0	10235(1)	2664(2)	22(1)
Al(2)	0	13387(1)	2018(2)	20(1)
Al(1)	1262(1)	11368(1)	-160(1)	26(1)
Al(3)	0	8142(2)	3976(2)	31(1)
N(1)	1000(2)	12248(3)	1818(4)	18(1)
C(10)	0	13983(5)	4173(7)	29(1)
C(1)	899(3)	11256(3)	2998(4)	21(1)
C(12)	0	8604(7)	6179(8)	55(2)
C(9)	1191(3)	12188(4)	-2175(5)	38(1)
C(2)	1790(3)	12950(3)	2086(5)	22(1)
C(8)	2248(3)	10319(4)	224(7)	40(1)
C(6)	2815(3)	14370(4)	1066(5)	35(1)
C(7)	2047(3)	13762(4)	938(5)	29(1)
C(5)	3329(3)	14178(4)	2340(6)	38(1)
C(3)	2305(3)	12790(4)	3396(5)	30(1)
C(4)	3068(3)	13405(4)	3503(6)	35(1)
C(11)	0	14620(5)	375(6)	25(1)
C(13)	1053(3)	7525(4)	3035(6)	47(1)

**Table A 1.22** Positional parameters and U(eq) for P[CH<sub>2</sub>N-3,5-(CF<sub>3</sub>)<sub>2</sub>C<sub>6</sub>H<sub>3</sub>]<sub>3</sub>Al<sub>2</sub>Me<sub>3</sub> (25a)

	x	y	z	U(eq)
Al(1)	7985(1)	1039(1)	2503(1)	34(1)
Al(2)	10123(1)	-728(1)	2862(1)	38(1)
P(1)	8677(1)	644(1)	639(1)	41(1)
N(1)	7027(2)	2002(2)	1506(2)	39(1)
N(2)	8421(2)	-698(2)	2565(2)	37(1)
N(3)	9670(2)	1092(2)	2118(2)	35(1)
C(28)	7580(4)	1209(3)	3674(2)	57(1)
C(29)	10300(4)	-1097(3)	4171(2)	58(1)
C(30)	11361(3)	-1588(3)	2269(3)	57(1)
C(31)	4330(8)	1126(6)	9514(6)	112(2)
C(32)	4003(7)	467(9)	10382(8)	125(3)
C(33)	5309(10)	658(8)	9138(5)	119(2)
C(1)	7239(3)	1686(3)	679(2)	45(1)
C(2)	8428(3)	-766(3)	1616(2)	42(1)
C(3)	9756(3)	1283(3)	1105(2)	42(1)
C(4)	6001(3)	2892(3)	1485(2)	39(1)
C(5)	5927(3)	3611(3)	2039(2)	45(1)
C(6)	4913(3)	4492(3)	2031(2)	49(1)
C(7)	3942(3)	4712(3)	1467(2)	51(1)
C(8)	4008(3)	4017(3)	915(2)	48(1)
C(9)	5016(3)	3128(3)	909(2)	45(1)
C(10)	4901(3)	5250(3)	2625(3)	67(1)
C(11)	2948(3)	4159(4)	338(3)	57(1)
C(12)	7773(3)	-1648(3)	3175(2)	40(1)
C(13)	6558(3)	-1344(3)	3331(2)	50(1)
C(14)	5927(3)	-2263(4)	3883(3)	56(1)
C(15)	6505(4)	-3481(3)	4272(2)	59(1)
C(16)	7719(3)	-3791(3)	4106(3)	55(1)
C(17)	8357(3)	-2875(3)	3568(2)	50(1)
C(18)	4623(4)	-1925(5)	4062(4)	85(1)
C(19)	8326(5)	-5138(4)	4503(4)	84(2)
C(20)	10211(3)	2010(3)	2298(2)	37(1)

Appendix One: X-ray Crystal Structure Data

C(21)	11231(3)	1659(3)	2840(2)	45(1)
C(22)	11706(3)	2547(3)	3035(2)	49(1)
C(23)	11192(3)	3792(3)	2673(2)	50(1)
C(24)	10194(3)	4144(3)	2109(2)	48(1)
C(25)	9697(3)	3265(3)	1925(2)	44(1)
C(26)	12804(4)	2133(4)	3635(3)	72(1)
C(27)	9640(4)	5496(4)	1678(4)	71(1)
F(1)	4968(9)	4556(7)	3516(4)	75(2)
F(2)	5913(6)	5814(7)	2475(5)	64(2)
F(3)	3980(7)	6179(7)	2481(6)	83(2)
F(3B)	5407(9)	6220(7)	2245(5)	82(2)
F(1B)	3718(5)	5616(8)	2854(6)	66(2)
F(2B)	5428(8)	4566(7)	3456(4)	67(2)
F(1C)	4065(17)	5094(17)	3266(12)	91(4)
F(3C)	4569(14)	6476(8)	2089(8)	71(3)
F(2C)	5902(15)	5102(19)	3034(14)	98(4)
F(4)	2185(2)	5228(3)	182(2)	100(1)
F(5)	2302(2)	3260(3)	731(2)	78(1)
F(6)	3265(2)	4089(3)	-476(2)	85(1)
F(7)	4058(4)	-2843(4)	4311(6)	226(3)
F(8)	4027(3)	-1080(5)	3345(3)	139(2)
F(9)	4435(4)	-1399(6)	4658(3)	182(2)
F(10)	7783(4)	-5865(3)	4277(4)	183(3)
F(11)	8355(4)	-5548(4)	5396(3)	148(2)
F(12)	9453(3)	-5346(2)	4253(3)	112(1)
F(13)	8521(3)	5743(3)	1963(3)	117(1)
F(14)	9509(3)	5858(2)	774(2)	105(1)
F(15)	10243(4)	6236(2)	1829(4)	169(2)
F(16)	13130(4)	3029(3)	3805(3)	135(2)
F(17)	13792(3)	1759(4)	3201(3)	123(1)
F(18)	12734(3)	1177(3)	4364(2)	130(2)

**Table A 1.23** Positional parameters and U(eq) for Me<sub>3</sub>Al·P(CH<sub>2</sub>NPh)<sub>3</sub>Al<sub>2</sub>Me<sub>3</sub> (**26b**)

	x	y	z	U(eq)
P(1)	8182(1)	2349(1)	4204(1)	23(1)
Al(1)	7951(1)	3509(1)	3445(1)	20(1)
Al(3)	8395(1)	1346(1)	4807(1)	29(1)
Al(2)	10192(1)	2902(1)	3451(1)	22(1)
N(3)	8690(1)	2326(1)	3382(1)	21(1)
C(2)	9168(2)	3307(1)	4189(1)	25(1)
N(2)	9294(1)	3760(1)	3786(1)	22(1)
N(1)	6697(1)	3350(1)	3755(1)	24(1)
C(16)	8589(2)	1818(1)	3011(1)	23(1)
C(1)	6820(2)	2911(1)	4145(1)	26(1)
C(10)	9799(2)	4653(1)	3834(1)	26(1)
C(4)	5614(2)	3715(1)	3680(1)	24(1)
C(3)	8392(2)	1734(1)	3730(1)	24(1)
C(23)	10692(2)	3457(1)	2953(1)	34(1)
C(21)	9461(2)	1253(1)	2894(1)	36(1)
C(22)	7804(2)	4217(1)	2956(1)	32(1)
C(17)	7649(2)	1893(1)	2771(1)	34(1)
C(13)	10766(2)	6369(1)	3911(1)	45(1)
C(11)	9430(2)	5369(1)	3604(1)	36(1)
C(20)	9421(2)	822(2)	2528(1)	45(1)
C(24)	11286(2)	2190(2)	3751(1)	35(1)
C(5)	5179(2)	3729(2)	3292(1)	36(1)
C(7)	3464(2)	4433(2)	3516(1)	44(1)
C(25)	10042(2)	1196(2)	4803(1)	48(1)
C(18)	7614(2)	1459(2)	2403(1)	43(1)
C(15)	10667(2)	4807(2)	4102(1)	47(1)
C(9)	4931(2)	4063(2)	3982(1)	37(1)
C(6)	4120(2)	4084(2)	3213(1)	45(1)
C(19)	8509(2)	938(1)	2278(1)	40(1)
C(8)	3878(2)	4417(2)	3899(1)	46(1)
C(14)	11141(2)	5663(2)	4138(1)	56(1)
C(12)	9917(2)	6221(2)	3642(1)	45(1)
C(26)	7474(2)	311(2)	4631(1)	56(1)

**Table A 1.24** Positional parameters and U(eq) for  $\{P[CH_2N-3,5-(CF_3)_2C_6H_3]_2MgTHF_2\}_2$  (27)

	x	y	z	U(eq)
C(1)	3929(4)	6283(4)	8310(4)	33(1)
C(10)	5230(4)	6857(4)	9805(4)	33(1)
P(1)	4269(1)	5788(1)	9871(1)	28(1)
Mg(1)	3323(1)	3926(1)	11964(1)	29(1)
O(2)	1783(3)	5098(3)	12089(3)	41(1)
N(1)	4986(3)	6160(3)	7522(3)	32(1)
N(2)	3565(3)	3164(3)	10828(3)	33(1)
O(1)	2741(3)	2508(3)	13483(3)	46(1)
C(11)	2838(4)	2434(4)	10795(4)	33(1)
C(15)	843(4)	1708(4)	11364(4)	41(1)
C(12)	3178(4)	1624(4)	10284(4)	38(1)
F(7)	3807(4)	210(4)	9097(4)	87(1)
C(2)	4688(4)	6483(4)	6395(4)	32(1)
C(7)	5624(4)	6298(4)	5596(4)	39(1)
F(5)	6138(4)	6242(5)	2789(4)	111(2)
C(13)	2386(5)	890(4)	10319(5)	43(1)
C(6)	5411(5)	6627(5)	4442(4)	44(1)
F(6)	7353(4)	5515(4)	4194(3)	93(1)
F(4)	7043(4)	7394(4)	3085(4)	107(2)
C(16)	1627(4)	2442(5)	11335(4)	41(1)
C(14)	1199(5)	918(4)	10865(5)	45(1)
C(4)	3302(5)	7343(5)	4757(4)	45(1)
C(5)	4243(5)	7172(5)	3986(4)	53(1)
C(3)	3500(4)	7011(4)	5931(4)	38(1)
F(3)	1907(4)	8221(6)	3215(4)	130(2)
C(9)	6470(6)	6446(6)	3633(5)	58(2)
F(9)	1991(5)	91(8)	9099(8)	192(4)
F(12)	-1185(4)	1369(8)	11731(7)	200(4)
F(10)	-369(5)	1229(7)	13128(5)	158(3)
F(11)	-884(4)	2851(5)	11872(7)	155(3)
C(18)	-396(6)	1777(6)	11949(6)	65(2)
F(2)	1239(4)	7117(6)	4835(5)	146(2)

Appendix One: X-ray Crystal Structure Data

F(1)	1498(5)	8761(6)	4574(6)	169(3)
C(8)	2026(6)	7883(7)	4332(6)	67(2)
C(20)	1882(8)	1195(7)	15303(7)	101(3)
C(19)	1698(5)	2451(6)	14326(5)	67(2)
C(23)	1821(7)	6095(7)	12339(8)	90(2)
C(21)	3171(9)	690(7)	15181(7)	103(3)
F(8)	3055(9)	-1090(4)	10598(6)	201(4)
C(17)	2788(6)	31(6)	9789(7)	73(2)
C(26)	612(6)	5337(7)	11594(9)	96(3)
C(24)	613(10)	6895(11)	12017(13)	177(7)
C(22)	3519(6)	1322(5)	13872(6)	72(2)
C(25)	-216(6)	6234(7)	11890(8)	94(3)

**Table A 1.25** Positional parameters and U(eq) for {P[CH<sub>2</sub>NH-3,5-(CF<sub>3</sub>)<sub>2</sub>C<sub>6</sub>H<sub>3</sub>]<sub>2</sub>Se<sub>2</sub>}<sup>-</sup>[HNEt<sub>3</sub>]<sup>+</sup> (35)

	x	y	z	U(eq)
C(88)	2652(11)	2985(5)	1476(8)	31(4)
C(110)	616(15)	1806(7)	2421(11)	81(7)
C(111)	529(12)	1510(6)	1755(9)	44(5)
C(113)	1320(12)	1061(6)	882(9)	46(5)
C(114)	2239(13)	876(6)	641(10)	62(6)
C(221)	1864(13)	982(6)	2216(10)	53(5)
C(222)	1239(15)	566(7)	2310(11)	81(7)
C(223)	2772(12)	1039(6)	6320(9)	45(5)
C(224)	3275(15)	583(7)	6174(11)	78(7)
C(300)	2927(17)	738(8)	4136(12)	82(7)
C(301)	3341(15)	1159(8)	4124(11)	71(6)
C(302)	2863(17)	1538(8)	4207(11)	78(7)
C(303)	1886(18)	1527(8)	4348(12)	82(7)
C(304)	1468(16)	1117(8)	4378(12)	84(7)
C(305)	1973(17)	712(8)	4280(11)	80(7)
C(700)	1180(30)	1918(13)	4600(20)	59(11)
C(701)	3520(40)	1952(17)	3990(30)	102(16)
C(800)	1095(17)	2612(8)	4737(14)	59(11)
C(801)	712(14)	2859(9)	4125(14)	73(13)
C(802)	1260(20)	3199(9)	3832(12)	60(12)
C(803)	2195(19)	3293(8)	4151(15)	76(14)
C(804)	2578(14)	3046(9)	4763(14)	54(11)
C(805)	2028(17)	2706(8)	5055(11)	47(10)
C(900)	3600(20)	2589(8)	3793(17)	194(16)
C(901)	2690(20)	2719(9)	3478(10)	144(11)
C(902)	2159(14)	3047(10)	3819(16)	162(13)
C(903)	2540(20)	3245(8)	4475(16)	220(19)
C(904)	3460(20)	3115(10)	4789(11)	153(13)
C(905)	3989(15)	2787(11)	4448(18)	290(30)
N(40)	1440(9)	1290(4)	1616(7)	35(4)
F(70)	4070(13)	4612(6)	1227(9)	178(10)
F(71)	5403(14)	4604(6)	851(6)	159(8)

## Appendix One: X-ray Crystal Structure Data

F(72)	5040(9)	4106(4)	1528(6)	86(4)
C(806)	3690(60)	3220(30)	5300(40)	180(30)
C(906)	1100(30)	3135(14)	3390(20)	70(13)
C(1)	3718(11)	3361(5)	-218(8)	30(4)
C(2)	3525(11)	3598(5)	-884(9)	35(4)
C(3)	3701(11)	4065(5)	-919(9)	35(5)
C(4)	4048(11)	4311(6)	-325(9)	38(5)
C(5)	4258(11)	4073(5)	326(9)	30(4)
C(6)	4084(11)	3613(5)	387(8)	30(4)
C(8)	4654(15)	4347(7)	970(11)	50(5)
C(9)	3458(12)	3516(5)	2399(9)	34(4)
C(10)	2658(11)	3812(5)	2343(8)	31(4)
C(11)	2670(12)	4194(5)	2801(9)	38(5)
C(12)	3413(12)	4288(6)	3318(9)	43(5)
C(13)	4213(12)	3989(6)	3361(9)	39(5)
C(14)	4243(12)	3608(6)	2915(9)	40(5)
C(15)	1788(13)	4503(6)	2710(10)	42(5)
C(16)	5043(17)	4095(8)	3921(12)	64(6)
C(17)	6342(11)	1431(5)	1133(8)	27(4)
C(18)	5533(11)	1321(5)	626(8)	32(4)
C(19)	5573(12)	952(5)	179(9)	34(4)
C(20)	6343(11)	654(5)	249(9)	35(5)
C(21)	7116(12)	753(5)	728(9)	33(4)
C(22)	7136(11)	1131(5)	1184(8)	30(4)
C(23)	4687(16)	836(7)	-334(11)	57(6)
C(24)	7973(14)	439(7)	822(11)	50(5)
C(25)	5980(11)	2358(5)	3125(8)	31(4)
C(26)	6072(11)	1599(5)	3777(8)	30(4)
C(27)	5765(11)	1340(5)	3182(9)	31(4)
C(28)	5558(12)	878(5)	3264(9)	36(5)
C(29)	5701(11)	657(6)	3939(9)	39(5)
C(30)	6015(11)	931(5)	4529(8)	31(4)
C(31)	5216(16)	597(7)	2613(11)	55(6)
C(32)	6155(14)	714(6)	5247(10)	43(5)
C(50)	3800(11)	2597(5)	391(8)	34(4)
C(51)	6224(10)	1383(5)	4463(8)	25(4)

Appendix One: X-ray Crystal Structure Data

C(55)	7141(11)	1968(5)	2046(8)	26(4)
C(71)	3563(17)	4294(8)	-1638(12)	61(6)
N(1)	6287(9)	1822(4)	1568(7)	32(3)
N(2)	6315(9)	2065(4)	3751(6)	30(3)
N(3)	3511(9)	2900(4)	-210(7)	33(3)
N(4)	3521(8)	3127(4)	1956(6)	27(3)
F(1)	4102(8)	1188(4)	-485(6)	78(4)
F(2)	4941(8)	686(6)	-978(6)	124(6)
F(3)	4151(8)	512(4)	-111(8)	103(5)
F(4)	8089(9)	189(4)	254(8)	117(6)
F(5)	7916(10)	147(5)	1341(9)	135(6)
F(6)	8792(8)	647(4)	969(7)	90(4)
F(7)	1836(8)	4767(4)	2102(6)	81(4)
F(8)	1744(8)	4791(4)	3252(6)	78(4)
F(9)	981(7)	4284(3)	2596(7)	75(4)
F(10)	5551(9)	4444(5)	3703(8)	110(5)
F(11)	4796(9)	4221(5)	4542(7)	118(6)
F(20)	5666(8)	3757(4)	4023(6)	77(4)
F(21)	5565(11)	378(5)	5371(6)	123(6)
F(22)	6040(13)	991(4)	5805(6)	126(6)
F(23)	7003(10)	560(8)	5439(8)	186(10)
F(24)	4438(13)	728(5)	2290(10)	200(11)
F(25)	5094(11)	155(4)	2734(6)	103(5)
F(26)	5812(14)	581(6)	2109(7)	160(8)
F(31)	4205(11)	4555(5)	-1819(7)	124(6)
F(32)	2867(14)	4579(10)	-1683(10)	230(14)
F(33)	3330(20)	4050(5)	-2184(8)	240(15)
P(1)	6914(3)	2502(1)	2514(2)	28(1)
P(5)	2853(3)	2458(2)	990(2)	30(1)
Se(1)	3505(1)	1964(1)	1763(1)	38(1)
Se(2)	1517(1)	2301(1)	374(1)	42(1)
Se(3)	6246(1)	2986(1)	1745(1)	36(1)
Se(4)	8266(1)	2679(1)	3115(1)	39(1)
C(100)	2498(14)	899(7)	7889(11)	74(7)
C(101)	3404(12)	1075(6)	7644(9)	45(5)
C(103)	4234(13)	1524(6)	6766(9)	52(5)

Appendix One: X-ray Crystal Structure Data

C(104)	4155(16)	1836(7)	6120(11)	84(7)
N(41)	3285(10)	1314(5)	6942(7)	45(4)

**Table A 1.26** Positional parameters and U(eq) for P[CH<sub>2</sub>N-3,5-Me<sub>2</sub>C<sub>6</sub>H<sub>3</sub>]<sub>2</sub>SeZrN(-3,5-Me<sub>2</sub>C<sub>6</sub>H<sub>3</sub>)CH<sub>2</sub>NEt<sub>2</sub> (**37c**)

	x	y	z	U(eq)
Zr(1)	9212(1)	4908(1)	1012(1)	43(1)
Se(1)	7931(1)	6094(1)	725(1)	82(1)
P(1)	9128(1)	6738(1)	1101(1)	67(1)
N(3)	9534(2)	3620(2)	1038(1)	42(1)
N(1)	10713(2)	5487(2)	865(1)	47(1)
C(20)	10315(3)	3084(2)	1210(1)	40(1)
C(5)	11964(3)	4455(2)	603(1)	53(1)
C(4)	11755(3)	5285(2)	703(1)	46(1)
C(25)	11314(3)	3421(2)	1343(1)	46(1)
C(9)	12591(3)	5874(3)	634(1)	55(1)
C(21)	10125(3)	2231(2)	1250(1)	48(1)
C(23)	11903(4)	2077(3)	1544(1)	61(1)
C(8)	13613(3)	5645(3)	473(1)	58(1)
C(6)	12967(4)	4217(3)	447(1)	65(1)
C(22)	10917(4)	1723(2)	1418(1)	59(1)
C(24)	12119(3)	2930(3)	1505(1)	54(1)
C(7)	13785(4)	4821(3)	383(1)	64(1)
C(26)	10701(5)	791(3)	1450(2)	90(2)
C(10)	13155(5)	3307(3)	349(2)	104(2)
C(27)	13221(4)	3309(3)	1636(1)	84(2)
C(11)	14489(4)	6312(3)	393(1)	89(2)
N(4)	7965(3)	3966(2)	708(1)	57(1)
N(2)	8940(3)	5260(2)	1531(1)	56(1)
C(3)	8566(3)	3234(2)	868(1)	50(1)
C(1)	10548(3)	6380(2)	940(1)	58(1)
C(12)	8757(3)	4867(3)	1863(1)	60(1)
C(2)	8925(4)	6175(3)	1528(1)	70(1)
C(16)	8641(4)	3572(3)	2203(1)	74(1)
C(17)	8774(4)	3994(3)	1882(1)	65(1)
C(13)	8595(4)	5307(3)	2180(1)	74(1)
C(28)	6745(4)	3974(3)	798(2)	81(2)

Appendix One: X-ray Crystal Structure Data

C(19)	8676(6)	2622(3)	2210(2)	113(2)
C(30)	8089(5)	3969(3)	313(1)	83(2)
C(29)	6508(4)	4097(3)	1188(2)	106(2)
C(31)	9288(5)	4021(4)	185(1)	97(2)
C(14)	8464(4)	4894(4)	2501(1)	79(1)
C(15)	8496(4)	4032(4)	2511(1)	84(1)
C(18)	8289(5)	5394(4)	2840(2)	108(2)
C(34)	5609(7)	4069(5)	2263(2)	144(3)
C(33)	5000	4530(10)	2500	184(5)
C(32)	5000	5385(8)	2500	168(5)
C(36)	5000	2708(10)	2500	180(5)
C(35)	5581(9)	3208(7)	2281(3)	196(4)

## Vita Auctoris

**Name:** Hua Han

**Education:** Tianjin University, Tianjin, China, 1991-1995 B.S.

Nankai University, Tianjin, China, 1999-2002 M.S.

University of Windsor, Windsor, On. Canada,

2003-2007 Ph.D

### Publication:

1. **Hua Han** and Samuel. A. Johnson. "Ligand Design for the Assembly of Polynuclear Complexes: Syntheses and Structures of Trinuclear and Tetranuclear Aluminum Alkyl Complexes Bearing Tripodal Diamidoselenophosphinito Ligands and a Comparison to Related Tripodal Triamidophosphine Complexes". *Organometallics* **2006**, 25(23); 5594-5602.
2. **Hua Han**, Mona Elsmaili, and Samuel A. Johnson. "A Diligating Tripodal Amido-Phosphine Ligand Building Block for Heterobimetallic Polynuclear Complexes and The Effect of a Proximal Early Transition Metal on the Donor Ability of a Phosphine". *Inorg. Chem.* **2006**, 45(18), 7435-7445.
3. Keen, A. L.; Doster, M.; **Han, Hua.**; Johnson, S. A. "Facile assembly of a Cu<sub>9</sub> amido complex: a new tripodal ligand design that promotes transition metal cluster formation". *Chem. Comm.* **2006**, 1221-1223.
4. **Han, Hua**; Johnson, S. A.\* "Bridged Dinuclear Tripodal Tris(amido)phosphine Complexes of Titanium and Zirconium as Diligating Building Blocks for Organometallic Polymers" *Eur. J. Inorg. Chem.*, **2007**, in press.
5. **Hua Han**, Jillian A. Hatnean and Samuel. A. Johnson\*. "Magnesium Bimetallic Complexes with P-P Bond: a New Method to Synthesize Diamido- Phosphine Complexes From Phosphine Selenides by P-C Bond Cleavage". 2007, in preparation.